Université de Montréal

Monoacylglycerol, α/β-hydrolase domain-6, and the regulation of insulin secretion and energy metabolism

par

Shangang Zhao

Département de biochimie

Faculté de médecine

Thèse présentée à la Faculté de médecine
en vue de l'obtention du grade de PhD en biochimie

August, 2015

Université de Montréal

Faculté des études supérieures

Cette thèse intitulée:

Monoacylglycerol, α/β-hydrolase domain-6, and the regulation of insulin secretion and energy metabolism

Présentée par : Shangang Zhao

a été évaluée par un jury composé des personnes suivantes :

Sylvie Mader, président-rapporteur

Marc Prentki, directeur de recherche

Jennifer Estall, membre du jury

Andre Carpentier, examinateur externe

Rejean Couture, Représentante du doyen de la FES

Résumé

Le cycle glycérolipides/acides gras libres (GL/FFA) est une voie métabolique clé qui relie le métabolisme du glucose et des acides gras et il est composé de deux processus métaboliques appelés lipogenèse et lipolyse. Le cycle GL/FFA, en particulier la lipolyse des triglycérides, génère diverses molécules de signalisation pour réguler la sécrétion d'insuline dans les cellules bêta pancréatiques et la thermogenèse non-frissonnante dans les adipocytes. Actuellement, les lipides provenant spécifiquement de la lipolyse impliqués dans ce processus sont mal connus.

L'hydrolyse des triglycérides dans les cellules β est réalisée par les actions successives de la triglycéride lipase adipocytaire pour produire le diacylglycérol, ensuite par la lipase hormono-sensible pour produire le monoacylglycérol (MAG) et enfin par la MAG lipase (MAGL) qui relâche du glycerol et des acides gras. Dans les cellules bêta, la MAGL classique est très peu exprimée et cette étude a démontré que l'hydrolyse de MAG dans les cellules β est principalement réalisée par l'α/β-Hydrolase Domain-6 (ABHD6) nouvellement identifiée. L'inhibition d'ABHD6 par son inhibiteur spécifique WWL70, conduit à une accumulation des 1-MAG à longues chaines saturées à l'intérieur des cellules, accompagnée d'une augmentation de la sécrétion d'insuline stimulée par le glucose (GSIS). Baisser les niveaux de MAG en surexprimant ABHD6 dans la lignée cellulaire bêta INS832/13 réduit la GSIS, tandis qu'une augmentation des niveaux de MAG par le « knockdown » d'ABHD6 améliore la GSIS. L'exposition aiguë des monoacylglycérols exogènes stimule la sécrétion d'insuline de manière dose-dépendante et restaure la GSIS supprimée par un inhibiteur de lipases appelé orlistat. En outre, les souris avec une inactivation du gène ABHD6 dans tous les tissus (ABHD6-KO) et celles avec une inactivation du gène ABHD6 spécifiquement dans la cellule β présentent une GSIS stimulée, et leurs îlots montrent une augmentation de la production de monoacylglycérol et de la sécrétion d'insuline en réponse au glucose. L'inhibition d'ABHD6 chez les souris diabétiques (modèle induit par de faibles doses de streptozotocine) restaure la GSIS et améliore la tolérance au glucose. De plus, les résultats montrent que les MAGs non seulement améliorent la GSIS, mais potentialisent également la sécrétion d'insuline induite par les acides gras libres ainsi que la sécrétion d'insuline induite par divers agents et hormones, sans altération de l'oxydation et l'utilisation du glucose ainsi que l'oxydation des acides gras. Nous avons démontré que le MAG se lie à la protéine d'amorçage des vésicules appelée Munc13-1

et l'active, induisant ainsi l'exocytose de l'insuline. Sur la base de ces observations, nous proposons que le 1-MAG à chaines saturées agit comme facteur de couplage métabolique pour réguler la sécrétion d'insuline et que ABHD6 est un modulateur négatif de la sécrétion d'insuline.

En plus de son rôle dans les cellules bêta, ABHD6 est également fortement exprimé dans les adipocytes et son niveau est augmenté avec l'obésité. Les souris dépourvues globalement d'ABHD6 et nourris avec une diète riche en gras (HFD) montrent une faible diminution de la prise alimentaire, une diminution du gain de poids corporel et de la glycémie à jeun et une amélioration de la tolérance au glucose et de la sensibilité à l'insuline et ont une activité locomotrice accrue. En outre, les souris ABHD6-KO affichent une augmentation de la dépense énergétique et de la thermogenèse induite par le froid. En conformité avec ceci, ces souris présentent des niveaux élevés d'UCP1 dans les adipocytes blancs et bruns, indiquant le brunissement des adipocytes blancs. Le phénotype de brunissement est reproduit dans les souris soit en les traitant de manière chronique avec WWL70 (inhibiteur d'ABHD6) ou des oligonucléotides anti-sense ciblant l'ABHD6. Les tissus adipeux blanc et brun isolés de souris ABHD6-KO montrent des niveaux très élevés de 1-MAG, mais pas de 2-MAG. L'augmentation des niveaux de MAG soit par administration exogène *in vitro* de 1-MAG ou par inhibition ou délétion génétique d'ABHD6 provoque le brunissement des adipocytes blancs. Une autre évidence indique que les 1-MAGs sont capables de transactiver PPARα et PPARγ et que l'effet de brunissement induit par WWL70 ou le MAG exogène est aboli par les antagonistes de PPARα et PPARγ. L'administration *in vivo* de l'antagoniste de PPARα GW6471 à des souris ABHD6-KO inverse partiellement les effets causés par l'inactivation du gène ABHD6 sur le gain de poids corporel, et abolit l'augmentation de la thermogenèse, le brunissement du tissu adipeux blanc et l'oxydation des acides gras dans le tissu adipeux brun. L'ensemble de ces observations indique que ABHD6 régule non seulement l'homéostasie de l'insuline et du glucose, mais aussi l'homéostasie énergétique et la fonction des tissus adipeux.

Ainsi, 1-MAG agit non seulement comme un facteur de couplage métabolique pour réguler la sécrétion d'insuline en activant Munc13-1 dans les cellules bêta, mais régule aussi le brunissement des adipocytes blancs et améliore la fonction de la graisse brune par l'activation

de PPARα et PPARγ. Ces résultats indiquent que ABHD6 est une cible prometteuse pour le développement de thérapies contre l'obésité, le diabète de type 2 et le syndrome métabolique.

Mots-clés: Métabolisme énergétique, obésité, diabète de type 2, cycle glycérolipides/acides gras, AB-hydrolase domain 6, monoacylglycérol, cellule pancréatique beta, sécrétion d'insuline, résistance à l'insuline, brunissement des adipocytes, tissu adipeux brun

Abstract

The glycerolipid/ free fatty acid (GL/FFA) cycle is a key metabolic pathway that links glucose and fatty acid metabolism and it consists of lipogenesis and lipolysis. GL/FFA cycling, especially in its lipolysis arm, generates various lipid signaling molecules to regulate insulin secretion in pancreatic ß-cells and non-shivering thermogenesis in adipocytes. Currently, the lipolysis-derived lipid signals involved in this process are uncertain.

Triglyceride hydrolysis in mammalian cells is accomplished by the sequential actions of adipose triglyceride lipase to produce diacylglycerol, by hormone sensitive lipase to produce monoacylglycerol (MAG) and by MAG lipase (MAGL) that releases free fatty acid and glycerol. Our work shows that in pancreatic ß-cell, the classical MAGL is poorly expressed and that MAG hydrolysis is mainly conducted by the newly identified α/β-Hydrolase Domain-6 (ABHD6). Inhibition of ABHD6 by its specific inhibitor WWL70, leads to long-chain saturated 1-MAG accumulation inside the cells, accompanied by enhanced glucose-stimulated insulin secretion (GSIS). Decreasing the MAG levels by overexpression of ABHD6 in the ß-cell line INS832/13 reduces GSIS, while increasing MAG levels by ABHD6 knockdown enhances GSIS. Acute exposure of INS832/13 cells to various MAG species dose-dependently stimulates insulin secretion and restores GSIS suppressed by the pan-lipase inhibitor orlistat. Also, various biochemical and pharmacological experiments show that saturated 1-MAG levels species rather than unsaturated or 2-MAG species best correlate with insulin secretion. Furthermore, whole-body and β-cell-specific ABHD6-KO mice exhibit enhanced GSIS *in vivo*, and their isolated islets show elevated MAG production and GSIS. Inhibition of ABHD6 in low dose streptozotocin diabetic mice restores GSIS and improves glucose tolerance. Results further show that ABHD6-accessible MAGs not only enhance GSIS, but also potentiate fatty acid and non-fuel-induced insulin secretion without alteration in glucose oxidation and utilization as well as fatty acid oxidation. We have identified that MAG binds and activates the vesicle priming protein Munc13-1, thereby inducing insulin exocytosis. Based on all these observations, we propose that lipolysis-derived saturated 1-MAG acts as a metabolic coupling factor to regulate insulin secretion and ABHD6 is a negative modulator of insulin secretion.

Besides its role in ß-cells, ABHD6 is also highly expressed in adipocytes and its level is increased with obesity. Mice globally lacking ABHD6 on high fat diet (HFD) show modestly

reduced food intake, decreased body weight gain, insulinemia and fasting glycemia and improved glucose tolerance and insulin sensitivity and enhanced locomotor activity. In addition, ABHD6-KO mice display increased energy expenditure and cold-induced thermogenesis. In accordance with this, these mice show elevated UCP1 level in white and brown adipocytes, indicating browning of white adipocytes. The browning phenotype is reproduced in the mice either chronically treated with the ABHD6 inhibitor WWL70 or an antisense oligonucleotides targeting ABHD6. White and brown adipose tissues isolated from whole body ABHD6 KO mice show greatly elevated levels of 1-MAG, but not 2-MAG. Increasing MAG levels by either exogenous administration of 1-MAG or ABHD6 inhibition or genetic deletion induces browning of white adipocytes in a cell-autonomous manner. Further evidence indicates that 1-MAGs can transactivate PPARα and PPARγ and the browning effect induced by WWL70 or exogenous MAG is abolished by PPARα and PPARγ antagonists. *In vivo* administration of the PPARα antagonist GW6471 to ABHD6 KO mice partially reversed the ABHD6-KO effects on body weight gain, and abolishes the enhanced thermogenesis, white adipose browning and fatty acid oxidation in brown adipose tissue. All these observations indicate that ABHD6 regulates not only insulin and glucose homeostasis but also energy homeostasis and adipose tissue function.

Thus, ABHD6-accessible 1-MAG not only acts as a metabolic coupling factor to regulate fuel and non-fuel induced insulin secretion by activating Munc13-1 in beta cells, but also regulates glucose, insulin and energy homeostasis. The latter effects are mediated at least in part via browning of white adipocytes and enhanced brown fat function through the activation of PPARα and PPARγ. Collectively these findings suggest that ABHD6 is a promising target for developing therapeutics against obesity, type 2 diabetes and metabolic syndrome.

Keywords: Energy metabolism, obesity, type 2 diabetes, glycerolipid/fatty acid cycling, AB-hydrolase domain 6, monoacylglycerol, pancreatic ß-cell, insulin secretion, adipose browning, brown adipose tissue,

Table des matières

Liste des figures

Liste des abréviations

2-AG: 2-arachidonoylglycerol

18FDG: 18F-fluorodeoxyglucose

ABHD6: α/β-Hydrolase Domain-6

Ach: Acetylcholine

AMPK: 5' AMP-activated protein kinase

ATF6: activating transcription factor 6

ATGL: adipocytes triglyceride lipase

BAIBA: β-aminoisobutyric acid

BMI: body mass index

BMP: bone morphogenetic proteins

CHOP: C/EBP homologous protein

COX2: cyclooxygenase-2

CPT1: carnitine palmitoyltransferase-1

CNS: central nervous system

CREB: cAMP response element-binding protein

DAGL: diacylglycerol lipase

DGAT: diacylglycerol acyltransferase

DHA: docosahexaenoic acid

DIO2: type II iodothyronine deiodinase

EPA: eicosapentaenoic acid

ER: endoplasmic reticulum

ERK: extracellular signal–related kinase

ETC: electron transport chain

FFA: free fatty acid

FGF21: fibroblast growth factor 21

FNDC5: fibronectin type III domain containing 5

G0S2: G0/G1 switch gene 2

GDM: gestational diabetes mellitus

GIP: glucose-dependent insulinotropic peptide

GL/FFA cycling: glycerolipid/ free fatty acid cycling

GLP1: glucagon-like peptide-1

GLUT: glucose transporter

GPAT: glycerolphosphate acyltransferase

HFD: high fat diet

HIF-1α: hypoxia inducible factor 1alpha

HSL: hormone sensitive lipase

IL-1β: interleukin-1β

InsP3: 1, 4, 5- inositiol trisphosphate

IRE1: inositol requiring protein1

JNK1: JUN N-terminal kinase 1

LCCoA: long-chain acyl-CoA

LPA: lysophosphatidic acid

LPAAT: lysophophatidic acid acyltransferase

MAG: monoacylglycerol

MAGL: monoacylglycerol lipase

MCD: malonyl-CoA decarboxylase

MCF: metabolic coupling factor

MDP: the morphologically docked pool

MODY: maturity onset diabetes of youth

Myf5: myogenic factor 5

NAFLD: nonalcoholic fatty liver disease

NP: natriuretic peptides

PA: phosphatidic acid

PAP: phosphatidic acid phosphatase

PDX1: pancreas-duodenum homeobox-1

PERK: PKR-like kinase

PGC1α: peroxisome proliferator-activated receptor gamma coactivator 1α

PIP3: phosphatidylinositol 3, 4, 5- triphosphate

PKA: protein kinase A

PKG: GMP-dependent protein kinase

PL: phospholipids

PPAR: Peroxisome proliferator-activated receptor

POMC: proopiomelanocortin

PRDM16: PRD1-BF-1-RIZ1 homologous domain-containing protein-16

RAR: retinoid acid receptor

ROS: reactive oxygen species

RRP: readily released pool of granules

RXR: retinoid X receptor

SNAP: synaptosomal-associated protein 25

SNARE: soluble *N*-ethylmaleimide-sensitive factor (NSF) attachment protein receptor

SSRS5: somatostatin receptor subtype 5

STAT: signal transducer and activator of transcription

STZ: streptozotocin

TBX1: T-box transcription factor-1

Tmem26: transmembrane protein 26

TG: triacylglycerol

TG/FFA cycling: triacylglycerol/ free fatty acid cycling

T1D : type 1 diabetes

T2D: type 2 diabetes

UCP: uncoupling proteins

VEGF: vascular endothelial growth factor

ZDF: Zucker Diabetic Fatty

It is not because things are difficult that we do not dare; it is because we do not dare that they are difficult. ~ Seneca

Remerciements

Many thanks to my supervisor- Dr. Marc Prentki, who gave me the chance to join his lab and it completely changed my life. Without Marc, all the achievements do not exist. Marc is such a nice boss that he always puts the student's need as his priority. And he always made some time to talk to me about my strong points and my weak points to give reasonable advice to improve myself. In the last few years, I learned a lot from him.

Many thanks to my co-supervisor Dr. Murthy Madiraju, who always treats me as his son. He helped a lot not only in science, but also in my personal life. He helped me with everything in such a detail and through discussions with him, I could get lots of good advice to solve the problems. When issues raised among people inside or outside the lab, he always tried his best to help me search for the best solutions, and gave me valuable advice on how to prevent such issues again.

Many thanks to Dr. Erik Joly and Dr. Marie-line Peyot. Through discussion during PLDD, lab meeting and MDRC seminars, new clues are given to help solve the experimental problems and to accelerate experimental process and also they both helped me in improving my oral presentations.

Many thanks to Mr. Yves Mugabo and Dr. José Iglesias. As close friends, they did everything they could to help me. Their encouragement helped me a lot for trouble-shooting the experiments and the issues with people.

Many thanks Dr. Annie, Mr. Marco and Dr. Julien, who gave me the training when I entered the lab. Special thanks to Annie, a really good and strict teacher, and made me learn a lot to start my experiments.

For sure, I do not forget the people in MDRC/CRCHUM. There is a long list of people in my mind and I am very grateful for all what they all brought to me.

At last, many thanks to my wife- Xiaomeng and my babies- Chloé, Chris and Christina, and my parents for their help in encouraging and supporting in my research and daily life. With babies, the first year is always difficult, but we always get more happiness than we expected.

1. Introduction

1.1 Energy metabolism, obesity and type 2 diabetes

The survival of all species depends on energy homeostasis, a precise balance between energy intake and expenditure (Woods et al., 1998). Through evolution, human and animals have developed multiple and complex mechanisms to regulate energy homeostasis to regulate body weight (Ebbeling et al., 2012). In order to maintain normal body weight, energy intake needs to be equal to energy expenditure. Besides this, macronutrient oxidation also has to be balanced with macronutrient intake (Imbeault et al., 1997). Several decades ago, most people in the developed world needed to work hard physically to obtain sufficient food for consumption, and at that time, energy intake and energy expenditure were more well-balanced. However, in our modern society with rapidly developing technology, economic development and industrialization, there is a wide choice of highly caloric food at relatively low cost. Also more and more people prefer to choose meals rich in saturated fatty acids and starch but low in fiber, together with sugar-sweetened beverages (Mela, 2001). In conjunction with more sedentary lifestyle, energy from food intake has often considerably surpassed the daily energy expenditure. The surplus energy is predominantly stored in the form of triacylglycerol (TG) in the subcutaneous and visceral fat depots and other tissues, such as liver, and muscle thereby contributing to obesity among these people and this is particularly marked for individuals with low basal metabolic rate and physical activity (Alappat and Awad, 2010).

As a result of imbalance between energy intake and energy expenditure, the incidence of obesity has increased greatly over the last decades and has become a major socio-economic burden all over the world, especially in developed countries. According to the American Diabetes Association, nearly one third of the total US (Halter et al., 2014) population is affected by obesity and a similar situation is observed in Canada. A report from the National Diabetes Surveillance System indicated that approximately 25% of all Canadian adults are obese as are 10% of the children (Anis et al., 2010).

Obesity-associated systemic insulin resistance is generally thought to be a primary cause for many disorders, such as cardiovascular diseases, hypertension, and type 2 diabetes (T2D)

(Guo, 2014). The parallel rapid increase of individuals with obesity and T2D all over the world is striking and the term 'diabesity' has been created to emphasize the potential link between these two conditions (Astrup and Finer, 2000). Besides obesity-associated insulin resistance, insufficient insulin secretion resulting from beta cell dysfunction is another major cause of T2D and type 1 diabetes (T1D) (Eizirik and Darville, 2001; Kahn, 2003). According to the World Health Organization and the International Diabetes Federation, the number of diabetic patients has climbed from 100–135 million in 1994–1995 up to approximately 382 million in 2013, and this number is expected to rise to 592 million by 2035 (Guariguata et al., 2014). In Canada, approximately 1.9 million men and women have been diagnosed with diabetes in 2005-2006, which represents about 1 in 17 Canadians - 5.5% of all women and 6.2% of all men. According to recent statistics in 2013, more than 9 million Canadians live with undiagnosed or diagnosed diabetes or pre-diabetes (Baillot et al., 2014).

1.1.1 Glucose and lipid metabolism in obesity and type 2 diabetes

Impaired metabolism of glucose and lipid is observed in humans with obesity and T2D (Fujioka et al., 1987). Glucose metabolism in mammalian cells requires specific transporter to transport glucose inside the cells. The translocation of the glucose transporter 4 (GLUT4) from cytoplasm to plasma membrane is regulated by the insulin signaling pathway. However, insulin resistance in subjects with obesity or T2D curtails the translocation of GLUT4 to the plasma membrane and thus glucose metabolism inside the cells, in particular in skeletal muscle, is impaired, leading to hyperglycemia, a hallmark of T2D (Mackenzie and Elliott, 2014). The main pathway for glucose utilization is its oxidation through glycolysis and Krebs cycle to produce energy. In the case of obesity or T2D, nutrient oversupply leads to excess ROS production in the mitochondria or increases ER work load, and eventually causes oxidative and ER stress, which in turn have detrimental effects on cellular function. Also, if the TCA cycle is saturated with intermediates, some of the glucose carbons enter other metabolic pathways, which will generate metabolites that become toxic when in excess, such as lysophospatidate (LPA), 1,2 diacylglycerol (DAG) and ceramides, which further affect cell function (Nolan and Prentki, 2008; Poitout and Robertson, 2002).

Lipid metabolism is also altered in subjects with obesity and T2D. Many cells predominately use glucose rather than lipids as energy source when they coexist in abundance (Hue and

Taegtmeyer, 2009). In subjects with obesity and T2D, glucose supply is always present, and fatty acid oxidation is under strong inhibition, and thus most of the lipid precursors enter esterification pathway producing triglycerides (TG) and additional complex lipids, for storage in the adipocytes, which further contributes to obesity (Zechner et al., 2012). Once the limitation for fat storage in the adipocytes is reached, the newly synthesized fat is ectopically accumulated in muscle tissues and liver, and further contributes to insulin resistance and increased circulating glucose levels (Shulman, 2014).

1.1.2 Glycerolipid/ free fatty acid (GL/FFA) cycling

GL/FFA cycling, previously named as triacylglycerol/ free fatty acid cycling (TG/FFA cycling), was first described in 1965. With the rapidly increasing knowledge of the mechanisms of obesity and diabetes and the implication of altered lipogenesis and lipolysis in these diseases, it is gradually becoming evident that this cycling is located at the center of metabolic networks, tightly linking glucose and FFA metabolism, with important roles in regulating many signaling molecules controlling numerous biological processes (Prentki and Madiraju, 2008, 2012).

1.1.2.1 Enzymology and metabolites

GL/FFA cycling is active under both fed and fasting states and occurs in almost every cell, tissue, organ and organism. The biological process of this cycle involves the esterification of FFA onto a glycerol backbone to synthesize glycerolipids followed by their hydrolysis with the release of the FFA that can be re-esterified to reenter the cycle (Prentki and Madiraju, 2008). Lipogenesis and lipolysis, two essential parts of GL/FFA cycling, were generally regarded as two separate independent processes. In the Prentki`s laboratory, we found that these two processes are closely linked to each other: thus some TG, once synthesized during lipogenesis, goes through lipolysis to generate glycerol and FFA.

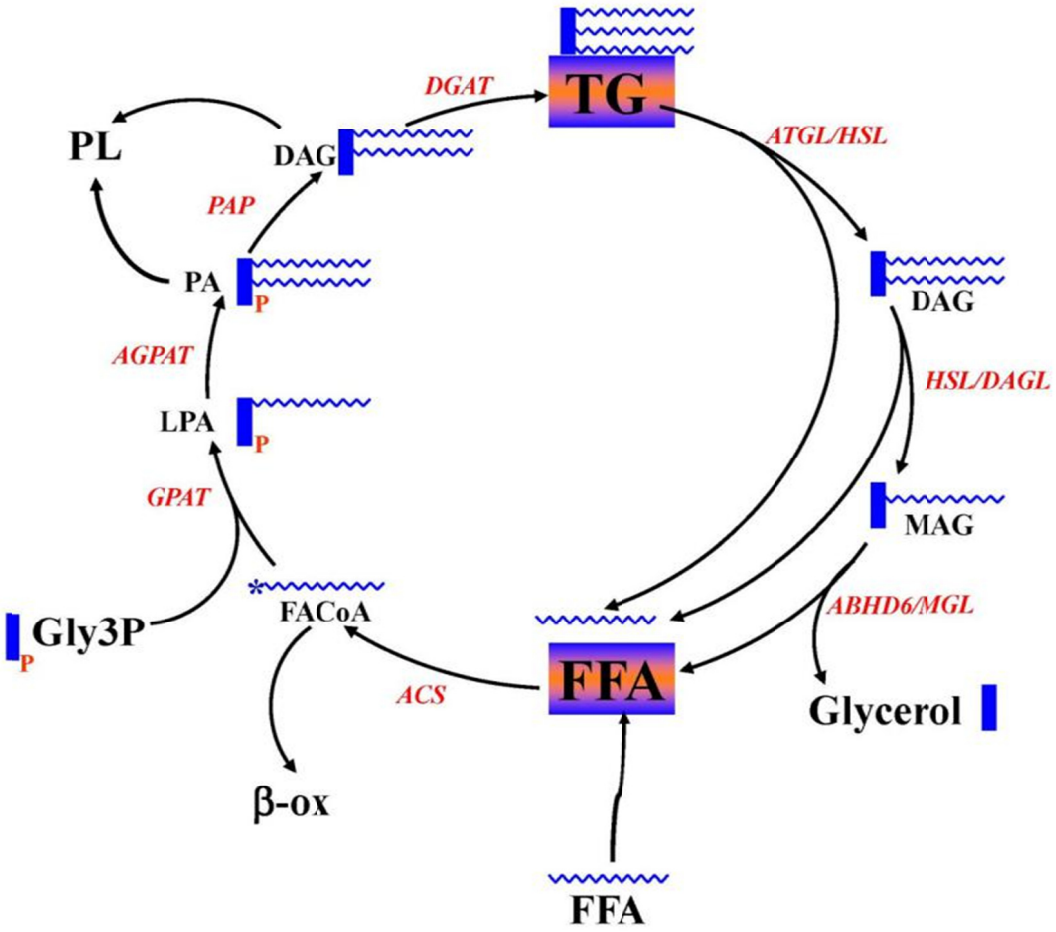

Figure 1 Enzymes and intermediates of GL/FFA cycling. The detailed description of this cycling can be found in the chapter. The figure is modified from *Endocr Rev. 2008 Oct; 29(6):647-76.*

The initial step in lipogenesis is to synthesize lysophosphatidic acid (LPA) catalyzed by the enzyme glycerolphosphate acyltransferace (GPAT) using substrates glycerol-3-phosphate and fatty acid-CoA (Figure 1) (Takeuchi and Reue, 2009). Glycerol-3-phosphate is derived via glycolysis of glucose or gluconeogenesis in the liver (Pages et al., 2001). Fatty acid-CoA is generated from *de novo* fatty acid synthesis or exogenous fatty acids from food digestion or from the lipolysis process. LPA is further esterified to phosphatidic acid (PA), catalyzed by 1-acyl-sn-glycerol-3-phosphate acyltransferase. The formation of diacylglycerol is from PA, and this process is catalyzed by PA phosphatase (PAP). Finally, triglyceride (TG) synthesis is completed with the enzyme diacylglycerol acyltransferase (DGAT) (Takeuchi and Reue, 2009). LPA, PA and diacylglycerol (DAG) generated from lipogenesis process can also be

incorporated into phospholipids (PL) (Vance and Tasseva, 2013). Following lipogenesis, the synthesized metabolites, such as TG, DAG and phospholipids (PL), could go through lipolysis process. The full lipolysis process involves the complete breakdown of TG into glycerol and FFA (Prentki et al., 2013b; Zechner et al., 2012). In this process, TG is first degraded to DAG by the enzyme adipocytes triacylglycerol lipase (ATGL) (Smirnova et al., 2006), and then DAG is hydrolyzed to monoacylglycerol (MAG), catalyzed by hormone sensitive lipase (HSL) (Vaughan et al., 1964) and DAG lipase (DAGL) (Bisogno et al., 2003), and finally MAG is hydrolyzed to glycerol and FFA using the enzyme monoacylglycerol lipase (MAGL) (Fredrikson et al., 1986) and α/β-Hydrolase Domain-6 (ABHD6) (Blankman et al., 2007a; Zhao et al., 2014).

It is now well-accepted that the GL/FFA cycle is under stringent control via separate enzymes for forward and backward reactions. The rate-limiting step in this cycle lies in the initial step using glycerol-3-phosphate and fatty acid-CoA to produce LPA (Pages et al., 2001). So the enzyme glycerol-3-phosphate acyltransferase (GPAT) involved in this step is of special importance. Currently, four isoforms of GPAT have been cloned and identified, viz., GPAT1 to GPAT4. GPAT1 and GPAT2 are mainly localized in the mitochondria, while GPAT3 and 4 are in the endoplasmic reticulum **(**ER) (Wendel et al., 2009). Mitochondrial GPAT1 has been characterized more thoroughly than the other isoforms and shown to represent more than 50% of total enzymatic activity (Wendel et al., 2013). GPAT1 deficient mice display markedly lower hepatic TG and DAG concentration, and are protected from hepatic steatosis (Xu et al., 2006) and hepatic insulin resistance possibly because of a lower DAG-mediated PKC activation (Neschen et al., 2005). Further study using metabolomics analysis shows that several metabolites, including palmitate, 1-mono-16:0-acyl-glycerol, 1,2-di-16:0-acyl-glycerol are decreased, and other metabolites involved in carbohydrate metabolism are increased in the GPAT1 KO mice (Li et al., 2010), which may provide important clues to explain high insulin sensitivity in these mice. Besides GPAT1, mice deficient in GPAT4 have also been generated (Nagle et al., 2008), and these mice show 49% lower total GPAT activity and exhibit a 25% reduction in body weight and resistance to both diet-induced and genetically induced obesity with increased thermogenesis (Vergnes et al., 2006).

The second enzyme involved in this cycle is 1-acyl-sn-glycerol-3-phosphate acyltransferase (AGPAT), also named as lysophophatidic acid acyltransferase (LPAAT), catalyzing the reaction from LPA to PA. Several isoforms of LPAAT have been identified, and only AGPAT1 and AGPAT2 show high activity (Agarwal et al., 2011). Mice deficient in AGPAT2 develop severe lipodystrophy affecting both white and brown adipose tissues, displaying extreme insulin resistance, diabetes, and hepatic steatosis associated with high expression of lipogenic genes and high rates of *de novo* fatty acid biosynthesis (Cortes et al., 2009).

PA phosphatase (PAP) is responsible for converting PA to DAG. In mammals, two types of PAP (PAP1 and PAP2) have been recognized (Takeuchi and Reue, 2009). PAP-1 is found mainly in the ER and believed to be involved in the synthesis of TG and PL. PAP-2 is located near the plasma membrane and may be producing DAG from PA released from membrane. The next important enzyme involved in acylating DAG to TG is diacylglycerol acyltransferase (DGAT), with important roles in regulating energy storage and metabolism (Smith et al., 2000). Two types of DGAT (DGAT1 and DGAT2) exist in the mammals. DGAT1 has been reported to be highly expressed in skeletal muscle, intestine as well as other tissues, whereas DGAT2 is mostly expressed in the adipocytes and liver. Overexpression of DGAT1 in rat islets has been shown to increase palmitate incorporation into TG resulting in a modest accumulation in TG content and decreased glucose-stimulated insulin secretion, which may be due to "glucolipotoxicity" (Poitout and Robertson, 2002). DGAT-1 knockout mice were shown to have increased insulin sensitivity and enhanced glucose tolerance, and protected from diet induced obesity (Harris et al., 2011); DGAT2 also plays a fundamental role in mammalian triglyceride synthesis and is required for survival based on the fact that DGAT2-deficient mice are lipopenic and die soon after birth, apparently from profound reductions in substrates for energy metabolism and from impaired permeability barrier function in the skin (Yen et al., 2008). Also in both KO mice, DGAT1 was unable to compensate for the absence of DGAT2, supporting the hypothesis that the two enzymes play fundamentally distinct roles in mammalian triglyceride metabolism.

The process of lipolysis is also highly dependent on several enzymes, depending on different reactions. TG hydrolysis is conducted by adipose TG lipase (ATGL), (previously named desnutrin and patatin-like domain containing phospholipase A2, PNPLA2) (Smirnova et al.,

2006), which is the rate-limiting step of lipolysis. It is now known that ATGL when stimulated by CGI58, hydrolyses TG at sn-1 position (Mayer et al., 2015), releasing 2,3-DAG, which is not known as a signaling molecule as 1,2-DAG. On the other hand, ATGL when not associated with CGI58, prefers to hydrolyze TG at the sn-2 position, producing 1,3-DAG (Eichmann et al., 2012).

The product of TG hydrolysis is either 2,3 DAG or 1,3 DAG, and both of these are hydrolyzed by hormone sensitive lipase (HSL) to generate either 2- or 1-MAG. However, the membrane-bound sn-1 DAG lipase hydrolyzes 1,2-DAG that primarily arises from phospholipase C action on the membrane phospholipids. HSL displays a broad specificity for its substrates *in vitro*, including TG, DAG, MAG and cholesterol esters (CE). However, under *in vivo* conditions and inside the cells HSL preferentially hydrolyzes DAG to MAG, than TG to DAG and far better than MAG to glycerol (Fredrikson et al., 1981). The activity of HSL is markedly activated by protein kinase A and cAMP raising agents. sn-1 DAG lipases show high activity in brain and pancreatic beta cells compared to other tissues. This enzyme shows remarkable specificity to sn1,2-DAG containing arachidonic acid (AA) at position 2 and releases 2-arachidonoylglycerol (2-AG), an endocannabinoid, which is an important signaling molecule for activating CB-1 and CB-2 receptors (Hoover et al., 2008).

Hydrolysis of MAG is mainly conducted by the classical MAGL in many tissues. Besides the classical MAGL, other enzymes that can hydrolyze MAG have been identified recently and these include α/β- Hydrolase domain 6 (ABHD6) and ABHD12. MAGL is highly expressed in adipose tissue, liver and brain and responsible for most of the MAG hydrolysis activity in these tissues. MAGL is mainly a cytosolic enzyme. ABHD6 and ABHD12 are shown to hydrolyze MAG in brain, and both of the enzymes account for 15% of total MAG hydrolysis activity. ABHD6 and ABHD12 are located in the plasma membrane, with the catalytic site of ABHD6 facing the cytosolic side of the membrane, and the catalytic site of ABHD12 facing the exterior of the cell. (Blankman et al., 2007a). ABHD6 is shown to be widely expressed in many tissues, including pancreatic islets, liver, adipose tissue and brain, while the tissue distribution of ABHD12 is not very clear. Besides their MAG hydrolyzing activity, ABHD6 and ABHD12 are also shown to hydrolyze other substrates with lower efficiency. Recently, ABHD6 is shown to hydrolyze lysophospholipids such as lysophosphatidylcholine (Thomas et

al., 2013) and also bis(monoacylglycero)phosphate (Pribasnig et al., 2015), even though the physiological relevance of these activities *in vivo* is not known. Similarly, ABHD12 is also shown to be the major brain lysophosphatidylserine (lyso-PS) lipase. Genetic deficiency of ABHD12 in humans leads to a neurodegenerative disease called polyneuropathy, hearing loss, ataxia, retinitis pigmentosa and cataract (PHARC) (Blankman et al., 2013).

1.1.2.2 Role in cellular signaling and fuel detoxification

As indicated above, GL/FFA cycling consists of multiple steps, catalyzed by separate enzymes in its lipogenic and lipolytic arms. Such a complex enzyme system offers several "regulating points" to better and more conveniently control this cycling, in order to meet the diverse needs of signaling metabolite supply for biological functions. Disturbance of this cycle leads to a wide range of pathophysiological conditions, including obesity, T2D, hypertension, cardiovascular disease and cancer (Prentki and Madiraju, 2008, 2012).

The GL/FFA cycle is able to generate signaling molecules regulating numerous biological functions. These roles could be grouped into three categories: established roles, emerging or likely roles and candidate roles (Figure 2). The established role refers to thermogenesis. In mammals, maintenance of body temperature is at least in part, if not largely dependent on lipolysis, an essential part of GL/FFA cycling. FFA released from lipolysis can activate mitochondrial uncoupling proteins (UCPs), which dissociate the respiration from ATP production to dissipate the respiratory energy as heat. Different rodent models, which show some defects in lipolysis, such as *ob/ob* mice, ATGL-KO mice and Zucker fatty rats, show intolerance to cold exposure, and the main reason for this may be due to their inability to increase lipolysis to generate sufficient heat to maintain normal body temperature (Triandafillou and Himms-Hagen, 1983).

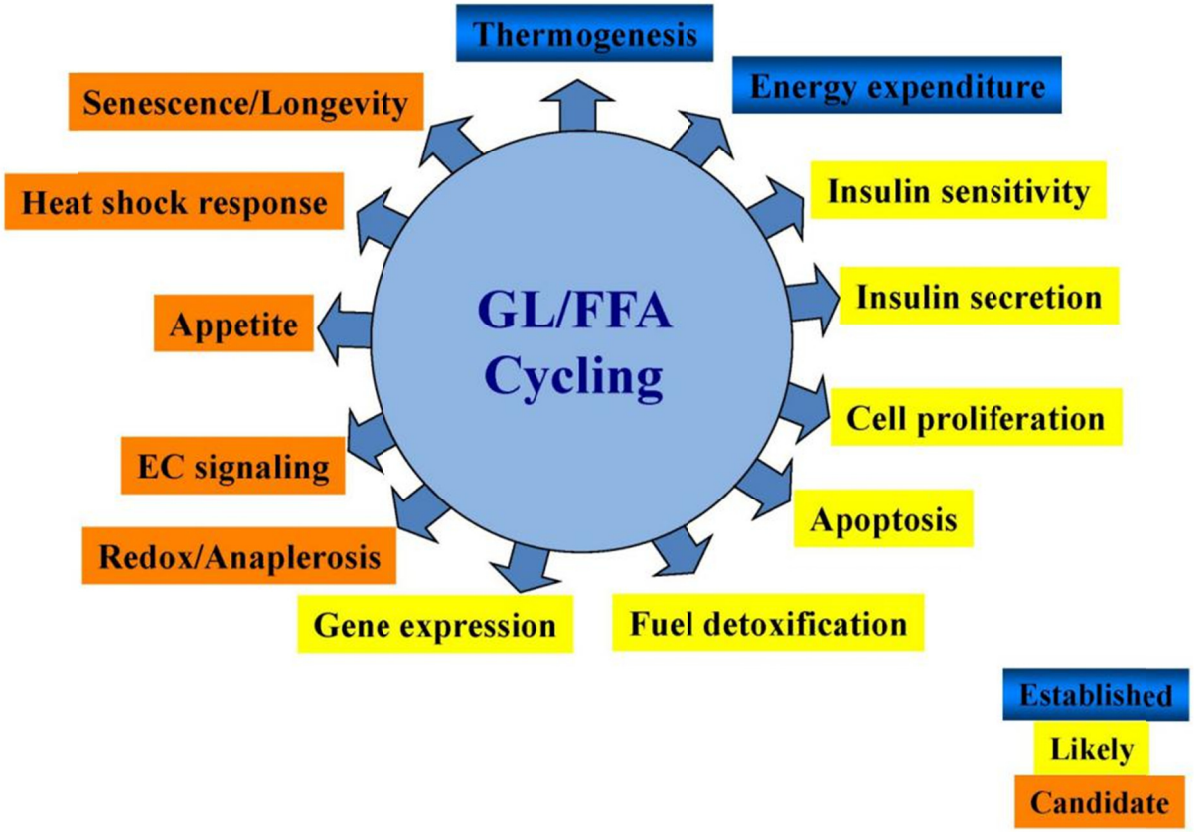

Figure 2: Biological processes regulated by GL/FFA cycling. GL/FFA cycling generates many lipid signals to regulate different biological processes. Some established roles are highlighted in blue. Some likely emerging roles are listed in yellow, and some candidate roles are indicated in red. The figure is adapted from *Endocr Rev. 2008 Oct;29(6):647-76*.

Among the emerging roles of GL/FFA cycling, recent research has suggested detoxification of fuel oversupply, regulation of cell survival and proliferation, as well as the regulation of gene expression and insulin secretion.

GL/FFA cycling allows for fuel detoxification (Nolan and Prentki, 2008) because in a "glucodetoxification" process it directs the glucose carbon to glycerol, which cannot be reincorporated in the cycle in most cell types, as they express very low levels of glycerol kinase. Also, in a "lipodetoxification" process, a large portion of glucose carbons is used for *de novo* synthesis of FFA, and these newly synthesized FFA and lipolysis-released FFA are either transported out of the cells or transported into mitochondria for beta oxidation. Further, as an energy-consuming and futile pathway (each turn of GL/FFA cycling consumes 7 ATP

molecules) this cycle releases energy in the form of heat. Thus, several steps in this cycling involve ATP usage, such as conversion of FFA into fatty acid-CoA and LPA and PA synthesis by acylglycerol kinase enzymes. The released heat is necessary to maintain normal body temperature.

Another emerging role of GL/FFA cycling is to regulate gene expression. Some intermediates generated in the cycling, such as DAG, could directly or indirectly activate hypoxia inducible factor 1alpha (HIF-1α), a transcription factor that regulates the expression of various glycolytic enzymes, vascular endothelial growth factor (VEGF) and cell survival. Recently, protein lysine acetylation has emerged as a key posttranslational modification in cell function regulation (Zhao et al., 2010), and some studies showed that lysine acetylation is a prevalent modification of enzymes that participate in intermediary metabolism according to cellular nutrition conditions. GL/FFA cycle is a highly active metabolic pathway, which continuously uses NADH and regenerates NAD, which is a substrate for the protein deacetylation enzymes, sirtuins, which regulate a wide range of cellular functions including gene expressions (Haigis and Guarente, 2006). Thus it is also possible that GL/FFA cycle controls gene expression by regulating redox state, sirtuin activity and protein lysine deacetylation. Also, because of the ability of GL/FFA cycle to activate sirtuins, which are well known for their involvement in promoting longevity, the possibility that GL/FFA cycle indirectly contributes to longevity exists (Park et al., 2013b).

GL/FFA cycle may also be implicated in the regulation of cell survival and proliferation through the distribution of metabolites into tissues and avoiding their toxic build up. High circulating levels of FFA in combination with elevated glucose levels (glucolipotoxicity) is toxic to non-adipose cells, such as beta cells, as these metabolites can disturb many cellular processes, in particular mitochondrial function and energy homeostasis (van Raalte and Diamant, 2011). Several reports have shown that TG accumulation in non-adipose cells could be regarded as a defensive mechanism against acute FFA toxicity (Cheon and Cho, 2014). TG build-up, together with highly active GL/FFA cycle could protect the cells as long as the cells retain the ability to hydrolyze TG to maintain normal amount of TG. The role of the GL/FFA cycle in the regulation of insulin secretion will be discussed in the next chapter in details.

1.1.2.3 Regulation of MAG levels in mammalian cells

The levels of MAG inside the cells are generally regulated by the synthesizing enzymes and degrading enzymes. MAG is mainly produced from lipolysis process through hydrolysis of DAG by HSL and DAGL. Overexpression of ATGL, the rate-limiting step in lipolysis was shown to increase the release of glycerol and FFA (Pulinilkunnil et al., 2013) and probably leads to elevated MAG in cells. Deletion of ATGL in mice leads to large amounts of TG accumulation, reduced glycerol and FFA release (Huijsman et al., 2009) and probably results in lowered MAG levels.

For MAG metabolizing enzymes, three different enzymes, including MAGL, ABHD6 and acyl CoA: monoacylglycerol acyltransferase (MGAT), have been identified. MAGL is considered as the main MAG hydrolyzing enzyme. MAGL is highly expressed in various tissues, including different fat depots, liver and brain (Taschler et al., 2011). Deletion of MAGL in mice leads to MAG accumulation in liver, adipose and brain, and protects mice from high fat diet (HFD)-induced insulin resistance as it reduces circulating FFA levels in the plasma. Even in the adipocytes isolated from MAGL KO mice, some MAG hydrolysis activity is still detectable, indicating that other enzyme(s) can hydrolyze MAG to a significant extent (Taschler et al., 2011). In 2007, another two enzymes ABHD6 and ABHD12 were identified using activity based protein profiling methods in brain tissue (Blankman et al., 2007a), and these two enzymes were shown to contribute to 15% of the total MAG lipase activity in the brain, while classical MAGL is responsible for the remaining 85%. Recent studies have shown that ABHD6 is highly expressed in several tumor cell lines, such as the breast cancer cell line MCF7, but the significance of this high expression is not clear (Li et al., 2009; Max et al., 2009). Another report demonstrated that inhibition of ABHD6 in brain produced the cannabinoid effect via accumulation of 2-AG, indicating the important roles of ABHD6 in regulating cell function (Marrs et al., 2010; Tchantchou and Zhang, 2013). However, the relative importance of ABHD6 in other tissues, including beta cells, adipose and liver, is not yet determined.

MGAT is another enzyme that uses MAG as substrate to synthesize DAG (Shi and Cheng, 2009). This enzyme is mainly expressed in the intestine and responsible for uptake of MAG released from nutrient digestion. Mice deficient in MGAT2 are protected from diet induced

obesity and metabolic disorders with increased thermogenesis. Consistent with this result, intestine-specific deletion of MGAT2 in mice reproduces the effect of global deletion (Nelson et al., 2014). Surprisingly, expression of MGAT1 in the liver is very low, however, deletion of this enzyme specifically in liver produces strong beneficial effects in glucose homeostasis (Hall et al., 2014). However, in all these KO mice models, MAG levels inside the cells were not measured and thus we cannot attribute the beneficial effects to MAG accumulation.

1.2 Pathogenesis of type 2 diabetes

1.2.1 The various forms of type 2 diabetes

In simple terms, T2D can be defined as the pathological situation where the amount of secreted insulin is insufficient to match the increasing needs of tissues with high degree of insulin resistance, resulting in hyperglycemia, the hallmark of diabetes (Prentki and Nolan, 2006). However, T2D is a complex metabolic disorder with a multitude of mechanisms for its causes, including both genetic (Morris et al., 2012; Sladek et al., 2007) and environmental factors (Figure 3). Depending on body mass index (BMI) of the subjects with freshly diagnosed T2D, T2D can be classified into two major groups: lean T2D and obese T2D (Perry et al., 2012). Lean T2D is usually found in elderly and in poor and developing countries. The onset of this lean T2D in some individuals is due to insufficient adipocyte development because of poor nutrition during childhood. The typical mouse model of lean T2D is low-dose streptozotocin-induced diabetes with normal fasting insulinemia, whereas in type 1 diabetes there are very low to non-detectable levels of insulin in the plasma. Obese T2D is the major form and represent most of the cases of T2D. The causes of obese T2D are complex, but we should put some emphasis on the environmental factors, as genetic modifications cannot occur in a short time frame and the genetic factors alone do not explain the pandemic of obese T2D.

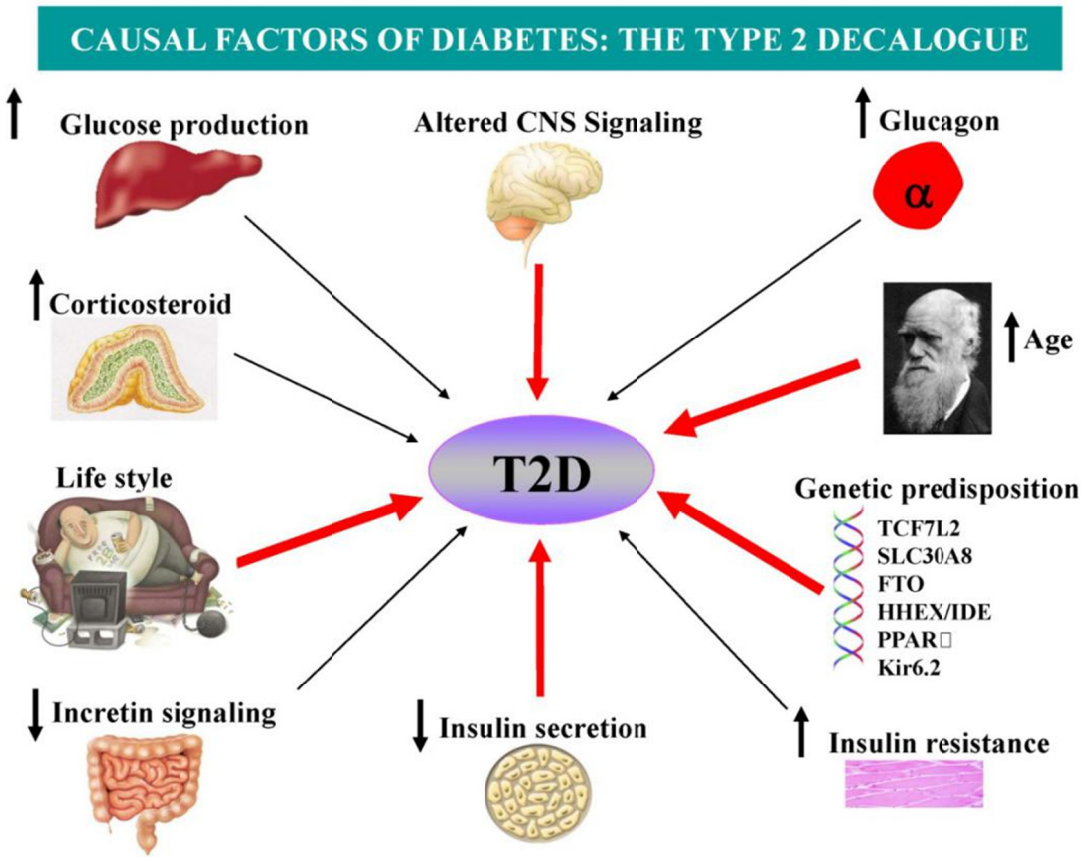

Figure 3. The possible causal factors of T2D. T2D is a complex disease involving both environmental factor and genetic variation. So far, many factors have been shown to implicate in this process. Red arrows highlight the factors that are currently thought to be most important.

T2D is generally regarded as a complex syndrome of polygenic nature. With the new high-density array technology that allows simultaneous genotyping of thousands of polymorphisms, many candidate loci, such as ACDC, CAPN10, ENPP1, HNF4A, SLC308A, IDE-KIF11, EXT2-ALX4 have been identified that significantly associate withT2D (Morris et al., 2012; Sladek et al., 2007). Some of the identified susceptible genes, such as zinc transporter SLC308A, are exclusively expressed in beta cells. Despite the numerous genes identified so far, their precise role in the pathogenesis of T2D is still unclear. Much effort is currently made to unravel the mechanisms implicated and this may eventually lead to novel targets for therapeutics.

T2D accounts for approximately 90 to 95 percent of all cases of diabetes and nearly 3 million Canadians suffered from T2D in 2010. Incidence of T2D is strongly associated with obesity, older age, family history of diabetes, previous history of gestational diabetes, physical inactivity and ethnicity (Stumvoll et al., 2005). There has been an alarming increase in childhood obesity associated with T2D (Lloyd et al., 2012). However, nationally representative data on prevalence of T2D in youth are not available.

The symptoms of T2D develop gradually with time. T2D is virtually considered as a chronic syndrome rather than an acute disease, such as anemia and hypothyroidism. Despite the lack of overt symptoms for T2D, unless the hyperglycemia is well controlled through pharmacological, nutritional or physical intervention, the function of several tissues and organs, such as kidney, nerves and eyes is gradually compromised (1998; Amos et al., 1997). Thus untreated or poorly-treated T2D can become a serious health and social problem as a result of secondary complications (Renard, 2009), greatly reducing the quality of life and even life span. With huge efforts made in elucidating the mechanisms of the onset and progression of T2D, some crucial factors, such as obesity-driven insulin resistance, adipose, liver and beta cell dysfunction, greatly contribute to the pathogenesis of T2D.

The global obesity epidemic significantly contributes to the rapid increase in T2D. Insulin resistance directly links obesity with T2D. However, obesity-induced insulin resistance is not the only cause for T2D and may even be protective for tissues such as the heart and skeletal muscle (Nolan et al., 2015). Hyperglycemia appears only when beta cells are unable to secrete sufficient insulin to compensate for the insulin resistance in peripheral tissues. Thus, obesity-induced insulin resistance and beta cell dysfunction are two major risk factors for the onset of T2D (Prentki and Nolan, 2006; Reaven, 1997). We will further discuss these two factors in more detail in the following chapters.

1.2.2 Obesity-induced insulin resistance

How does obesity cause insulin resistance? The question cannot be answered in a simple way. With huge efforts made in the past decades, major advance in our understanding of the relationship between obesity and insulin resistance has been greatly improved. Large number of metabolites and hormones, and inflammatory, neural and cell-intrinsic pathways are shown

to be affected by obesity. It is possible that some of these factors act either independently or synergistically to induce insulin resistance. Better understanding of the mechanism regarding obesity leading to insulin resistance may offer more efficient and powerful approaches to prevent or treat obesity-associated insulin resistance and its associated metabolic disorders.

1.2.2.1 Elevated free fatty acids in obesity and insulin resistance

FFA levels in the plasma of obese individuals are increased, and positively correlate to the degree of insulin resistance (Capurso and Capurso, 2012). Increased FFA is mainly generated from lipolysis in the adipocytes. In general, in the fasting state, insulin levels are decreased with elevated glucagon levels, and the increased glucagon will lead to the elevated activity of the lipase enzymes, in particular HSL, and lipolysis in the adipocytes. FFA generated in the lipolysis is taken up by other tissues, such as liver and muscle, where they go through fatty acid oxidation and provide energy. However, in obesity, the regulation of lipolysis enzymes in adipose tissues is disrupted, as insulin cannot suppress lipolysis, resulting in elevated lipolysis generated FFA in the plasma (Arner and Langin, 2014).

FFA may exert its effect on insulin signaling pathway mainly via intracellular metabolism in other tissues. Elevated FFA levels are associated with increased DAG, ceramide or acetyl-CoA. 1,2-DAG is a well-known second messenger, and through binding to C1-domain, it activates PKC, causing its translocation from cytoplasm to plasma membrane. Activated PKC phosphorylates insulin receptor and inhibits insulin signaling pathway (Yu et al., 2002). Deletion of PKCζ in liver protects the mice from obesity-induced insulin resistance, indicating DAG-PKC pathway contributes to FFA-induced insulin resistance in liver and muscle (Matsumoto et al., 2003; Perry et al., 2014; Samuel and Shulman, 2012). Besides DAG, ceramides also increase with prolonged FFA treatment, and their roles in insulin resistance are well-established (Holland et al., 2007). It has been shown that plasma ceramides are elevated in obese subjects with T2D and correlate with the severity of insulin resistance (Haus et al., 2009; Kanety et al., 1996). Inhibition of ceramide synthesis ameliorates glucocorticoid-, saturated fat- and obesity-induced insulin resistance via different mechanisms: first, ceramides possibly phosphorylate IRS-1 on inhibitory serine/ threonine residues through activation of extracellular signal-regulated kinase 2, JNK and P38 (Kanety et al., 1996); second, ceramides may directly block PI3K under unstimulated states; however, this observation is still under

debate (Hla and Kolesnick, 2014; Turpin et al., 2014); third, ceramides can directly inhibit Akt by activating protein phosphatase 2A or by activating PKCζ, which inhibits Akt translocation to the plasma membrane (Powell et al., 2004; Teruel et al., 2001).

1.2.2.2 Adipocytes secreted adipokines and insulin resistance

Adipose tissue participates in regulating energy homeostasis via secretion of adipokines, such as leptin and adiponectin (Rosen and Spiegelman, 2014). In response to excess energy intake, adipose tissue expansion, by the formation of new adipocytes or enlarging the existing adipocytes, is necessary to avoid the lipotoxic effects. With adipocyte remodeling, the adipokine secretion is also changed accordingly.

Among the adipokines, the functions of leptin and adiponectin are best understood (Meier and Gressner, 2004). Leptin is a hormone that directly regulates energy homeostasis by regulating energy intake and modulating energy expenditure, and its secretion is positively correlated to obesity (Moran and Phillip, 2003). The discovery of leptin was once regarded as a cure for obesity; however, leptin resistance in the brain makes it impossible to treat human obesity in the context of excess food intake (Caro et al., 1996). Adiponectin was identified in 1995 and 1996 by two different groups, and is specifically expressed in different adipose depots, such as visceral fat and brown fat (Matsuzawa, 2005). Further studies indicated that circulating adipinectin level is decreased with obesity, and restoring its levels curtails insulin resistance in different animal models (Yamauchi and Kadowaki, 2013). In line with this, mice deficient in adiponectin are glucose intolerant and show severe insulin resistance, associated with increased circulating FFA levels (Maeda et al., 2002). Various mechanisms are proposed to explain the beneficial effects of adiponectin in energy homeostasis. It has been demonstrated that adiponectin can increase FFA oxidation and reduce hepatic glucose output (Xu et al., 2003; Yamauchi et al., 2002), while in the muscle, it activates the energy sensor AMPK to increase glucose uptake and usage as well as fatty acid oxidation (Yoon et al., 2006).

1.2.2.3 Obesity-associated inflammation and insulin resistance

Chronic inflammation builds a crucial link between obesity and insulin resistance (Dandona et al., 2004). It is well accepted that the circulating inflammation markers, such as TNF alpha, IL-6 and C-reactive protein, are elevated in obese individuals, and these markers are predictive

of future development of T2D (Mugabo et al., 2010; Mugabo et al., 2011). Activation of inflammation pathway is directly associated with systemic insulin resistance in different tissues, such as liver (Gauthier et al., 2011). In white adipose tissue, obesity increased macrophage infiltration, which leads to local inflammation. Inhibition of macrophage infiltration in the adipose ameliorates obesity-induced insulin resistance (Apovian et al., 2008).

With respect to the mechanisms related to inflammation and insulin resistance, several signaling proteins, such as JUN N-terminal kinase 1(JNK1) (Hirosumi et al., 2002), IKKβ (Arkan et al., 2005), and SOCS proteins (Ueki et al., 2005; Ueki et al., 2004) have been implicated in this process. Many inflammation markers, such as TNFα activate JNK1 (Nguyen et al., 2005). In obese animal models, such as *ob/ob* mouse, or diet-induced obese mouse, JNK1 activity in different tissues positively correlates with inflammation markers and insulin resistance (Han et al., 2013). Suppression of JNK activity in liver improves obesity-induced insulin resistance and energy homeostasis, emphasizing the importance of this pathway in the liver (Seki et al., 2012). Further studies have shown that JNK-1 directly acts through insulin signaling pathway via serine phosphorylation of IRS-1 (Lee et al., 2003); IKKβ has been shown to be a mediator of TNFα-induced insulin resistance. Transgenic mice with constitutive expression of IKKβ in liver show activation of NFκB, and systemic insulin resistance. In line with this, inhibition of IKKβ by high dose of aspirin (Yuan et al., 2001) (Yin et al., 1998) improves insulin resistance in obese individuals with T2D. Furthermore, IKKβ directly phosphorylates IRS-1 on serine residues (Zhang et al., 2008). Besides JNK1 and IKKβ, SOCS proteins (SOCS1, SOSC3 and SOCS6) have also been shown to be implicated in inflammation-induced insulin resistance. SOCS3 protein levels are increased with obesity. Inhibition of SOCS3 protein activity increases insulin sensitivity, while overexpression of SOCS1 and SOCS3 in liver decreases insulin sensitivity. Furthermore, SOCS proteins work through insulin signaling pathway by phosphorylation of IRS-1 on serine residues.

1.2.2.4 Neural mechanisms links to obesity-induced insulin resistance

The central nervous system (CNS) receives various signals from peripheral tissues, such as insulin from beta cells and leptin from adipocytes, and signals from local nutrient metabolism, such as oleate and ketone bodies, and integrates all this information, and sends signals to

control food intake and metabolism in peripheral tissues to balance energy intake, storage and expenditure.

The central role of leptin and insulin in the regulation of energy metabolism in peripheral tissues is well-accepted (Balthasar et al., 2004; Plum et al., 2006). Lipodystrophic and leptin-deficient mice show high degree of insulin resistance, and this can be reversed by central administration of leptin. Also, deletion of insulin receptors in the hypothalamus leads to insulin resistance and elevated glucose output in liver and impaired energy homeostasis. Multiple evidences show that the central effect of insulin and leptin depends on signal transducer and activator of transcription (STAT) 3 (Bates et al., 2003). It has been shown that STAT3 accounts for essential effects of leptin in energy homeostasis and deletion of STAT3 in mice mirrors the mice with deletion of leptin receptors (Takeda et al., 1997).

In addition to leptin and insulin, local brain FFA and its metabolism have also proven to be implicated in regulation of energy homeostasis. With obesity, increased circulating levels of FFA in the brain lead to hepatic insulin resistance, which is recaptured by central infusion of high amounts of oleate (Obici et al., 2002). Also, central administration of a carnitine palmitoyltransferase-1 (CPT-1) inhibitor, which reduces fatty acid oxidation, ameliorates liver insulin resistance (Kim et al., 2004). The beneficial effects of CPT1 inhibitor are partially mediated by activation of vagal efferent fibers connecting between the brain and liver.

Disturbed circadian rhythm is one of the risk factors in insulin resistance and T2D (Perciaccante et al., 2006). It is well-documented that the CLOCK transcription factor is one of the essential components of the circadian clock within hypothalamic neurons. Deletion of Clock in mice leads to a disturbed feeding behavior, and increased susceptibility to diet-induced obesity with hyperleptinemia, hyperlipidemia, hepatic steatosis, hyperglycemia, and hypoinsulinemia, indicating that circadian rhythm works via central mechanism to regulate energy homeostasis (Rudic et al., 2004).

1.2.3 Beta cell dysfunction and its underlying mechanisms

The main role of the beta cell is to secrete insulin in response to different signals in order to maintain glycemia in a narrow range. In the context of insulin resistance, beta cells need to secrete higher amounts of insulin to compensate increased needs of tissues. Hyperglycemia

arises only when beta cells fail to compensate. From this perspective, diabetes could be regarded as a beta cell disease (Figure 4) (Prentki et al., 2013b). Regarding the cause of beta cell dysfunction, several mechanisms have been proposed, and better understanding of these different mechanisms may help us find better promising approaches to prevent beta cell dysfunction.

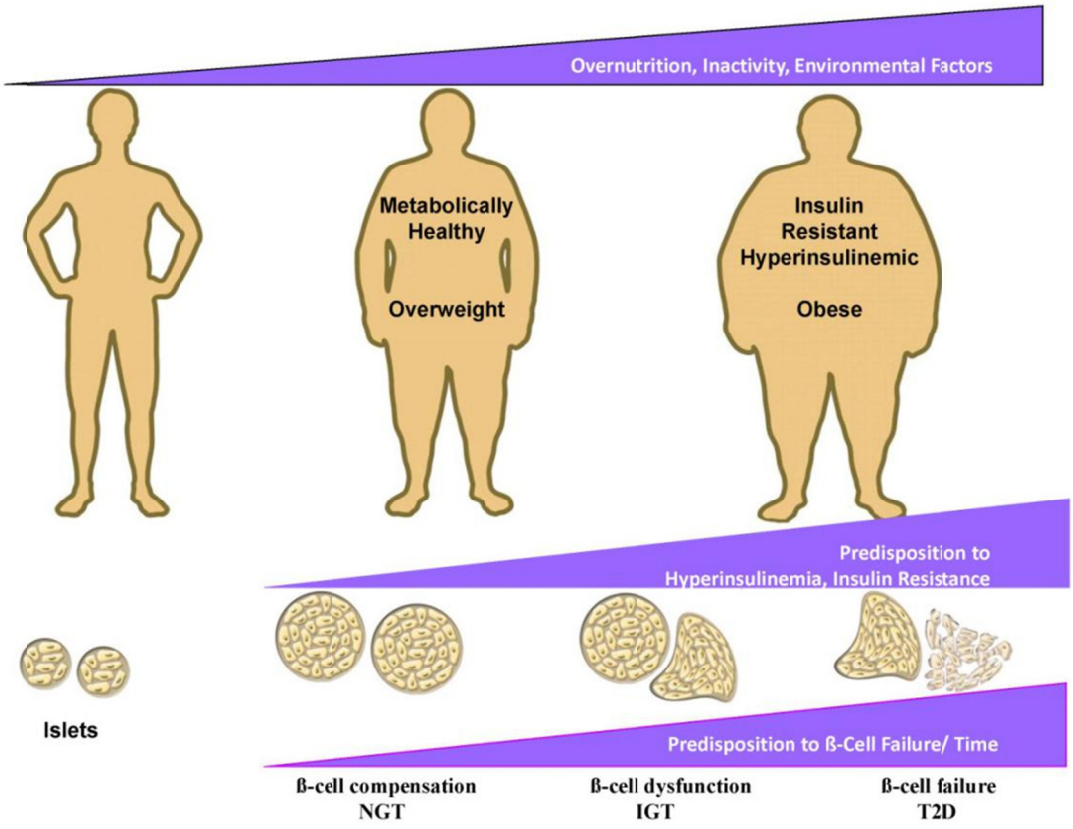

Figure 4 Islet beta cell failure and natural history of T2D. Over-nutrition, inactivity and various environmental factors contribute to obesity, which is associated with insulin resistance. Increased insulin resistance in peripheral tissues forces the beta cells to proliferate and to secrete more insulin to maintain euglycemia. Once the beta cells fail to compensate the increased need for insulin, hyperglycemia occurs. This figure is adapted from *J Clin Invest. 2006 Jul;116(7):1802-12.*

1.2.3.1 Glucotoxicity

It is well-accepted that glucotoxicity of beta cells is defined as dysfunction induced by the chronic exposure of these cells to high concentrations of glucose, resulting in impaired glucose stimulated insulin secretion and insulin gene expression as well as apoptosis under certain

conditions (Harmon et al., 1999). After chronic high glucose exposure, several commonly used beta cell lines, such as HIT-T15 and INS-1 as well as rodent and human islets show reduced glucose-stimulated insulin secretion (GSIS) and also reduced insulin content (Boyd and Moss, 1993; Olson et al., 1993). In line with this, insulin promoter activity and pancreas-duodenum homobox-1 (PDX-1) and MafA binding activity to the insulin promoter are also decreased (Sharma et al., 1995; Ye et al., 2006). Similar results have been obtained in rat islets cultured *ex vivo* for up to six weeks (Jacqueminet et al., 2000).

The proposed mechanism with regard to glucotoxicity is closely related to the remodeling of glucose metabolism in the beta cell (Robertson et al., 2003). Instead of glucose being metabolized via glycolysis and Krebs' cycle, additional pathways are activated that include glyceraldehyde autoxidation, lipogenesis with DAG formation and PKC activation, sorbitol metabolism leading to the accumulation of reactive oxygen species (ROS) (Poitout and Robertson, 2002). Due to poor defense mechanisms against ROS available in the beta cells (low levels of superoxide dismutases and virtually no expression of catalase or glutathione peroxidase), ROS produced from altered glucose metabolism pathways eventually leads to beta cell dysfunction. In support of this hypothesis, beta cells with overexpression of glutathione peroxidase preserve intra-nuclear MafA binding activity and beta cell function, and thus slow down the progression of diabetes in *db/db* mice (Harmon et al., 2009).

Due to the role of increased oxidative stress in causing glucotoxicity, some antioxidants may be beneficial in protecting beta cell from this insult. This hypothesis has been supported in studies using the anti-oxidants N-acetylcysteine and aminoguanidine. In the Zucker Diabetic Fatty (ZDF) rats, treatment with these antioxidants has been shown to decrease markers of oxidative stress and improve glucose tolerance (Briaud et al., 1999). In *db/db* mice, treatment with N-acetylcysteine enhanced insulin secretion, ameliorated glycemia, reduced apoptosis and increased beta cell mass (Kaneto et al., 1999).

1.2.3.2 Lipotoxicity

The concept of lipotoxicity is derived from the phenomenon that T2D is commonly associated with elevated levels of TG and FFA in the plasma. Similar to glucotoxicity, lipotoxocity refers to chronically elevated levels of FFA eventually causing beta cell dysfunction (Gremlich et al.,

1997). Different fatty acid species have distinct effects in inducing beta cell apoptosis. Saturated fatty acids, such as palmitate and stearate have strong effect in inducing cell apoptosis. By contrast, monounsaturated fatty acids, such as oleate and palmitoleate, have been shown to protect beta-cells from apoptosis (Cnop et al., 2001) (El-Assaad et al., 2003). Of special interest, mixture of equimolar saturated and monounsaturated fatty acid is also not toxic to cells. And this protective effect may be due to the strong ability of unsaturated fatty acid in inducing TG synthesis. But this conclusion has been under debate, as other results indicate the protective effect lies in the fatty acid structure rather than the metabolism of FFA (Diakogiannaki et al., 2008). Even though the concept of lipotoxicity has been proposed for many years, it is still short of strong experimental support. We and others reported that FFA can induce beta cell dysfunction only in combination with elevated levels of glucose. In the presence of low glucose, high FFA (at reasonable concentrations) does not change both *in vitro* and *in vivo* the total insulin content of the ß-cell and only slightly affects GSIS. So from this standpoint, the concept of glucolipotoxicity (Prentki et al., 1998), combined chronic effect of both high glucose and FFA, is more appropriate to explain the toxic effect of FFA in beta cells and therefore gained more focus in recent research.

1.2.3.3 Glucolipotoxicity

Glucolipotoxicity is a combination of glucotoxicity and lipotoxicity, but importantly incorporates the concept of synergy of the toxicity of these fuels when present in excess simultaneously. This concept has been initially advanced by our lab together with Dr B Corkey and has been widely accepted. Glucolipotoxicity indicates the synergistic chronic effect of glucose and fatty acid in inducing beta cell dysfunction, and therefore glucolipotoxicity shows some similar features as glucotoxicity, such as decreased glucose-stimulated insulin secretion and decreased total insulin content of beta cells. Glucolipotoxicity also induces beta cell dysfunction in a unique fashion. When INS832/13 cells, derived from rat beta cells, are incubated in different conditions with high glucose (20mM glucose, no FFA), or high FFA (0.4mM palmitate, 5mM glucose), or high glucose (20mM) plus high FFA (0.4mM), high FFA alone has no effect in comparison to high glucose, indicating that high FFA *per se* have no significant toxic effect. Of special importance, the combination of high glucose and high FFA showed highest apoptosis, compared to the group with low glucose (El-Assaad et al.,

2003; El-Assaad et al., 2010). Further study indicated that this strong apoptosis inducing effect was closely related to lipid esterification processes, TG accumulation and ceramide deposition as well as activation of caspase-3 pathway in the cells (El-Assaad et al., 2010). Similar results were also reported in dispersed rat and human islets (Buteau et al., 2004). Some *in vivo* results also favor the concept of glucolipotoxicity. A 72 h infusion of glucose and intravenous fat emulsion in 6- month-old rats leads to insulin resistance and reduced insulin secretion *in vivo*. This was associated with diminished glucose-stimulated second-phase insulin secretion and proinsulin biosynthesis and lower insulin content as well as reduced expression of typical beta cell genes in isolated islets (Fontes et al., 2010). The mechanisms related to glucolipotoxicity are associated with glucose and FFA metabolism. As proposed by our lab, glucose is the main determinant of fatty acid partitioning inside the beta cells. When glucose concentration is in the low to normal range, fatty acids are transported into mitochondria through CPT-1, for beta oxidation without causing any toxic effect. When glucose and fatty acids are both elevated, glucose is converted to citrate through TCA cycle and then leads to the synthesis of malonyl-CoA, which inhibits CPT-1 activity. Inhibition of fatty acid oxidation, at the CPT-1 step causes fatty acid partitioning from beta oxidation to esterification (Prentki et al., 2002). High glucose also leads to enhanced lipolysis (Hu et al., 2005), and if the rates of esterification and lipolysis are the same, there is little toxic effect even in the presence of high glucose and high fatty acid. But if these rates of esterification and lipolysis are not balanced, many lipid derivatives may accumulate and induce beta cell dysfunction (Poitout et al., 2010; Prentki and Madiraju, 2012).

1.2.3.4 ER STRESS

The main function of pancreatic beta cell is insulin synthesis and secretion according to the body's demand. Beta cell needs to produce huge amounts of insulin in face of hyperglycemia. This large amount underscores the special "insulin factory" characteristic of beta cells with a highly developed ER, which is the major site responsible for posttranslational modification, folding and assembly of newly synthesized secretory proteins, and a cellular calcium store. ER is also an organelle that controls cell survival. A myriad of pathological and physiological factors, such as impaired protein transport from the ER to the Golgi, and calcium depletion from the ER lumen, can compromise the function of the ER, termed as ER stress (Laybutt et

al., 2007). Beta cells have to employ certain cytoprotective mechanisms to mitigate ER stress, referred to as the unfolded protein response (UPR), also named as ER stress signaling, which is elicited by ER stress (Eizirik and Cnop, 2010). The UPR can reduce ER stress and maintain ER function to produce and process proper amounts of proteins. In the event that the UPR cannot maintain ER homeostasis, cells activate at least three apoptosis pathways to induce cell apoptosis (Janikiewicz et al., 2015): the transcriptional induction of the genes for CHOP (C/EBP homologous protein)/ GADD153 pathway, the c-JUN NH2-terminal kinase (JNK) pathway and the ER-localized cysteine protease caspase-12 pathway. Multiple studies have implicated ER stress in beta cell apoptosis and this may be responsible for the reduction of beta cell mass in individuals with T2D.

Three ER membrane-associated proteins, inositol requiring protein 1 (IRE1), PKR-like kinase (PERK), and activating transcription factor 6 (ATF6), have been identified as master regulators in ER stress signaling and shown to regulate glucose homeostasis. Pancreatic beta cells deficient in PERK are more susceptible to ER stress-induced apoptosis. And PERK-deficient mice develop severe hyperglycemia soon after birth due to defects in islet proliferation and increased apoptosis. However, our understanding of the UPR in beta-cells is incomplete. The complexity of UPR pathways as well as its master regulators has not been completely investigated. We need to identify the cross talk between UPR pathway and other signaling pathways, such as mTOR, which have been shown to decrease ER stress, and also to focus on identifying endogenous molecules and chemical compounds that could modulate ER stress and protecting beta cells from metabolic stress-induced apoptosis.

1.2.3.5 Inflammation

In response to inflammation resulting from injuries or infection, the immune system plays a key role in restoring the normal function. Excess energy intake also leads to inflammation in different tissues, including pancreatic islets. Generally speaking, inflammation induced by circulating cytokines, such as interleukin-1β (IL-1β), tissue necrosis factor 1α and interferon-γ, plays a major role in inducing beta cell apoptosis seen in type 1 diabetes, and now it is also observed in T2D (Donath, 2013). In response to chronic high glucose exposure, human islets will secrete high amount of IL-1β, and in combination high glucose and IL-1β synergize in causing beta cell dysfunction (Boni-Schnetzler et al., 2008; Fei et al., 2008). The synergistic

effect of high glucose and IL-1β in inducing beta cell dysfunction is also observed in isolated rat islets cultured *ex-vivo*. Most recently, it has been observed in a clinical trial that blocking of IL-1β receptor by specific antagonist greatly improved beta cell function and ameliorated the hyperglycemia in patients with T2D, indicating the possible roles of IL-1β-induced inflammation in progression of T2D. However, large-scale clinical studies in human T2D are needed to further confirm these findings. Studies using different animal models indicate that the potential mechanisms related to inflammation of islet tissue involve hypoxia, cell death and the JNK-NFκB pathway.

1.2.3.6 Additional mechanisms

Autophagy is characterized by the process that intracellular long-lived proteins or damaged organelles are recycled to maintain cellular homeostasis (Levine and Klionsky, 2004). And it is regarded as a defense mechanism to protect beta cells from ER stress and oxidative stress (Jung et al., 2008). It has been reported that in different rodent models, such as *ob/ob*, *db/db* and Akita mice, the number of autophagosomes and autophagolysosomes is increased in beta cells. In islets isolated from human subjects with T2D, autophagy-related cell death is observed (Hartley et al., 2009). However, currently, beta cell dysfunction cannot be directly ascribed to increased autophagy activity. To do so, we need to show that inhibition of autophagy in these conditions could protect the beta cells from different insults.

Recently, microRNA, a small non-coding RNA, found in different tissues has shown to play important role in multiple cellular processes, including beta cell function. Some reports have indicated that miRNA-24 is highly expressed in pancreatic beta cells and its level is elevated in the mice fed with HFD. Overexpression of this miRNA was shown to inhibit insulin secretion and beta cell proliferation via targeting with maturity onset diabetes of youth (MODY) genes (Guay and Regazzi, 2013; Zhu et al., 2013). Also, modifications in the levels of miR-34a, miR-146a, miR-199a-3p, miR-203, miR-210 and miR-383 primarily occur in diabetic mice with obesity and result in increased beta cell apoptosis (Nesca et al., 2013). Interestingly, miR-375 regulates the proliferation of islet cells and insulin secretion, contributing to the reduced beta-cell mass and function in the progeny of mothers fed a low protein diet that show hyperglycemia even at adult age (Dumortier et al., 2014).

Recent studies have documented the intestinal microbiota as an emerging factor that contributes to beta cell dysfunction. Microbiota-mediated inflammation may directly target beta cells and impair beta cell function (Vaarala et al., 2008). Also, it has been reported that change in circulating incretin levels, such as GLP-1 and GIP due to altered intestinal microbiota, may also play a role in beta cell dysfunction. The incretins have been shown to largely contribute to insulin secretion after meals, and in patients with T2D, the effect of incretins is greatly reduced. However, the exact mechanism by which intestinal microbes alter these processes is currently unknown (Michaliszyn et al., 2014).

1.3 Insulin secretion

As discussed above, the main role for the beta cell is to monitor circulating nutrient level and control blood glucose in a narrow range by secreting appropriate amounts of insulin. Insulin secretion is a complex and well-controlled process and we will discuss this in more detail.

1.3.1 Insulin exocytosis

The process of insulin release out of the granule is referred as insulin exocytosis. Insulin vesicle exocytosis is a complex process involving many steps, including vesicle movement via actin network, docking to plasma membrane, priming, and finally fusion with the plasma membrane and each step requires delicate regulation so that appropriate amount of insulin is released in response to various stimuli (Takahashi et al., 2002). In order to easily explain the dynamics of vesicle exocytosis, the vesicles can be divided into three different groups depending on their release competence following various stimulations: the readily releasable pool of granules (RRP), the morphologically docked pool (MDP) and the reserve pool (Bratanova-Tochkova et al., 2002). As its name implies, RRP is the pool of granules that are already docked to the plasma membrane and primed and available to be released after stimulation. MDP means that the granules have already docked on the plasma membrane and some of the granules are already primed and others not. With regard to the reserve pools, they are larger and more complex than RRP and need to be transported from the actin network to the plasma membrane and then are released after priming. The classification of granule pools may not be accurate; as some reports indicate that some newly formed insulin granules are immediately released as RRP. However, the mechanism is currently under investigation.

Capacitance studies show that in mouse beta cells, the total number of granules is estimated as 13,000 per beta cell, of which 0.3-0.7% belong to the RRP group, 1-7% to the MDP, and the rest are comprised in the reserve pool. That is, the total number of RRP granules ranges from 40 to 100, while the total number of granules in the MDP and reserve pools is approximately 1,000 and 11,600, respectively (Bratanova-Tochkova et al., 2002). In response to physiological stimulations, beta cells only release a small portion of insulin granules with approximately less than 10% of total insulin granules.

Insulin secretion is a biphasic process with a rapid first phase and a long sustained second phase (Straub and Sharp, 2002). When beta cells receive signals from different stimulations, insulin is released from the granules and generally the peak reaches within 5min. It has been proposed that RRP is the main contributor for the first phase insulin secretion. Some reports have indicated that in the patients with T2D there is defective first phase secretion (O'Rahilly et al., 1988). After first phase, insulin is released at a much lower rate and involves translocation of granules from reserve pools to the readily releasable pool or transformation of morphologically docked granules to release competency before exocytosis. Depending on different species, there is considerable variation in the second phase insulin secretion. In the mouse islets, the second phase insulin secretion is small and even negligible, while in the islets from rats and humans, there is an evident and efficient second phase insulin secretion contributing to more than 50% of total insulin released during 1hr.

Several hypotheses have been proposed to explain the process of insulin vesicle exocytosis. Of all the hypothesis, the one that is wildly accepted is the soluble *N*-ethylmaleimide-sensitive factor (NSF) attachment protein receptor (SNARE) hypothesis (Rorsman et al., 2000), which proposes the formation of complex between the proteins located in the plasma membrane, syntaxin and synaptosomal-associated protein 25 (SNAP-25) and the protein from the vesicle-associated membrane protein 2 (VAMP-2)/synaptobrevin-2 (Lang and Jahn, 2008). At least 5 protein super-families have been identified to be involved in this process, such as SNAREs, Sec1/Munc18 (SM) proteins, synaptotagmins, Rab proteins and endocytotic proteins. Different proteins participate at different steps and play crucial roles. Loss of the fusion between the membrane protein and vesicle completely blocked vesicle exocytosis. Knocking down the protein “Munc18-1” decreased the first and second phase of insulin secretion (Oh et al., 2012;

Tareste et al., 2008). Rab plays a critical role in the formation, trafficking, and tethering of vesicles to the target compartment in endocrine and nonendocrine cells. Rab27a deficient mice showed decreased number of docked granules and insulin secretion (Kasai et al., 2005). Besides these core proteins, the remodeling of F-actin also plays important roles in insulin exocytosis. F-actin negatively regulates exocytosis via binding and blocking Syntaxin 4 accessibility (Jewell et al., 2008). But further studies indicated that metabolic amplification pathway increases both phases of insulin secretion and is independent on actin microfilaments. It has been reported that SNARE complex assembly is regulated by Munc13-1, a synaptic protein that determines the priming of synaptic vesicles, a rate-limiting step in insulin granule release (Kwan et al., 2006a). Munc13-1 is highly expressed in mouse, rat and human islets and some reports show that the level of Munc13-1 is reduced in the islets isolated from rodent models of T2D as well as humans with T2D (Sheu et al., 2003). Overexpression of Munc13-1 in INS832/13 cell line greatly elevated glucose-stimulated insulin secretion and this elevation is dependent on DAG production, as blocking of phospholipase C completely abolishes the effect of overexpression (Sheu et al., 2003). Munc13-1 knockout is embryonic lethal and mice with complete deficiency in Munc13-1 do not survive, as Munc13-1 is not only an important determinant in insulin secretion, but also plays important roles in neurotransmitter release (Augustin et al., 1999). Heterozygous Munc13-1 knockout mice display glucose intolerance with decreased insulin levels in the plasma, indicating that the cause of glucose intolerance is mainly due to a primary islet β-cell secretory defect. Also, the defect in insulin secretion in heterozygous Munc13-1 knockout mice could be partially rescued by phorbol ester potentiation, which was interpreted to support the view that Munc13-1 is a DAG receptor, as confirmed in neurotransmitter release in the brain.

1.3.1.1 Triggering and amplification pathways in glucose induced insulin secretion

The mechanism that underlies the biphasic nature of glucose-induced insulin secretion process is still poorly understood, but some well-established pathways have been implicated: the K_{ATP} dependent/ triggering pathway and the K_{ATP} -independent/amplification pathway (Rorsman and Renstrom, 2003). The K_{ATP} dependent/triggering pathway is well-established and gained strong experimental support. Once nutrient enters the cells, intracellular metabolism of these nutrients by different metabolic pathways produces ATP and elevates the ratio of ATP-to-

ADP, and then closes ATP-sensitive K+ (K_{ATP}) channels, leading to membrane depolarization and opening of voltage-operated Ca2+ channels, which in turn causes Ca2+ influx. The rise in cytoplasmic free Ca^{2+} concentration ([Ca^{2+}]i) activates the exocytotic machinery leading to insulin secretion.

Compared to the K_{ATP} dependent/triggering pathway, the KATP-independent/amplification pathway is more complex and poorly understood. This hypothesis is based on the observation that insulin secretion is still enhanced under the conditions that beta-cell [Ca2+]i is maintained at a higher level with either a high concentration of sulfonylurea or a high concentration of K+ in the presence of diazoxide to open the K(ATP) channels, indicating that other mechanisms are responsible for elevated insulin secretion (Nolan et al., 2006d). This amplification pathway depends on the production of various metabolic coupling factors (MCF) (Prentki et al., 2013b). Several MCFs have been identified and are shown to implicate the amplification pathways. We will discuss this in the following chapter.

1.3.2 Fuel and non-fuel induced insulin secretion

It is well-accepted that in some cases, beta cells need some signal to switch from "quiescence state" to "release state" to control elevated glycemia, while in other cases, beta cells need to stop insulin secretion in order not to lead to hypoglycemia. Beta cells employ different sensors to sense fuels and non-fuels in the plasma in response to different situations. Some fuels, such as glucose, fatty acid and amino acids, and some non-fuels, including GLP-1, GIP, acetylcholine, somatostain and (nor)epinephrine are important regulators in insulin exocytosis (Figure 5). In the following part, we will discuss these regulators in more detail.

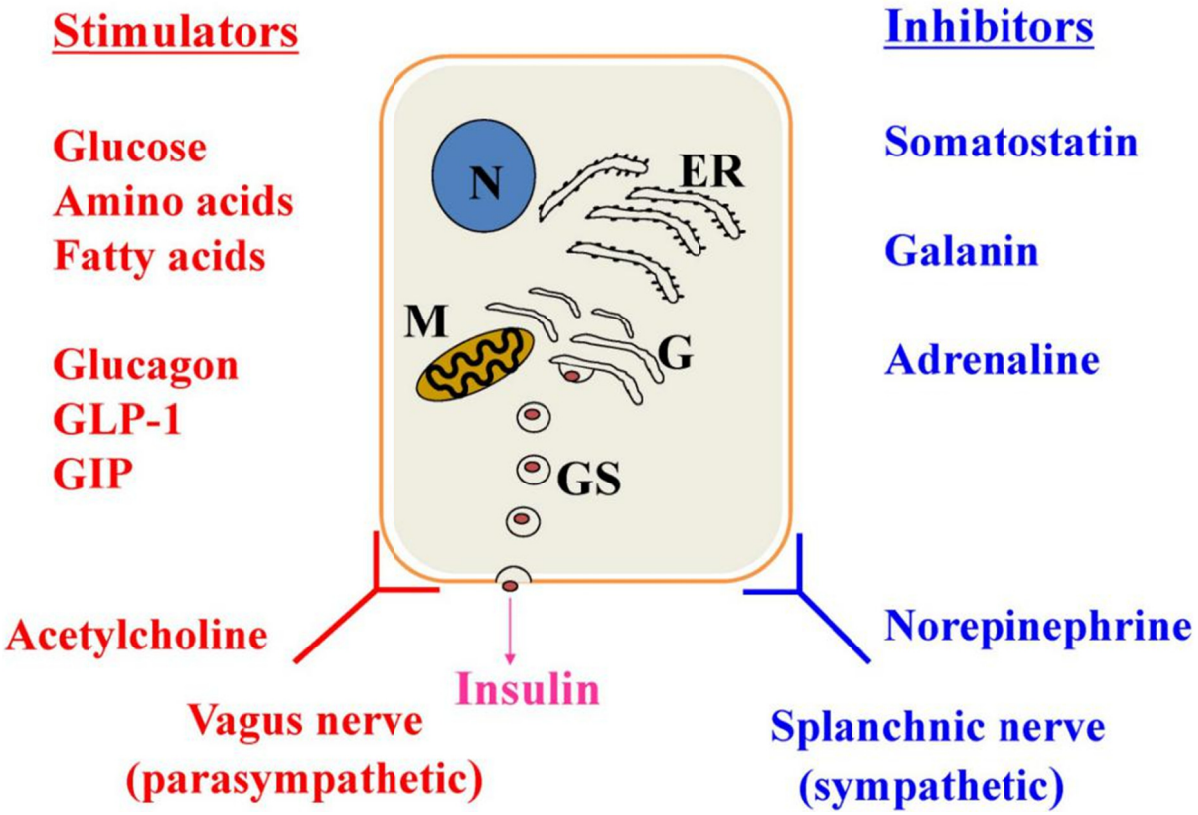

Figure 5 Fuel and non-fuel- modulators of insulin secretion. Various types of fuel and non-fuel stimuli regulate insulin secretion by different mechanisms.

1.3.2.1 Glucose

Glucose is the most powerful nutrient to regulate insulin secretion in the beta cell. The perfusion studies in mouse, rat and human islets have shown that elevated glucose induces a biphasic release of insulin. The efficacy of glucose as a potent signal is closely related to its metabolism inside the beta cell (Prentki et al., 1997; Zhang et al., 2008). After food digestion, glucose level rises in the blood and is rapidly transported into beta cells via the high K_M and high Vmax glucose transporters GLUT2 in rat and GLUT1 in human (Schuit, 1997). Glucose is phosphoryalated by the high K_M glucokinase, the rate limiting step in its metabolism, and subsequently oxidized via glycolysis and the TCA cycle to produce ATP. An increase in the ratio ATP-to-ADP closes the ATP-sensitive K+ (K+ATP) channels, causing depolarization of the plasma membrane, which in turn opens L-type voltage dependent Ca2+ channels. Ca2+

influx along with Ca2+ efflux from ER take part in priming the secretory vesicles for exocytosis (Figure 6). Additional mechanisms implicated in glucose signaling to insulin secretion are discussed below.

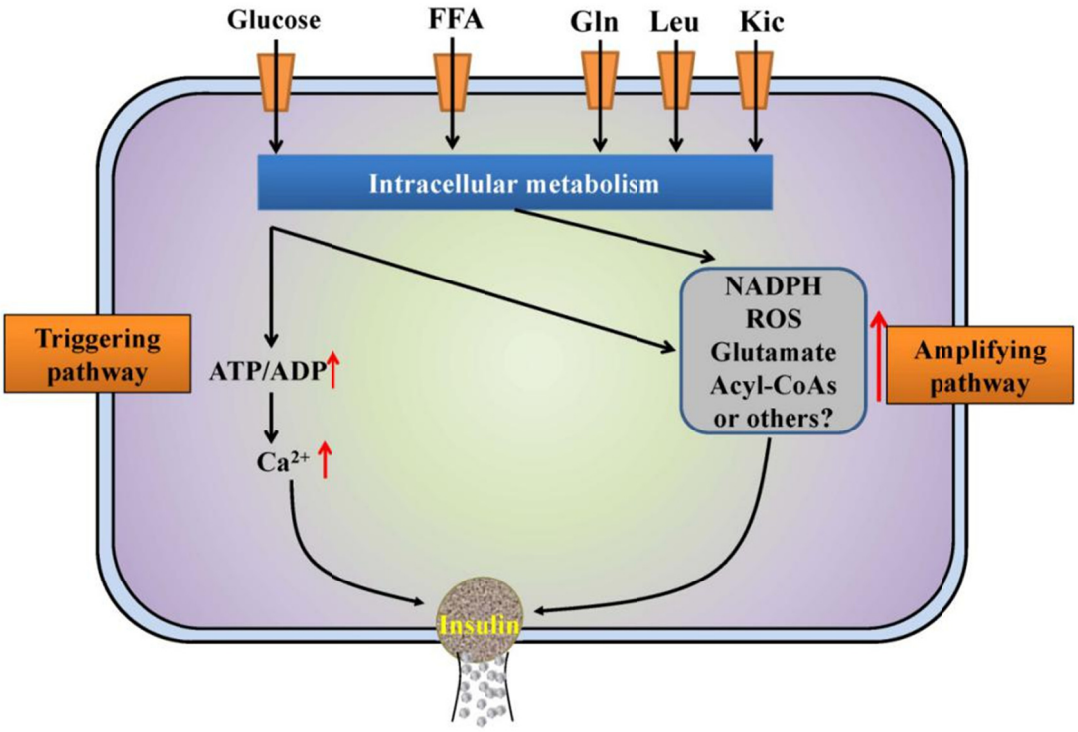

Figure 6 Triggering and K+-ATP independent/ amplification pathways in beta cell metabolic signaling.

1.3.2.2 Free fatty acids

The effect of FFA on insulin secretion is dependent on the duration of exposure of the beta cells. Short time exposure to FFA of beta cells enhances insulin secretion at high glucose concentrations and has very modest effect at basal glucose levels (Carpentier et al., 1999). However, chronic exposure of FFA to beta cells can lead to beta cell dysfunction as discussed in the previous chapter.

The mechanism of the potentiation effect of FFA can be explained by the "trident model" (Nolan et al., 2006d). The first two arms of this model relate to the intracellular metabolism of FFA, and the third arm involves the FFA receptor 1 (also known as GPR40) located in the plasma membrane (Itoh et al., 2003). The first arm is the AMP-activated protein kinase (AMPK)/malonyl-CoA/long-chain acyl-CoA (LCCoA) signaling network (Prentki et al., 2002;

Roduit et al., 2004). In the presence of high glucose, which elevates malonyl-CoA in the cell, FFA metabolism is switched from beta oxidation to lipid esterification, resulting in the availability of LC-CoA and acylglycerol (DAG, lysophosphatidic acid, phosphatidic acid) intermediates for signaling purpose. Overexpression of malonyl-CoA decarboxylase (MCD) blocks the increase of malonyl-CoA levels, enhances fat oxidation and reduces FFA esterification and this is associated with reduced GSIS in the absence and presence of exogenous FFA (Prentki et al., 2002). The second arm is related to glycerolipid/ free fatty acid (GL/FFA) cycling, which will be discussed in detail in the next chapter. The third arm acts through FFA receptor GPR40. GPR40 is highly expressed in mouse, rat and human islets as well as in various beta cell lines. GPR40 is activated by medium to long chain FFA. Overexpression of GPR40 in pancreatic β-cells enhances glucose-stimulated insulin secretion and improves glucose tolerance in normal and diabetic mice (Nagasumi et al., 2009). In line with this, mice deficient in GPR40 specifically decreases FFA-amplified glucose-stimulated insulin secretion. It is estimated that 50% of FFA-amplified insulin secretion is contributed by GRP40 receptor and the remaining 50% is contributed by the other two arms (Kebede et al., 2008; Latour et al., 2007).

1.3.2.3 Amino acids

Individual amino acids alone do not induce insulin secretion at their physiological concentrations. However, combination of several amino acids at high concentrations, such as L-alanine and glutamine and leucine (Fajans et al., 1967), shows strong effect in inducing insulin secretion. The mechanisms vary differently dependent on the type of amino acids. L-Arginine, a cationically charged amino acid, can directly depolarize the plasma membrane and causes insulin secretion; but this effect is dependent on the presence of glucose. L-alanine has a more complex mechanism to stimulate insulin secretion. On one hand, L-alanine can be co-transported with Na+, and thus can depolarize the plasma membrane; on the other hand, L-alanine can be metabolized, to produce ATP, leading to KATP channel closure (Newsholme et al., 2010). Both pathways appear to promote Ca2+ influx and insulin secretion. Leucine is known to activate glutamate dehydrogenase and thus strongly potentiates the effect of L-glutamine in inducing insulin secretion via anaplerotic input (discussed in more details below) into the Krebs cycle (Malaisse et al., 1982).

1.3.2.4 GLP-1 and GIP

Glucose-dependent insulinotropic peptide (GIP) and glucagon-like peptide-1 (GLP-1) are two important gluco-incretins that play important roles in regulating glucose homeostasis via enhancing insulin secretion. The identification of GIP and GLP-1 followed the interesting observation of different insulin levels in response to oral gavage vs intraperitoneal injection of glucose. Oral gavage induces higher insulin levels than intraperitoneal injection, indicating that some gastrointestinal tract hormones or signals are contributing to this process. It is now estimated that GIP and GLP1 contribute to more than 50% of the total post-prandial insulin secretion (Vilsboll et al., 2003).

GIP is produced from endocrine K-cells in the duodenum after ingestion of carbohydrate and fat, while GLP-1 is produced from enteroendocrine L- cells of the intestinal mucosa and both are released into the portal circulation in response to meal ingestion (Phillips and Prins, 2011). GLP-1 mediated enhancement of insulin secretion does not involve driving fuel and energy metabolism in primary rodent pancreatic beta-cells (Peyot et al., 2009a). Both GLP-1 and GIP play their roles in insulin secretion via binding to their specific cell surface receptors to generate signaling molecules, such as cAMP and Ca^{2+}, which trigger insulin exocytosis. Mice deficient in GIP receptor show glucose intolerance with impaired initial insulin response after oral glucose load (Yabe and Seino, 2011). Consistent with this, ectopic GIP expression in β-cells maintains insulin secretion in the absence of proglucagon-derived peptides, revealing a novel compensatory mechanism for sustaining incretin hormone action in islets (Fukami et al., 2013). Similarly, mice deficient in GLP-1 receptor are also glucose intolerant with reduced insulin levels in plasma.

The effect of GLP-1 receptor agonists in inducing insulin secretion is glucose-dependent. Without high glucose, GLP-1 shows very little or no effect on insulin secretion. It has been shown that intraportal GLP-1 stimulates insulin secretion predominantly through the hepatoportal-pancreatic vagal reflex pathways (Nishizawa et al., 2013). Besides this, GLP-1 regulates insulin secretion possibly also via central action, as acute activation of central GLP-1 receptors enhances hepatic insulin action and insulin secretion in HFD-fed insulin resistant mice. The combination of GIP and GLP-1 for therapeutics is not promising, as GIP is unable

to further amplify the insulinotropic and glucose-lowering effects of GLP-1 alone in type 2 diabetics (Mentis et al., 2011).

1.3.2.5 Acetylcholine

Acetylcholine (Ach) is a major stimulatory neurotransmitter released from parasympathetic nerve endings reaching pancreatic islets in rodents. Ach is synthesized by choline acetyltransferase using acetyl-CoA and choline in the cytoplasm. Then ACh is transported from the cytoplasm into the vesicles by an antiporter (Lawal and Krantz, 2013). Several reports indicated that released Ach plays important role in stimulating insulin secretion, particularly during the "cephalic phase" of insulin secretion that occurs prior to food intake when one sees a meal. The effect of Ach in insulin secretion is dependent on binding to M3 muscarinic receptors and activation of G protein-coupled phospholipase C to produce DAG and IP3, both of which can activate downstream targets, such as PKC, PKD, Munc13-1 and Ca2+ signaling to promote insulin secretion. Mice deficient in the M3 muscarinic receptor are hypophagic and lean (Yamada et al., 2001). Further studies indicated that the potentiation effect of Ach in insulin secretion is abolished in islets isolated from M3 muscarinic receptor KO mice (Duttaroy et al., 2004).

Compared to mouse islets, human islets do not show high cholinergic innervation. It is mainly alpha cells of human islets that release Ach in response to kainate or a lowering in glucose concentration to offer paracrine cholinergic input to beta cells to regulate insulin secretion (Rodriguez-Diaz et al., 2011).

1.3.2.6 Somatostatin

Somatostatin, a hypothalamic growth-hormone-inhibiting factor, decreases insulin secretion in response to various stimulations, including L-arginine and isoproterenol in mouse, rat and human islets. The effect of somatostatin in insulin secretion *in vivo* is attributed to a direct paracrine effect on pancreatic beta cells and is not mediated via the CNS (Hauge-Evans et al., 2015), and it can inhibit first and second phase of insulin secretion (Alberti et al., 1973). The function of somatostatin is mainly mediated by one of the G protein-coupled receptors-somatostatin receptor subtype 5 (SSRS5), the major receptor expressed in the pancreatic beta cells. Some recent reports indicate that SSRS5 functions as a negative regulator for PDX-1

expression and that somatostatin's inhibitory effect on cell proliferation and insulin expression/secretion is mediated by SSRS5 via down-regulating PDX-1 expression. The effect of SSTR5 on PDX-1 is regulated both the transcriptional level and the post-translational level by increasing PDX-1 degradation (Zhou et al., 2014). Mice lacking of somatostatin receptor subtype show decreased blood glucose and plasma insulin and increased leptin and glucagon concentrations (Strowski et al., 2000).

1.3.2.7 Galanin

Galanin is a neuropeptide composed of 29 amino acids, and is highly expressed in the brain, spinal cord, and peripheral tissues. It has been noticed that patients with gestational diabetes mellitus (GDM) display high levels of plasma galanin (Fang et al., 2013). And further studies indicate that galanin is an effective biomarker for prediction of GDM. Besides the role in increasing insulin sensitivity in muscle and adipocytes, earlier studies in dogs clearly indicated that galanin strongly inhibits insulin secretion in pancreatic beta cells and induces hyperglycemia in dog (McDonald et al., 1985). Further studies have shown that galanin inhibits insulin secretion by direct interference with exocytosis through a pathway involving a pertussis toxin- sensitive, guanine-nucleotide-binding regulatory protein, negatively coupled to adenylate cyclase (Ullrich and Wollheim, 1989). Recent reports have revealed some new mechanisms regarding its regulatory effect in insulin secretion. It has been shown that galanin's inhibitory effect on insulin release is partially mediated by G_o2 G protein in pancreatic β cells (Tang et al., 2012). The inhibitory effect of galanin is lost in islets isolated from mice lacking G_o2, but not other $G_{i/o}$ proteins.

1.3.2.8 (Nor) epinephrine

Epinephrine (also called adrenaline) is a hormone and a neurotransmitter. Both epinephrine and norepinephrine are produced by adrenergic nerve terminals and play various roles in regulating glucose production in the liver and insulin secretion in the pancreatic beta cells (Sharara-Chami et al., 2012). Elevated levels of epinephrine by either endogenous release in response to stress or exogenous infusion are known to cause glucose intolerance, and the effect is mainly mediated by inhibitory effect in insulin secretion and enhanced glucose production in the liver. The effect of norepinephrine and epinephrine on insulin secretion is

mediated by α2-adrenergic receptor and β1-adrenergic receptor. Ghrelin is a strong inhibitor of insulin secretion in rodents and healthy humans and norepinephrine stimulates ghrelin secretion through the β1-adrenergic receptor via increased cAMP and protein kinase A activity. The effect of epinephrine in decreasing insulin secretion via its specific receptors is particularly important to prevent hypoglycemia during exercise when muscle contraction promotes glucose uptake by tissues, and when enhanced whole body glucose oxidation is required.

1.3.3 Metabolic signals promoting insulin secretion

Nutrient secretagogues, such as glucose and FFA, activate beta cell metabolism and elevate ATP production, which precedes the rise in Ca^{2+} and insulin secretion. The availability of substrates and their metabolism leads to the production of various metabolic coupling factors (MCF) to promote insulin release (Prentki et al., 2013b). The initial metabolism of fuels in the beta cells appears to be governed by a "push" (substrate availability) rather than a "pull" mechanism (Ca^{2+} influx driving mitochondrial metabolism), unlike other tissues (Peyot et al., 2009a). This occurs possibly because of the specific characteristics of beta cells. In beta cells, glucose transport inside the cells is not a rate-limiting step, and rapid equalization of extra and intracellular is reached with glucose transporters. Also, glycolysis is governed by glucokinase with low affinity, around 8mM, for glucose.

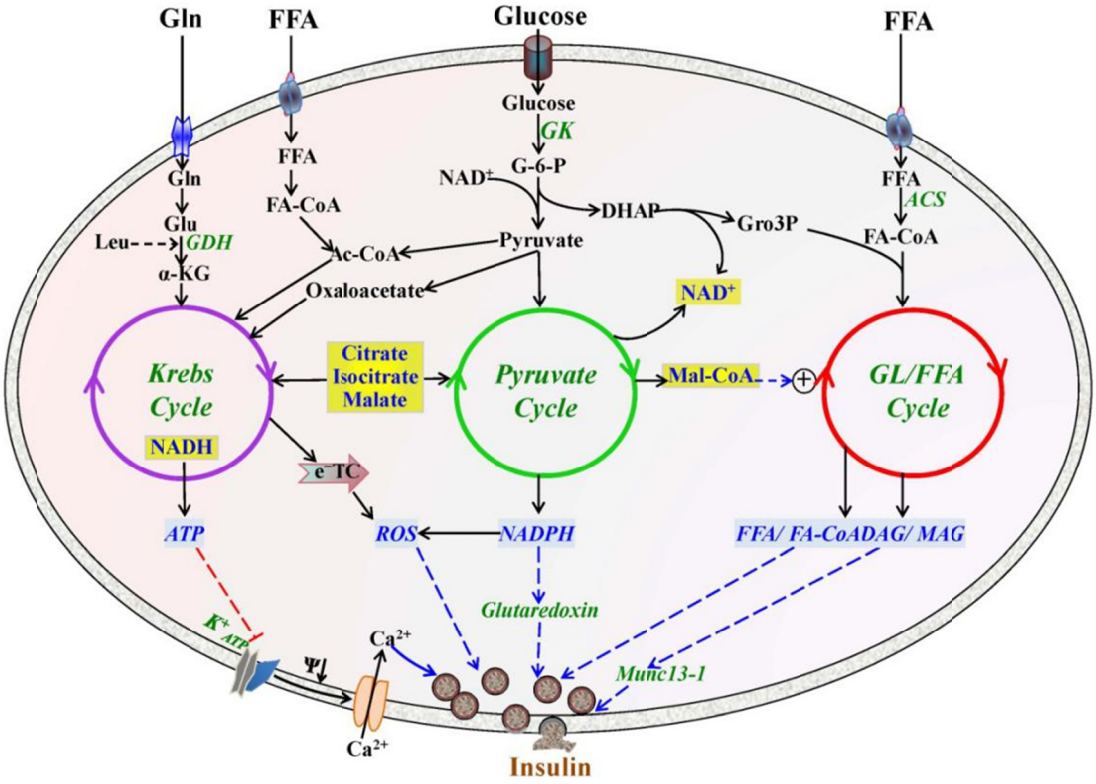

Figure 7 Intergrated view of metabolic pathways generating metabolic coupling factors for insulin secretion. This figure is adapted from *Cell Metab. 2013 Aug 6; 18(2):162-85.*

1.3.3.1 Anaplerosis and cataplerosis-derived signals

Cataplerosis and anaplerosis are processes that represent the efflux of Krebs' cycle intermediates from mitochondria into the cytosol, and their replenishment, respectively. Both processes are quantitatively similar because the Krebs' cycle is not a sink for glucose carbons (Schuit et al., 1997). In the beta cells, anaplerosis and cataplerosis pathways are thought to provide the carbon precursors (eg citrate) of MCF for insulin secretion (Figure 8).

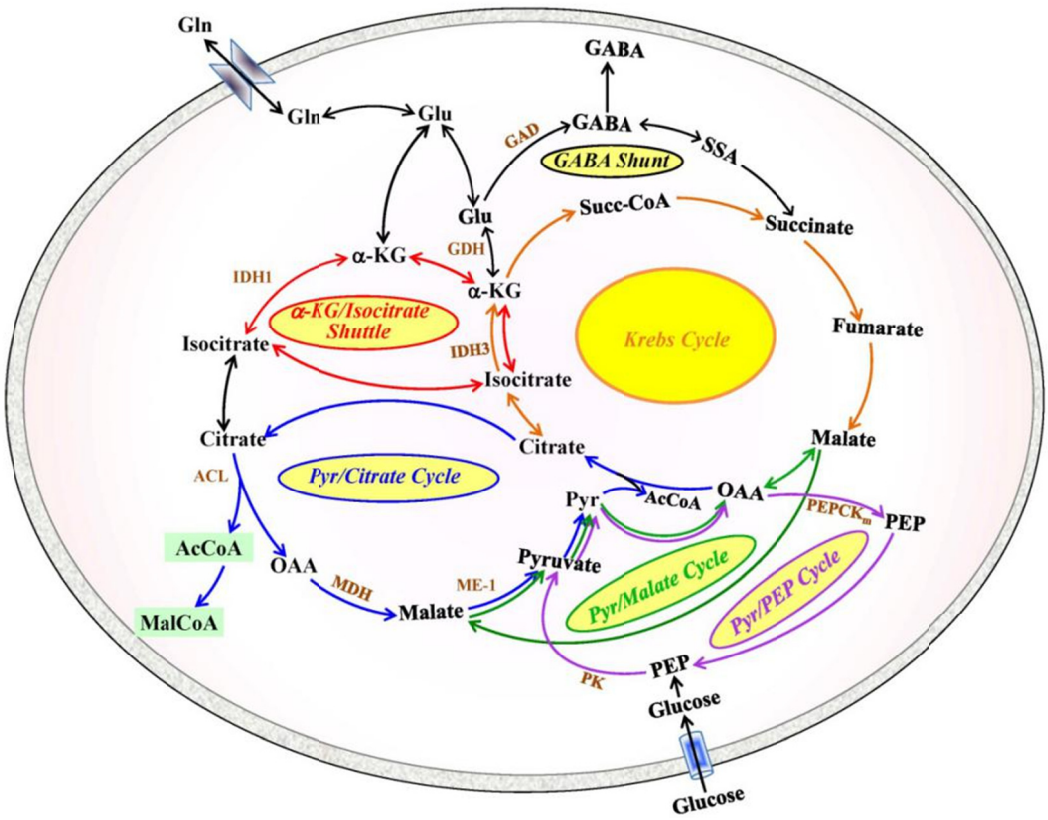

Figure 8 Anaplerotic- and Cataplerotic-Derived Signals for Insulin Secretion. This figure is adapted from *Cell Metab. 2013 Aug 6; 18(2):162-85*.

Multiple studies have shown that pyruvate cycling is important in glucose-stimulated insulin secretion. Pyruvate carboxylase (PC) is well expressed in the beta cells, and its level is reduced in the islets isolated from patients with T2D (Jensen et al., 2006). The rate of pyruvate carboxylase is dose-dependently correlated with GSIS. Decreasing activity of PC either by a pharmacological inhibitor or down-regulation decreases glucose-stimulated insulin secretion, while increasing its activity by overexpression increases insulin secretion (Farfari et al., 2000).

Pyruvate cycling allows for high glycolytic flux via NADH re-oxidation and the production of different MCFs, malonyl-CoA (MalCoA), NADPH (Guay et al., 2007), glutamate and GTP. MalCoA is formed by carboxylation of acetyl-CoA, catalyzed by acetyl-CoA carboxylase (ACC). MalCoA is an important metabolite that regulates fatty acid oxidation through allosteric inhibition of carnitine palmitoyltransferase 1 (CPT1). The hypothesis that MalCoA acts as a MCF is supported by many experimental results (Prentki et al., 2002; Roduit et al., 2004). The level of MalCoA is well-correlated with GSIS. Decreasing ACC activity by

specific inhibitors or downregulation leads to reduce GSIS, while overexpression of ACC reduces the level of MalCoA and thus GSIS in the presence of FFA.

Some reports strongly support NADPH as a MCF for insulin secretion (MacDonald et al., 2006; Pongratz et al., 2007). The ratio of NADPH/NADP is well-correlated with GSIS in mouse and rat islets as well as in different beta cell lines. Increasing NADPH level by exogenous administration enhances GSIS in patch-clamping studies, and decreasing NADPH by knockdown of malic enzyme reduces GSIS. Regarding the mechanism of NADPH action, two targets have been proposed: one is the redox protein glutaredoxin (GRX) and the other is voltage-dependent K^+ channel. It has been suggested that NADPH and NADP+ control reduced and oxidized forms of GRX and GRX may directly regulate exocytosis via a posttranslational modification (change in the redox state of exocytotic proteins). Also, injection of GRX potentiates NADPH-induced insulin secretion. Overexpression of GRX1 increases GSIS, and down-regulation of GRX1 reduces GSIS in rat islets (Reinbothe et al., 2009). Kv channel is an important regulator of voltage-gated calcium channel. Inhibition of Kv channel results in Ca^{2+} influx and thus GSIS. It has been hypothesized that the NADPH could directly bind to β unit of Kv channel to regulate its channel activity. However, more experimental support needs to prove this hypothesis.

The notion that glutamate acts as a MCF is supported by the observation that glutamate directly enhances insulin granule exocytosis in beta cell lines. Glutamate is produced during cataplerosis and anaplerosis via reductive amination or transamination. The glutamate level is well-correlated with GSIS, and reduction of glutamate level by overexpression of glutamate decarboxylase curtails GSIS (Straub and Sharp, 2002). Furthermore, human and mice deficient in glutamate dehydrogenase are associated with hyperinsulinemia (Stanley et al., 1998). However, the view that glutamate acts as a MCF has been challenged, and the evidence indicates that anaplerotic oxidative deamination of glutamate via GDH, producing alphaketoglutarate in the Krebs cycle, is implicated in this type of hypersulinemia (Palladino and Stanley, 2010).

Besides ATP, GTP has been proposed to be a MCF. GTP level is increased with increasing glucose concentration (Kibbey et al., 2007). The production of GTP in the mitochondrion is catalyzed by GTP-specific isoform succinyl-CoA synthase (GTP-SCS). It has been shown that

GTP could directly promote insulin secretion in a calcium-independent manner. Further studies show that the effect of GTP in insulin secretion may involve some small G proteins. Reduced level of GTP-SCS is associated with decreased insulin secretion, supporting the role of GTP as a MCF.

1.3.3.2 Electron transport-derived signals

Activation of TCA cycle is associated with transferring electrons to mitochondrial respiratory chain, leading to ATP generation. Many reports indicate that the mitochondrial electron transport chain plays important role in generating various MCFs, including ATP, ADP, AMP, cAMP, reactive oxygen species (ROS) and reduced cytochrome c, to promote insulin secretion, as inhibition of different complexes of electron transport chain (ETC) is associated with reduced GSIS (Prentki et al., 2013b).

The role of different adenine nucleotides, including ATP, ADP and AMP in regulating K^+_{ATP} channels is well-established (Ghosh et al., 1991; Loubatieres-Mariani et al., 1979). Increased ATP levels inhibit K^+_{ATP} channels, while MgADP is responsible for opening the channels. At high glucose, reduced ADP level contributes to closure of K^+_{ATP} channels. ATP is proposed to be required for priming of insulin granules, and may directly be implicated in the exocytosis machinery. Studies show correlation between elevated ATP levels and second phase insulin secretion in mouse islets. With increasing glucose levels, the ratio of AMP/ATP is lower, which may play an important role in reducing AMPK activity, a fuel sensor and a negative regulator of insulin secretion (Lamontagne et al., 2009). Furthermore, cAMP is also proposed to be a MCF in insulin secretion, as the level of cAMP is elevated with increasing glucose concentration possibly because its formation is limited by ATP acting as a substrate for some adenylate cyclase isoforms (Prentki and Matschinsky, 1987), and oscillations of cAMP content in beta cells is well-correlated with insulin secretion (Yajima et al., 1999). cAMP in insulin secretion works through cAMP-dependent protein kinase A (PKA) and Epac2, which directly regulate insulin exocytosis.

The role of ROS in beta cell function is dependent on its concentration and time of elevation. As discussed in the previous chapter, chronic ROS exposure results in beta cell dysfunction. In contrast, acute ROS may function as a MCF to promote insulin secretion (Leloup et al., 2009).

Multiple reports support this hypothesis. It has been noticed that glucose increases ROS levels in rodent islets and beta cell lines. Decreasing ROS levels by ROS scavengers reduces GSIS (Pi et al., 2007). Moreover, the increased insulin secretion by low micromolar of H_2O_2 is abolished by ROS scavengers, and overexpression of antioxidant enzymes superoxide dismutase in beta cells reduces GSIS (Alfadda and Sallam, 2012). However, some evidences are against this hypothesis, as mice lacking NADPH oxidase NOX2 show increased GSIS rather than reduction in insulin secretion (Li et al., 2012b). In addition, GSIS does not change in the islets with overexpression of H_2O_2 –inactivating catalase (Gurgul et al., 2004). Further work is needed to evaluate the role of ROS acting as MCF for insulin secretion.

Reduced cytochrome C is emerging as an MCF (Jung et al., 2011). Some evidence supports this hypothesis, as change in the level of cytochrome C is associated with variation in GSIS. But more work is needed to further evaluate this view.

1.3.3.3 Inositol lipids and polyphosphates

Glucose metabolism leads to a rapid turnover in phosphatidylinositol 4,5-bisphosphate (PIP2), phosphatidylinositol 3,4,5- triphosphate (PIP3) and inositol 1,4,5- triphosphate (InsP3), and it seems that the role of PIP2, PIP3 and InsP3 in insulin secretion are different. Some reports indicate that there is no major change in GSIS with reduction in the level of PIP2. In contrast, increasing PIP2 levels is associated with increased insulin secretion (Berggren and Barker, 2008). The enzyme G-protein-coupled PI3-kinase catalytic subunit (P110γ) is responsible for generation of PIP3 using its substrate PIP2. Islets isolated from mice lacking P110γ show decreased insulin secretion with complete loss of first-phase insulin secretion and a blunted second phase insulin secretion (MacDonald et al., 2004; Pigeau et al., 2009). The role of InsIP3 in insulin secretion promoted by glucose is related to Ca2+ mobilization from the ER (Prentki et al., 1984) and also as a precursor for generating other inositol polyphosphates, such as InsP5 and InsP6, both of which may also potentiate calcium induced secretion via unknown mechanisms (Barker et al., 2009).

1.3.3.4 GL/FFA cycling and lipid signaling for insulin secretion

The role of GL/FFA cycling in regulating insulin secretion is well-established. Glucose metabolism increases both lipogenesis and lipolysis, two essential parts of GL/FFA cycling

(Prentki and Madiraju, 2012). And it has also been shown that both parts of GL/FFA important for GSIS. Increasing GL/FFA cycling by liver X receptor activation or by deletion of PKCε is associated with enhanced insulin secretion (Calkin and Tontonoz, 2012; Schmitz-Peiffer et al., 2007). Inhibition of fatty acid esterification by triacsin-C decreases the amplification of FFA of GSIS. Also, blocking lipolysis by the panlipase inhibitor orlistat curtails GSIS. Similarly, decreasing various lipase (ATGL and HSL) activities by either specific inhibitors or downregulation or gene deletion reduces GSIS (Peyot et al., 2009c; Peyot et al., 2004; Tang et al., 2013). All these reports strongly support the role of GL/FFA cycling in insulin secretion.

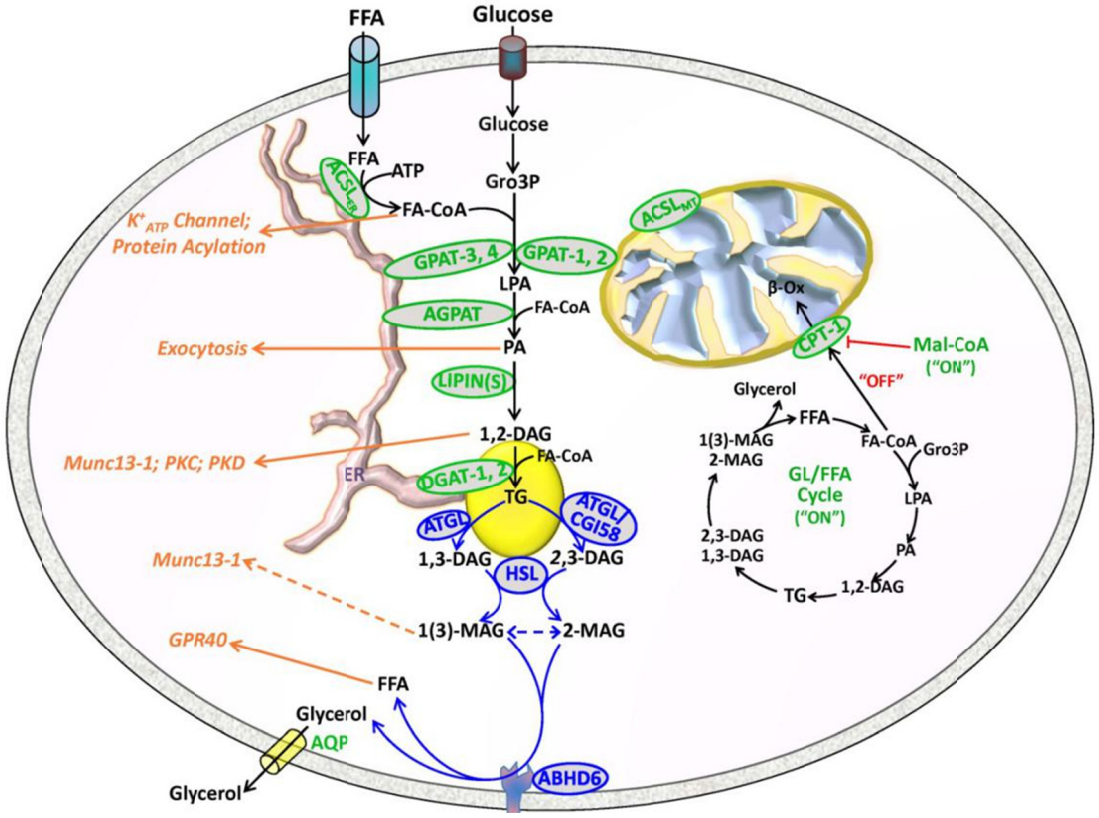

Figure 9 GL/FFA cycling and lipid signals in insulin secretion. This figure is adapted from *Cell Metab. 2013 Aug 6; 18(2):162-85*.

Different lipid species, including DAG, FFA and FA-CoA, generated via GL/FFA cycling may function as MCF to promote insulin secretion (Figure 9) (Prentki et al., 2013b). The roles of FFA and FA-CoA in insulin secretion have been discussed in the previous chapter. Nutrient inhibition of fatty acid oxidation is accompanied by elevated glycerolipid (GL) formation and

significant increases in the total mass of DAG, triacylglycerol (TG) and phosphatidic acid (PA) are shown to occur in glucose-stimulated beta cells and correlate with GSIS. Furthermore, increasing DAG levels by exogenous administration or the DAG analog PMA enhances GSIS (Zawalich and Rasmussen, 1990). However, some recent evidence in the stereospecificity of lipase questions the role of lipolysis-derived DAG in insulin secretion (Eichmann et al., 2012). It has been shown that hydrolysis of TG by ATGL generates 1,3-DAG or 2,3-DAG, other than 1,2-DAG, a classical second messenger that activate PKC and Munc13-1. Thus, DAG generated from TG hydrolysis cannot activate PKC or Munc13-1. In addition, deletion of HSL, leading to the accumulation of 2,3-DAG inside the cells, decreases GSIS. All these evidence do not favor the hypothesis that lipolysis-derived DAG is a signaling molecule in regulating insulin secretion. Besides DAG, other lipolysis-derived lipid signals that may function as MCF must be considered, in particular MAG. This stems from the observation that HSL produces MAG and HSL deletion impairs GSIS.

1.4 Adipocytes and energy metabolism

Besides the regulation of insulin secretion, pathogenesis of diabetes also has its roots in obesity. Adipose tissue, which stores fat, plays an important role in secreying several hormones and adipokines that regulate metabolic homeostasis, which is often disturbed in obese individuals. Also, adipose tissue is the prime source of circulating fatty acids, which contribute to insulin resistance, a primary problem in type 2 diabetes. Thus it is important to understand the metabolic and physiological changes in adipose tissues in relation to the pathogenesis of diabetes and obesity. With increasing rate of obesity epidemic, advances in our understanding of adipose tissue function led to the appreciation that the adipocytes are not just a lipid storage place, but also important in their function as regulators of energy metabolism. In the past few years, significant advances have been made in the classification of adipocytes as well as in deducing the mechanisms of adipocyte differentiation and development (Rosen and Spiegelman, 2014). The new roles of adipocytes in a various pathological conditions and their communication with other tissues are increasingly elucidated, giving more clues to understand metabolic diseases and shedding light on new avenues for the prevention and cure of such diseases. In this chapter, we will discuss this in more detail.

1.4.1 The different types of adipocytes and their lineage

In general, adipocytes have been traditionally classified into two different groups: white and brown adipocytes. Recently, new type of adipocytes has been identified and is named as 'beige' or 'brite' adipocytes (Wu et al., 2012). Regarding the differences and similarities among white, brown and beige adipocytes in lineage and relative contribution to overall energy metabolism, progress has been made but much is still unknown.

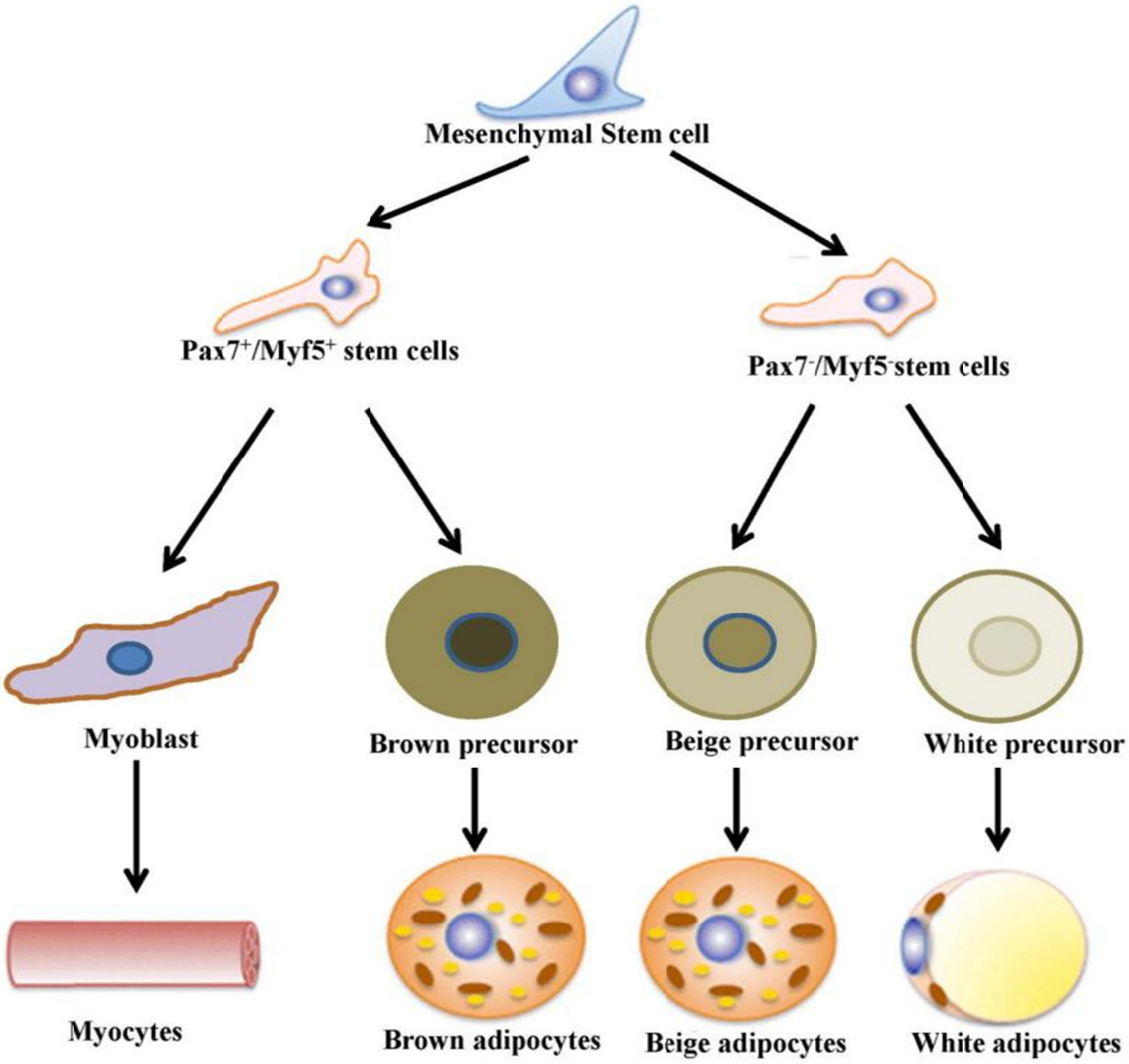

Figure 10 Lineage of white, beige and brown adipocytes. The detailed decription of this figure could be found in the text.

1.4.1.1 White adipocytes

Mature white adipocytes contain large lipid droplets and nucleus squeezed at the periphery. Generally speaking, in non-overweight healthy humans, white adipocytes make up 20% of total body weight in man, while up to 25% in women. Depending on its location, white fat can be further divided into visceral and subcutaneous fat. Visceral fat is generally regarded as "bad fat" because of its close relationship with metabolic disease, while subcutaneous fat has protective effect. However, this classification is oversimplified, as clear distinctions between visceral fat depots, such as perigonadal and retroperitoneal fat, have been observed. Also, the fat depots in humans cannot be easily correlated with those in mice, as the vast majority of visceral fat in human is found in the omentum, while it is barely detectable in mice. In contrast, epididymal fat in mice is generally regarded as representative of visceral fat, while in human, it does not exist.

Visceral fat and subcutaneous fat behave differently, as they display different rates of lipogenesis and lipolysis as well as different adipokine secretion. There is still no clear explanation for these differences. Some evidence suggests that these difference are intrinsic, as transplanted visceral fat into subcutaneous region shows no effect on energy metabolism, whereas transplantation of subcutaneous fat into visceral depot clearly shows protective effect in reducing adiposity and improving glucose tolerance (Tchkonia et al., 2013; Tran and Kahn, 2010).

Regarding the developmental origins of white adipocytes, it is not completely understood (Figure 10). With new technologies developed, it has been shown that adipocytes originate from mesenchyme. The earliest observation, dated from 1965, showed that a cluster of blood vessels, named as "primitive organ", identified in different species, such as mice and humans, become a fat pad in the later time point during development. This observation is strongly supported by lineage-tracing experiments. Besides the primitive organ, it seems that part of the adipocytes may originate from a subpopulation of endothelial cells as identified by a different lineage-tracing using the VE-cadherin promoter derived cre recombinase (Tran et al., 2012). However, this finding could not be repeated by another linage-tracing study (Berry and Rodeheffer, 2013). Also, since 1944, it has been suggested that some adipocytes develop from hematopoietic precursors. With help from sophisticated imaging and bone marrow transfer

techniques, one group was able to prove this hypothesis (Berry and Rodeheffer, 2013; Majka et al., 2010). It may be true that a small population of white adipocytes may originate from hematopoietic precursors, but this may not be the major pathway as later studies suggested.

With nutrient oversupply, adipocytes need to dramatically alter their dimensions. This can be achieved by two different ways: one is to increase the cell volume (hypertrophy); the other is to increase cell number by proliferation and /or differentiation of preadipocytes (hyperplasia). Recent studies have shown that adipose hypertrophy and hyperplasia both exist in response to over-nutrition (Wang et al., 2013c). Some isotope labeling experiments suggest that adipocytes number is fixed during childhood, and it is hard to lose, as dramatic weight loss only reduces the cell volume rather than cell number (Eto et al., 2012). This statement does not mean that adipocytes never die, and it just indicates that the birth and death rates are well-matched to keep the stable number.

1.4.1.2 Brown adipocytes

Compared to white adipocytes with a big lipid droplet, brown adipocytes contain many small lipid droplets and high density of mitochondria. Brown adipocytes are found in most of the mammals, to less extent in protoendothermic animals. Human newborns possess significant amount of brown adipose tissue to protect them from cold environments. Until recently the presence of brown adipose in adult humans and its relative contribution to overall energy metabolism were thought to be minimal or insignificant. With the new technology of PET scan with 18F-fluorodeoxyglucose (18FDG), human brown adipose tissue was identified in different regions of human body and was shown to effectively oxidize glucose and FFA under cold exposure (Sacks et al., 2009). This is encouraging, considering the main function of brown adipose is in dissipating stored chemical energy in the form of heat, especially in the face of energy oversupply in the modern society (Sidossis and Kajimura, 2015).

The main function of brown adipose is in non-shivering thermogenesis, for which, the uncoupling protein 1 (UCP1), a specific protein highly expressed in brown adipocytes, is responsible. UCP1 is generally located and densely packaged in the mitochondria. Once activated by long-chain fatty acids, UCP1 catalyzes proton leak across the inner mitochondrial membrane, resulting in uncoupling of mitochondria during glucose or FFA oxidation leading

to heat generation rather than ATP production. Many hypotheses have been proposed to explain how UCP1 works inside the cells. One recent study implied that UCP1 may function as a long-chain fatty acid /H+ synporter as UCP1 effectively operates as a H(+) carrier activated by long chain fatty acids (Fedorenko et al., 2012).

Regarding the origin of classical brown adipocytes, it was initially hypothesized that they have the same origin as white adipocytes, as they both share so many similarities (Figure 10). However, this hypothesis has been proved to be incorrect. Multiple evidences show that brown adipocytes have a totally different origin compared to white adipocytes. Over the last few years, evidence has favored the notion that classical brown adipocytes and muscle cells share the same or similar precursor. This notion is proved with the identification of the transcription cofactor PRD1-BF-1-RIZ1 homologous domain-containing protein-16 (PRDM16), a dominant regulator of brown fat development. With deletion or down-regulation of PRDM16 in primary brown adipocytes, brown adipocytes are switched to skeletal muscle; in contrast, overexpression of PRDM16 in skeletal muscle, a phenotypic switch to classical brown adipocytes is seen (Cohen et al., 2014; Kajimura et al., 2009; Seale et al., 2008). Moreover, using lineage-tracing techniques with muscle-selective myogenic factor 5 (Myf5)-Cre, classical brown adipocytes and skeletal muscle were shown to be derived from the same precursors. These observations strongly support the hypothesis that classical brown adipocytes and skeletal muscle derived from the same or similar precursors, also explains why some myogenic genes exists in brown preadipocytes.

Considering the role of classical brown adipose in energy metabolism, it may be an effective and potential therapeutic target to combat against obesity. Based on some calculations made in mice, it is estimated that 40-50g of brown fat could account for 20% of total energy expenditure (Cannon and Nedergaard, 2004). However, this calculation cannot be applied to human beings at the thermoneutrality conditions in the modern society. Nevertheless, brown fat still accounts for a high portion of human energy expenditure, approximately from 2.7% to 5% depending on the body size (van Marken Lichtenbelt and Schrauwen, 2011).

Brown fat therapy is proven to be successful in rodents, as increasing brown fat mass greatly improves glucose homeostasis (Schrauwen et al., 2015). Transplantation of brown adipocytes to adult mice increases glucose tolerance on chow diet and protects the mice from diet-induced

obesity. These beneficial effects are dependent on circulating IL-6, as transplantation of brown adipocytes isolated from mice deficient in IL-6 lose the protection effect (Liu et al., 2013). Surprisingly, transplantation of embryonic brown fat adipocytes into streptozotocin (STZ)-treated mice reversed STZ-induced type 1 diabetes (Gunawardana and Piston, 2012, 2015). This effect is independent of increased insulin secretion, and indeed depends on increased circulating adiponectin and lepin levels, as leptin has been shown to reverse STZ-induced diabetes in mice. However, the results of clinical trials in humans to increase brown fat mass are not promising, so far (Grundlingh et al., 2011). Some chemical agents, such as dinitrophenol, were shown some 40 years ago to have beneficial effects to induce weight loss; however, these agents are associated with major side effects, such as rash, cataracts, and hyperpyrexia and are not considered anymore. Other classical brown fat inducers, such as catecholamine and thyroid hormone, cannot be used in humans, as high doses of catecholamine and thyroid hormones lead to some side effects, such as increasing blood presssure. Beta3-adrenergic receptor-specific agonists increase brown fat mass and non-shivering thermogenesis in rodents and was thought as a promising way to use in humans; however, selection of an agonist specifically targeting this receptor in human has proven difficult. As cold exposure is effective in increasing brown fat mass and activity, simple cold-exposure could perhaps be enough to reach beneficial effect in humans. However, this is quite difficult to practice in real life. Based on these, we still have a long way to go to harness brown fat for the therapy of metabolic syndrome related disorders.

1.4.1.3 Beige adipocytes

Beige adipocytes are a distinct type of thermogenic adipocytes that share some similarities and distinctions to both white and brown adipocytes. Under normal conditions, they express extremely low levels of UCP1 and store excess energy in lipid droplets, similar to white adipocytes. However, under some physiological conditions, such as cold exposure or exercise, beige adipocytes express high amounts of UCP1 and greatly increase non-shivering thermogenesis, similar to classical brown adipocytes (Wu et al., 2012). Also, beige adipocytes show a unique gene signature compared to brown and white adipocytes, such as T-box transcription factor-1 (TBX-1), transmembrane protein 26 (Tmem26) and an inducible T-cell costimulatory receptor CD137, which form gene makers for selecting beige adipocytes (Wu et

al., 2012). Beige adipocytes are enriched in inguinal and retroperitoneal fat, and to a lesser extent in perigonadal fat. Recent studies show that the identified brown adipocytes in adult human are mainly composed of beige adipocytes, which provide a basis for studying the importance of this new cell type in treating metabolic disorders (Sharp et al., 2012).

Beige adipocytes were only identified in recent years, however, the existence of UCP1 positive cell in white fat depots is known since decades but with poor characterization. Recent studies helped in understanding their function better by isolation and immortalization of beige preadipocytes cell lines, providing a 'pure' system to investigate the specific gene signatures as well as the specific roles in cell function (Wu et al., 2012).

The precursors of beige adipocytes appear to be totally distinct from classical brown and white adipocytes (Figure 10). Lineage-tracing experiments indicate that beige adipocytes are not derived from Myf5 positive cells, which give rise to brown adipocytes. At least two dominant hypotheses are proposed to explain the origin of beige adipocytes. One hypothesis states that the beige adipocytes originate from transdifferentiation of existing mature white adipocytes. This notion is supported by the observation showing no proliferation in the formation of beige adipocytes during cold exposure or β3 agonist treatment. The second hypothesis favors that beige adipocytes originate from specific precursors within white adipocytes depots. This hypothesis has gained more support by gene-lineage study. Thus, after cold exposure, new adipogenesis is required for forming beige adipocytes; these beige adipocytes, upon removing cold stress, switch to white adipocytes (Ye et al., 2013). This pattern could be repeated several times, suggesting one unique precursor plays an important role in this process. Further studies indicate that beige adipocytes could be induced only from a small portion of stromal vascular fraction, indicating the existence of different precursors from white adipocytes. With a ribosomal profiling approach, it has been shown that approximately 20% beige adipocytes are derived from smooth muscle-like precursors (Long et al., 2014). So far, it is still hard to make any conclusion with regard to the origin of beige adipocytes, due to the different technical issues raised from the specificity of antibodies used for sorting or staining, together with some leakage of different Cre mice used in lineage tracing studies. However, with development of new techniques, the origin of beige adipocytes should be solved rapidly.

Since both beige and brown adipocytes express UCP1, it is important to address whether these two types of adipocytes have similar functions. The simple answer to this question is still unknown. Some reports indicate that beige adipocytes have the same capacity as classical brown adipocytes to induce UCP1 expression, indicating they may play similar role in non-shivering thermogenesis. Besides this, whether beige and classical brown adipocytes have some cell type specific roles is still unknown. It is likely that beige and brown adipocytes may have different secreting adipokines, which may directly affect whole body metabolism. It has been shown that classical brown adipocytes secrete an epidermal growth factor (EGF) family member extracellular ligand- neuregulin 4 (Nrg4), a brown adipocytes specific endocrine factor that shows therapeutic potential for the treatment of obesity-associated disorders, including T2D and nonalcoholic fatty liver disease (NAFLD) (Wang et al., 2014).

1.4.2 Adipocyte 'browning pathways' and signals

As a new type of thermogenic fat, beige adipocytes hold tremendous promise for treating obesity, T2D and its associated disorders. The existence of beige adipocytes in adult humans and the established beneficial effects of increasing beige adipocytes in mouse models point towards the significance of studies that identify agents or therapies to induce browning of white adipocytes. In this chapter, we will focus on adipocyte browning pathways and signals, and we will discuss various agents and pathways that modulate the activity of beige adipocytes (Figure 11).

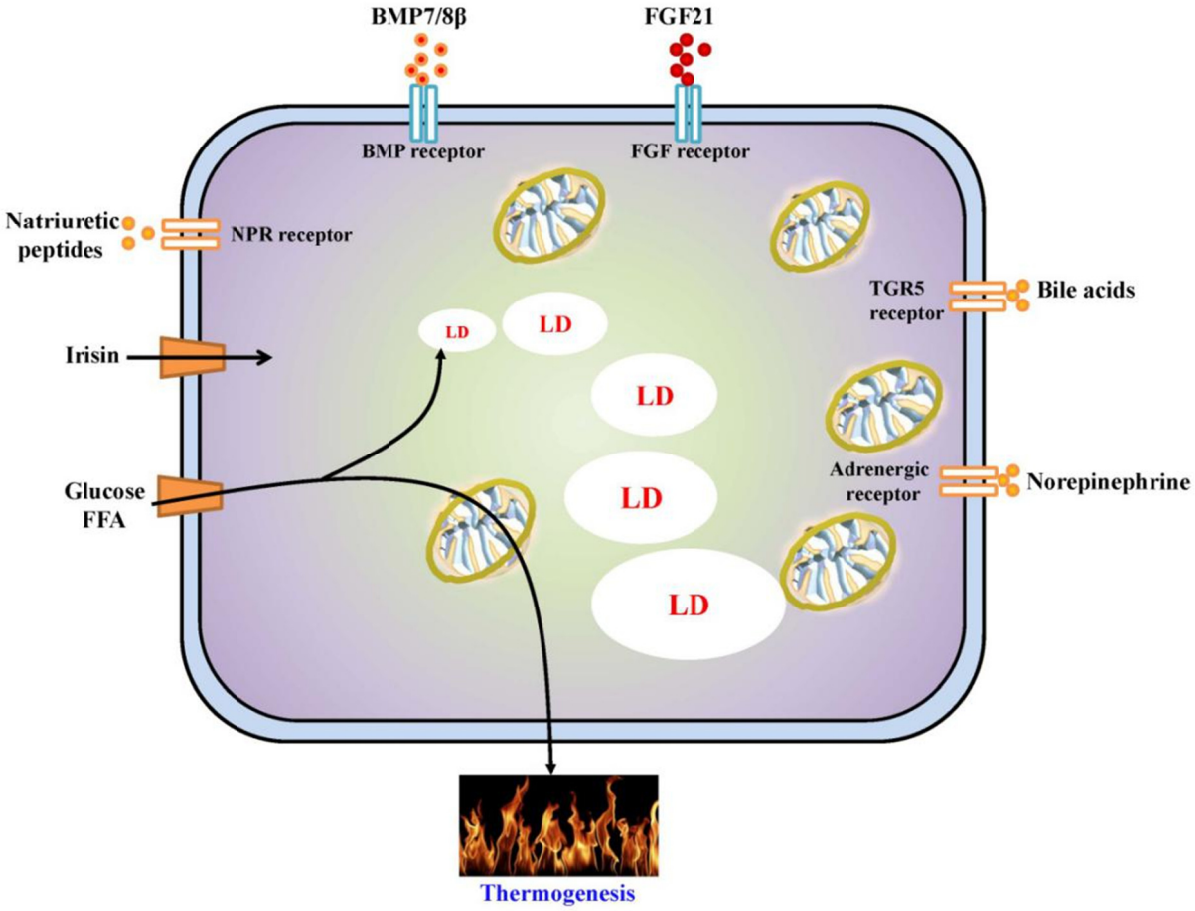

Figure 11 Different agents induced browning of white adipocytes. Many physiological intervention and some peptides have been shown to induce browning of white adipocytes via binding their specific receptor. LD, lipid droplets; TGR5, G protein-coupled bile acid receptor 1; BMP, Bone morphogenetic protein.

1.4.2.1 Cold exposure

In response to cold exposure, non-shivering thermogenesis is increased in most young and middle-aged human beings to maintain normal body temperature. The increased non-shivering thermogenesis is mainly conducted by classical brown adipocytes and inducible beige adipocytes, whose existence in adult human is now widely accepted (Cypess et al., 2009; Sidossis and Kajimura, 2015; Virtanen et al., 2009). Cold exposure is the most efficient way to induce beige adipocytes formation and to enhance brown fat function. It has been shown that acute cold acclimatization recruits human beige/ brown adipocytes (van der Lans et al., 2013)

and enhances fatty acid oxidation as well as glucose and FFA uptake in adult humans greatly increasing whole-body energy expenditure (Ouellet et al., 2012). In T2D patients, cold-induced FFA uptake and oxidative metabolism are not defective despite reduced glucose uptake by brown/ beige fat (Blondin et al., 2015), implying that increasing thermogenesis by cold exposure may provide an efficient method to treat T2D, although it likely may prove difficult in most patients. Besides the beneficial effect in T2D, cold exposure may also be applied to treat T1D, at least in mouse model. It has been shown that browning of white adipose tissue *via* cold exposure in combination with activation of liver X receptors is an alternative and effective strategy to manage insulin-dependent diabetes in mice (Gao et al., 2015).

Cold exposure induced formation of beige adipocytes is largely dependent on the sympathetic nervous system. It has been known that central neural circuits orchestrate the homeostatic repertoire to maintain stable body temperature during cold exposure (Morrison, 2011). Based on some observations in rodents, it appears that cold sensing by skin sends signal to spinal cord and then to hypothalamus in the brain, where different signals are integrated and projects to neurons of the peripheral sympathetic nervous system (SNS), leading to the release of norepinephrine to induce UCP1 and beige adipocytes. However, the pathways of inducing beige fat are highly specific and not mimicked by generalized pharmacological activation of the SNS (Cypess et al., 2012). Besides SNS, fibroblast growth factor 21 (FGF21) and irisin were shown to participate in cold-induced increase in beige fat volume and non-shivering thermogenesis (Lee et al., 2014). FGF21 was shown to play crucial role in inducing of beige adipocytes as deletion of FGF21 in mice impairs beige fat induction and thus reduced cold-induced thermogenesis. FGF21 regulates UCP1 levels in an autocrine/paracrine manner via directly elevating the protein level of PGC-1α in adipocytes (Fisher et al., 2012). Some studies have indicated that mild cold exposure in rodents and human increases circulating FGF21 and irisin levels (Lee et al., 2014), predicting greater lipolysis and cold-induced thermogenesis (Lee et al., 2013).

1.4.2.2 **Exercise, Irisin and IL6**

The beneficial effect of exercise in combating obesity and insulin resistance is well-established. Exercise is known to reduce the risk of coronary heart disease, osteoporosis, and

colon and breast cancer in humans. Besides this, exercise can improve life quality by improving mental well-beings and reducing clinical depression. Participation in an exercise training program has moderately positive effects on sleep quality in middle-aged and older adults (Yang et al., 2012). Of special interest, the beneficial effect of exercise persists also in the people with T2D and to some extent, in the people with T1D (Chimen et al., 2012). It has been shown that exercise increases insulin sensitivity in normal as well as insulin resistant populations (Borghouts and Keizer, 2000). The major contribution to exercise-induced whole body glucose homeostasis is skeletal muscle (Holloszy and Coyle, 1984), and recent studies showed that subcutaneous adipocytes also play a role in exercise-induced improvement in glucose homeostasis, as mice transplanted with subcutaneous fat isolated from exercise-trained mice show better glucose tolerance with a significant increase in glucose uptake by soleus muscle and brown fat (Stanford et al., 2015; Wallberg-Henriksson and Zierath, 2015). However, it is still not clear whether the protective effect of subcutaneous fat is dependent on exercise-induced browning of white adipocytes, as many reports in rodents strongly support that exercise-derived secreted myokines, such as irisin, promote browning of white adipocytes and thus increase whole body energy expenditure during exercise (Bostrom et al., 2012; Kelly, 2012).

Irisin, a newly identified exercise-associated hormone, is cleaved from a type 1 membrane protein named “fibronectin type III domain containing 5” (FNDC5), and then secreted mainly by skeletal muscles and partially by subcutaneous fat (Roca-Rivada et al., 2013) into circulation and promotes browning of white adipocytes. This browning effect induced by irisin is possibly mediated by activation of extracellular signal–related kinase (ERK) and p38 protein kinase signaling cascades (Wu and Spiegelman, 2014; Zhang et al., 2014c).

Considering the beneficial effects of irisin in inducing browning of white adipocytes and improving metabolic health in mice, it gained great interest over the last three years to translate these findings from mice to human. Even though there were some doubts, the existence of irisin in human plasma is confirmed (Swick et al., 2013) with different antibodies and methods and its levels are negatively correlated with T2D, as circulating irisin levels are not detectable in human subjects with T2D, compared to normal people (Choi et al., 2013; Park et al., 2013a). However, the positive correlation of irisin levels and exercise is not

consistently observed in humans. In one study, the parent polypeptide FNDC5 mRNA is reported to increase in skeletal muscle in exercise-trained aged humans (Bostrom et al., 2012), while in other studies, no difference or decrease of FNDC5 levels are observed in endurance trained humans (Lecker et al., 2012; Norheim et al., 2014; Pekkala et al., 2013). Also, the role of irisin in inducing browning of human pre-adipocytes is not observed, raising great concerns regarding the possible role of irisin as a potential therapeutic agent in humans. Further studies reveal that there are some differences in start codon of irisin between human and rodents, which greatly affect the efficiency of translation (Raschke et al., 2013). This difference may help explain the inconsistent observation between rodent and human studies. More experiments are needed to confirm the beneficial effect of irisin in humans, including inducing browning of white adipocytes and improve metabolic health.

Besides irisin, interleukin (IL)-6 released during exercise is shown to play important role in inducing browning of white adipocytes (Knudsen et al., 2014). As a cytokine, IL-6 is produced and released from many cell types, including skeletal muscle during contraction. It has been demonstrated that IL-6 promote lipolysis, fatty acid oxidation and glucose uptake in skeletal muscle (Pedersen, 2007). Recent study indicates the beneficial effect of IL-6 in glucose and fatty acid metabolism is partially explained by induction of beige adipocytes. IL-6 is necessary for exercise-induced beige adipocytes formation, as deletion of IL-6 in mice impairs exercise-induced browning effect. The browning effect induced by IL-6 may be associated with the activation of 5' AMP-activated protein kinase (AMPK), which is an important regulation factor in inducing beige adipocytes.

1.4.2.3 Hormones and peptides

Sympathetic neuronal activity is undoubtedly a physiological signal to induce beige adipocytes and enhance brown fat activity. Besides this, several other hormones and peptides, including norepinephrine, FGF21, irisin, bone morphogenetic protein (BMP)-7, BMP4, BMP8b, vascular endothelial growth factor (VEGF), natriuretic peptides, prostaglandin, thyroid hormone, insulin and leptin are also regulators of beige adipocytes. In the previous chapter, we already discussed about the role of norepinephrine, FGF21 and irisin; we will now focus on other hormones and peptides.

As multi-functional growth factors, bone morphogenetic proteins (BMPs) belong to the transforming growth factor (TGF)-beta superfamily. It is well-documented that BMPs are implicated in the regulation of cell proliferation, survival, differentiation and apoptosis. Recent studies indicate that BMPs regulate adipogenesis. While BMP4, mainly secreted by white adipose cells, acts as an integral feedback regulator of both white and beige adipogenic commitment and differentiation (Qian et al., 2013), BMP7 and BMP8b induce both brown and beige adipogenesis in rodent and human progenitors (Okla et al., 2015; Whittle et al., 2012). BMPs may act through enhanced p38MAPK/CREB signaling and increased lipase activity to induce browning effect.

VEGF was shown to be an important regulator of angiogenesis during embryogenesis, reproductive function and skeletal growth. It has been implicated in many pathological conditions, such as tumors and neovascular disorders (Ferrara et al., 2003). Recent study has revealed a new role of VEGF in adipocytes: it promotes survival, proliferation and normal mitochondrial development (Bagchi et al., 2013) and in white adipocytes, it induces beige adipocytes formation. Overexpression of VEGF-A specifically in adipocytes improves vascularization and causes a "browning" of white adipose tissue, with massive up-regulation of UCP1 and PGC1α. As a consequence, the mice show increased energy expenditure and are resistant to diet-induced obesity (Sun et al., 2012).

Natriuretic peptides (NP) can be divided into three different subgroups: atrial NP (ANP), brain NP (BNP) and C-type NP (CNP). These peptides are predominantly released from the heart in response to heart failure and increased pressure and play important roles in reducing blood volume, blood pressure and cardiac output. Recent studies indicate that NPs also play some roles in regulating lipolysis in adipocytes and induce beige adipocytes formation in mouse and humans (Bordicchia et al., 2012). This is associated with increased heat production and weight loss in mice. NPs promote browning of white adipocytes in a cell-autonomous manner. Mechanistically, NPs activate cyclic GMP-dependent protein kinase (PKG), which acts in parallel with beta-adrenergic-PKA pathway to increase lipolysis and thermogenesis. Besides PKG, some reports suggest that p38/MAPK pathway may play a role in NP-induced browning, but not yet confirmed.

As FFA-derived lipid species, the prostaglandins (PG) have multiple functions, such as regulation of blood pressure, blood clotting and induction of child birth. Recent study showed that PGs are important regulators of beige adipocytes. The rate-limiting step in the synthesis of PG is catalyzed by cyclooxygenase-2 (COX2), a key regulator of local PG levels. Increased PG levels by increasing COX2 activity was shown to increase beige adipocyte formation in both subcutaneous and visceral fat depots. Beta3-adrenergic receptor agonist increases COX2 in parallel with increasing browning of white adipocytes. Deletion of inhibition of COX2 in mice impairs β3-adrengergic receptor agonist-induced browning effect in white fat depots, rather than brown fat. Overexpression of COX2 in mice is sufficient to increase thermogenesis and protects the mice from diet-induced obesity (Vegiopoulos et al., 2010). Currently, it is still not clear through which pathway PGs regulate beige adipocytes formation.

Thyroid hormones play crucial roles in regulating the differentiation in many tissues, including preadipocytes differentiation (Obregon, 2014). Also, thyroid hormones T3 and T4 regulate adiponectin and its receptors' *AdipoR1* and *AdipoR2* gene expression in adipose tissue at the translation levels (Seifi et al., 2013; Seifi et al., 2012). T3 is much more active one and it is converted from T4 by the enzyme type II iodothyronine deiodinase (DIO2). T3 regulates genes involved in lipogenesis, lipolysis, thermogenesis, mitochondrial function and transcription factors. In the fully differentiated human mature adipocytes, T3 treatment increases UCP1 levels and oxygen consumption via binding to thyroid hormone receptor β (Lee et al., 2012a). However, abnormally high circulating thyroid hormone levels in human may not increase beige or brown adipose tissue activity (Zhang et al., 2014b).

Insulin and leptin work together on hypothalamic neurons to induce browning of white adipocytes and weight loss (Dodd et al., 2015). Mice deficient in PTP1B phosphatase have enhanced insulin and leptin signaling in proopiomelanocortin (POMC) neurons and are resistant to diet-induced obesity because of increased energy expenditure conducted by beige adipocytes. Also, increased insulin and leptin levels by intracerebroventricular infusion or activation of POMC neurons also increased browning of white adipocytes. All these results reveal an important role of insulin and leptin in adipocytes biology.

1.4.2.4 Metabolites and browning

Some metabolites, such as lactate, β-aminoisobutyric acid (BAIBA), retinoic acid and prostaglandins, have been shown to induce formation of beige adipocytes. Here, we will discuss the effects of metabolites that can induce browning.

Lactate provides fuel for different organs, such as liver and brain and some studies showed that lactate may act as a signaling molecule (Brooks, 2009). After production during exercise, lactate can be shuttled between white-glycolytic and red-oxidative fibers in muscle, or between different organs, including skeletal muscle, heart, liver and brain. Exchange of lactate to pyruvate in peroxisomes regulates cell redox state and may function as a ROS generator. High levels of circulating lactate in blood leads to reduced uptake of glucose and FFA by various organs. Also, in adipocytes, lactate may directly regulate metabolism via binding to G-protein coupled receptor to inhibit lipolysis to feedback to the circulating FFA levels (Liu et al., 2009). In line with a role in regulation of cell redox state, recent study indicates that lactate induces browning of white adipose cells with elevation of UCP1 levels in rodent and human adipocytes. Lactate-induction of UCP1 is probably mediated by changes in cell redox state following lactate transport via monocarboxylate transporters. This regulation is apparently dependent on PPARγ signaling rather than hypoxia-inducible factor-1α (HIF1α) and PPARα pathways (Carriere et al., 2014).

Besides lactate, ß-aminoisobutyric acid (BAIBA) appears to play an important role in browning of white adipocytes (Kammoun and Febbraio, 2014; Roberts et al., 2014). BAIBA is a catabolite of thymine metabolism and is derived from thymine of both DNA and transfer RNA. Its determination can be used to probe the metabolism of DNA and RNA in normal and tumoral tissues (Nielsen et al., 1974) and it is a biomarker for some cancers. The beneficial effect of BAIBA has been reviewed recently (Begriche et al., 2010). BAIBA can regulate body fat mass and lipid homeostasis through its direct role in liver and adipocytes (Jung et al., 2015). In liver, BAIBA increases fatty acid oxidation, reduce inflammation and *de novo* lipogenesis in a leptin-independent manner, while in adipocytes, it increases leptin secretion, fatty acid oxidation and reduces the weight of visceral fat. Further study shows that the beneficial effect in adipocytes is mediated by the browning effect induced by BAIBA in a PPARα-dependent manner (Begriche et al., 2010).

Retinoic acid is derived from vitamin A and was originally shown to play an important role in growth and development. Recently, increasing evidence shows that it functions as a strong regulator of intercellular metabolism and induction of beige adipocytes. Administration of retinoic acid to murine 3T3-L1 white adipocytes leads to increased lipolysis and fatty acid oxidation as well as expression of some regulatory genes implicated in this process (Mercader et al., 2007). In line with this, increasing level of retinoic acid increases UCP1 levels in a cell-autonomous manner in isolated mouse pre-adipocytes (Mercader et al., 2010). Chronic retinoic acid-treated mice show increased thermogenesis and are resistant to diet-induced obesity with great improvement in glucose tolerance (Bonet et al., 2012). The possible mechanism for retinoic-acid induced browning may lie in PPAR activation. The activity of PPAR requires heterodimerization with retinoid X receptor (RXR), which also binds to and forms heterodimer in a specific DNA region with the retinoic acid receptor (RAR). The ability of RXR to bind both PPAR and RAR affects its transcriptional activity. Some studies show that retinoic acid-induced browning is dependent on P38-MAPK signaling, which could link between retinoid acid and PPAR activation (Yu et al., 2012).

Long-chain n-3 polyunsaturated fatty acids, such as eicosapentaenoic acid (EPA; 20:5 n−3) and docosahexaenoic acid (DHA, 22:6 n−3), have been implicated in the browning process of white adipocytes. EPA and DHA are enriched in marine fish oil, whose intake shows beneficial effect in reducing weight gain and visceral fat mass in mice. The beneficial effect may be associated with the browning effect. The mechanism possibly involves PPAR activation, as DHA and EPA are efficient ligands for various PPARs (Peters et al., 2001).

1.4.2.5 Gene-manipulations and browning

Manipulation (overexpression, knockdown or knock out) of many genes in mice protect from diet-induced obesity and are associated with browning effect in white adipocytes. Because of space limitation, we will not include all these genes here. We only discuss some key transcriptional factors (e.g. PRDM16 and PGC1a) and lipase genes (e.g. ATGL and HSL) that code for metabolic enzymes in GL/FFA cycling.

<u>PRDM16</u>

PR Domain containing 16 (PRDM16) is a transcriptional factor that contains a large zinc finger and plays crucial roles in adipocytes differentiation and in the formation of beige adipocytes. PRDM16 is highly expressed in brown adipocytes in mouse and human and acts as a driver for brown adipocytes fate. Overexpression of PRDM16 in myoblasts leads to a brown adipocytes phenotype (Kajimura et al., 2009), while silencing of this gene in brown adipocytes impairs the thermogenic program and increases some muscle-specific genes. Besides the role in brown fat cell differentiation, PRDM16 also plays a role in the formation of beige adipocytes. The level of PRDM16 is higher in fat depots prone to become beige adipocytes (Cohen et al., 2014). In line with correlative expression level results, down-regulation of PRDM16 in white adipocytes *in vitro* decreases the induction of thermogenic program and impairs the browning response after cold exposure, while overexpression of PRDM16 increase the formation of beige adipocytes and protects mice from diet-induced obesity (Seale et al., 2011). Recently, adipocytes-specific PRDM16-KO mice have been generated and studies with these mice strongly support the role of PRDM16 in the induction of beige adipocytes (Cohen et al., 2014).

Peroxisome proliferator-activated receptor gamma coactivator 1- alpha (PGC1α)

As a transcription co-activator, PGC1α is implicated in the regulation of energy metabolism via modulating mitochondrial biogenesis and promoting remodeling of muscle fiber composition to more oxidative and less glycolytic capacity (Liang and Ward, 2006). PGC1α can directly interact with cAMP response element-binding protein (CREB), which builds a link between external stimuli driving cAMP signaling to mitochondrial biogenesis. Also, evidence shows that PGC1α is highly induced by cold exposure (Puigserver et al., 1998), which may offer a link for PGC1α in browning of white adipocytes (Enerback, 2010). PGC1α has been shown to directly induce UCP1 and other browning markers in white adipocytes. Further studies have been shown that PGC1α is essential for cold-induced browning of white adipocytes (Bostrom et al., 2012). Thus, PGC1α can be regarded as a central transcriptional effector in inducing browning of adipocytes. However, mice deficient in PGC1α develop normal brown adipocytes, indicating that PGC1α does not participate in the development of brown adipocytes.

UCP1

Expression of UCP1 is a gold standard marker for browning of white adipocytes, and modulation of UCP1 levels affects non-shivering thermogenesis. Consistent with this, transgenic expression of UCP1 in adipocytes increases thermogenesis and prevents diet-induced obesity (Stefl et al., 1998). Deletion of UCP1 in mice accelerates diet-induced obesity and abolishes diet-induced thermogenesis under thermoneutral conditions (Feldmann et al., 2009). However, when UCP1 deficient mice are placed at normal temperature (22℃), they only show cold-sensitivity, but do not become obese on chow diet or HFD (Enerback et al., 1997), indicating the importance of other sources of thermogenesis in regulating body weight.

Forkhead box protein C2 (FoxC2)

As a forkhead/winged helix transcription factor, FoxC2 has been shown to regulate both beige and brown adipocyte function. Overexpression of FoxC2 in white adipocytes leads to browning of white adipocytes with significant increase in mitochondrial density and thermogenic gene expression, including UCP1 (Cederberg et al., 2001). As a result, these mice show higher insulin sensitivity and are resistant to diet-induced obesity. These beneficial effects are mediated by β-adrenergic receptor-cAMP-PKA pathway possibly due to the direct induction of RIα subunit by FoxC2 (Cederberg et al., 2001).

Receptor interacting protein (RIP140)

As a nuclear receptor, RIP140 plays important role in regulating lipid and glucose metabolism via modulating gene expression in different metabolic tissues, such as skeletal muscle and liver. In adipocytes, RIP40 can directly interact with PGC1α and block its ability to induce browning of white adipocytes (Chechi et al., 2013). Overexpression of RIP140 in adipocytes decreases the expression of thermogenic gene and oxidative metabolism. In contrast, deletion of RIP140 in adipocytes induces browning of white adipocytes (Leonardsson et al., 2004).

ATGL

During formation of beige adipocytes, dynamic change has been observed in lipid droplet associated proteins to increase lipolysis rate, which facilitate the transformation from the white adipocytes-like to brown adipocyte-like shape (Barneda et al., 2013). As a rate-limiting step in lipolysis, ATGL activity is crucial in controlling of energy metabolism. Deletion of ATGL in

mice impairs lipolysis, and results in TG accumulation in different tissues, including heart, which makes the mice to develop cardiac related problems at early age. These mice show cold intolerance, which may result from decreased thermogenesis (Haemmerle et al., 2006). Further study indicates that ATGL is regulated by AMPK and is required for a browning phenotype (Ahmadian et al., 2011). In consistent with this, mice with overexpression of ATGL are resistant to diet-induced obesity (Watt and Spriet, 2010).

G0/G1 switch gene 2 (G0S2) is a protein that interacts with and inhibits ATGL activity (Cerk et al., 2014; Lu et al., 2010). Deletion of G0S2 in mice increases ATGL activity, improves acute cold intolerance, increases browning of white adipocytes and allows resistance to diet-induced obesity (El-Assaad et al., 2015; Ma et al., 2014).

Stearoyl-CoA desaturase-1 (SCD1)

SCD1 catalyzes the rate-limiting step in the synthesis of unsaturated fatty acids and is an important regulator of whole body energy homeostasis. Mice with skin-specific deletion of SCD1 display severe cold intolerance because of rapid depletion of fuel substrates to maintain core body temperature, and show increased browning of white adipocytes and enhanced brown fat activity (Sampath et al., 2009). However, the browning effect observed in this mouse needs to be examined carefully, as there are some burning issues raised in this model (Nedergaard and Cannon, 2014). In some cases, the evidence indicates that skin and fur defects are sufficient to cause browning of white adipocytes. As SCD1 mice show skin and fur problems, the browning effect may not be related to the gene deletion mediated changes in thermogenesis *per se*, but could be simply explained by improper fur development.

Monoacylglycerol lipase

Overexpression of MAGL in mouse forebrain neurons decreases MAG levels in forebrain, and protects the mice from diet-induced obesity. The beneficial effect is partially mediated by effects on brown adipocytes. How MAG levels in the brain regulate brown adipocytes is not known, and endocannabinoid 2-arachidonoyl-sn-glycerol signaling may be involved (Jung et al., 2012).

Elongation of very long chain fatty acid protein 3 (ELOVL3)

The fatty acid elongase ELOVL3 is the rate-limiting enzyme in the synthesis of C20-C24 saturated and monounsaturated very long chain fatty acids (VLCFAs) in different tissues, including brown and white adipose tissues (Westerberg et al., 2004). During cold exposure, the mRNA level of ELOVL3 is increased 200 fold and this correlates with the higher rate of lipid mobilization (Westerberg et al., 2006). Ablation of ELOVL3 leads to constrained expansion of adipose tissue, and resistance against diet-induced obesity. The basis for these phenotypes may lie in increased energy expenditure induced by increased browning of white adipocytes (Zadravec et al., 2010). Female mice show more pronounced phenotype than male mice for unknown reasons. However, ELOVL3 has been shown to play an important role in skin barrier, so the browning effect induced by deletion of ELOVL3 needs to be interpreted with caution (Westerberg et al., 2004).

1.4.3 Peroxisome proliferator-activated receptors (PPARs) in energy metabolism

The nuclear receptor PPARs play crucial roles in regulating energy homeostasis. The different isoforms of PPARs show distinct yet overlapping functions and wide tissue distribution. PPARs regulate different gene expression at the transcriptional levels to modulate different aspects of energy metabolism. Reduced activity of these receptors by down-regulation or gene deletion leads to a variety of metabolic diseases, while increasing the activity by some specific agonists provides many metabolic benefits. Studies on these receptors have greatly increased our knowledge with regard to regulation of energy metabolism at the molecular levels and pave the road to design new therapies for the metabolic syndrome (Wang, 2010).

1.4.3.1 PPAR isoforms and their tissue distribution

So far, three different PPARs have been cloned and identified: PPARα, PPARβ and PPARγ. PPARα is the first PPAR to be cloned in 1990s by Stephen Green. The expression of PPARα is different between rodents and humans. In rodents, it is shown to be widely expressed among different tissues: the highest expression of PPARα is found in liver and brown adipocytes, followed by heart and kidney, and then lower expression in small and large intestine, skeletal muscle and adrenal gland (Braissant et al., 1996). However, in humans, it is equally expressed among tissues with higher expression in liver, intestine, kidney and heart (Auboeuf et al., 1997); Compared to PPARα, PPARβ is equally distributed in different tissues. It has been

shown to express in a variety of tissues/cells in multiple systems including cardiovascular, urinary, respiratory, digestive, endocrine, nervous, hematopoietic, immune, musculoskeletal, sensory and reproductive organ systems (Higashiyama et al., 2007); PPARγ is highly and specifically expressed in adipocytes and immune system, and seldom expressed in other tissues (Jones et al., 2005).

1.4.3.2 PPARs and lipid metabolism

PPARα plays an important role in regulating liver and skeletal muscle lipid metabolism and glucose homeostasis. Activation of PPARα by endogenous ligands is a mechanism to sense the circulating levels of endogenous FFAs or their derivatives and regulate the expression of various genes that code enzymes and some protein transporters to maintain lipid homeostasis by stimulating FA oxidation and increasing lipoprotein metabolism (Fruchart et al., 1999). Also, PPARα plays a role in cholesterol homeostasis as its activation prevents excess cholesterol accumulation in macrophages by increasing cholesterol efflux from these cells. Mice deficient in PPARα are intolerant to fasting, and display high serum apoB associated with VLDL and increased hepatic triglyceride secretion and liver steatosis (Higashiyama et al., 2007). Surprisingly however, mice deficient in PPARα are resistant to diet-induced obesity and show improved insulin sensitivity (Wang et al., 2013a). There is no clear explanation regarding this discrepancy with a role of this transcription factor in fat detoxification and oxidation. It may involve compensatory mechanisms related to total KO of this gene and it may also involve effects on skeletal muscles, as overexpression of PPARα leads to glucose intolerance (Iglesias et al., 2012).

Similar to PPARα, PPARβ also plays important role in regulating fatty acid oxidation in several tissues, including skeletal muscle, liver and adipose tissues. Also, some evidence indicates that PPARβ can control mitochondrial biogenesis. Activation of PPARβ stimulates keratinocyte differentiation, improves barrier homeostasis and leads to TG accumulation in keratinocytes (Woods et al., 1998). Mice deficient in PPARβ exhibit exacerbated epithelial cell proliferation and are sensitive to skin carcinogenesis (Ebbeling et al., 2012). In adipocytes, activation of PPARβ by its specific agonist GW501516 prevents IL-6-induced STAT3 activation by inhibiting ERK1/2 and preventing the STAT3-Hsp90 association (Imbeault et al., 1997) as well as ameliorating fructose-induced insulin resistance by preventing Nrf2

activation (Neel, 1999). In skeletal muscle, activation of PPARβ induces myogenesis by modulating myostain activity (Neel, 1962) as well as preventing ER stress and improving insulin resistance (Mela, 2001). In pancreatic beta cells, PPARβ regulates beta cell mass and insulin secretion (Iglesias et al., 2012).

Compared to PPARα and PPARβ, PPARγ does not play a direct role in regulating fatty acid oxidation. In contrast, it plays key role in adipocytes differentiation. In the mouse and human, PPARγ can be further divided into two isoforms by alternative splicing: PPARγ1 and PPARγ2 (Anis et al., 2010). PPARγ1 isoform is mainly expressed in liver and other tissues, whereas PPARγ2 isoform is exclusively expressed in adipose tissue to function as a regulator of adipogenesis and lipogenesis. Overexpression of PPARγ1 in mouse liver results in high induction of adipocyte-specific and lipogenesis-related genes and leads to hepatic steatosis in PPARα$^{-/-}$ mice (Halter et al., 2014). Selective deletion of PPARγ2 in adipose tissue impairs the development of adipose tissue and causes insulin resistance (Guo, 2014). Global deletion of PPARγ in mice is lethal as PPARγ is required for placental, cardiac and adipose tissue development (Astrup and Finer, 2000). Muscle specific deletion of PPARγ causes increased adiposity and insulin resistance but maintains normal response to thiazolidinediones (Relimpio, 2003). Adipocytes specific PPARγ knockout mice generated in various laboratories show different phenotypes. In one report, deletion of PPARγ in adipose tissues protects against diet-induced obesity and insulin resistance (Jones et al., 2005), while in another report it caused lipoatrophy and severe metabolic disturbance (Wang et al., 2013a). The reason for this discrepancy is currently unknown.

1.4.3.3 PPARs and browning of white adipocytes

Of all three PPARs, PPARα and PPARγ play important roles in inducing browning of white adipocytes. The role of PPARβ in adipose browning has been seldom reported. Increasing PPARα activity by the specific agonists fenofibrate or GW6471 induces beige cell formation in subcutaneous white adipocytes from diet-induced male obese mice (Rachid et al., 2015). The β-aminoisobutyric acid induced browning of white adipocytes is dependent on PPARα (Badman et al., 2007). How does PPARα induce the browning of white adipocytes? This may occur partially through FGF21, a direct target of PPARα that clearly shows browning effects in white adipocytes (Roberts et al., 2014). Another possible explanation may lie in the direct

regulation of thermogenic gene networks. Some reports indicate that UCP1 is a direct target gene of PPARα, and that PPARα activation in white adipocytes is associated with increased UCP1 levels and browning effects (Kelly et al., 1998).

The effect of PPARγ in browning of white adipocytes is well-documented. The first observation of beige adipocytes was made with chronic treatment of white adipocytes with the PPARγ agonist rosiglitazone (Petrovic et al., 2010) This drug not only increases the expression of PGC-1α and mitochondriogenesis in these cells but also causes a norepinephrine-augmentable UCP1 gene expression in a subset adipocytes with increased thermogenic capacity. The browning effect is mediated at least in part through the stabilization of the PRDM16 protein (Ohno et al., 2012). Further studies have indicated that the browning effect induced by the PPARγ agonist leads to the formation of PPARγ "superenhancers" to maintain the browning phenotype without further requiring rosiglitazone (Loft et al., 2015).

Overall rationale and hypothesis of the thesis

The biochemical basis of fuel induced insulin secretion is not fully understood and we need to define additional metabolic coupling factors (MCF), besides adenine nucleotides, that mediate the link between glucose metabolism in the ß-cell and the exocytotic release of insulin. There is much evidence that endogenous lipid signals derived from the lipolysis segment of GL/FFA cycling in the ß-cell regulate insulin secretion. However, the molecular identity of these lipid signals is currently uncertain. In whole body or ß-cell specific ATGL KO mice there is TG accumulation in islet tissue and reduced GSIS, thus ruling out TG itself as a possible metabolic signal for insulin secretion. Therefore, downstream signals in the lipolysis cascade contribute to glucose action on insulin secretion. If DAG were a signal for GSIS, suppression or inhibition of HSL or DAG lipase, which transform DAG to MAG, should enhance GSIS rather than reducing it. However, several studies showed that HSL-KO leads to reduced GSIS, suggesting that DAG is not the lipid signal for GSIS. In addition lipolysis does not produce 1,2 DAG, a known lipid signals that activate protein kinase enzymes, but 1,3- and 2,3-DAG that are not known to possess signaling properties so far. Thus, the remaining candidate signals are MAG, FFA and glycerol. Exogenous glycerol does not alter insulin secretion and exogenous FFA cause modest restoration of GSIS in islet from ATGL and HSL KO mice. Thus, the most likely candidate signal for insulin secretion in the lipolysis cascade is MAG. It should be added that MAG is degraded by MAGL in various cell types but we find that this enzyme is poorly expressed in the ß-cell and that ABHD6 is the predominant enzyme that degrades MAG in islet tissue.

The first central hypothesis of this thesis is that lipolysis-derived MAG that is accessible to ABHD6 for its degradation functions as a MCF to promote insulin secretion in ß-cells.

Lipolysis plays an important role in regulating non-shivering thermogenesis and lipolysis-derived lipids participate in the activation of PPARα and PPARγ, even though the specific lipid involved is not yet identified. In view of our entirely novel concept that MAG acts as a signaling molecule at large and the recent evidence indicating that ABHD6 controls its degradation in many cell types, we were interested in assessing the role of MAG and ABHD6

in adipose tissues besides islets and at the whole body level. To this end we wished to study various aspects of energy homeostasis in mice deficient of ABHD6.

The second central hypothesis of this thesis is that MAG and ABHD6 play a role in energy homeostasis, body weight control and thermogenesis via MAG activation of some PPAR isoforms involved in browning of white adipocytes and brown fat function.

Article 1

α/β-Hydrolase Domain 6 accessible monoacylglycerol as a signal for glucose-stimulated insulin secretion

Authors:

Shangang Zhao[1], Yves Mugabo[1], Jose Iglesias[1], Li Xie[2], Viviane Delghingaro-Augusto[1], Roxane Lussier[1], Marie-Line Peyot[1], Erik Joly[1], Bouchra Taïb[3], Matthew A. Davis[4], J. Mark Brown[4], Abdelkarim Abousalham[5], Herbert Gaisano[2], S.R. Murthy Madiraju[1] and Marc Prentki[1]

[1] Molecular Nutrition Unit and Montreal Diabetes Research Center, CRCHUM, and Departments of Nutrition, Biochemistry and Molecular Medicine, Université de Montréal, Montréal, QC, Canada; [2]Department of Medicine, University of Toronto, Toronto, Ontario, Canada; [3] Department of Pathology and Cell Biology, Université de Montréal; [4]Section on Lipid Sciences, Department of Pathology, Wake Forest University School of Medicine, Medical Center Boulevard, Winston-Salem, NC 27157, USA. [5]Organization and Dynamics of Biological Membranes, UMR 5246 ICBMS, CNRS-Université Claude Bernard Lyon 1, Bâtiment Raulin, 43, boulevard du 11 novembre 1918, 69622 Villeurbanne, Cedex, France

Running title: Monoacylglycerol and insulin secetion.

Published in: Cell Metabolism 2014 Jun 3;19(6):993-1007.

Correspondence to:

Dr. Marc Prentki, Montreal Diabetes Research Center, CRCHUM-Viger Tower, 900 Saint Denis St, Rm R08-412, Montreal, QC H2X 0A9, Canada

Dr. S.R. Murthy Madiraju, Montreal Diabetes Research Center, CRCHUM-Viger Tower, 900 Saint Denis St, Rm R08-414, Montreal, QC H2X 0A9, Canada.

Detailed contribution of authors in this work:

Shangang Zhao mainly contributed to characterize the role of ABHD6 in insulin secretion using in vitro, ex vivo and in vivo mouse models, and partially contributed to develop the method to quanlify 1-MAG and 2-MAG, together with looking into the effect of Munc13-1 translocation induced by increasing MAG levels. The overall contribution to this work is around 60% of all the generated data. The detailed figures are as follows: Fig 1B; Fig 2 (parts of work), Fig 3, Fig 4, Fig 5, Fig 6, Fig 7C , most of the supplementary Figures (expect Sup Fig S1A, Fig S2D, S2E, S2F; Fig S4I; Fig S6A, Fig S6C).

Yves Mugabo was responsible for characterizing the MAG species by HPLC after modulating ABHD6 levels, and help in oral glucose tolerance test and MAG hydrolysis activity. The detailed figures are as follows: Fig 1A, Fig 2 (most of the work) and Fig S4E-G.

Jose Iglesias was responsible for testing the binding effect of MAG to Munc13-1 C1 domain using various in vitro techniques, and MAG hydrolysis activity, together with helping in many oral glucose tolerance tests. The detailed figures are as follows: Fig 1A-B (mRNA level); Fig 1C-D; Fig 7A-B; Fig S4I and Fig S6A.

Li Xie was responsible for the work related to the effect of MAG in Munc13-1 heterozygous islets using patch-clamp study. The detailed figures are as follows: Fig 7E and Fig S6C.

Viviane Delghingaro-Augusto was responsible for 2-AG effect in insulin secretion. The detailed figures include Fig S1A and S2D-F.

Roxane Lussier was responsible for helping in oral glucose tolerance test and ip injection of WWL70 to mice.

Bouchra Taïb was responsible for hypothalamus isolation, RNA extraction and cDNA synthesis.

Marie-line Peyot and Erik Joly were responsible for the analysis of the results and through discussions.

Matthew A. Davis, J. Mark Brown, Abdelkarim Abousalham contributed to provide reagents.

S.R. Murthy Madiraju and Marc Prentki conceived the project, designed the study, analyzed the results, and wrote the manuscript.

SUMMARY

Glucose metabolism in pancreatic β-cells stimulates insulin granule exocytosis and this process requires generation of a lipid signal. However, the signals involved in lipid amplification of glucose-stimulated insulin secretion (GSIS) are unknown. Here we show that in β-cells glucose stimulates production of lipolysis-derived long-chain saturated monoacylglycerols, which further increase upon inhibition of the membrane bound monoacylglycerol lipase α/β-Hydrolase Domain-6 (ABHD6). ABHD6 expression in β-cells is inversely proportional to GSIS. Exogenous monoacylglycerols stimulate β-cell insulin secretion and restore GSIS suppressed by the pan-lipase inhibitor orlistat. Whole-body and β-cell specific ABHD6-KO mice exhibit enhanced GSIS and their islets show elevated monoacylglycerol production and insulin secretion in response to glucose. Inhibition of ABHD6 in diabetic mice restores GSIS and improves glucose tolerance. Monoacylglycerol binds and activates the vesicle priming protein Munc13-1 thereby inducing insulin exocytosis. We propose saturated monoacylglycerol as a signal for GSIS and ABHD6 as a negative modulator of insulin secretion.

INTRODUCTION

Insulin is secreted from the pancreatic β-cell upon fusion of insulin containing secretory granules with the plasma membrane (Ashcroft and Rorsman, 2012; Kwan and Gaisano, 2009; MacDonald, 2011), and glucose stimulated insulin secretion (GSIS) occurs via intracellular glucose metabolism in the β-cell (MacDonald, 2011; Maechler and Wollheim, 1998; Prentki et al., 2013a). Insulin secretion is altered in diabetes, and despite decades of research the signaling pathways involved in GSIS largely remain to be defined (Nolan and Prentki, 2008). Glucose metabolism leads to a rise in ATP concentration in the β-cell, causing closure of potassium channels (K_{ATP}), which triggers an elevation in cytosolic Ca^{2+} necessary for insulin granule exocytosis (Prentki and Matschinsky, 1987). However, glucose signaling for insulin exocytosis also occurs via other metabolic coupling factors besides ATP (Henquin, 2011; Jitrapakdee et al., 2010; Maechler and Wollheim, 1998; Prentki and Madiraju, 2012).

The glycerolipid/free fatty acid (GL/FFA) cycle (Nolan et al., 2006b; Nolan and Prentki, 2008), which conducts synthesis of glycerolipids including mono-, di-, & tri-acylglycerols (MAG; DAG; TG) and phospholipids followed by their lipolysis to FFA and glycerol, plays a key role in GSIS (Nolan and Prentki, 2008; Prentki and Madiraju, 2012) via the production of lipolysis-derived signaling molecule(s) that remain to be defined (Prentki et al., 2013a). GSIS is reduced in isolated islets obtained from mice deficient in either adipose triglyceride lipase (Peyot et al., 2009b), which hydrolyzes TG to DAG (Nolan and Prentki, 2008), hormone sensitive lipase (Fex et al., 2009; Peyot et al., 2004) which forms MAG from DAG (Haemmerle et al., 2002), or when DAG lipase (which also forms MAG) is inhibited by RHC80267 (Guenifi et al., 2001). On the basis of these observations, we hypothesized that MAG is a key signal mediating the link between glucose and intracellular fatty acid signaling and insulin secretion.

If DAG were a signal for GSIS (Eliasson et al., 2008; Green et al., 2009; Kwan et al., 2006b), then suppression or inhibition of HSL or DAG lipase, which elevates DAG levels, should enhance GSIS instead of reducing it. MAG can be hydrolyzed not only by MAG lipase (MAGL) but also by the recently discovered plasma membrane bound enzymes α/β-hydrolase domain containing-6 (ABHD6), with its catalytic site facing the cytosol, and ABHD12 with an exterior facing catalytic site (Blankman et al., 2007b). Recent studies suggested a potential

role for ABHD6 in the control of metabolic syndrome (Thomas et al., 2013) and also inflammation (Alhouayek et al., 2013).

Here we show that glucose stimulation elevates various MAG species in the β-cells, particularly saturated 1-MAG species, and that MAG accessible to ABHD6 but not to MAGL acts as a signal for promoting insulin granule exocytosis by binding to the vesicle priming protein Munc13-1. Suppression of ABHD6 either genetically or pharmacologically leads to MAG accumulation in β-cells with a resultant increase in GSIS *in vitro, ex vivo* and *in vivo*. The data indicate that ABHD6 is a negative regulator of GSIS and that MAG is a metabolic coupling factor for insulin secretion in response to glucose and fatty acids.

RESULTS

Membrane Bound ABHD6 is the Predominant MAG Lipase in β-cells

We found that in β-cell lines and islets from rat, mouse and human, MAGL is expressed at very low levels, unlike other tissues (Figure 1A). However, ABHD6 is well expressed both at the mRNA and protein levels in islets and β-cell lines (Figure 1B). Using 1-oleoylglycerol as the substrate, we found that MAG hydrolyzing activity in INS832/13 β-cells primarily resides in the membrane fraction (Figure 1C) and is inhibited by the ABHD6 inhibitor WWL70, which does not affect MAGL, ATGL and HSL (Bachovchin et al., 2010; Blankman et al., 2007b) and by orlistat, which inhibits most lipases. We found that WWL70-sensitive ABHD6 activity in INS832/13 cell extracts with 1-palmitoylglycerol is ~3-fold higher than with 1-oleoylglycerol, even though both the MAG species could serve as substrates (Figure 1E). However, ABHD12 expression is low in β-cells and rodent islets while it is higher in human islets (data not shown).

Elevation of 1-MAG by Glucose and ABHD6 Inhibition in β-cells correlate with GSIS

If MAG is a mediator of GSIS, its level is expected to respond to an increase in glucose concentration and pharmacological agents that either increase or reduce MAG levels should modulate insulin secretion accordingly. The incorporation of [1-^{14}C]-arachidonic acid into both 1- and 2-MAG, besides other glycerolipids, increased in INS832/13 cells at high glucose

(Figure S1A). We also tested the effect of WWL70 and orlistat on the incorporation of [^{14}C]-glucose into different lipids. Under conditions where the lipid carbons are pre-labeled with [^{14}C]-glucose, incubation with 10 mM glucose led to elevated lipolysis, measured as ^{14}C-FFA release (Figure S1B), and a rise in the content of neutral glycerolipids, particularly 1- and 2-MAG (Figure S1C). TG accumulated with orlistat but not with WWL70 (Figure S1D). Neither of these inhibitors had an effect on total DAG levels (Figure S1D). While orlistat had no effect on 2-MAG levels, WWL70 (Figure S1C) increased this lipid. On the other hand, orlistat which inhibits GSIS (Nolan et al., 2006c), reduced the formation of 1-MAG, while WWL70 which enhances GSIS (see below Fig 3) caused an increase in 1-MAG (Figure S1C). Thus, elevated glucose promotes lipolysis and FFA release in β-cells, and causes a rise in 1-MAG and 2-MAG levels that is amplified in the presence of the ABHD6 inhibitor WWL70. In addition, GSIS in the presence of lipolysis (orlistat) or ABHD6 (WWL70) inhibitors correlates only with 1-MAG and not with 2-MAG, DAG or TG.

Glucose Specifically Increases Saturated Long Chain Fatty Acid and MAG Species

As ABHD6 inhibition reduced glucose stimulated FFA release from INS cells (Figure S1B), we examined if this is specific for any particular species of FFA. In rat islets high glucose (16.7 mM) specifically increased the release of long chain saturated FFA (Figure 2A), e.g., palmitate (C16:0) and stearate (C18:0), and this increase was abolished by WWL70 (Figure 2B), while the release of unsaturated FFA species or saturated FFA of <C16 chain length were not affected (Figure 2A,B). Similar changes were noticed in the total FFA present in the islet cells (Figure 2C). Thus, WWL70 is a useful tool to study the role of ABHD6 and MAG in glucose signaling as it shows the anticipated effects on lipid metabolism. It reduces MAG hydrolysis *in vitro*, and increases MAG levels and reduces FFA content and release in intact β-cells.

The pattern of lipolysis (FFA release) with glucose and WWL70 was largely related to the MAG species in the cells. As glucose and WWL70 led to an accumulation of MAG in INS cells incubated with [^{14}C]-glucose, we examined the effect of WWL70 on individual species of MAG (Figure 2D). Thus, a 2 to 10 mM increase in glucose elevated total cellular MAG (both 1- and 2-MAG) more than 2-fold and this was further increased by WWL70 (Figure 2E). Glucose primarily and quantitatively increased both 1- and 2-isomers of palmitoylglycerol

(Figure 2F) and stearoylglycerol (Figure 2G), though there was noticeable effect on other MAG species. WWL70 appeared to be specific in further elevating the levels of 1-MAG species, in particular, 1-palmitoylglycerol and 1-stearoylglycerol (Figure 2F, G), and other saturated fatty acid containing MAGs (Figure 2D). This indicates that ABHD6 has preferential access to 1-MAG species with saturated FFA.

MAG Enhances Insulin Release and Restores GSIS Suppressed by Orlistat

Since glucose primarily elevates long chain saturated MAG, we tested whether these MAG species are efficient secretagogues when provided exogenously. 1-Palmitoylglycerol and 1-stearoylglycerol were most effective in enhancing GSIS in INS832/13 cells (Figure 3A), whereas and 1-oleoylglycerol (Figure 3A) and 1-linoleoylglycerol (Figure S2A) were less effective. The GSIS enhancing effect by 1-palmitoylglycerol was also seen in human and rat islets (Figure 3B). 1-Stearoylglycerol caused similar effects in both rat and human islets (Figure S2B).

We noticed that exogenous MAG (1-palmitoylglycerol, Figure 3C; 1-stearoylglycerol, Figure S2C and 2-arachidonoylglycerol, Figure S2D,E,F) was not only effective in enhancing GSIS but also in restoring GSIS suppressed by the lipolysis inhibitor orlistat in INS832/13 cells. This provides strong pharmacological evidence for the view that lipolysis-derived MAG is a signal for GSIS.

Cannabinoid Receptors are not Implicated in Glucose Signaling for Insulin Secretion

A specific antagonist (AM251) of the CB1 receptor (Lan et al., 1999) known to be present in β-cell (Matias et al., 2006), and an inverse agonist (AM630) of the CB2 receptor (Ross et al., 1999) whose presence in β-cells is controversial (Kim et al., 2011), did not alter GSIS (Figure S2E and S2F). In addition, the restoration of orlistat-inhibited GSIS by 2-arachidonoylglycerol was not affected by AM251 (Figure S2F).

ABHD6 Inhibition Amplifies GSIS

Inhibition of ABHD6 by WWL70 in INS832/13 cells, which causes MAG accumulation, almost doubled insulin secretion at 10 mM glucose both in the presence and absence of exogenous palmitate (Figure 3D). In contrast, orlistat, which decreased 1-MAG levels (Figure

S1C), strongly inhibited GSIS (Figure 3D). WWL70 had no effect on insulin secretion at low glucose and amplified only GSIS, with maximal effect at 10 μM (Figure S2G), without affecting the total insulin content of the cells (not shown). WWL70 was also effective in enhancing GSIS in islets from CD1 mice (Figure 3E) and C57Bl6 mice and Wistar rats (not shown), as well as from non-diabetic human donors (Figure 3E). Insulin secretion induced by membrane depolarization with 10 mM arginine or 35 mM KCl was not affected by WWL70 in INS832/13 cells (not shown).

Insulin Secretion is Inversely Proportional to ABHD6 Levels

In order to further ascertain the role of ABHD6 in GSIS regulation, we modified the expression of ABHD6 in INS832/13 cells by overexpression or RNAi-knockdown. A ~3 fold increase in ABHD6 protein (Figure 4A) decreased GSIS (Figure 4B), as compared to GFP expressing control cells, both in the presence and absence of palmitate. In contrast, a decrease in ABHD6 content by >80% using two different siRNA oligomers (A1 & A2) led to ~2-fold increase in GSIS, in comparison to control RNAi-transfected cells (Figures 4C, 4D and 4E). An ABHD6 gene expression dosage effect on GSIS with the two siRNA oligomers is apparent.

MAG Hydrolysis by ABHD6 but not by MAG Lipase Controls Insulin Secretion

We tested whether the signaling competent MAG for insulin secretion is accessible not only to ABHD6 but also to the small amount of MAGL present in the β-cell. MAG lipase is a an amphiphilic enzyme distributed between cytosol and membrane fractions (Severson and Hee-Cheong, 1988), unlike ABHD6 which is largely membrane bound (Blankman et al., 2007b) (Figure 1C). Inhibition of MAGL by JZL184 (Long et al., 2009b) caused a modest increase in MAG levels in INS832/13 cells but had no effect on GSIS (Figure S3). In addition, RNAi silencing of MAGL (Figures 4F and 4G) or overexpressing MAGL (Figures 4H and 4I) in INS832/13 cells was without effect on GSIS. Thus, ABHD6-accessible MAG only acts as a signal for insulin secretion.

Enhanced Insulin Secretion in Whole Body ABHD6 Deficient Mice

Whole body deletion of the mouse ABHD6 gene was obtained by a knockout-first technique (Figure S4A) (Skarnes et al., 2011). Gene deletion was verified by genotyping. Genomic PCR

of *abhd6* locus yielding a single fragment of 517bp is indicative of complete loss of the gene in the homozygous mice, whereas a fragment of 200bp is indicative of wild-type (WT) (Figure S4B). Both fragments were noticed in heterozygous (HZ) mice. ABHD6 deletion was also confirmed in the Western-blots showing complete loss of the 37 kDa ABHD6 protein (Figure 5A) in the homozygous knockout (KO) mice. There was no difference in the growth and food intake of ABHD6-KO and HZ mice in comparison to WT mice up to 25 weeks of age (Figures S4C and S4D).

We examined if the isolated islets, *ex vivo,* from ABHD6-KO mice also exhibit enhanced GSIS and elevated MAG content, similar to the *in vitro* experiments using the ABHD6 inhibitor and RNAi-knockdown approaches. The *ex vivo* (16wk old mice) experiments revealed an increase in GSIS in the ABHD6-KO islets at 8.3 and 16.7 mM glucose while the islets from HZ mice also showed significantly elevated GSIS at 16.7 mM glucose (Figure 5B). Interestingly, the KO islets also had elevated KCl-stimulated insulin secretion (Figure 5B).

We measured the content of MAG *ex vivo*, in islets from ABHD6-KO, HZ and WT mice after incubation at 2.8 and 16.7 mM glucose. Total MAG (Figure 5C) and 1-MAG (Figure 5D) levels were elevated in the islets from all animal types at high glucose. The increase in 2-MAG was moderate and significant only in the KO islets (Figure S4E). Importantly, there was an inverse effect of ABHD6 'gene dosage' on total MAG, 1-MAG and 2-MAG levels at high glucose (Figures 5C, 5D and S4E). Thus, genetic deletion of ABHD6 was associated with enhanced *ex vivo* GSIS and total MAG as well as 1-MAG and 2-MAG species in the islets. Similar to the observations with INS832/13 cells (Figure 2D), maximal changes in the ABHD6-KO islets were seen in saturated fatty acid containing MAG species (Figure S4F and S4G). Thus in ABHD6-KO islets, high glucose induced ~4-fold increase in 1-palmitoyl MAG and a more than 2-fold increase in 1-stearoyl MAG and these increases were higher than in WT and HZ islets (Figure S4F). While similar trend was seen in corresponding 2-MAG levels, the total amounts were lower than 1-MAG (Figure S4G). Other 1-and 2-MAG species contributed quantitatively much less to total MAG (data not shown).

We then assessed the impact of ABHD6 deletion on GSIS *in vivo* by performing an oral glucose tolerance test (OGTT) in 26-week-old male ABDH6-KO and HZ mice and wild-type

littermates. Results indicated unaltered glucose tolerance in both ABHD6-KO and HZ mice, as compared to WT mice (Figure 5E). Plasma insulin levels during OGTT were increased significantly in both the KO and HZ mice (Figure 5F; inset showing AUC), consistent with the results obtained with the normal mice administered with ABHD6 inhibitor WWL70 (see below). The increase in GSIS appeared to be ABHD6 gene dosage dependent, as evident from area under the curve calculations (Figure 5F inset). Since there was elevated insulinemia response with unchanged glycemia in the KO and HZ mice upon glucose load, we tested if the insulin sensitivity is altered in these mice. Hyperinsulinemic euglycemic clamp revealed unaltered insulin sensitivity in either KO or HZ mice fed chow diet for 26 weeks (Figure 5G) confirming the results obtained by insulin tolerance test, (Figure S4H). Both the basal glycemia and insulinemia were similar in the KO, HZ and the WT mice.

Lack of Effect of WWL70 on GSIS and MAG Hydrolyzing Activity in ABHD6-KO Islets

Extracts from ABHD6-KO mouse islets showed about 50% reduced MAG hydrolytic activity that was insensitive to inhibition by ABHD6 inhibitor WWL70, unlike the MAG hydrolysis activity in wild-type islet extracts (Figure S4I). The residual MAG hydrolysis activity in the whole islet extracts of KO mice could be due to HSL, MAGL and other non-specific hydrolases. ABHD6 inhibition by WWL70 enhanced GSIS in wild-type islets *ex vivo* but this enhancement was not seen in whole body KO mouse islets, which show already enhanced GSIS (Figure S4J). These results reinforce the view that WWL70 is a specific inhibitor of ABHD6 and importantly that its effect on GSIS in β-cells is exclusively due to ABHD6 inhibition.

ABHD6 Inhibition Enhances GSIS and Restores Glucose Tolerance in Diabetic Mice

We examined if the GSIS enhancing effect of ABHD6 inhibition by WWL70 is noticeable *in vivo* in control CD1 mice, and in the low-dose streptozotocin (LD-STZ) diabetes mouse model. We chose to employ the LD-STZ mouse model as this presents with ~50% reduced β-cell mass, fed hyperglycemia of approximately 20 mM, slightly elevated fasting glycemia and significantly lowered fed insulinemia (Hayashi et al., 2006). Thus, in order to study the *in vivo* effects of ABHD6 inhibition specifically on insulin secretion, we felt it important to choose an animal model that is not insulin resistant and hyperinsulinemic (e.g., db/db, ob/ob,

high fat fed mice etc.) and where β-cell mass is not drastically decreased. Administration (i.p.) of WWL70 for 3 days enhanced insulinemia in control mice during OGTT but did not affect glycemia (Figures 5H and 5I). In LD-STZ diabetic mice WWL70 restored glucose responsive insulin release, normalized basal glycemia and markedly improved glucose tolerance (Figures 5J and 5K).

Enhanced GSIS *in vivo* and *ex vivo* in β-Cell Specific ABHD6 KO Mice

In order to ascertain whether the insulin secretion effects seen in whole body ABHD6-KO mice are indeed due to the lack of ABHD6 in pancreatic β-cells *per se*, we generated β-cell specific ABHD6 KO (BKO) mice. Floxed ABHD6 mice were produced from the knockout-first mice (whole-body ABHD6-KO) by crossing with Flpo transgenic mice on pure C57Bl6N genetic background, so that the resulting floxed ABHD6 mice are on pure C57Bl6N background. Floxed ABHD6 mice were crossed with tamoxifen-inducible mip-*cre* transgenic mice (Wicksteed et al., 2010) that were back-crossed to C57Bl6N for 8 generations, to produce mice that carried floxed ABHD6 gene and tamoxifen-inducible mip-*cre* transgene, which were used for generating β-cell specific ABHD6-KO mice. After 2 weeks following 5 consecutive tamoxifen injections, ABHD6 expression was abrogated only in pancreatic islets (β-cells) (Figure 6A) but not in other tissues (Figure 6B,C,D) of the BKO mice. ABHD6 mRNA levels were unchanged in ventromedial hypothalamus (Figure S5A) and arcuate nucleus (Figure S5B) regions of hypothalamus, indicating no leakage of *cre* expression in these regions and thus there is no central nervous system involvement in the altered β-cell function of BKO mice. Similar to whole body KO mice, there were no significant alterations in body weight gain (Figure S5C), food intake (Figure S5D) up to 5 weeks post-tamoxifen injection. BKO mice did not show any changes in β-cell mass compared to floxed and mip-*cre* control mice (Figure S5E). BKO male mice, 2 weeks post tamoxifen injection, showed slightly improved glucose tolerance (Figure 6E) and elevated insulinemia (Figure 6F) during OGTT. Similar to the whole body KO mice, isolated islets from BKO mice showed enhanced GSIS *ex vivo* (Figure 6G).

MAG Binds to the Exocytosis Effector Munc13-1

Among the potential targets for MAG action relevant for insulin secretion, Munc13-1 seemed plausible as this protein orchestrates membrane fusion events in various cell types (Ma et al., 2013), binds diacylglycerol and participates in the final stages of exocytotic process in β-cells (Kwan and Gaisano, 2009). However, the C1-domain of Munc13-1 shows lower affinity for DAG, the proposed physiological ligand (Rhee et al., 2002), than for phorbol myristate acetate (PMA), due to occlusion of the binding site by a Trp residue (Shen et al., 2005). We assessed if MAG is a better ligand than DAG for Munc13-1 C1-domain. Using three independent approaches we proved it to be the case. 1) Tryptophan fluorescence quenching of the Munc13-1 C1-domain showed that 1-palmitoylglycerol binds as effectively as PMA, a well-known C1-domain ligand, and better than dioctanoylglycerol (Figure 7A). Palmitate did not show any binding. Similar high efficient binding was also observed with 1-stearoylglycerol (not shown). 2) Protein-lipid overlay showed that GST-Munc13-C1 fusion protein (but not GST alone) binds to 1-palmitoylglycerol and 1-stearoylglycerol, similar to or better than dioctanoylglycerol, whereas binding with palmitate, stearate and TG was insignificant (Figure 7B). 3) Munc13-1 C1 domain peptide could bind to the NBD-MAG and quenched its fluorescence (emission λ540 nm) in comparison to a control peptide (Figure S6A). Thus, NBD-MAG fluorescence in the presence of a similar sized unrelated peptide used as negative control (glucagon-like peptide 1) was higher than in the presence of the Munc13-1 peptide.

Glucose and MAG Cause Munc13-1 Translocation to Plasma Membrane

Confocal microscopy studies (Figure 7C) revealed that, in INS832/13 cells expressing EGFP-tagged Munc13-1, high glucose concentration promotes the translocation of Munc13-1-EGFP to plasma membrane and this translocation is not seen with H567K mutant Munc13-1-EGFP (mutation in the C1 domain). Phorbol myristate acetate (PMA) caused much higher Munc13-1 translocation independent of glucose levels. ABHD6 inhibitor WWL70, which increases intracellular MAG levels, and also exogenous 1-palmitoylglycerol caused significantly increased translocation of Munc13-1 at 10 mM glucose and to a lesser extent at 2 mM glucose (Figure 7C, D). These effects were lost with H567K mutant Munc13-1. In a complementary approach using cell fractionation and Western blotting we noticed that in wild type islets high glucose increased Munc13-1 translocation to a membrane fraction. In addition, incubation of

whole body ABHD6-KO mouse islets at high glucose (which elevates their MAG levels, see Figure 5C,D) led to a larger increased Munc13-1 migration to plasma membrane in comparison to wild type mouse islets and also to KO islets incubated at low glucose concentration (Figure S6B). These results further support the view that MAG binds with Munc13-1 at its C1-domain, *in situ*, and causes its translocation to plasma membrane, an important step in insulin granule exocytosis.

MAG directly Promotes Exocytosis in Single β-cells at least in part via Munc13-1

We examined whether MAG promotes exocytosis by acting on Munc13-1 by performing cell membrane capacitance (Cm) measurements by patch clamp, using islet β-cells from Munc13-$1^{+/+}$ and Munc13-$1^{+/-}$ mice (Munc13-1-/- mice are not viable). Insulin exocytosis was induced by a train of ten 500-ms depolarization pulses. Cell Cm changes elicited by the first two pulses approximate the size of the ready releasable pool (RRP) of primed and fusion-ready granules, reflecting the first phase insulin secretion. Subsequent pulses estimate the rate of granule refilling or mobilization from the reserve pool(s) to the RRP (Gillis et al., 1996), which correlates with the second phase of insulin secretion (Rorsman and Renstrom, 2003). In Munc13-$1^{+/+}$ β-cells 1-palmitoylglycerol increased Cm at every depolarizing pulse (Figure 7E) and enhanced insulin exocytosis in both the size of RRP and the rate of granule pool refilling compared with control. In Munc13-$1^{+/-}$ β-cells exocytosis was reduced by ~50% and MAG stimulation of exocytosis was also decreased proportionally. While 1-palmitoylglycerol could significantly enhance insulin exocytosis in the RRP in Munc13-$1^{+/-}$ β-cells, the rate of refilling was not significantly stimulated unlike in the Munc13-$1^{+/+}$ β-cells.

We examined if MAG affects voltage-gated Ca^{2+} channel activity, which plays key role in GSIS (Prentki and Matschinsky, 1987; Rorsman and Renstrom, 2003). In the β-cells from both Munc$13^{+/+}$ and Munc$13^{+/-}$ mice, no significant changes in Ca^{2+} current amplitudes and current densities were observed with or without MAG or WWL70 pretreatment (Figure S6C).

Recent studies (Iwasaki et al., 2008; Zygmunt et al., 2013) suggested that MAG activates the transient receptor potential vanilloid-1 (TRPV1), which when stimulated acts as a Ca^{2+} channel. We examined this possibility of TRPV1 involvement in β-cells by employing

TRPV1-KO mice for both *in vivo* and *ex vivo* studies and also a pharmacological antagonist, AMG9810. The results ruled out this possibility (data not shown).

DISCUSSION

This study provides biochemical, pharmacological, cell biology and genetic evidence in support of the hypothesis, depicted in Figure 7F, proposing that the enigmatic lipolysis-derived molecule mediating the link between glucose metabolism and insulin granule exocytosis in the β-cell is MAG that targets munc13-1, and that the signaling competent MAG level is controlled by ABHD6. The overwhelming set of data and complementary approaches that collectively support this view is summarized as follows: 1) GSIS is reduced both *in vivo* and *ex-vivo* in mice deficient in ATGL (Peyot et al., 2009b) and HSL (Fex et al., 2009; Peyot et al., 2004), the first two enzymes of the lipolysis pathway. 2) Elevated glucose promotes β-cell lipolysis, as shown by a rise FFA levels inside and released from β-cells. 3) GSIS in INS832/13 cells is associated with a rise in total MAG levels, in particular, saturated FA containing 1-MAG. 4) Exogenous MAG amplifies GSIS in INS832/13 cells and islet tissues. 5) GSIS is curtailed by the panlipase inhibitor orlistat, which suppresses lipolysis and the glucose induced rise in MAG. 6) Orlistat-inhibited GSIS is restored by exogenous MAG. 7) ABHD6 is expressed at high levels in the β-cell and islet tissues, whereas MAGL is poorly expressed. 8) The ABHD6 inhibitor WWL70 enhances glucose induced MAG accumulation and insulin secretion. 9) Overexpression of ABHD6 in the β-cell reduces GSIS, whereas RNAi silencing of the enzyme enhances insulin release. 10) Islets from whole body ABHD6-KO mouse show elevated GSIS *ex vivo*. 11) MAG hydrolyzing activity of ABHD6-KO islets is reduced by ~50% and the remaining activity is insensitive to inhibition by WWL70. 12) The enhanced GSIS seen in ABHD6-KO mouse islets *ex vivo*, is not further increased by ABHD6 inhibitor, WWL70. 13) While total and 1-MAG levels increase in islets from ABHD6-KO, HZ and WT mice at high glucose concentration, this increase is inversely proportional to 'ABHD6-gene dosage'. 14) GSIS *in vivo* is enhanced in whole bodyABHD6-deficient mice. 15) Beta-cell specific deletion of ABHD6 in mice also led to enhanced GSIS both *in vivo* and in islets *ex vivo* thus excluding any involvement of central nervous system or peripheral tissues in the enhanced GSIS. 16) WWL70 enhances GSIS *in vivo* in control mice

and restores GSIS in low dose streptozotocin-diabetic mice. 17) MAG binds efficiently the exocytotic effector Munc13-1. 18) Addition of either WWL70 or exogenous MAG increased the glucose-stimulated translocation of Munc13-1 to plasma membrane in INS832/13 β-cells and this effect is lost with C1-domain mutated Munc13-1. 19) Glucose stimulation of ABHD6-KO mouse islets caused increased migration of Munc13-1 to plasma membrane 20) MAG causes exocytosis in single patch-clamped β-cells. 21) MAG induced exocytosis is reduced in Munc13-$1^{+/-}$ β-cells.

Saturated long chain 1-MAG (e.g., 1-palmitoyl- or 1-stearoyl-glycerol) is likely the physiologically relevant MAG with regard to metabolic coupling for GSIS. Thus, glucose stimulation and suppression of ABHD6 either by its inhibition by WWL 70 or its genetic deletion caused more prominent rises in saturated 1-MAG than 2-MAG species. In addition, glucose only triggered the release of lipolysis-derived saturated long chain fatty acids. Furthermore, saturated long chain fatty acyl 1-MAG were better secretagogues than monounsaturated or polyunsaturated 1-MAG species. In addition, elevated glucose caused a prominent rise in the incorporation of labeled glucose into 1-MAG, whereas incorporation into 2-MAG was largely unaltered. Also, the lipolysis inhibitor orlistat suppressed the impact of glucose on 1-MAG levels, but barely affected the incorporation of glucose into 2-MAG or DAG. These findings are completely congruent with the fact that lipolysis of TG by ATGL generates primarily 1,3-DAG (Eichmann et al., 2012; Lass et al., 2011), which is further hydrolyzed to 1-MAG by HSL. Interestingly, a recent study documented that ABHD6 has preferential activity for 1-MAG species, and saturated long chain 1-MAG species are efficiently hydrolyzed by the enzyme (Navia-Paldanius et al., 2012a). Although ABHD6 was reported to hydrolyze lysophosphatidylglycerol in a recent study (Thomas et al., 2013), this activity is only about 5% of this enzyme's MAG hydrolyzing activity, indicating that ABHD6 is predominantly a MAG hydrolase.

The results indicate that there is a "signaling competent pool" of 1-MAG, likely close to or associated to the inner side of the plasma membrane that plays a role in insulin exocytosis. ABHD6 controls the level of this pool, thereby regulating GSIS, whereas this pool of 1-MAG is not influenced by MAGL. Thus, using pharmacological and siRNA agents we observed that ABHD6 inhibition, but not MAGL inhibition, alters GSIS. Notably, MAGL is an amphiphilic

enzyme distributed between cytosol and membrane fractions (Severson and Hee-Cheong, 1988), whereas ABHD6 is exclusively membrane bound (Marrs et al., 2010). Similar intracellular compartmentalization having an impact on the signaling functions of eicosanoids (Bozza et al., 2011) and sphingolipids (Siow and Wattenberg, 2011), because of the intracellular distribution of the involved enzymes, has been described.

We ruled out the possibility that endocannabinoid receptors (Matias et al., 2006) that bind 2-arachidonoylglycerol, but not saturated MAG, are involved in the MAG-mediated effects on insulin secretion. Thus, a specific antagonist of the CB1 receptor (AM251) (Lan et al., 1999) and an inverse agonist (AM630) of the CB2 receptor (Ross et al., 1999) did not alter GSIS. In addition, the restoration of orlistat-inhibited GSIS by 2-arachidonoylglycerol was not affected by AM251. Finally, 2-arachidonoylglycerol levels even at high glucose were <1% of the total β-cell MAG, whereas the saturated MAG that rose in the presence of glucose were 100 fold higher as compared to 2-arachidonylglycerol and stimulated insulin secretion. Noteworthy, only 2-arachidonoylglycerol binds CB receptors but not saturated MAG (Ben-Shabat et al., 1998). It was earlier suggested (Li et al., 2012a) that MAGL is important in GSIS regulation in MIN6 cells and islets by regulating 2-arachidonoylglycerol levels. However, these authors employed URB602, which has low affinity for MAGL (Ki ~28 μM) and is not selective (Vandevoorde et al., 2007; Wiskerke et al., 2012). In fact URB602 at 50 μM caused glucose independent insulin secretion (at 2 mM glucose) and reduced GSIS at 20 mM glucose (Li et al., 2012a), a clear indication of this drug's toxic effects on β-cell. In our studies, we employed 1 μM JZL184 (IC50 25 nM for rat MAGL; (Long et al., 2009b)) to inhibit MAGL, which does not exert any toxic effects and our results rule out the involvement of CB1/2 receptors in GSIS regulation.

Since the components of exocytotic machinery, including Munc13-1, are needed also for non-fuel induced insulin secretion (e.g. high KCl) (Roduit et al., 2004) it is anticipated that elevated levels of MAG can influence KCl induced secretion via Munc13-1 activation. Thus in the islets from ABHD6-KO mice the elevated secretion by KCl (at 2.8 mM glucose) could be due to increased MAG levels even at 2.8 mM glucose in these islets. However, in INS832/13 cells, ABHD6 inhibition by WWL70 had no effect on KCl induced secretion (at 1 mM glucose), as under these conditions, MAG levels did not increase in these cells.

How is MAG signaling linked to insulin secretion? Munc-13-1, a vesicle priming protein (Kwan et al., 2006b; Sheu et al., 2003), was proposed to be activated upon DAG binding to its C1-domain (Rhee et al., 2002) and to translocate to plasma membrane and promote insulin granule exocytosis (Kwan et al., 2006b; Sheu et al., 2003). However, NMR studies revealed that DAG binds with low affinity to Munc13-1 due to an occluding tryptophan residue in the C1-domain (Shen et al., 2005). We now demonstrate that the C1 domain of Munc13-1 binds to MAG more efficiently than to DAG. Hence, the accumulation of MAG at high glucose likely results in the activation of Munc13-1 and exocytosis. Inasmuch as high glucose and also ABHD6 inhibition lead to much higher rise in 1-MAG levels than in total DAG and because orlistat, which suppresses GSIS completely, reduces MAG but not DAG in β-cells, MAG rather than DAG is the more plausible activator of Munc13-1 linked to insulin exocytosis. Wild-type Munc13-1, but not the C1-domain mutant (H567K) Munc13-1, showed glucose-stimulated translocation to plasma membrane and exogenous MAG or the ABHD6 inhibitor WWL70 also increased Munc13-1 translocation to the plasma membrane to the same extent as high glucose, which strongly implicates MAG as the physiological modulator of Munc13-1 migration. We further found in patch clamp experiments in wild type β-cells that 1-palmitoylglycerol increases exocytosis from granules located in both the readily releasable and reserve/refilling pools that correspond to first- and second-phase GSIS, respectively. Exocytosis from granules derived from the two pools was reduced in Munc13$^{+/-}$β-cells both in the absence and presence of MAG, again supporting the view that Munc13-1 is a target of MAG action.

Overall, the present study identifies MAG, in particular long chain saturated 1-MAG species, as a lipid metabolic coupling factor linking glucose metabolism in the pancreatic islet β-cell to insulin secretion. MAG appears to target at least in part Munc13-1, a key exocytotic effector that orchestrates membrane fusion events. The results also show that the MAG signal for insulin secretion is modulated by the membrane bound MAG hydrolase ABHD6. Identifying MAG species other than the endocannabinoid 2-arachidonoylglycerol as signaling molecules may prove to be of broad significance in various cell types and diseases. In addition, it will be of interest to determine whether ABHD6 inhibition may provide a useful approach to develop antidiabetic agents and insulin secretagogues.

ACKNOWLEDGEMENTS

This work was supported by grants from the Canadian Institutes of Health Research (M.P. & S.R.M.M.). M.P. holds the Canada Research Chair in Diabetes and Metabolism. H.G. is supported by grants from the Canadian Institutes of Health Research. SZ was supported by studentships from Diabète Québec and the Montreal Diabetes Research Center. YM was supported by studentships from the Fonds de Recherche Québec-Santé, the department of Nutrition of Université de Montréal and Diabète Québec and BT received a fellowship from Diabète Québec. We thank Robert Zimmermann, Christopher Nolan, Vincent Poitout, Robert Farese, Jr. and Stephanie Fulton, for critical review of the manuscript. We thank Dr Thierry Alquier for his advise for hypothalamic measurements of ABHD6 and Dr. Josep Rizo, University of Texas, for a gift of Munc13-1-C1-GST expression plasmid.

EXPERIMENTAL PROCEDURES

Islet Isolation

Pancreatic islets were isolated from Wistar rats, C57Bl6 or CD1 mice (all males) as described before (Peyot et al., 2009b). Human islets (75 to 90% pure) were obtained from Beta-Pro LLC, VA, USA.

Insulin Secretion in Isolated Islets and INS832/13 Cells

Insulin secretion in isolated islets and INS832/13 cells (Hohmeier et al., 2000) was measured in static incubations as described earlier (Peyot et al., 2009b) in the absence or presence of the pharmacological agents WWL70, orlistat and JZL184.

Over-expression and RNAi Knockdown of ABHD6 and MAGL

The pCMV-based plasmids expressing human ABHD6, MAGL and Green Fluorescent Protein (GFP) were from Origene. pCMV-AC plasmids coding for either ABHD6, MAGL or GFP (control) were introduced into INS832/13 cells using the Amaxa Nucleofector method (Program T-27, solution V; Amaxa Inc). After transfection, cells were cultured for 72h in 12-well and 6-well plates, for insulin secretion and Western blot analysis, respectively. Silencer select pre-designed siRNA against ABHD6 and 2 Scrambled-siRNA were from Ambion. For RNAi-knockdown of MAGL, 2 siRNA were used. siRNA constructs were introduced into INS832/13 cells by reverse transfection using RNAiMAX (Invitrogen) and used 24h after transfection for Western blotting and insulin secretion determination.

Effect of ABHD6 Inhibitor in Low-dose Streptozotocin Mouse Diabetes Model

In vivo efficacy of the ABHD6 inhibitor WWL70 was assessed in a low-dose streptozotocin (STZ)-type-2 diabetes mouse model with impaired insulin secretion and reduced β-cell mass (Hayashi et al., 2006).

Analysis of MAG Binding to Munc13-1 C1-Domain

Rat Munc13-1 C1 domain (residues 567-617) was cloned as GST fusion protein(Shen et al., 2005). The Munc13-1 C1-GST fusion protein was expressed in *E. coli* and the C1-peptide

was purified after thrombin cleavage. Synthetic rat Munc13-1-C1 peptide was from Biomatik. MAG binding to Munc13-C1 domain was assessed by: 1) tryptophan fluorescence quenching; 2) 1-(12-(7-Nitrobenz-2-oxa-1,3-diazol-4-yl)amino)dodecanoylglycerol (NBD-MAG) fluorescence quenching; and 3) protein-lipid overlay.

Assessment of MAG-Induced Munc13-1 Translocation, *in situ*, in INS832/13 Cells

INS832/13 cells were transfected with plasmids expressing either Munc13-1-EGFP or H567K-mutated Munc13-1-EGFP and plated on coverslips. After 48h, the cells were incubated at 2 and 10 mM glucose, with and without 1 μM PMA, 10 μM WWL70 or 100 μM 1-PG, for 10 min. Then the coverslips with the cells were processed for confocal microscopy.

Studies in Munc13-1$^{+/-}$ Mouse Islets

Munc13-1$^{+/-}$ mouse (Augustin et al., 1999; Rhee et al., 2002) islets were isolated as described before (Kwan et al., 2006b) and dispersed into single cells that were plated on glass coverslips and allowed to adhere for 48 h before cell capacitance measurements.

ABHD6 Knockout Mice

Whole-body and β-cell specific ABHD6 knockout mice were generated by employing "knockout-first" design (Skarnes et al., 2011). The mice used were a pure background of C57/BL6N and the ES cells (JM8A3.N1 (Agouti), also derived from C57Bl6N) with confirmed conditional vector targeting for ABHD6 (HEPD0651_8_C07) were obtained from European Conditional Mouse Mutagenesis Program (Germany). Details are given in Extended Experimental Procedures.

Determination of Free Fatty Acid and Monoacylglycerol Species

Free fatty acids accumulated in the rat islets and INS832/13 cells and released into the medium were extracted, derivatized with phenacylbromide and quantified by reverse phase HPLC. Total lipids from rat islets and INS832/13 cells were extracted, separated on boric acid/silica gel-TLC with two solvent systems to allow 1- and 2-MAG separation. The separated 1- and 2-MAG spots were scraped from the TLC plates and used to determine different MAG species, with respect to the attached fatty acid. For this purpose total MAG extracts were saponified, neutralized and extracted in n-heptane. After extraction, the fatty

acids were derivatized with phenacylbromide and quantified by reverse-phase HPLC.

Statistical Analysis

Values are expressed as means ± SEM. Statistical analysis was performed using one-way ANOVA with Dunnett's post-test for multiple comparisons or two-way ANOVA with Bonferroni's post-test for multiple comparisons using GraphPad Prism. For electrophysiology experiments, comparisons were by unpaired two-tailed Student's *t* test.

SUPPLEMENTAL INFORMATION

Supplemental Information includes Extended Experimental Procedures, six figures, and legends and can be found online.

FIGURE LEGENDS

Figure 1. Expression and Distribution of Monoacylglycerol Lipase and ABHD6 in Rat Tissues, Pancreatic Islets and β-Cell Lines.

(A) Upper panel: protein level of MAGL as indicated by a Western blot. Lower panel: MAGL mRNA expression relative to 18S mRNA. (B) Upper panel: ABHD6 protein level. Lower panel: ABHD6 mRNA level. (C, D) Assessment of MAG hydrolytic activity using 1-oleoylglycerol (50 μM) as substrate in INS832/13 cell without and with the ABHD6 inhibitor WWL70 (10 μM) and the panlipase inhibitor orlistat (25 μM) in (C) membranes and (D) cytosolic (supernatant) fractions. $n = 6$. *P<0.05; ***P<0.001 compared with control (Cont). (E) WWL70-sensitive MAG hydrolysis activity in INS832/13 cell extracts is higher with 1-palmitoylglycerol than with 1-oleoylglycerol. MAG hydrolysis was measured using 50μM 1-palmitoylglycerol (1-PG) or 1-oleoylglycerol (1-OG) as described in the Extended Experimental Procedures. Briefly, in a volume of 100 μl 8μg INS cell extract; 50 μM MAG without or with 10 μM WWL70, were incubated for 30 min at 30°C and fatty acids released were extracted and analyzed by HPLC. ***P<0.001 compared with 1-OG (n = 3 separate cell extracts, done in duplicates).

Figure 2. Glucose Specifically Enhances the Production and Release of Saturated Free Fatty Acid From Rat Islets and Increases the Differential Production of Monoacylglycerol Species in β-Cells.

(A-C) Release and cellular content of different FFA species by isolated rat islets at 2.8 and 16.7 mM glucose with and without WWL70 (10 μM) after 2 h incubation. $n = 12$. *P<0.05; **P<0.01; ***P<0.001 compared with 2.8G. (B) The release of palmitate (C16:0), stearate (C18:0) and oleate (C18:1) into incubation medium; (C) Cellular content of palmitate, oleate and stearate in rat islets. (D-G) Effect of glucose and WWL70 (10 μM) on the content of MAG species in INS832/13 cells after 2 h incubation. 2G, 2 mM glucose; 10G, 10 mM glucose. (D) All measured MAG species; ##P<0.01 compared with 2G; *P<0.05; **P<0.01;

***P<0.001 compared with 10G. (E) Total MAG corresponding to the sum of all measured MAG species; (F) 1- and 2-palmitoyglycerol (PG) (C16:0) and (G) 1- and 2-stearoylglycerol (SG) (C18:0). n = 15; *P<0.05, compared with 2G; #P<0.05; ##P<0.01 compared with 10G.

Figure 3. Monoacylglycerol and the ABHD6 Inhibitor WWL70 Enhance Insulin Secretion in β-Cells.

(A) Dose-dependent effect of different MAG species on GSIS at 5mM glucose in INS832/13 cells. n = 12. *P<0.05; ***P<0.001 compared with no MAG addition. (B) 1-Palmitoylglycerol (1-PG) (100 μM) enhances GSIS in human islets and rat islets. Mean ± SEM of 4 (human islets) and 6 (rat islets) separate experiments with triplicate determinations. **P<0.01 compared with control value. (C) Exogenous MAG restores GSIS inhibited by the pan-lipase inhibitor orlistat. 1-Palmitoylglycerol (50 μM) restoration of 25 μM orlistat-inhibited GSIS (at 5 & 10 mM glucose) in INS832/13 cells. n = 12. ***P<0.001 compared with control; ###P<0.001 compared with the orlistat group. (D) Effect of WWL70 (10 μM) and orlistat (25 μM) on GSIS in INS832/13 cells. Insulin secretion was measured at the indicated glucose concentrations without and with 0.3 mM palmitate. n = 12. ***P<0.001 compared to control. (E) Effect of WWL70 (10 μM) on insulin secretion in CD1-mouse islets and human islets at different glucose concentrations. n = 12. *P<0.05; **P<0.01 compared with no WWL70 addition.

Figure 4. Expression Level of ABHD6 but not MAGL Affects Glucose Stimulated Insulin Secretion in β-Cells.

ABHD6 over-expression (A, B) and RNAi-knockdown (C-E) experiments in INS832/13 cells. (A) Western blot showing ABHD6 expression in cells transfected with pCMV6-based ABHD6 expression plasmid (48 h post transfection) as compared to cells expressing green fluorescent protein (GFP). (B) Insulin secretion in control cells (GFP) and cells over-expressing ABHD6, at 2 and 10mM glucose without and with palmitate. n = 9. *P<0.05; ***P<0.001 vs GFP expressing cells. (C) Western blot showing reduced ABHD6 expression

by RNAi-knockdown for 24h. A1 and A2 siRNAs reduce the protein level as compared to the control siRNAs C1 and C2; NT, not transfected. (D) Corresponding ABHD6 mRNA levels. (E) Insulin secretion at 2 and 10 mM glucose in control cells and after RNAi-knockdown of ABHD6. $^{**}P<0.01$ vs control (C1 and C2) groups; $n = 9$. (F, G) MAGL RNAi-knockdown experiments. (F) MAGL mRNA levels decreased after RNAi knockdown for 48h. M-1 and M-2 are the siRNAs; Cont, RNAi control. (G) Insulin secretion in INS832/13 cells at 1 and 10 mM glucose after MAGL RNAi-knockdown. (H, I) MAGL overexpression experiments. (H) Western blot showing elevated expression of MAGL in INS cells transfected with pCMV6-based MAGL expression plasmid (48h post transfection) as compared to cells expressing GFP and untransfected cells (NT). (I) Insulin secretion at 2 and 10 mM glucose in the presence and absence of WWL70 (10 μM); $n = 9$.

Figure 5. Enhanced Glucose Induced Insulin Secretion by Genetic Deletion or Pharmacological Suppression of ABHD6 in Mice.

(A) Western blot analysis of different tissues reveals complete loss of the ~37kDa ABHD6 protein in homozygous ABHD6-KO mice, a partial loss in heterozygote ABHD6-Ko mice as compared to the wild-type mice. (B-D) Elevated GSIS in ABHD6-KO mouse islets*, ex vivo*, is associated with glucose-dependent increase in the islet MAG content. (B) *Ex vivo* GSIS in islets from ABHD6-KO, heterozygote (HZ) and wild-type (WT) mice. GSIS was measured as described in Methods, at basal (2.8 G), intermediate (8.3G) and high (16.7G) glucose concentrations (n=6 mice per group); $^{*}P<0.05$; $^{**}P<0.01$; $^{***}P<0.001$ vs WT group at the same glucose concentration. (C) Total MAG content of islets from ABHD6-KO, HZ and WT mice. Isolated islets were incubated at 2.8 mM (2.8G) and 16.7 mM (16.7G) glucose for 1 h in KRBH and islet MAG levels were analyzed (n=3 separate experiments). $^{*}P<0.05$ vs 2.8 G in the same genotype; $\#\#P<0.01$ vs value of WT islets. (D) Total 1-MAG levels in the islets incubated as in (B) (n=3). $^{**}P<0.01$ vs 2.8 G in the same genotype; $\#\#P<0.01$ vs WT islets. (E-G) Effect of *in vivo* suppression of ABHD6 by gene knockout in male mice on glucose induced insulin secretion and insulin sensitivity. (E) Glycemia during oral glucose tolerance test (OGTT) in 26-week-old WT, HZ and KO mice (n = 5-8 per group). OGTT was performed after a 6h food withdrawal (0700h to 1300h). Inset depicts area under the curve. (F)

Corresponding insulinemia in the OGTT. Inset depicts area under the curve for insulinemia. * *P*<0.05 vs WT. (G) Insulin sensitivity assessment by hyperinsulinemic euglycemic clamp in 26 week old chow diet fed ABHD6-KO male mice. Glycemia was clamped at 7.2 mM in both WT and KO mice and blood samples were collected at different intervals to measure blood glucose. Glucose infusion rate was calculated and shown as inset for 90 to 120 min time period of the clamp. (H-K) Effect of *in vivo* pharmacological suppression of ABHD6 by WWL70 (i.p.) on glucose induced insulin secretion in normal and diabetic mice. Diabetes was induced by a single and low-dose of streptozotocin in CD1 mice. After 4 weeks the diabetic and control mice were treated daily with WWL70 (i.p., 5 mg/kg BW) or vehicle for 3 days. Oral glucose tolerance test (OGTT) was conducted in these mice after WWL70 treatment (8-10 mice per group) and after a 6h food withdrawal (0700h to 1300h). (H) Glycemia and (I) insulinemia in normal mice. Insets depict area under the curve. *P<0.05; **P<0.01 compared with vehicle treated. (J) Glycemia and (K) insulinemia in STZ-diabetic mice. Insets depict area under the curve. *P<0.05; **P<0.01 compared with vehicle treated.

Figure 6. Enhanced Glucose Induced Insulin Secretion by β-Cell Specific Deletion of ABHD6 in Mice.

(A-D) Expression of ABHD6 protein in different tissues from β-cell specific ABHD6-KO (BKO) mice. Two weeks post-tamoxifen injection to induce the expression of cre recombinase and deletion of ABHD6 in pancreatic β-cells, tissues were collected from the mip*cre*+, WT, flox/flox and BKO mice and analyzed for ABHD6 expression by Western blot. (A) Pancreatic islets, (B) Skeletal muscle, (C) White adipose (visceral) and (D) Liver. Representative blots of two separate experiments were shown. Tubulin was probed as loading control in the same blots.

(E-G) Effect of β-cell specific ABHD6-KO on glucose tolerance and glucose induced insulin secretion *in vivo* and *ex vivo* in islets. (E) Glycemia during oral glucose tolerance test (OGTT) in mip*cre*+ (n=9), flox/flox (n=12) and BKO (n=9) mice. OGTT was performed after a 6h food withdrawal (0700h to 1300h). Inset depicts area under the curve. * P<0.05 vs flox/flox. (F) Corresponding insulinemia in the OGTT. Inset depicts area under the curve for insulinemia.

* $P<0.05$ vs flox/flox. (G) *Ex vivo* GSIS at 2.8, 8.3 and 16.7 mM glucose in islets isolated from mip*cre*+ mice (n=7), flox/flox mice (n=8) and BKO mice (n=8). Insulin secretion is shown as percentage of total insulin content. *$P<0.05$ vs flox/flox or mip*cre*+.

Figure 7. Monoacylglycerol Binds to Munc13-1 C1 Domain, Facilitates Munc13-1 Translocation to Plasma Membrane and Stimulates Insulin Exocytosis in Single β-Cells.

(A) Ligand binding to Munc13-1 C1 domain assessed by tryptophan fluorescence quenching. Representative graph of fluorescence emission spectra of Munc13-1 C1 peptide (1 μM) incubated with 1 μM of either palmitic acid (PA), 1,2-dioctanoylglycerol (DOG), phorbol-12-myristate-13-acetate (PMA), 1-palmitoylglycerol (1-PG) or the DMSO control. Inset: Peak fluorescence emission at 350 nm. Means ± SEM. of 3 experiments with 10 spectra per experiment. **$P<0.001$ and ***$P<0.00001$. (B) Protein-lipid overlay assay. At indicated amounts, 1-PG, PA, 1,2-DOG, triglycerides (TG), 1-SG and stearic acid (SA) were spotted on nitrocellulose membrane, and after blocking membranes were incubated with 10 μg/ml of Munc13-1-C1-GST fusion protein or GST (negative control) and processed as described in Methods for assessing the bound Munc13-1-C1-GST. (C) INS832/13 cells were transfected with pEGFP plasmids expressing either Munc13-1 (wild-type) or H567K mutant Munc13-1 and were grown on cover-slips. Three days after transfection, the cells were incubated in KRBH at 2 or 10 mM glucose, containing 0.3 μM PMA, 10 μM WWL70, 100 μM 1-PG or DMSO vehicle for 10 min at 37°C. Then the coverslips were washed in cold PBS, fixed with ProLong Gold antifade reagent (Life Technologies) and the cells were imaged using confocal microscope (Leica TCS SP5) with 63× objective. Representative images are shown. (D) Munc13-1 translocation to plasma membrane was quantified using Image J software. About 6 to 10 individual cells were imaged per each treatment. Results are expressed as pixel intensity in the plasma membrane as a percentage of whole cell intensity. *$P<0.05$, ***$P<0.001$ as compared to 2G DMSO control; #$P<0.05$, ##$P<0.01$ as compared to corresponding 2G control; †$P<0.05$, ††$P<0.01$ as compared to 10G DMSO control. See Supplementary Information for Detailed Methods. (E) MAG induction of exocytosis is dependent on Munc13-1. Changes in cell membrane capacitance (Cm) were measured in Munc13-1$^{+/+}$ and

$^{+/-}$ mice β-cells with or without 1-PG (MAG) pretreatment using a train of ten depolarization pulses (500 ms in duration) from -70 mV to 0 mV. Panel I: Representative recordings of exocytosis from Munc13-1$^{+/+}$ and Munc13$^{+/-}$ mice β-cells with or without MAG pretreatment. Panel II: Cumulative changes in cell capacitance normalized to basal cell membrane capacitance (fF/pF) in Munc13-1$^{+/+}$ and $^{+/-}$ mice β-cells with or without MAG pretreatment (*n* = 11-16 cells, from 3-4 mice). **P*<0.05. Panel-III: Statistical analysis showing the size of the readily releasable pool (RRP) of insulin granules ($\Delta Cm_{1st–2nd\ pulse}$) and the rate of granule mobilization (refilling) ($\Delta Cm_{3rd–\ 10th\ pulse}$) (*n* = 11-16 cells, from 3-4 mice). **P*<0.05. (F) Scheme illustrating the role of monoacylglycerol as a metabolic coupling factor in glucose stimulated insulin secretion. The triggering arm of GSIS involves a rise in cytosolic ATP, the closure of metabolically sensitive K_{ATP} channels resulting in plasma membrane depolarization and the opening of voltage gated Ca^{2+} channels, and a rise in cytosolic Ca^{2+} that induces the exocytosis of insulin granules. The scheme illustrates that the amplification arm of GSIS involves MAG which acts as a metabolic coupling factor mediating the link between glucose metabolism in the β-cell and insulin secretion. Glucose stimulates glycerolipid/ FFA cycling, and lipolysis of triglycerides (TG) by adipose triglyceride lipases (ATGL) and of diacylglycerol (DAG) by hormone sensitive lipase (HSL) to generate MAG. The concentration of MAG produced in the vicinity of the plasma membrane is controlled by its hydrolysis by the membrane bound ABHD6 to produce glycerol and free fatty acids (FFA), which can leave the cell. Some FFA can re-enter the glycerolipid fatty acid cycle. MAG generated close to the plasma membrane binds and activates Munc13-1, an exocytosis facilitating and insulin secretory vesicle priming protein, which enhances insulin granule fusion with the plasma membrane and the release of insulin. Inhibition of membrane bound ABHD6 by WWL70 leads to a build up of MAG in the β-cell when glucose concentration is high, enhancing insulin secretion. Gro-3-P, glycerol 3-phosphate; 1-MAG, 1-monoacylglycerol; 2-MAG, 2-monoacylglycerol; FACoA, long chain fatty acyl-CoA, LPA, lysophosphatidate; PA, phosphatidate.

REFERENCES

Alhouayek, M., Masquelier, J., Cani, P.D., Lambert, D.M., and Muccioli, G.G. (2013). Implication of the anti-inflammatory bioactive lipid prostaglandin D2-glycerol ester in the control of macrophage activation and inflammation by ABHD6. Proc. Natl. Acad. Sci. USA 110, 17558-17563.

Ashcroft, F.M., and Rorsman, P. (2012). Diabetes mellitus and the beta cell: the last ten years. Cell 148, 1160-1171.

Augustin, I., Rosenmund, C., Sudhof, T.C., and Brose, N. (1999). Munc13-1 is essential for fusion competence of glutamatergic synaptic vesicles. Nature 400, 457-461.

Bachovchin, D.A., Ji, T., Li, W., Simon, G.M., Blankman, J.L., Adibekian, A., Hoover, H., Niessen, S., and Cravatt, B.F. (2010). Superfamily-wide portrait of serine hydrolase inhibition achieved by library-versus-library screening. Proc. Natl. Acad. Sci. USA 107, 20941-20946.

Ben-Shabat, S., Fride, E., Sheskin, T., Tamiri, T., Rhee, M.H., Vogel, Z., Bisogno, T., De Petrocellis, L., Di Marzo, V., and Mechoulam, R. (1998). An entourage effect: inactive endogenous fatty acid glycerol esters enhance 2-arachidonoyl-glycerol cannabinoid activity. Eur. J. Pharmacol. 353, 23-31.

Blankman, J.L., Simon, G.M., and Cravatt, B.F. (2007). A comprehensive profile of brain enzymes that hydrolyze the endocannabinoid 2-arachidonoylglycerol. Chem. Biol. 14, 1347-1356.

Bozza, P.T., Bakker-Abreu, I., Navarro-Xavier, R.A., and Bandeira-Melo, C. (2011). Lipid body function in eicosanoid synthesis: an update. Prostaglandins Leukot. Essent. Fatty Acids 85, 205-213.

Eichmann, T.O., Kumari, M., Haas, J.T., Farese, R.V., Jr., Zimmermann, R., Lass, A., and Zechner, R. (2012). Studies on the substrate and stereo/regioselectivity of adipose triglyceride lipase, hormone-sensitive lipase, and diacylglycerol-O-acyltransferases. J. Biol. Chem. 287, 41446-41457.

Eliasson, L., Abdulkader, F., Braun, M., Galvanovskis, J., Hoppa, M.B., and Rorsman, P. (2008). Novel aspects of the molecular mechanisms controlling insulin secretion. J. Physiol. 586, 3313-3324.

Fex, M., Haemmerle, G., Wierup, N., Dekker-Nitert, M., Rehn, M., Ristow, M., Zechner, R., Sundler, F., Holm, C., Eliasson, L., and Mulder, H. (2009). A beta cell-specific knockout of hormone-sensitive lipase in mice results in hyperglycaemia and disruption of exocytosis. Diabetologia 52, 271-280.

Gillis, K.D., Mossner, R., and Neher, E. (1996). Protein kinase C enhances exocytosis from chromaffin cells by increasing the size of the readily releasable pool of secretory granules. Neuron 16, 1209-1220.

Green, C.D., Jump, D.B., and Olson, L.K. (2009). Elevated insulin secretion from liver X receptor-activated pancreatic beta-cells involves increased de novo lipid synthesis and triacylglyceride turnover. Endocrinology 150, 2637-2645.

Guenifi, A., Simonsson, E., Karlsson, S., Ahren, B., and Abdel-Halim, S.M. (2001). Carbachol restores insulin release in diabetic GK rat islets by mechanisms largely involving hydrolysis of diacylglycerol and direct interaction with the exocytotic machinery. Pancreas 22, 164-171.

Haemmerle, G., Zimmermann, R., Hayn, M., Theussl, C., Waeg, G., Wagner, E., Sattler, W., Magin, T.M., Wagner, E.F., and Zechner, R. (2002). Hormone-sensitive lipase deficiency in mice causes diglyceride accumulation in adipose tissue, muscle, and testis. J. Biol. Chem. 277, 4806-4815.

Hayashi, K., Kojima, R., and Ito, M. (2006). Strain differences in the diabetogenic activity of streptozotocin in mice. Biol. Pharm. Bull. 29, 1110-1119.

Henquin, J.C. (2011). The dual control of insulin secretion by glucose involves triggering and amplifying pathways in beta-cells. Diabetes Res. Clin. Pract. 93 Suppl 1, S27-31.

Hohmeier, H.E., Mulder, H., Chen, G., Henkel-Rieger, R., Prentki, M., and Newgard, C.B. (2000). Isolation of INS-1-derived cell lines with robust ATP-sensitive K+ channel-dependent and -independent glucose-stimulated insulin secretion. Diabetes 49, 424-430.

Iwasaki, Y., Saito, O., Tanabe, M., Inayoshi, K., Kobata, K., Uno, S., Morita, A., and Watanabe, T. (2008). Monoacylglycerols activate capsaicin receptor, TRPV1. Lipids 43, 471-483.

Jitrapakdee, S., Wutthisathapornchai, A., Wallace, J.C., and MacDonald, M.J. (2010). Regulation of insulin secretion: role of mitochondrial signalling. Diabetologia 53, 1019-1032.

Kim, W., Doyle, M.E., Liu, Z., Lao, Q., Shin, Y.K., Carlson, O.D., Kim, H.S., Thomas, S., Napora, J.K., Lee, E.K., Moaddel, R., Wang, Y., Maudsley, S., Martin, B., Kulkarni, R.N., and Egan, J.M. (2011). Cannabinoids inhibit insulin receptor signaling in pancreatic beta-cells. Diabetes 60, 1198-1209.

Kwan, E.P., and Gaisano, H.Y. (2009). Rescuing the subprime meltdown in insulin exocytosis in diabetes. Ann. NY Acad. Sci. 1152, 154-164.

Kwan, E.P., Xie, L., Sheu, L., Nolan, C.J., Prentki, M., Betz, A., Brose, N., and Gaisano, H.Y. (2006). Munc13-1 deficiency reduces insulin secretion and causes abnormal glucose tolerance. Diabetes 55, 1421-1429.

Lan, R., Liu, Q., Fan, P., Lin, S., Fernando, S.R., McCallion, D., Pertwee, R., and Makriyannis, A. (1999). Structure-activity relationships of pyrazole derivatives as cannabinoid receptor antagonists. J. Med. Chem. 42, 769-776.

Lass, A., Zimmermann, R., Oberer, M., and Zechner, R. (2011). Lipolysis - a highly regulated multi-enzyme complex mediates the catabolism of cellular fat stores. Prog. Lipid Res. 50, 14-27.

Li, C., Vilches-Flores, A., Zhao, M., Amiel, S.A., Jones, P.M., and Persaud, S.J. (2012). Expression and function of monoacylglycerol lipase in mouse beta-cells and human islets of Langerhans. Cell. Physiol. Biochem. 30, 347-358.

Long, J.Z., Nomura, D.K., and Cravatt, B.F. (2009). Characterization of monoacylglycerol lipase inhibition reveals differences in central and peripheral endocannabinoid metabolism. Chem. Biol. 16, 744-753.

Ma, C., Su, L., Seven, A.B., Xu, Y., and Rizo, J. (2013). Reconstitution of the vital functions of Munc18 and Munc13 in neurotransmitter release. Science 339, 421-425.

MacDonald, P.E. (2011). Signal integration at the level of ion channel and exocytotic function in pancreatic beta-cells. Am. J. Physiol. Endocrinol. Metabol. 301, E1065-1069.

Maechler, P., and Wollheim, C.B. (1998). Role of mitochondria in metabolism-secretion coupling of insulin release in the pancreatic beta-cell. Biofactors 8, 255-262.

Marrs, W.R., Blankman, J.L., Horne, E.A., Thomazeau, A., Lin, Y.H., Coy, J., Bodor, A.L., Muccioli, G.G., Hu, S.S., Woodruff, G., Fung, S., Lafourcade, M., Alexander, J.P., Long, J.Z., Li, W., Xu, C., Moller, T., Mackie, K., Manzoni, O.J., Cravatt, B.F., and Stella, N. (2010). The serine hydrolase ABHD6 controls the accumulation and efficacy of 2-AG at cannabinoid receptors. Nature Neurosci. 13, 951-957.

Matias, I., Gonthier, M.P., Orlando, P., Martiadis, V., De Petrocellis, L., Cervino, C., Petrosino, S., Hoareau, L., Festy, F., Pasquali, R., Roche, R., Maj, M., Pagotto, U., Monteleone, P., and Di Marzo, V. (2006). Regulation, function, and dysregulation of endocannabinoids in models of adipose and beta-pancreatic cells and in obesity and hyperglycemia. J. Clin. Endocrinol. Metabol. 91, 3171-3180.

Navia-Paldanius, D., Savinainen, J.R., and Laitinen, J.T. (2012). Biochemical and pharmacological characterization of human alpha/beta-hydrolase domain containing 6 (ABHD6) and 12 (ABHD12). J. Lipid Res. 53, 2413-2424.

Nolan, C.J., Leahy, J.L., Delghingaro-Augusto, V., Moibi, J., Soni, K., Peyot, M.L., Fortier, M., Guay, C., Lamontagne, J., Barbeau, A., Przybytkowski, E., Joly, E., Masiello, P., Wang, S., Mitchell, G.A., and Prentki, M. (2006a). Beta cell compensation for insulin resistance in Zucker fatty rats: increased lipolysis and fatty acid signalling. Diabetologia 49, 2120-2130.

Nolan, C.J., Madiraju, M.S., Delghingaro-Augusto, V., Peyot, M.L., and Prentki, M. (2006b). Fatty Acid Signaling in the {beta}-Cell and Insulin Secretion. Diabetes 55 Suppl 2, S16-23.

Nolan, C.J., and Prentki, M. (2008). The islet beta-cell: fuel responsive and vulnerable. Trends in endocrinology and metabolism: Trends Endocrinol. Metab. 19, 285-291.

Peyot, M.L., Guay, C., Latour, M.G., Lamontagne, J., Lussier, R., Pineda, M., Ruderman, N.B., Haemmerle, G., Zechner, R., Joly, E., Madiraju, S.R., Poitout, V., and Prentki, M.

(2009). Adipose triglyceride lipase is implicated in fuel- and non-fuel-stimulated insulin secretion. J. Biol. Chem. 284, 16848-16859.

Peyot, M.L., Nolan, C.J., Soni, K., Joly, E., Lussier, R., Corkey, B.E., Wang, S.P., Mitchell, G.A., and Prentki, M. (2004). Hormone-sensitive lipase has a role in lipid signaling for insulin secretion but is nonessential for the incretin action of glucagon-like peptide 1. Diabetes 53, 1733-1742.

Prentki, M., and Madiraju, S.R. (2012). Glycerolipid/free fatty acid cycle and islet beta-cell function in health, obesity and diabetes. Mol. Cell. Endocrinol. 353, 88-100.

Prentki, M., and Matschinsky, F.M. (1987). Ca2+, cAMP, and phospholipid-derived messengers in coupling mechanisms of insulin secretion. Physiol. Rev. 67, 1185-1248.

Prentki, M., Matschinsky, F.M., and Madiraju, M.S. (2013). Metabolic Signaling in Fuel-Induced Insulin Secretion Cell Metabol.18, 162-185.

Rhee, J.S., Betz, A., Pyott, S., Reim, K., Varoqueaux, F., Augustin, I., Hesse, D., Sudhof, T.C., Takahashi, M., Rosenmund, C., and Brose, N. (2002). Beta phorbol ester- and diacylglycerol-induced augmentation of transmitter release is mediated by Munc13s and not by PKCs. Cell 108, 121-133.

Roduit, R., Nolan, C., Alarcon, C., Moore, P., Barbeau, A., Delghingaro-Augusto, V., Przybykowski, E., Morin, J., Masse, F., Massie, B., Ruderman, N., Rhodes, C., Poitout, V., and Prentki, M. (2004). A role for the malonyl-CoA/long-chain acyl-CoA pathway of lipid signaling in the regulation of insulin secretion in response to both fuel and nonfuel stimuli. Diabetes 53, 1007-1019.

Rorsman, P., and Renstrom, E. (2003). Insulin granule dynamics in pancreatic beta cells. Diabetologia 46, 1029-1045.

Ross, R.A., Brockie, H.C., Stevenson, L.A., Murphy, V.L., Templeton, F., Makriyannis, A., and Pertwee, R.G. (1999). Agonist-inverse agonist characterization at CB1 and CB2 cannabinoid receptors of L759633, L759656, and AM630. Br. J. Pharmacol. 126, 665-672.

Severson, D.L., and Hee-Cheong, M. (1988). Monoacylglycerol lipase activity in cardiac myocytes. Biochem. Cell Biol. 66, 1013-1018.

Shen, N., Guryev, O., and Rizo, J. (2005). Intramolecular occlusion of the diacylglycerol-binding site in the C1 domain of munc13-1. Biochemistry 44, 1089-1096.

Sheu, L., Pasyk, E.A., Ji, J., Huang, X., Gao, X., Varoqueaux, F., Brose, N., and Gaisano, H.Y. (2003). Regulation of insulin exocytosis by Munc13-1. J. Biol. Chem. 278, 27556-27563.

Siow, D., and Wattenberg, B. (2011). The compartmentalization and translocation of the sphingosine kinases: mechanisms and functions in cell signaling and sphingolipid metabolism. Crit. Rev. Biochem. Mol. Biol. 46, 365-375.

Skarnes, W.C., Rosen, B., West, A.P., Koutsourakis, M., Bushell, W., Iyer, V., Mujica, A.O., Thomas, M., Harrow, J., Cox, T., Jackson, D., Severin, J., Biggs, P., Fu, J., Nefedov, M., de Jong, P.J., Stewart, A.F., and Bradley, A. (2011). A conditional knockout resource for the genome-wide study of mouse gene function. Nature 474, 337-342.

Thomas, G., Betters, J.L., Lord, C.C., Brown, A.L., Marshall, S., Ferguson, D., Sawyer, J., Davis, M.A., Melchior, J.T., Blume, L.C., Howlett, A.C., Ivanova, P.T., Milne, S.B., Myers, D.S., Mrak, I., Leber, V., Heier, C., Taschler, U., Blankman, J.L., Cravatt, B.F., Lee, R.G., Crooke, R.M., Graham, M.J., Zimmermann, R., Brown, H.A., and Brown, J.M. (2013). The serine hydrolase ABHD6 Is a critical regulator of the metabolic syndrome. Cell reports 5, 508-520.

Vandevoorde, S., Jonsson, K.O., Labar, G., Persson, E., Lambert, D.M., and Fowler, C.J. (2007). Lack of selectivity of URB602 for 2-oleoylglycerol compared to anandamide hydrolysis in vitro. Br. J. Pharmacol. 150, 186-191.

Wicksteed, B., Brissova, M., Yan, W., Opland, D.M., Plank, J.L., Reinert, R.B., Dickson, L.M., Tamarina, N.A., Philipson, L.H., Shostak, A., Bernal-Mizrachi, E., Elghazi, L., Roe, M.W., Labosky, P.A., Myers, M.G., Jr., Gannon, M., Powers, A.C., and Dempsey, P.J. (2010). Conditional gene targeting in mouse pancreatic ss-Cells: analysis of ectopic Cre transgene expression in the brain. Diabetes 59, 3090-3098.

Wiskerke, J., Irimia, C., Cravatt, B.F., De Vries, T.J., Schoffelmeer, A.N., Pattij, T., and Parsons, L.H. (2012). Characterization of the effects of reuptake and hydrolysis inhibition on interstitial endocannabinoid levels in the brain: an in vivo microdialysis study. ACS Chem. Neurosci. 3, 407-417.

Zygmunt, P.M., Ermund, A., Movahed, P., Andersson, D.A., Simonsen, C., Jonsson, B.A., Blomgren, A., Birnir, B., Bevan, S., Eschalier, A., Mallet, C., Gomis, A., and Hogestatt, E.D. (2013). Monoacylglycerols Activate TRPV1 - A Link between Phospholipase C and TRPV1. PloS one 8, e81618.

SUPPLEMENTAL FIGURE LEGENDS

Figure S1. Incorporation of Labeled Fatty Acids and Glucose into Different Lipids in INS832/13 Cells, Related to Figure 1.

(A) INS832/13 β-cells were incubated with [1-^{14}C]-arachidonic acid (100 μM) and its incorporation into various lipids in at low (2 mM, 2G) and high (10 mM, 10G) glucose concentration was analyzed. [1-^{14}C]-Arachidonic acid was present during 40 min pre-incubation (at 2G) and during 45 min incubation (at 2G or 10G); *n* = 9. (B-D) INS832/13 cells were incubated with [U-^{14}C]-glucose under equilibrium labeling conditions, followed by 2 h incubation at 1 and 10 mM glucose, without and with the pan-lipase inhibitor orlistat (50 μM) and WWL70 (10 μM). (B) Release of [^{14}C]-FFA into the medium; (C) Incorporation of glucose carbons into 1-monoacylglycerol (1-MAG) and 2-monoacylglycerol (2-MAG); and (D) Incorporation of glucose carbons into diacylglycerol (DAG) and triglyceride (TG); *n* = 9.

Figure S2. Effect of 1-Linoleoylglycerol, 1-Stearoylglycerol and WWL70 and Lack of Effect of CB1 and CB2 Receptor Antagonists on Insulin Secretion, Related to Figure 3.

(A) Dose-dependent effect of 1-linoleoylglycerol on glucose stimulated insulin secretion at 5mM glucose in INS832/13 cells; *n* = 12. ***p<0.0001 compared with no MAG addition. (B) 1-Stearoylglycerol (1-SG) (30 μM) enhances GSIS in rat and human islets. Mean ± SEM of 4 (human islets) and 6 (rat islets) separate experiments with triplicate determinations. * p<0.05 and **p<0.01 compared with corresponding DMSO control. (C) Exogenous 1-stearoylglycerol restores GSIS inhibited by the pan-lipase inhibitor orlistat. GSIS (at 5 & 10 mM glucose) inhibited by 25 μM orlistat in INS832/13 cells is partially restored by 1-stearoylglycerol (30 μM). *n* = 12. ***p<0.0001 compared with DMSO control; ##p<0.01 compared with the orlistat group. (D-F) CB1 and CB2 receptors are not involved in MAG-mediated effects on insulin secretion. Insulin secretion was measured at 2 (2G) and 10 mM (10G) glucose without or with 1 μM of 2-arachidonoylglycerol (2-AG). Where indicated pre-incubations (45min) and incubations (45 min) were done with 1 μM AM251 (CB1 receptor antagonist) or 1 μM AM630 (CB2 receptor inverse agonist); *n*=6-9. (D) Insulin secretion at low and high glucose expressed as ng/mg protein. (E) Lack of effect of CB1/CB2 receptor antagonists at 2 mM

glucose on insulin secretion. Results are expressed as fold over DMSO control (absolute values of insulin secretion are given in panel (D). Where indicated 25 μM orlistat (pan-lipase inhibitor) was added. (F) Lack of effect of CB1/CB2 receptor antagonists at 10 mM glucose on insulin secretion. Where indicated 25 μM orlistat was added. Orlistat inhibition of glucose stimulated insulin secretion was reversed by 2-AG, and the CB1 antagonist AM251 had no effect on this reversal caused by 2-AG. Results are expressed as fold over DMSO control; n = 12. * p<0.05 and ***p<0.001 compared with control; *#P<0.05*; *###P<0.001* compared with the orlistat (ORL) group. (G) Dose-dependent effect of WWL70 on glucose stimulated insulin secretion in INS832/13 cells at 1, 5 and 10 mM glucose; n = 12. * p<0.05; **p<0.01; ***p<0.0001 compared with no WWL70 addition.

Figure S3. Effect of the MAGL Inhibitor JZL184 on the Lipid Profiles and Insulin Secretion in INS832/13 Cells, Related to 4.

Cells were labeled under equilibrium conditions with [U-^{14}C] glucose followed by 2h incubation at 1 and 10 mM [U-^{14}C] glucose (at the same specific radioactivity) in the absence (DMSO vehicle) and presence of 1 μM JZL184. Then the neutral glycerolipids in the cells and the released FFA were analyzed. 1-MAG: *P<0.05 compared to corresponding DMSO control; ###P<0.001 compared to 1 mM glucose. 2-MAG: **P<0.05 compared to DMSO control; ###P<0.001 compared to 1 mM glucose. Total MAG: **P<0.05 compared to DMSO control; FFA released: ###P<0.001 compared to 1 mM glucose. TG, ### P<0.001 compared to 1 mM glucose. DAG: no significant differences. Lower right panel shows insulin secretion at 1, 5 and 10 mM glucose with or without JZL184; n = 12.

Figure S4. Generation and Characteristics of ABHD6-KO Mice and Loss of WWL70 Effect on Insulin Secretion and MAG Hydrolytic Activity in ABHD6-KO Mouse Islets, Related to Figure 5.

(**A**) ABHD6-KO mice were generated as described in Methods. Schematic of the conditional knockout-first cassette for producing ABHD6-KO mice. Positioning of primers for genotyping PCR is indicated, for an anticipated 517 bp DNA fragment (with primers, loxP-F & R1) for floxed mutant mice and a 200bp fragment (with primers, wtF & wtR) for wild-type mice. (B) Genomic PCR amplification of chromosomal DNA obtained from tails of 3 week old mice,

showing 517 bp DNA fragment in the -/- mice, 200 bp fragment in the +/+ mice and both fragments in the +/- mice. (C) Weight gain of WT, HZ and ABHD6-KO mice (all males) over 23 weeks is similar (n=5-11). (D) Average daily chow food intake of ABHD6-KO mice over a period of 22 weeks (n=5-9 mice per group). (E) Total 2-MAG levels in the islets incubated at 2.8 mM (2.8G) and 16.7 mM (16.7G) glucose for 1 h in KRBH (n=3 separate experiments). ***P*<0.01 vs 2.8 G in the same genotype; ##*P*<0.05 vs WT islets. (F, G) Glucose-dependent increase in major MAG species in islets from ABHD6-KO mice. Isolated islets from ABHD6-KO, HZ, and WT mice were incubated at 2.8 mM (2.8G) and 16.7 mM (16.7G) glucose for 1 h in KRBH and islet total 1-MAG and 2-MAG were resolved by TLC and analyzed for individual MAG species (n=3 separate experiments). (F) Total 1-palmitoylglycerol (C16:0), 1-stearoylglycerol (C18:0) and 1-oleoylglycerol (C18:1) levels. (G) Total 2-palmitoylglycerol (C16:0), 2-stearoylglycerol (C18:0) and 2-oleoylglycerol (C18:1) levels. **P*<0.05; ***P*<0.01 vs 2.8 G in the same genotype; #*P*<0.05; ##*P*<0.01 vs WT islets. (H) Insulin tolerance test in fed 26 week old WT, HZ and KO mice (n=5-7). Inset depicts area above the curve. (I) Pancreatic islets were isolated from male whole-body ABHD6-KO mice and wild-type littermates and islet extracts (n=4 mice per group) were prepared by freeze-thaw-sonication of islets in 250 mM sucrose, 50 mM Hepes, pH 7.2 for measuring MAG hydrolysis activity. MAG hydrolysis was measured using 1-arachidonoylthioglycerol as substrate in the absence (DMSO vehicle) or presence of 1 μM WWL70. For details see Supplementary Methods. Results are expressed as percentage of activity in wild-type islet extracts. ***P*<0.01 vs wild-type control. (J) Effect of WWL70 (10 μM) on GSIS in ABHD6-KO and WT islets (n= 4 mice per group) was measured at 2.8 and 16.7 mM glucose, as described in Methods. ***P*<0.01, ****P*<0.001 vs wild-type DMSO control.

Figure S5. ABHD6 mRNA Expression in Hypothalamic Areas, Body Weight Gain, Food Intake and β-Cell Mass of β-Cell Specific ABHD6-KO Mice, Related to Figure 6

Two weeks post-tamoxifen injection, hypothalamic regions, ventromedial hypothalamus (VMH) and arcuate nucleus, which are known to express proteins under Rip (rat insulin-2 promoter) control, were isolated from mip*cre*+ (n=6), flox/flox (n=8) and BKO (n=12) mice and analyzed for any ABHD6 deletion due to possible cre expression by qRT-PCR. (A) VMH and (B) arcuate nucleus. Results are expressed as ABHD6 mRNA expression relative to 18S

mRNA. (C) Body weight gain of BKO mice on chow diet, up to 6 weeks and (D) average daily food intake for 6 weeks following tamoxifen injection of mip*cre*+ (n=5), flox/flox (n=5) and BKO (n=6) mice. (E) Two weeks post-tamoxifen injection, pancreata were isolated from mip*cre*+, flox/flox and male BKO mice (n=6 or 7) and processed for assessing β-cell mass. Results are expressed as percentage of total pancreas mass.

Figure S6. Fluorescent Monoacylglycerol Binding to Munc13-1 C1 Domain, Munc13-1 Translocation to Membrane Fraction in ABHD6-KO islets and the Effect of Monoacylglycerol on Voltage-Gated Ca^{2+} Channel Activity in Mouse Islet β-Cells, Related to Figure 7.

(A) Fluorescence quenching of NBD-MAG by Munc13-1-C1. Representative emission spectra of 1.5 μM of 7-nitrobenz-2-oxa-1,3-dizole-4-yl (NBD)-MAG (12:0) incubated with 1 μM of purified Munc13-1-C1 peptide and 1 μM of GLP1 peptide (negative control). AU, arbitrary units. Inset: Relative decrease (as percentage) in peak fluorescence (at 540 nm) of NBD-MAG by Munc13-1-C1 as compared to the control peptide; n=4. $^{**}P<0.01$. (B) Munc13-1 translocation to membranes in islets from wild-type and whole body ABHD6-KO mice. Isolated islets (500 islets from 4 mice in each group) were incubated at 2.8 or 16.7 mM glucose for 45 min followed by homogenization and isolation of whole membrane fraction. Membrane pellets were processed for Western blotting using anti-Munc13-1 antibody as detailed in Supplementary Methods. (C) Voltage-gated Ca^{2+} (Ca_v) currents from Munc13-$1^{+/+}$ and $^{+/-}$ mice β-cells with or without 1-palmitoylglycerol (MAG) (50μM) or WWL70 (10 μM) pretreatment are shown. Panel-I shows representative traces of Ca_v currents recorded in the whole-cell mode from Munc13-1 $^{+/+}$ and $^{+/-}$ mice β-cells. Panel-II shows current-voltage relationship of Ca_v channels. Currents were normalized to cell capacitance to yield current density. Panel-III is a bar chart, showing maximum increases in current densities. Mean ± SEM; *n* = 11-16 cells from 3-4 mice. For measurements of depolarization voltage-activated (Cav) currents pipettes were filled with 120 mM CsCl, 20 mM tetraethylammonium chloride, 5 mM EGTA, 5 mM MgATP, and 5 mM Hepes (pH 7.2). The external solution contained, 100 mM NaCl, 20 mM $BaCl_2$, 20 mM tetraethylammonium chloride, 4 mM CsCl, 1 mM $MgCl_2$, 10 mM glucose, and 5 mM Hepes pH 7.4. β-Cells were held at -70 mV for 2 min after

formation of whole-cell mode and currents were elicited from -80 to +60 mV in 10 mV increments. For testing MAG effect, 50 μM 1-palmitoylglycerol was added both during preincubation and incubation. Recordings were conducted using EPC10 patch clamp amplifier and Pulse and X-Chart software programs (HEKA Electronik, Germany).

EXTENDED EXPERIMENTAL PROCEDURES

Islet Isolation

All procedures involving animals were approved by the Institutional Committee for the Protection of Animals. Pancreatic islets were isolated from male Wistar rats, C57Bl6 or CD1 mice (Charles River) (Peyot et al., 2009b). Human islets (75 to 90% pure; male donors without any known disease) were from Beta-Pro LLC (USA). Isolated islets were handpicked and cultured overnight in RPMI 1640 medium.

Insulin Secretion

Secretion in INS832/13 cells (Hohmeier et al., 2000) and isolated islets was measured in static incubations (Peyot et al., 2009b). Pre-incubation was for 45 min in medium consisting of Krebs Ringer buffer-Hepes (KRBH), 0.5% defatted BSA and either 2 mM glucose for INS cells or 2.8 mM glucose for islets. Incubations were for 1-2h at various glucose concentrations. The drugs WWL70 (Cayman), orlistat (Sigma) and JZL184 (Cayman) were present both during pre-incubation and incubation. Insulin in the media and in the cell and islet extracts was determined (Linco Research).

Over-expression and RNAi Knockdown of ABHD6 and MAGL

The pCMV- plasmids expressing human ABHD6, MAGL and Green Fluorescent Protein (GFP) (Origene) were introduced into INS832/13 cells using the Amaxa Nucleofector (Amaxa, Inc.). After 72h, cells were used for insulin secretion and Western blot analysis. Silencer-select ABHD6- siRNA and 2 control-siRNA (Ambion) were introduced into INS832/13 cells using RNAiMAX and after 24h cells were used for Western blotting and insulin secretion. The sequences for ABHD6 used were 5'-CAGUUUGUAGAAUGCCUUAtt-3' and 5'-CGGAAAUUGUUUUUGGAAAtt-3'. For

RNAi-knockdown of MAGL, the following sequences were used: 1) 5'-CAAAUUGGAAGAAACCCUAGUACCC-3'; and 2) 5'-GUCCUCCAUGAAAUAAAUACGUGGG-3'.

ABHD6 Polyclonal Antibody Generation

A maltose binding protein (MBP) ABHD6 fusion protein expression construct was produced by inserting the DNA sequence encoding amino acids 119-315 of mouse ABHD6 into the pMAL-C2 vector (New England Biolabs). The pMAL-mABHD6$^{119-315}$ vector was used to produce the fusion protein in *E.coli*. Recombinant MBP-mABHD6$^{119-315}$ fusion protein was affinity-purified and used for antibody production (Lampire, PA). The polyclonal antibodies were affinity-purified using MBP-mABHD6$^{119-315}$ coupled Amino-link gel (Pierce).

Immunoblotting

Tissue and cell lysates were prepared and extracted proteins were processed for immunoblotting (Peyot et al., 2009b). Membranes were incubated with antibodies for MAGL (Cayman) and ABHD6. Mouse monoclonal β-actin and rabbit polyclonal α-tubulin antibodies were from Sigma and Abcam (Cambridge, MA) respectively.

Cell Capacitance Studies.

Munc13-1$^{+/-}$ mouse (Augustin et al., 1999; Rhee et al., 2002) islets were isolated (Kwan et al., 2006b) and dispersed into single cells by digestion with 0.25 mg/ml trypsin and were plated on glass coverslips in RPMI-1640 medium containing 11 mM glucose and allowed to adhere for 48 h before use. Recording pipettes were from 1.5-mm borosilicate glass capillary tubes, heat-polished with tip resistances from 2-3 MOhm when filled with intracellular solution. β-Cells were identified by the lack of a transient voltage-dependent inward Na^+ current (Gopel et al., 1999). For cell membrane capacitance (Cm) determinations (at 30°C) the intracellular solution contained 125 mM cesium glutamate, 10 mM CsCl, 10 mM NaCl, 1 mM $MgCl_2$, 5 mM Hepes, 0.05 mM EGTA, 3 mM MgATP (pH 7.2). The extracellular solution consisted of 118 mM NaCl, 5.6 mM KCl, 1.2 mM $MgCl_2$, 10 mM $CaCl_2$, 20 mM tetraethylammonium chloride, 5 mM Hepes (pH 7.4) and 5 mM glucose. Cm was estimated by the Lindau-Neher technique, implementing the "Sine-DC" feature of the Lock-in module (40 mV peak-to-peak

and a frequency of 500 Hz) in the whole-cell configuration during a train of ten 500-ms depolarizations from -70 mV to 0 mV.

Quantitative Real-Time PCR

Total RNA was extracted from INS832/13 cells, islets and tissues and first strand cDNA was synthesized from 2 µg of total RNA using the Pd(N)6 random primers and MMLV reverse transcriptase. RT-qPCR was performed and the PCR products were quantified using the FastStart DNA Master PLUS SYBR green kit (Roche Diagnostics). Expression levels were normalized for the 18S mRNA transcript. The primer sequences were: 18S mRNA forward (5'-CTGAGAAACGGCTACCACATC-3'), reverse (5-GGCCTCGAAAGAGTCCTGTAT-3'); MAGL forward (5'-TTGAAGAGGCTGGACATGCTG-3'), reverse (5'-TAGTCCTTCTGGACGGTGTTC-3'); and ABHD6 forward (5'-AGGATATGTGGCTCAGTGTGG-3'), reverse (5'-GTGCCTATAAGGTGAAAGGGC-3').

Incorporation of [U-^{14}C]-Glucose into Lipids

After pre-labeling overnight at 11 mM [U-^{14}C]-glucose in RPMI medium INS832/13 cells were washed in KRBH (1 mM [U-^{14}C]-glucose; same radio-specific activity) and pre-incubated for 45 min at 1 mM [U-^{14}C]-glucose. Then the cells were incubated for 2h at 1 and 10 mM [U-^{14}C]-glucose with and without orlistat, WWL70 and JZL184, followed by wash with PBS, flash-freezing in liquid nitrogen and lipid extraction. Lipids were separated by thin layer chromatography (TLC) and the associated radioactivity was quantified. Neutral lipids were separated by boric acid impregnated silica gel-TLC, with two successive solvent systems for efficient separation of 1-MAG from 2-MAG; first, with petroleum ether: diethyl ether: acetic acid (70:30:1); then using a second solvent system, chloroform: acetone: acetic acid (60:40:1).

Determination of Free Fatty Acid and Monoacylglycerol Species

Rat islets were pre-incubated for 1h in KRBH at 2.8 mM glucose and then incubated for 2h at 2.8 mM or 16.7 mM glucose. With INS832/13 cells, the low and high glucose concentrations were 2 and 10 mM, respectively. Inhibitors, when used, were present during both pre-incubation and incubation. FFA accumulated in the cells and released into the medium were extracted by Dole-Meinertz extraction procedure (Puttmann et al., 1993). The dried fatty acids

were derivatized with phenacylbromide and quantified by reverse phase HPLC (Mehta et al., 1998) using a Zorbax Eclipse plus XDB analytical C18 column (4.6 × 250 mm; 5 μm; Agilent Technology). FFA were eluted using methanol/water (92.5:7.5) at a flow rate of 1.5 ml/ min and detected at 242 and 254 nm and quantified by the internal standard method. For MAG measurements, total lipids from INS832/13 cells incubated at 2 and 10 mM glucose without or with 10 μM WWL70 or ABHD6 -/-, +/- and +/+ mouse islets incubated at 2.8 and 16.7 mM glucose were extracted and separated on boric acid/silica gel-TLC. The separated 1- and 2-MAG spots were scraped and were saponified and released fatty acids were quantified by reverse-phase HPLC.

Studies in the Low-Dose Streptozotocin Diabetes Mouse Model

Diabetes was induced by a single injection of streptozotocin (i.p., 100 mg/kg BW) to 8 wk old male CD1 mice (Hayashi et al., 2006). The 'normal' mice received buffer only. WWL70 was dispersed as a microsuspension in polyethylene glycol-300: Tween-20 (18:1). Four weeks following STZ (fed glycemia, 16-25 mM) or buffer injection, STZ and normal mice were divided into 2 groups and were administered WWL70 or vehicle daily, i.p., for 3 consecutive days, as follows: vehicle (PEG/Tween-20) and WWL (WWL70, 5 mg/kg BW). On the third day, the mice received the drug 2 h prior to oral glucose tolerance test, and access to food was withdrawn for 6 h prior to the glucose load (2g/kg BW). Blood was collected from the tail vein (0-120 min) for blood glucose and plasma insulin measurements.

ABHD6 Activity Measurements

INS832/13 cell membranes and cytoplasmic fractions (100,000 g pellet and supernatant) were used. Incubations were in 0.5 ml containing 25 mM Tris-HCl pH 6.0, 150 mM NaCl, 0.05 mM EDTA, 0.1 mM DTT and 0.02% defatted BSA, 8 μg cell extract protein, 50 μM 1-oleoylglycerol without or with 10 μM WWL70 or 25 μM orlistat. Incubations were for 1h at 30°C, and oleic acid released was quantified by HPLC. The hydrolytic activity inhibited by WWL70 was considered due to ABHD6.

In order to assess whether the ABHD6 inhibitor WWL70 can inhibit the residual MAG hydrolysis activity of ABHD6-KO islets, we prepared extracts of islets isolated from wild type and whole body ABHD6-KO mice. The assay system for measuring MAG hydrolysis

contained in a final volume of 100 µl, 50 mM potassium phosphate, pH 7.2, 1 µg of islet extract protein, 13 µM ThioGlo-1 and 5 µM arachidonyl-1-thioglycerol as the substrate. Reactions were started with the addition of substrate after a pre-incubation of 15 min at 30°C. Arachidonyl-1-thioglycerol hydrolysis was followed by the reaction of released thioglycerol with ThioGlo-1. The resulting adduct is fluorescent, whose formation is measured continuously for 30 min at 380 nm excitation and 510 nm emission. Where indicated, WWL70 was added at 1 µM final concentration at pre-incubation stage.

MAG Binding to the Munc13-1 C1-Domain

Rat Munc13-1 C1 domain (residues 567-617) as a GST fusion protein (Shen et al., 2005) was expressed in *E. coli* and purified. Synthetic rat Munc13-1-C1 domain peptide (99% pure) (HNFEVWTATTPTYCYECEGLLWGIARQGMRCTECGVKCHEKCQDLLNADC) was from Biomatik Corporation. *(A) Liposomal preparation.* Phosphatidylcholine (80 µg) and phosphatidylserine (20 µg) were dried and hydrated with 0.1 ml of liposome buffer (50 mM Hepes-NaOH pH 6.8, 100 mM NaCl and 4 mM EGTA) followed by vigorous mixing for 20 min and sonication for 5 min to produce unilamellar liposomes. This liposomal suspension was centrifuged at 3000×g for 30 min at 4°C and the supernatant containing unilamellar liposomes was used to perform MAG binding assay. *(B) Binding assay by tryptophan fluorescence quenching.* Binding of MAG and other ligands (1 µM each) to the Munc13-1 C1 domain was followed as before (Shen et al., 2005). Emission spectra were recorded between 300 and 400 nm at an excitation λ295 nm. *(C) Binding of NBD-MAG to Munc13-1 C1-domain.* Fluorescently labeled MAG binding to Munc13-1 C1 domain was followed by using 7-nitrobenz-2-oxa-1,3-dizole-4-yl MAG (12:0) (NBD-MAG) (Petry et al., 2005). Liposomes with NBD-MAG were prepared by mixing 3.75 µg of phosphatidylcholine, 6.3 µg of phosphatidylinositol and 12.5 µg of NBD-MAG (Petry et al., 2005). Binding was measured by incubating 1 µM synthetic Munc13-1 C1 peptide (MW: 5728.51) with 100 µl of NBD-MAG—liposomes, at room temperature for 10 min. Emission spectra of NBD fluorescence were recorded between 500 and 620 nm at an excitation λ480 nm. The fluorescence quenching due to NBD-MAG binding to Munc13-C1 was used to calculate the binding. Glucagon like peptide-1, with similar molecular size as the C1-domain, was used as control. *(D) Protein-lipid overlay assay.* The method of Dowler et al. (Dowler et al., 2002) was adapted. Briefly,

25-400 nmol of lipids in chloroform/methanol/water (1:2:0.08) were spotted on a Hybond-C-extra membrane and after drying blocked with 3% defatted-BSA. The membrane was then incubated overnight at 4°C with 10 μg/ml purified Munc13-1 C1-GST fusion protein or purified GST in Tris-buffered saline (50mM, pH 7.5) with 0.2% Tween-20. Detection used anti-GST antibody (Santa Cruz Biotech) and a peroxidase conjugated second antibody.

Munc13-1 Translocation to Plasma Membrane in β-Cells

Confocal microscopy study. INS 832/13β-cells were transfected with pEGFP-MUNC13-1 (WT) and pEGFP-mutated MUNC13-1 (H567K) plasmids using Amaxa. The transfected cells were grown on coverslips for 72 h. Then the cells were starved in RPMI 1640 medium with 2 mM glucose, and pre-incubated in KRBH buffer with 0.5% BSA and 2 mM glucose for 45 min. After pre-incubation, the cells were incubated at 2 or 10 mM glucose in the absence (DMSO control) or presence of 100 μM 1-PG, 10 μM WWL70 and 300 nM PMA for 10 min. Then the cells were quickly washed with cold PBS twice, and the coverslips were fixed with ProLong Gold Antifade reagent (Life Technologies) and mounted on slides for imaging using confocal microscope (Leica).

Cell Fractionation study. To assess the effect of ABHD6 deletion on the translocation of Munc13-1 to plasma membrane, islets from wild-type and male whole body ABHD6-KO mice were isolated and allowed to recover overnight in RPMI-1640 medium with 10% FBS and 11 mM glucose. The following day, the islets were divided into two subgroups of 500 islets each and placed in 1.5ml tubes. Then the islets were starved in RPMI-1640 with 10%FBS and 2.8 mM glucose for 2h. Then the islets were washed with KRBH and pre-incubated in KRBH with 0.5% BSA and 2.8 mM glucose for 45 min. The islets were then incubated in KRBH with 2.8 or 16.7mM glucose for 30 min, followed by quick wash with cold PBS and frozen in liquid nitrogen till further analysis. The islets were subjected to freeze-thaw sonication in 250 mM sucrose, 25 mM Hepes, pH 7.2, followed by centrifugation at 150,000xg for 30 min. The pellets containing the membrane fraction were suspended in 250 mM sucrose, 25 mM Hepes, pH 7.2 and the protein concentration was measured by BCA assay. Islet membrane protein (30 μg) was processed for SDS-PAGE and immnoblotting using anti-Munc13-1 antibody (Synaptic Systems) at a dilution of 1:1000 (overnight incubation). The Munc13-1 bands were

visualized with SuperSignal West Pico Chemiluminescence Detection Kit (Thermo Scientific). As a protein loading control, IGFR1β was probed using anti-IGFR1β antibody from Cell Signaling at 1:1000 dilution.

Whole Body ABHD6 Knockout Mice

Whole-body ABHD6 knockout mice were generated by employing "knockout-first" design (Skarnes et al., 2011). The mice used were a pure background of C57/BL6N and the ES cells (JM8A3.N1 (Agouti), also derived from C57Bl6N) with confirmed conditional vector targeting for ABHD6 (HEPD0651_8_C07) were obtained from European Conditional Mouse Mutagenesis Program (Germany). Details on the ES cells and vectors are available at http://www.knockoutmouse.org/martsearch/project/72228. Knockout-first ABHD6-whole body KO mice were generated on C57Bl6N background in Mouse Biology Program, University of California, Davis. Following primers were used for genotyping the wild-type and mutant mice, at 3 wks age, from chromosomal DNA extracted from a piece of tail. For wild-type, the primer sequences are: forward (wtF), 5'-GCAGAAAGGAAAGTAATACCTTAAGAG-3' and reverse (wtR), 5'-AACATCTTAAAACTTAATGCTGATAGCTC-3'. Although, these sequences are present in the targeting vector also, they are spaced too far apart and do not give rise to the anticipated PCR product in the mutant mice (Figure S4A). For the mutant mice, the forward (loxP-F) and reverse (ABHD6-R1) primers are 5'-GAGATGGCGCAACGCAATTAATG-3' and 5'-CAAGTGATGCTATGTAACCTTGCCCC-3', respectively. A PCR product of 517 bp indicated mutation while 200 bp band indicated wild-type (Figure S4B).

Beta Cell Specific ABHD6-KO (BKO) Mice

Whole body ABHD6-KO mice were crossed with Flpo transgenic mice on pure C57Bl6N genetic background, to produce floxed ABHD6 mice that are on pure C57Bl6N background. Homozygous floxed ABHD6 mice were crossed with tamoxifen-inducible mip-*cre* transgenic mice (Wicksteed et al., 2010) that were back-crossed to C57Bl6N for 8 generations, to produce mice that carried floxed ABHD6 gene and tamoxifen-inducible mip-*cre* transgene (mip*cre*+, flox/-). Then the mip*cre*+, ABHD6$^{flox/-}$ mice were crossed with ABHD6$^{flox/-}$ mice to generate mip*cre*+, ABHD6$^{flox/flox}$, β-cell specific inducible ABHD6-KO (mip*cre*+,

ABHD6$^{flox/flox}$) and wild-type mice. At the age of 8 weeks, these mice were injected intraperitoneally, daily with tamoxifen (50 mg/kg body weight, dissolved in 90% corn oil plus 10% ethanol) for 5 consecutive days to generate BKO mice. After 2 weeks following tamoxifen injections, ABHD6 expression was found to be abrogated only in pancreatic islets (β-cells) (Figure 6A) but not in other tissues (Figure 6B,C,D) of the BKO mice.

Beta Cell Mass Measurement

Whole pancreata were removed from mip*cre*+, floxed and BKO mice, and were placed in cold PBS and carefully all the surrounding fat and tissue was removed. After removing excess buffer, the pancreata were weighted and fixed in freshly prepared 10% formalin at room temperature for 24 h, followed by embedding in wax blocks. Then 5 μm sections were cut using a microtome and 6 equally spaced sections from each pancreas were processed for β-cell mass measurement. Immunohistochemistry was done with anti-guinea pig insulin antibody (DAKO) to mark β-cells and alkaline phosphatase conjugated second antibody. Hematoxylin was used for counter-staining. The slides were monitored using a high-resolution scanner (Nikon Super Cool Scan 9000) to assess the β-cell area and the whole pancreas area, followed by calculation of the ratio of β-cell area to whole pancreas area.

Hyper Insulinemic Euglycemic Clamp Studies

Two-hour hyper insulinemic-euglycemic clamps (Peyot et al., 2010) were performed on wild-type and whole body ABHD6-KO mice after a 5 h food-restriction in the morning from 7 AM to 12:00 noon. The mice received a bolus insulin infusion (85 mU/kg; HumulinR) for 1 min followed by insulin infusion at constant rate of 5 mU/ kg/ min. Dextrose (20%, w/v) was infused starting 5 min after the beginning of insulin infusion in order to clamp glycemia at 7.2 mM. Blood was collected every 30 min starting from time 0, to quantify the glucose levels. Glucose infusion rate was calculated as an index of insulin sensitivity during the last 30 min of the clamp.

Intraperitoneal Insulin Tolerance Test

Intraperitoneal insulin tolerance test (IP-ITT) was performed in conscious mice in the afternoon under fed conditions. Insulin was administered intraperitoneally at a dose of 0.75U/ kg BW.

Blood was collected from tail at 0, 15, 30, 45, 60 and 90 min and glycemia was monitored using glucometer.

Statistical Analysis

Values are expressed as means ± SEM. Statistical analysis was performed using one-way ANOVA with Dunnett's post-test for multiple comparisons or two-way ANOVA with Bonferroni's post-test for multiple comparisons using GraphPad Prism. For electrophysiology experiments, comparisons were by unpaired two-tailed Student's *t* test.

SUPPLEMENTAL REFERENCES

Dowler, S., Kular, G., and Alessi, D.R. (2002). Protein lipid overlay assay. Sci. STKE. 2002, pl6.

Gopel, S., Kanno, T., Barg, S., Galvanovskis, J., and Rorsman, P. (1999). Voltage-gated and resting membrane currents recorded from B-cells in intact mouse pancreatic islets. J. Physiol. 521 Pt 3, 717-728.

Mehta, A., Oeser, A.M., and Carlson, M.G. (1998). Rapid quantitation of free fatty acids in human plasma by high-performance liquid chromatography. J. Chromatogr. B Biomed. Sci. Appl 719, 9-23.

Petry, S., Ben Ali, Y., Chahinian, H., Jordan, H., Kleine, H., Muller, G., Carriere, F., and Abousalham, A. (2005). Sensitive assay for hormone-sensitive lipase using NBD-labeled monoacylglycerol to detect low activities in rat adipocytes. J. Lipid Res. 46, 603-614.

Peyot, M.L., Pepin, E., Lamontagne, J., Latour, M.G., Zarrouki, B., Lussier, R., Pineda, M., Jetton, T.L., Madiraju, S.R., Joly, E., Prentki, M. (2010) Beta-cell failure in diet-induced obese mice stratified according to body weight gain: secretory dysfunction and altered islet lipid metabolism without steatosis or reduced beta-cell mass. Diabetes 59, 2178-2187.

Puttmann, M., Krug, H., von Ochsenstein, E., and Kattermann, R. (1993). Fast HPLC determination of serum free fatty acids in the picomole range. Clin. Chem. 39, 825-832.

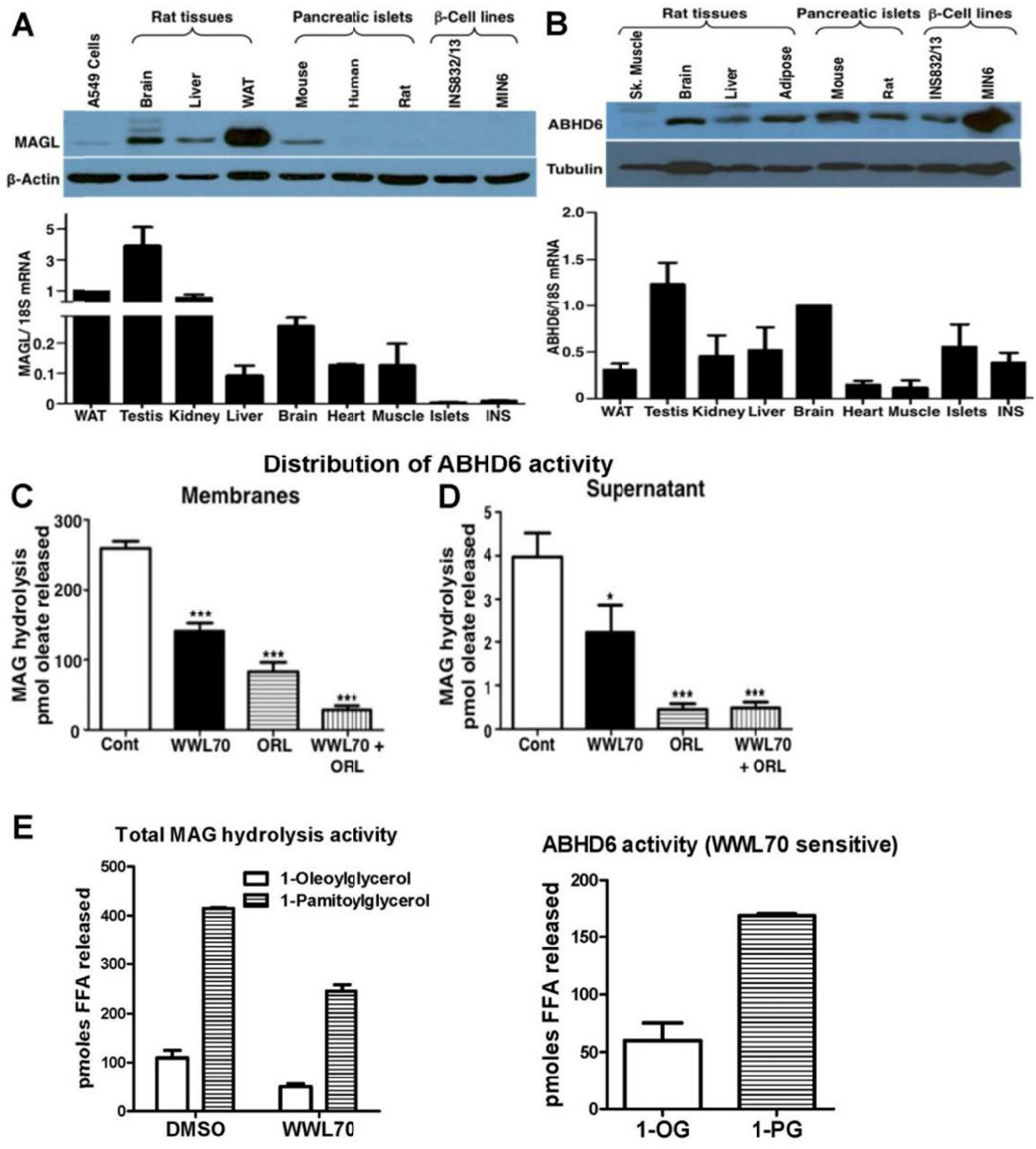
A
Rat tissues
Pancreatic islets
β-Cell lines
A549 Cells
Brain
Liver
WAT
Mouse
Human
Rat
INS832/13
MIN6
MAGL
β-Actin
MAGL/ 18S mRNA
WAT Testis Kidney Liver Brain Heart Muscle Islets INS
B
Rat tissues
Pancreatic islets
β-Cell lines
Sk. Muscle
Brain
Liver
Adipose
Mouse
Rat
INS832/13
MIN6
ABHD6
Tubulin
ABHD6/18S mRNA
WAT Testis Kidney Liver Brain Heart Muscle Islets INS
Distribution of ABHD6 activity
C
Membranes
MAG hydrolysis pmol oleate released
Cont
WWL70
ORL
WWL70 + ORL
D
Supernatant
MAG hydrolysis pmol oleate released
Cont
WWL70
ORL
WWL70 + ORL
E
Total MAG hydrolysis activity
1-Oleoylglycerol
1-Pamitoylglycerol
pmoles FFA released
DMSO
WWL70
ABHD6 activity (WWL70 sensitive)
pmoles FFA released
1-OG
1-PG

Figure 1

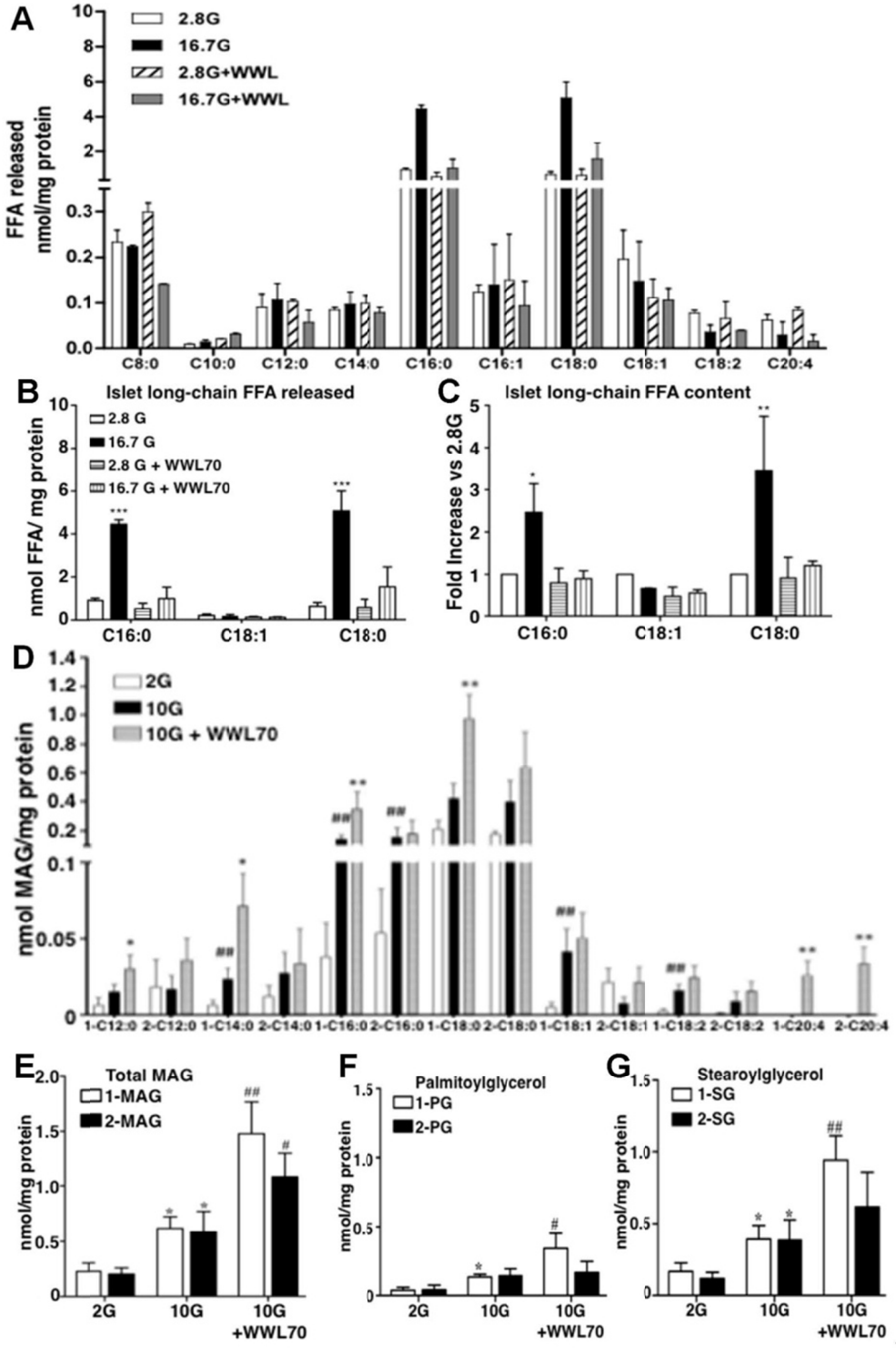
A
2.8G
16.7G
2.8G+WWL
16.7G+WWL
FFA released nmol/mg protein
C8:0
C10:0
C12:0
C14:0
C16:0
C16:1
C18:0
C18:1
C18:2
C20:4
B
Islet long-chain FFA released
2.8 G
16.7 G
2.8 G + WWL70
16.7 G + WWL70
nmol FFA/ mg protein
C16:0
C18:1
C18:0
C
Islet long-chain FFA content
Fold Increase vs 2.8G
C16:0
C18:1
C18:0
D
2G
10G
10G + WWL70
nmol MAG/mg protein
1-C12:0
2-C12:0
1-C14:0
2-C14:0
1-C16:0
2-C16:0
1-C18:0
2-C18:0
1-C18:1
2-C18:1
1-C18:2
2-C18:2
1-C20:4
2-C20:4
E
Total MAG
1-MAG
2-MAG
nmol/mg protein
2G
10G
10G +WWL70
F
Palmitoylglycerol
1-PG
2-PG
nmol/mg protein
2G
10G
10G +WWL70
G
Stearoylglycerol
1-SG
2-SG
nmol/mg protein
2G
10G
10G +WWL70

Figure 2

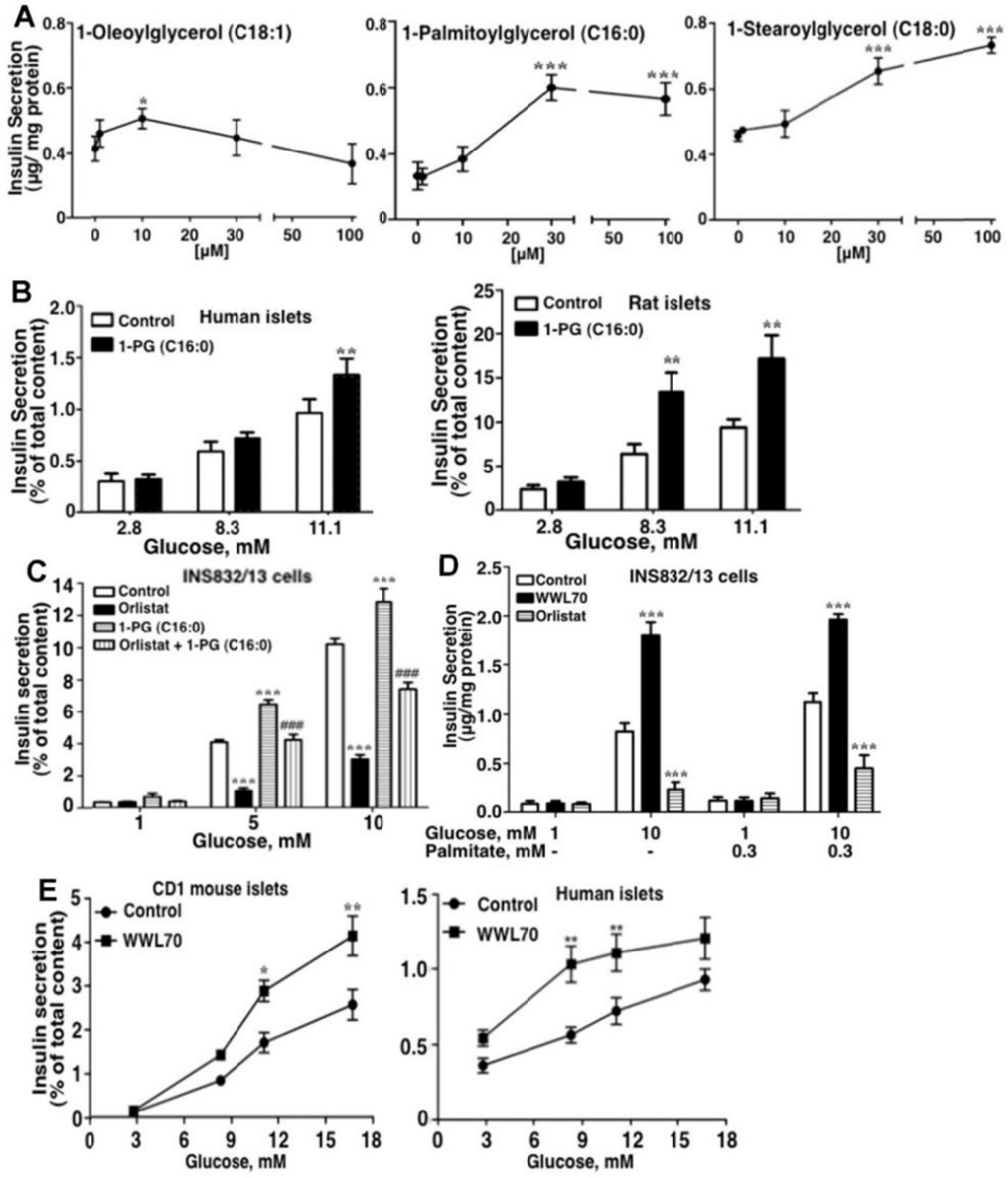
A
1-Oleoylglycerol (C18:1)
1-Palmitoylglycerol (C16:0)
1-Stearoylglycerol (C18:0)
Insulin Secretion (µg/ mg protein)
[µM]
B
Human islets
Rat islets
Control
1-PG (C16:0)
Insulin Secretion (% of total content)
Glucose, mM
C
INS832/13 cells
Control
Orlistat
1-PG (C16:0)
Orlistat + 1-PG (C16:0)
Insulin secretion (% of total content)
Glucose, mM
D
INS832/13 cells
Control
WWL70
Orlistat
Insulin Secretion (µg/mg protein)
Glucose, mM
Palmitate, mM
E
CD1 mouse islets
Human islets
Control
WWL70
Insulin secretion (% of total content)
Glucose, mM

Figure 3

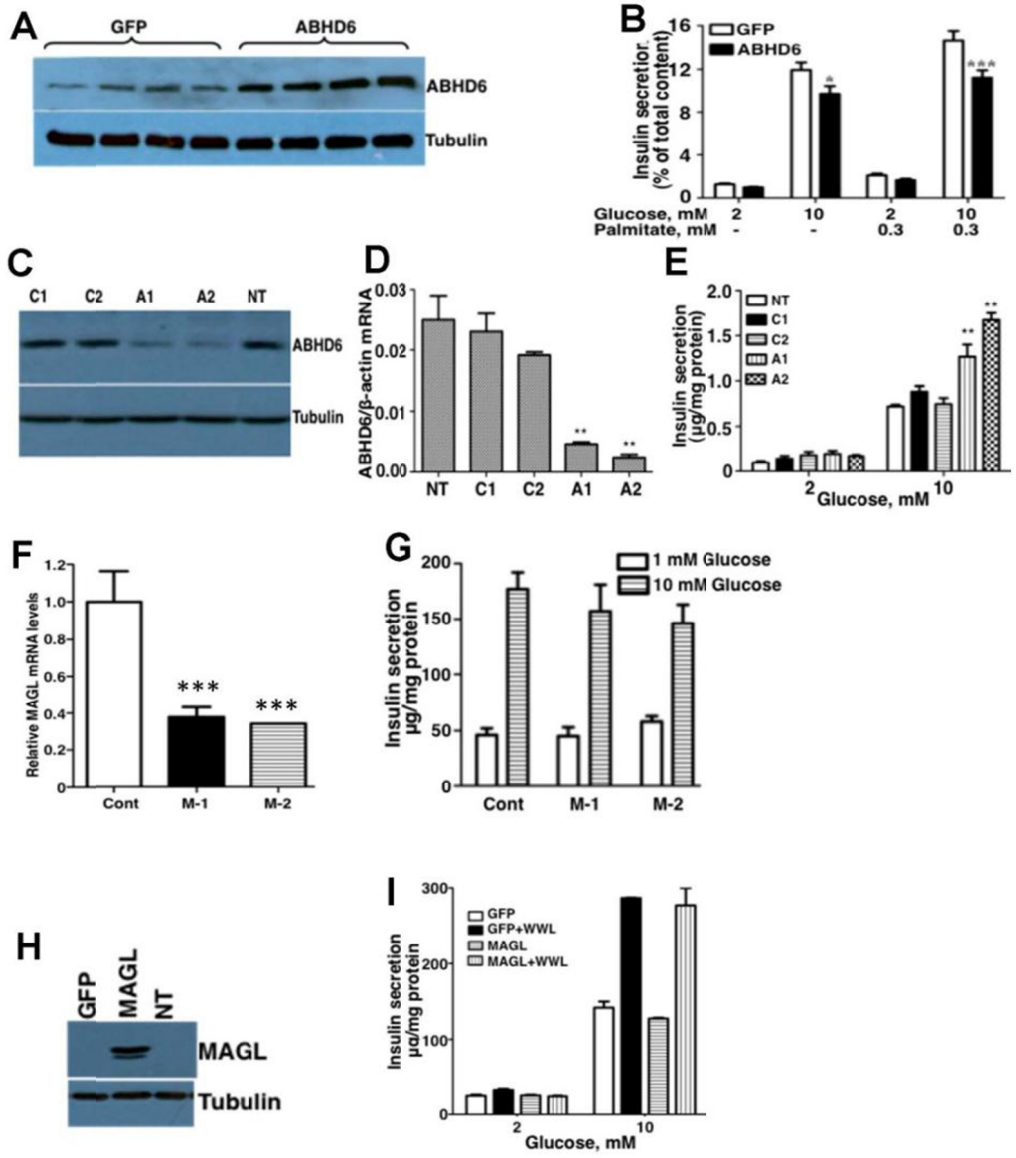
A
GFP
ABHD6
ABHD6
Tubulin
B
GFP
ABHD6
Insulin secretion (% of total content)
Glucose, mM
Palmitate, mM
C
C1
C2
A1
A2
NT
ABHD6
Tubulin
D
ABHD6/β-actin mRNA
NT
C1
C2
A1
A2
E
NT
C1
C2
A1
A2
Insulin secretion (μg/mg protein)
Glucose, mM
F
Relative MAGL mRNA levels
Cont
M-1
M-2
G
1 mM Glucose
10 mM Glucose
Insulin secretion μg/mg protein
Cont
M-1
M-2
H
GFP
MAGL
NT
MAGL
Tubulin
I
GFP
GFP+WWL
MAGL
MAGL+WWL
Insulin secretion μg/mg protein
Glucose, mM

Figure 4

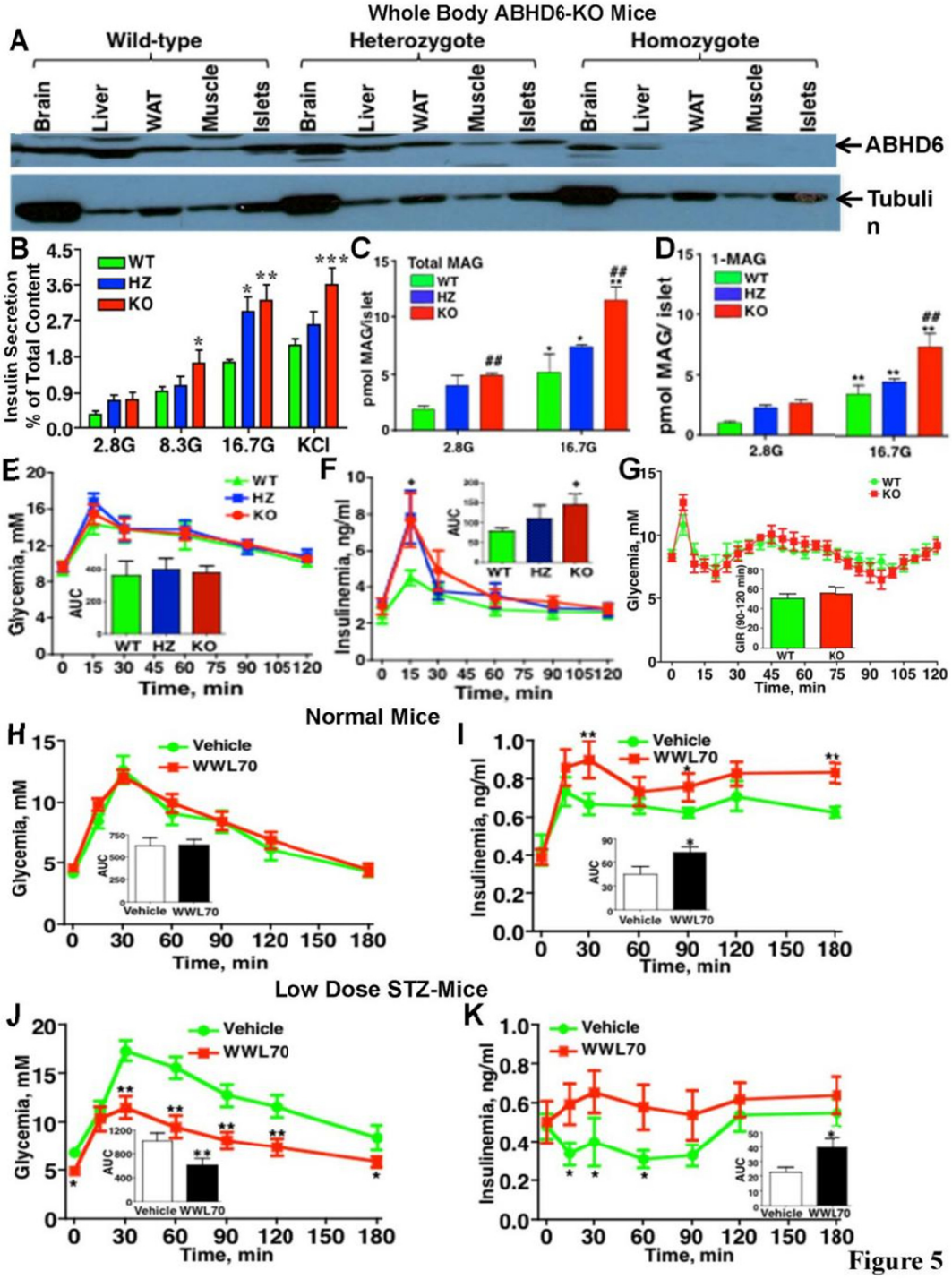
Whole Body ABHD6-KO Mice
A
Wild-type
Heterozygote
Homozygote
Brain
Liver
WAT
Muscle
Islets
ABHD6
Tubulin
B
Insulin Secretion % of Total Content
WT
HZ
KO
2.8G
8.3G
16.7G
KCl
C
Total MAG
pmol MAG/islet
D
1-MAG
pmol MAG/ islet
E
Glycemia, mM
AUC
Time, min
F
Insulinemia, ng/ml
G
GIR (90-120 min)
Normal Mice
H
Vehicle
WWL70
I
Low Dose STZ-Mice
J
K

Figure 5

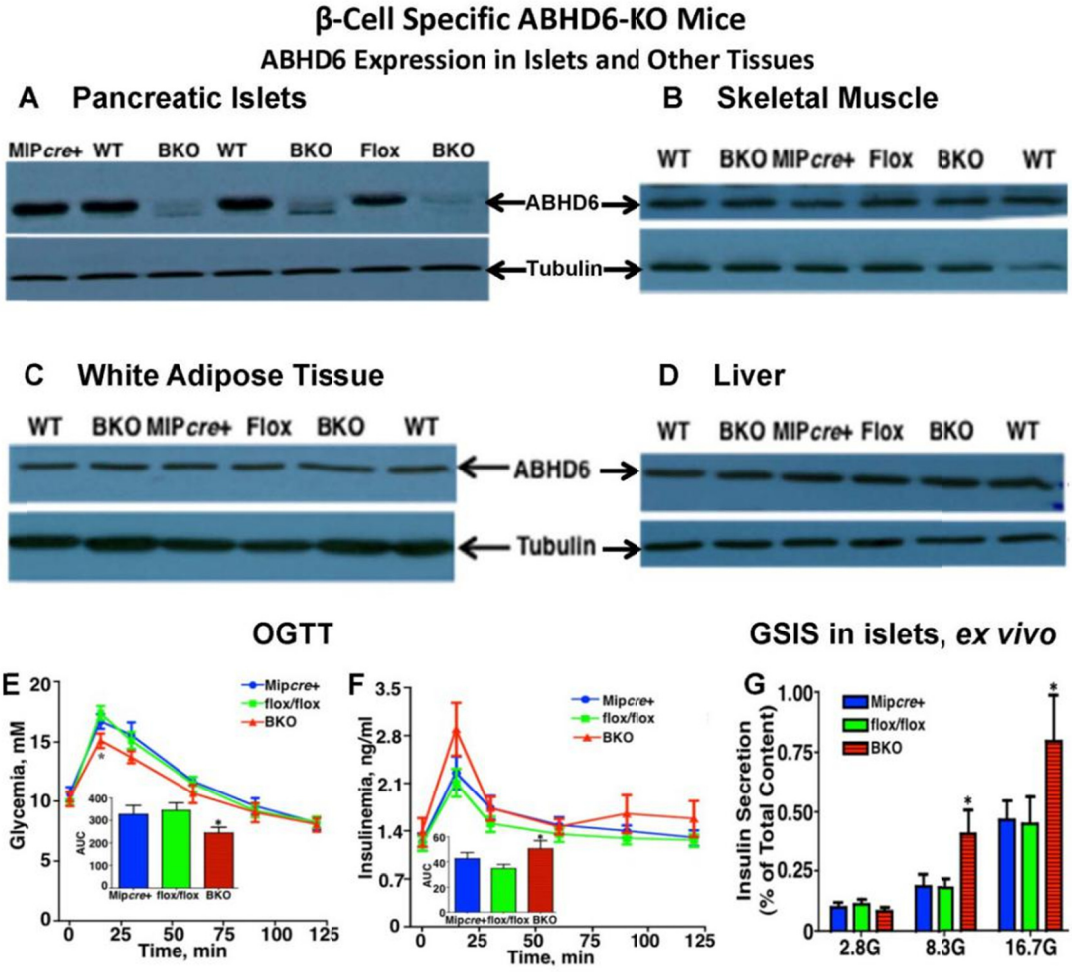
β-Cell Specific ABHD6-KO Mice
ABHD6 Expression in Islets and Other Tissues
A Pancreatic Islets
MIPcre+ WT BKO WT BKO Flox BKO
ABHD6
Tubulin
B Skeletal Muscle
WT BKO MIPcre+ Flox BKO WT
C White Adipose Tissue
WT BKO MIPcre+ Flox BKO WT
D Liver
WT BKO MIPcre+ Flox BKO WT
OGTT
GSIS in islets, ex vivo
E
Glycemia, mM
Time, min
AUC
Mipcre+
flox/flox
BKO
F
Insulinemia, ng/ml
Time, min
G
Insulin Secretion (% of Total Content)
2.8G
8.3G
16.7G

Figure 6

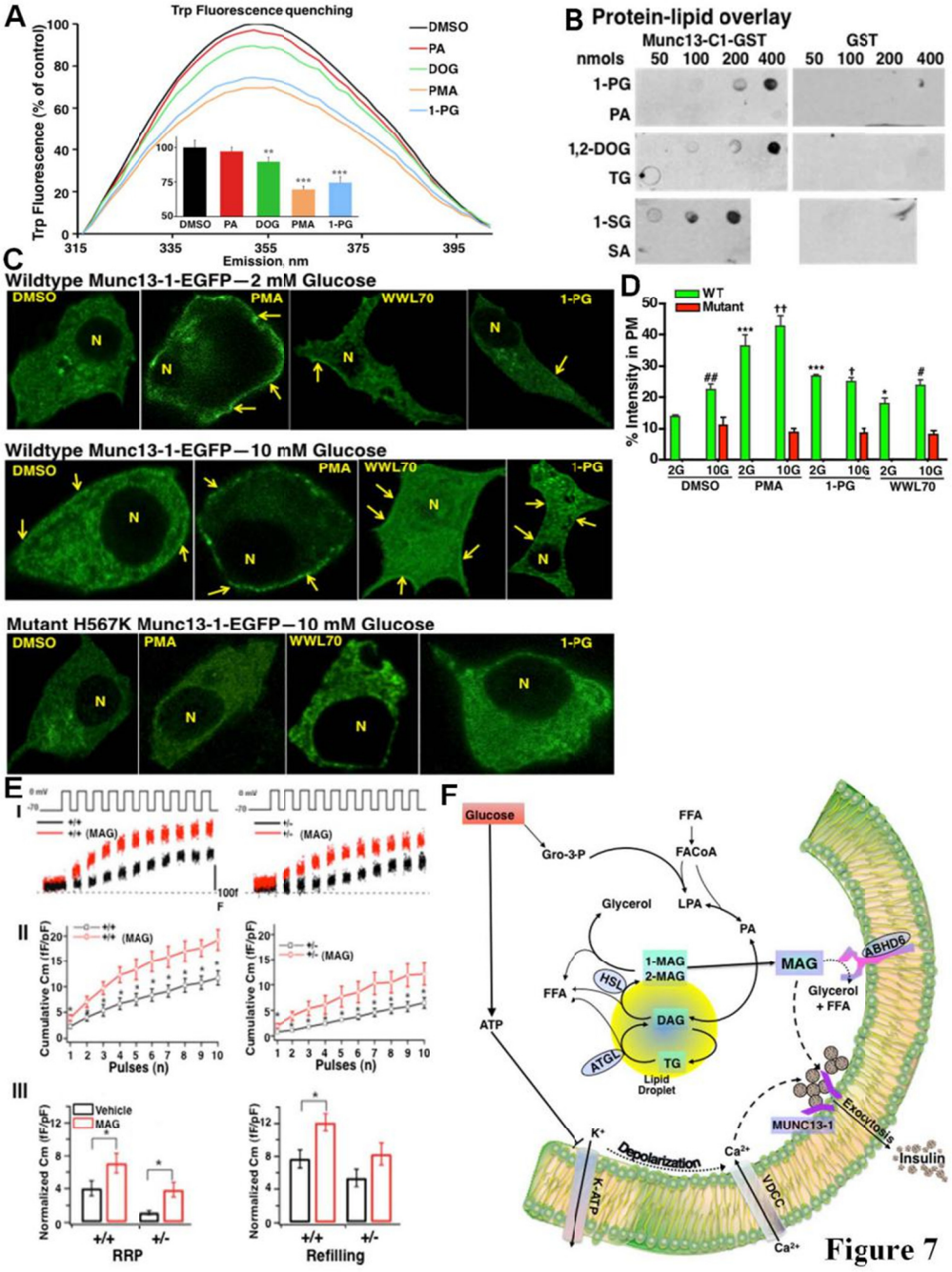
A
Trp Fluorescence quenching
Trp Fluorescence (% of control)
Emission, nm
DMSO
PA
DOG
PMA
1-PG
B Protein-lipid overlay
Munc13-C1-GST
GST
nmols 50 100 200 400
1-PG
PA
1,2-DOG
TG
1-SG
SA
C
Wildtype Munc13-1-EGFP—2 mM Glucose
Wildtype Munc13-1-EGFP—10 mM Glucose
Mutant H567K Munc13-1-EGFP—10 mM Glucose
DMSO
PMA
WWL70
1-PG
N
D
WT
Mutant
% Intensity in PM
2G 10G 2G 10G 2G 10G 2G 10G
DMSO PMA 1-PG WWL70
E
I
II
III
Cumulative Cm (fF/pF)
Pulses (n)
Normalized Cm (fF/pF)
Vehicle
MAG
RRP
Refilling
F
Glucose
Gro-3-P
FFA
FACoA
Glycerol
LPA
PA
1-MAG
2-MAG
MAG
ABHD6
HSL
FFA
DAG
TG
ATGL
Lipid Droplet
Glycerol + FFA
ATP
K+
Depolarization
Ca2+
MUNC13-1
Exocytosis
Insulin
K-ATP
VDCC

Figure 7

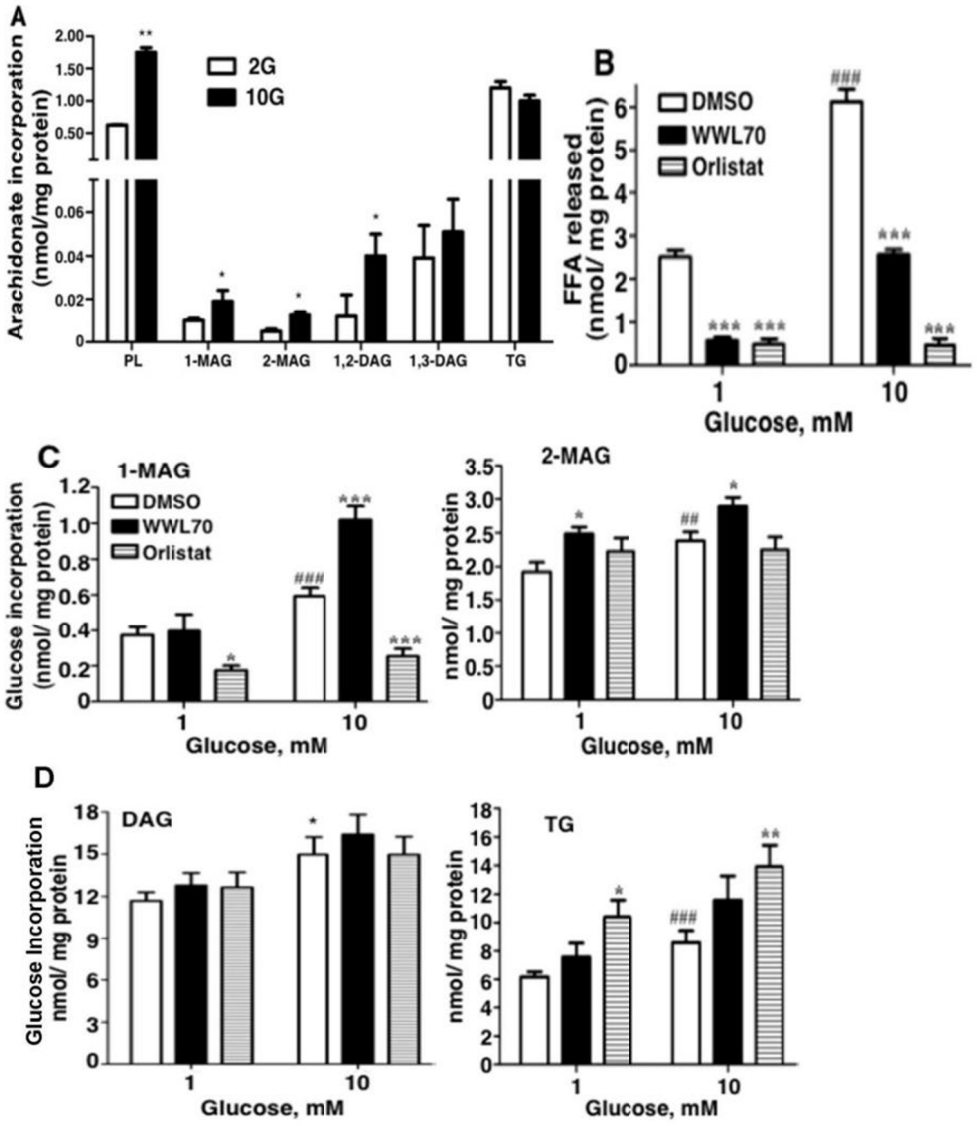
A
Arachidonate incorporation (nmol/mg protein)
2G
10G
PL
1-MAG
2-MAG
1,2-DAG
1,3-DAG
TG
B
FFA released (nmol/ mg protein)
DMSO
WWL70
Orlistat
Glucose, mM
C
1-MAG
Glucose incorporation (nmol/ mg protein)
2-MAG
nmol/ mg protein
D
DAG
Glucose Incorporation nmol/ mg protein
TG

Figure S1

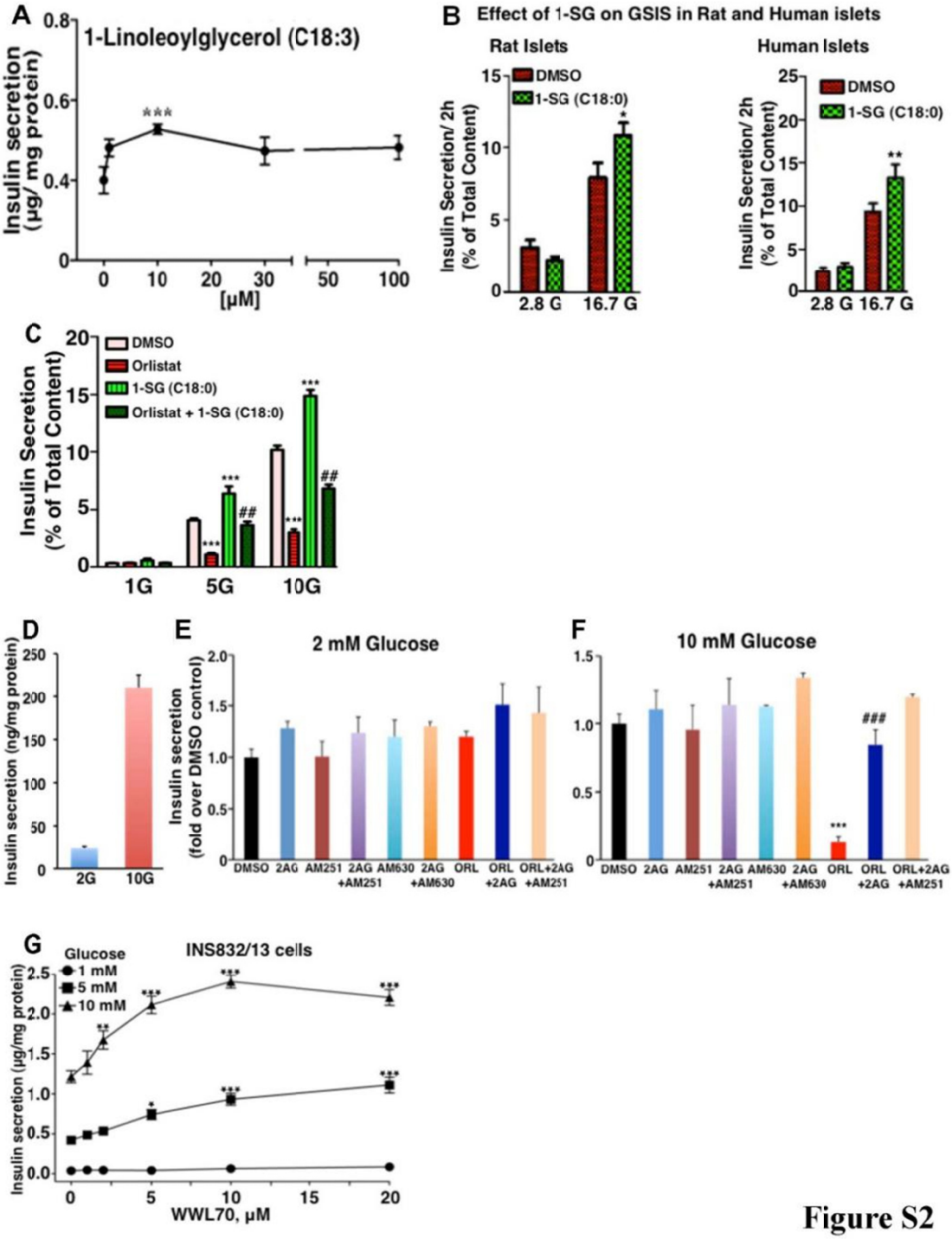
A
1-Linoleoylglycerol (C18:3)
Insulin secretion (µg/ mg protein)
[µM]
B
Effect of 1-SG on GSIS in Rat and Human islets
Rat Islets
Human Islets
DMSO
1-SG (C18:0)
Insulin Secretion/ 2h (% of Total Content)
2.8 G
16.7 G
C
DMSO
Orlistat
1-SG (C18:0)
Orlistat + 1-SG (C18:0)
Insulin Secretion (% of Total Content)
1G
5G
10G
D
Insulin secretion (ng/mg protein)
2G
10G
E
2 mM Glucose
Insulin secretion (fold over DMSO control)
DMSO
2AG
AM251
2AG +AM251
AM630
2AG +AM630
ORL
ORL +2AG
ORL+2AG +AM251
F
10 mM Glucose
G
Glucose
1 mM
5 mM
10 mM
INS832/13 cells
Insulin secretion (µg/mg protein)
WWL70, µM

Figure S2

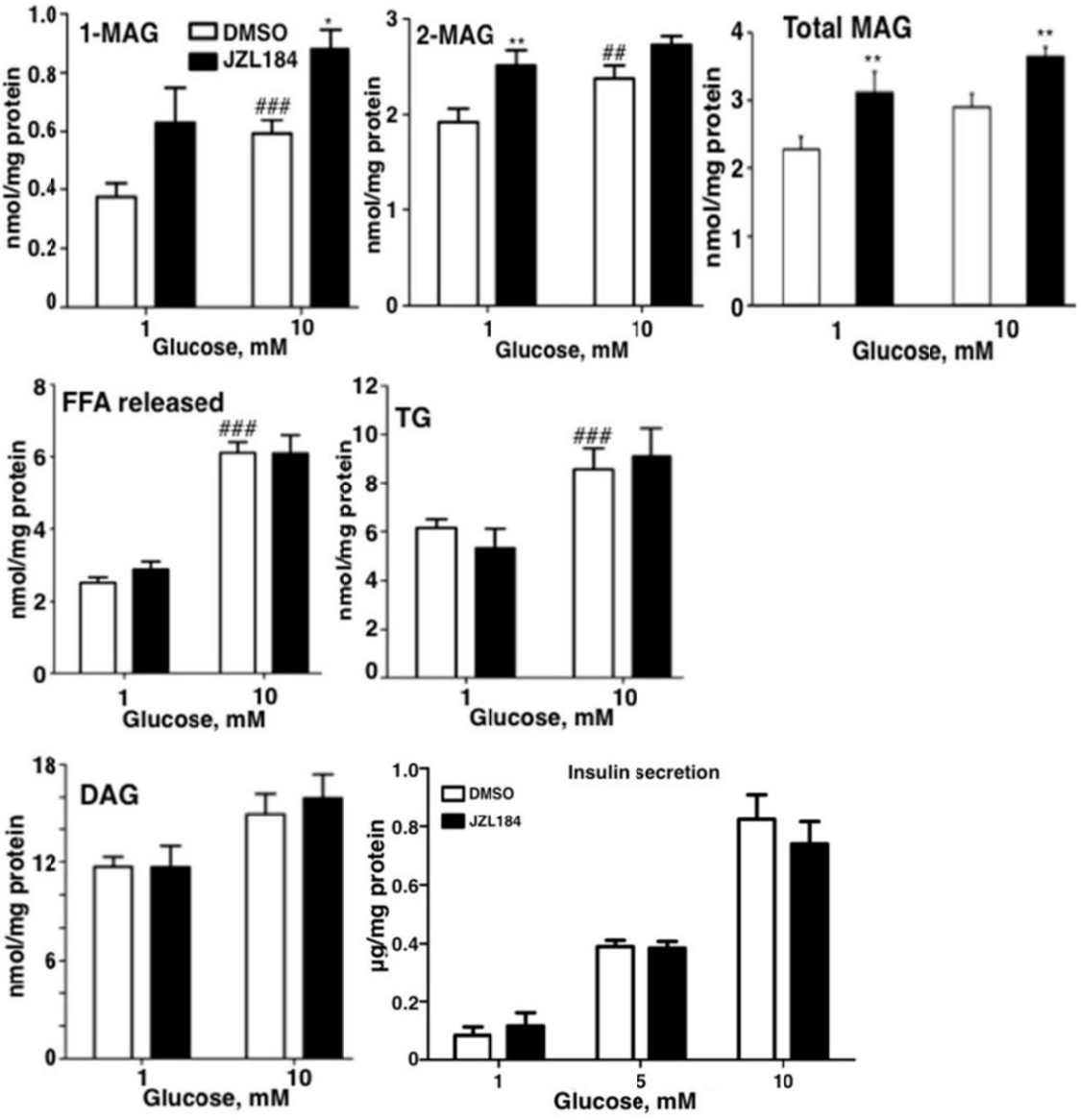
1-MAG
DMSO
JZL184
nmol/mg protein
Glucose, mM
2-MAG
Total MAG
FFA released
TG
DAG
Insulin secretion
µg/mg protein

Figure S3

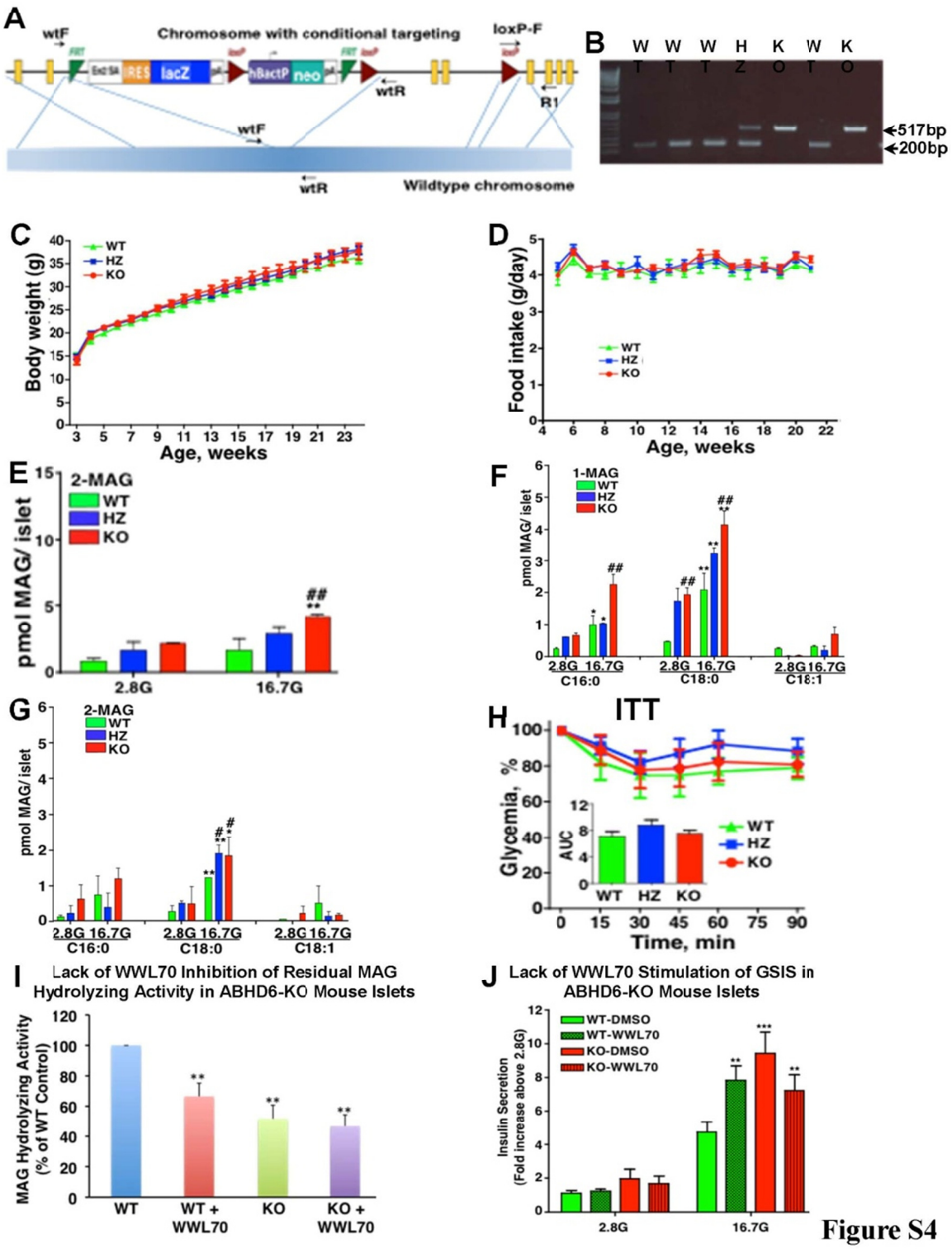
A
wtF
Chromosome with conditional targeting
loxP-F
Ex1 SA
IRES
lacZ
hBactP
neo
FRT
wtR
R1
wtF
wtR
Wildtype chromosome
B
W T
W T
W T
H Z
K O
W T
K O
517bp
200bp
C
Body weight (g)
WT
HZ
KO
Age, weeks
D
Food intake (g/day)
WT
HZ
KO
Age, weeks
E
2-MAG
WT
HZ
KO
pmol MAG/ islet
2.8G
16.7G
F
1-MAG
WT
HZ
KO
pmol MAG/ islet
2.8G 16.7G
C16:0
2.8G 16.7G
C18:0
2.8G 16.7G
C18:1
G
2-MAG
WT
HZ
KO
pmol MAG/ islet
2.8G 16.7G
C16:0
2.8G 16.7G
C18:0
2.8G 16.7G
C18:1
H
ITT
Glycemia, %
AUC
WT
HZ
KO
Time, min
I
Lack of WWL70 Inhibition of Residual MAG Hydrolyzing Activity in ABHD6-KO Mouse Islets
MAG Hydrolyzing Activity (% of WT Control)
WT
WT + WWL70
KO
KO + WWL70
J
Lack of WWL70 Stimulation of GSIS in ABHD6-KO Mouse Islets
WT-DMSO
WT-WWL70
KO-DMSO
KO-WWL70
Insulin Secretion (Fold increase above 2.8G)
2.8G
16.7G

Figure S4

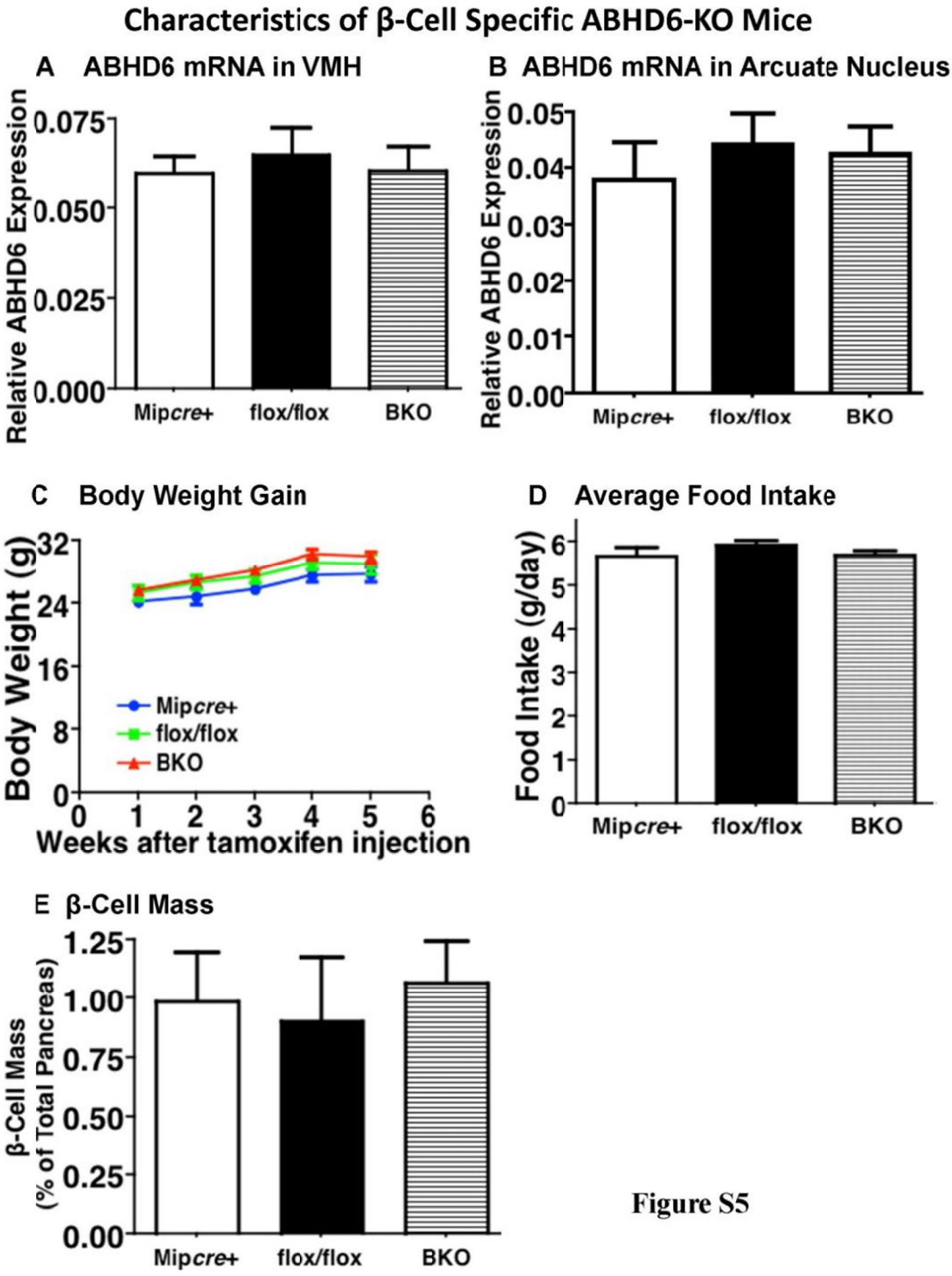
Characteristics of β-Cell Specific ABHD6-KO Mice
A ABHD6 mRNA in VMH
Relative ABHD6 Expression
0.075
0.050
0.025
0.000
Mipcre+
flox/flox
BKO
B ABHD6 mRNA in Arcuate Nucleus
Relative ABHD6 Expression
0.05
0.04
0.03
0.02
0.01
0.00
Mipcre+
flox/flox
BKO
C Body Weight Gain
Body Weight (g)
32
24
16
8
0
0 1 2 3 4 5 6
Weeks after tamoxifen injection
Mipcre+
flox/flox
BKO
D Average Food Intake
Food Intake (g/day)
6
5
4
3
2
1
0
Mipcre+
flox/flox
BKO
E β-Cell Mass
β-Cell Mass (% of Total Pancreas)
1.25
1.00
0.75
0.50
0.25
0.00
Mipcre+
flox/flox
BKO

Figure S5

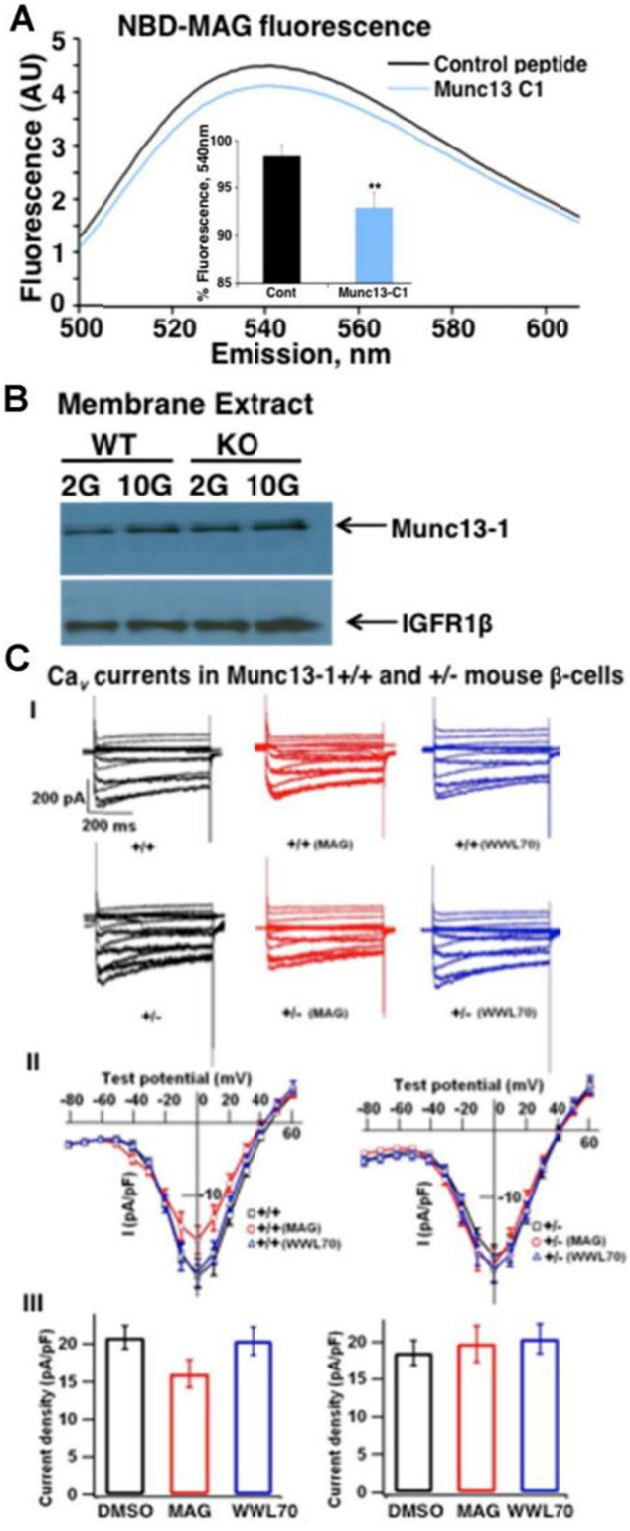
A
NBD-MAG fluorescence
Control peptide
Munc13 C1
Fluorescence (AU)
Emission, nm
% Fluorescence, 540nm
Cont
Munc13-C1
B
Membrane Extract
WT
KO
2G 10G 2G 10G
Munc13-1
IGFR1β
C
Cav currents in Munc13-1+/+ and +/- mouse β-cells
200 pA
200 ms
+/+
+/+ (MAG)
+/+ (WWL70)
+/-
+/- (MAG)
+/- (WWL70)
Test potential (mV)
I (pA/pF)
Current density (pA/pF)
DMSO
MAG
WWL70

Figure S6

Article 2

α/β-hydrolase domain-6 and saturated long chain monoacylglycerol regulate insulin secretion promoted by both fuel and non-fuel stimuli

Shangang Zhao[1], Pegah Poursharafi[1], Yves Mugabo, Emily J. Levens, Kevin Vivot, Camille Attane, Jose Iglesias[2], Marie-line Peyot, Erik Joly, Murthy Madiraju, Marc Prentki

Departments of Nutrition, Biochemistry and Molecular Medicine, Montreal Diabetes Research Center, CRCHUM and Université de Montréal, Montreal, QC, Canada

[1]Equally contributed to this project.

[2]Current address: Departamento de Nutricion y Bioquímica, Pontificia Universidad Javeriana, Cra 7, No. 43-82, Edf. Carlos Ortiz., Bogotá, Colombia

Running title: α/β-hydrolase domain-6 and insulin secretion

Published in: Molecular Metabolism, 2015.

Correspondence to:

Dr. Marc Prentki, Montreal Diabetes Research Center, CRCHUM, 900 St-Denis (Viger Tower), Rm R08-412, Montreal, QC H1W 4A4, Canada.

Dr. S.R. Murthy Madiraju, Montreal Diabetes Research Center, CRCHUM, 900 St-Denis (Viger Tower), Rm R08-414, Montreal, QC H1W 4A4, Canada.

Abbreviations: ABHD6, α/β-hydrolase domain-6; ATGL, adipose triglyceride lipase; BKO, β cell specific ABHD6-knockout; Carb, carbamylcholine; DAG, diacylglycerol; FFA, free fatty acid; Flox, Flox/Flox; GL/FFA, glycerolipid/ free fatty acid; GLP1, glucagon-like peptide 1; GPCR, G-protein coupled receptor; GSIS, glucose stimulated insulin secretion; HSL, hormone sensitive lipase; Kic, α-ketoisocaproate; KO, knockout; MAG, monoacylglycerol; OGTT, oral glucose tolerance test; ROS, reactive oxygen species; TG, triacylglycerol; WT, wild type; 1-OG, 1-oleoylglycerol; 1-PG, 1-palmitoylglycerol; 1-SG, 1-stearoylglycerol;

Detailed contributions of authors in this work:

Shangang Zhao was responsible most of the work presented in this chapter. The overall contribution to this work was up to 70%. The detailed contribution included: neutral lipid hydrolysis activity, mouse colony maintenance, islet isolation, ex vivo insulin secretion, calcium measurement, fatty acid oxidation and ex vivo MAG adding experiments. Also, Shangang Zhao participated in manuscript writing and revision of the manuscript.

Pegah Poursharafi helped in most of the experiments, and she contributed to mouse islet isolation, ex-vivo insulin secretion and fatty acid oxidation.

Yves Mugabo involved in the experiments of glucose utilization and oxidation, and helped in MAG species analysis.

Emily J. Levens helped in Western blotting of ABHD6, MAG addition experiments and MAG species analysis (Sample preparation parts).

Kevin Vivot performed perifusion experiments.

Camille Attane helped in calcium measurement and participated in discussion.

Jose Iglesias helped in measuring MAG hydrolysis activity and discussion.

Marie-line Peyot and Erik Joly helped for the analysis of the results and through discussions.

Murthy Madiraju and Marc Prentki conceived the project, designed the study, analyzed the results, and wrote the manuscript.

ABSTRACT

Objective: α/β-hydrolase domain-6 (ABHD6) is a newly identified monoacylglycerol (MAG) lipase. We recently reported that it negatively regulates glucose stimulated insulin secretion (GSIS) in the β cells by hydrolyzing lipolysis-derived MAG that acts as a metabolic coupling factor and signaling molecule via exocytotic regulator Munc13-1. Whether ABHD6 and MAG play a role in response to all classes of insulin secretagogues, in particular various fuel and non-fuel stimuli, is unknown.

Methods: Insulin secretion in response to various classes of secretagogues, exogenous MAG and pharmacological agents was measured in islets of mice deficient in ABHD6 specifically in the β cell (BKO). Islet perifusion experiments and determinations of glucose and fatty acid metabolism, cytosolic Ca^{2+} and MAG species levels were carried out.

Results: Deletion of ABHD6 potentiated insulin secretion in response to the fuels glutamine plus leucine and α-ketoisocaproate and to the non-fuel stimuli glucagon-like peptide 1, carbamylcholine and elevated KCl. Fatty acids amplified GSIS in control and BKO mice to the same extent. Exogenous 1-MAG amplified insulin secretion in response to fuel and non-fuel stimuli. MAG hydrolysis activity was greatly reduced in BKO islets without changes in total diacylglycerol and triacylglycerol lipase activity. ABHD6 deletion induced insulin secretion independently from KATP channels and did not alter the glucose induced rise in intracellular Ca^{2+}. Perifusion studies showed elevated insulin secretion during second phase of GSIS in BKO islets that was not due to altered cytosolic Ca^{2+} signaling or because of changes in glucose and fatty acid metabolism. Glucose increased islet saturated long chain 1-MAG species and ABHD6 deletion caused accumulation of these 1-MAG species at both low and elevated glucose.

Conclusion: ABHD6 regulates insulin secretion in response to fuel stimuli at large and some non-fuel stimuli by controlling long chain saturated 1-MAG levels that synergize with other signalling pathways for secretion.

Keywords α/β-hydrolase domain-6; monoacylglycerol; insulin secretion; pancreatic islets; cytosolic Ca^{2+}

1. INTRODUCTION

Insulin secretion plays a central role in glucose homeostasis, and glucose is the most prominent secretagogue for the pancreatic islet β cell (Prentki et al., 2013b). Yet, despite decades of research, we still do not fully understand how the intracellular metabolism of glucose and other fuel stimuli, such as fatty acids and some amino acids, is coupled to the exocytotic release of insulin containing granules. Glucose stimulated insulin secretion (GSIS) is a biphasic process with a rapid first phase followed by a sustained second phase (Bratanova-Tochkova et al., 2002). Glucose stimulation of the β cell results in rise in the ATP/ADP ratio with associated closure of KATP channels and a rise in intracellular Ca^{2+} that acts as a trigger for insulin release that can be amplified by additional metabolic coupling factors besides adenine nucleotides (Ashcroft and Rorsman, 2013; Prentki et al., 2013b). Candidate metabolic coupling factors include NADPH (Ivarsson et al., 2005), reactive oxygen species (ROS) (Pi et al., 2007), glutamate (Maechler and Wollheim, 1999), acyl-CoA compounds (Brun et al., 1996; Prentki et al., 1992) and additional lipid signaling molecules (Kaneko and Ishikawa, 2015). Although there is a general consensus that some lipid signaling molecules play key role in the amplification pathway of GSIS, the nature of these signals has remained elusive (Prentki et al., 2013b).

Glucose and free fatty acid (FFA) both increase flux through the glycerolipid/ free fatty acid (GL/FFA) cycle in β cells, with its lipogenesis and lipolysis arms (Prentki et al., 2013b). We (Nolan et al., 2006a; Peyot et al., 2009c; Peyot et al., 2004; Roduit et al., 2001) and others (Fex et al., 2009; Mulder et al., 2004) have proposed that the lipolysis segment of the GL/FFA cycle generates signal(s) involved in ß cell activation for insulin release. Deletion in the β cell of adipose triglyceride lipase (ATGL) (Peyot et al., 2009c) and hormone sensitive lipase (HSL) (Fex et al., 2009; Peyot et al., 2004; Roduit et al., 2001), that respectively catalyze the hydrolysis of triacylglycerol (TG) to diacylglycerol (DAG) and DAG to monoacylglycerol (MAG), resulted in reduced GSIS. On the basis of these observations, we hypothesized that one of the molecules downstream of DAG in the lipolysis cascade (MAG, FFA or glycerol) acts as a metabolic coupling factor (Zhao et al., 2014). MAG hydrolysis provides FFA and glycerol. Since reduced GSIS in ATGL knockout (KO) islets was not rescued by exogenous FFA (Peyot et al., 2009c) and glycerol is not a secretagogue, we hypothesized that this long-searched metabolic coupling factor is MAG.

We recently demonstrated that in the β cell MAG hydrolysis is conducted by α/β-hydrolase domain-6 (ABHD6), a newly identified MAG hydrolase and that in these cells the expression of the classical MAG lipase is very low (Zhao et al., 2014). We further showed that 1-MAG, which is produced in response to glucose stimulation of β cells, acts as a coupling factor for GSIS and that the level of 1-MAG increases by the suppression of ABHD6 activity either pharmacologically or by its genetic deletion. MAG was found to mediate its effect via activation of the exocytosis regulator protein Munc13-1, thereby enhancing insulin granule exocytosis (Zhao et al., 2014). The bulk of the evidence for a role of MAG as a coupling factor was obtained using whole body ABHD6-KO mice and we also showed that GSIS is enhanced *in vivo* and *ex vivo* in islets from ß cell specific ABHD6-KO (BKO) mice. However several questions remained with respect to the role of ABHD6 and MAG in the regulation of insulin secretion that are addressed here using islets from BKO mice, where ABHD6 was deleted in β cells at adult stage by tamoxifen-induced Cre expression. Are ABHD6 and MAG

involved more globally in β cell activation, that is in the regulation of insulin secretion in response to other fuels besides glucose and non-fuel stimuli as well? Are they implicated in: the KATP-dependent or independent pathway of secretion; the first or second phase of GSIS; and glucose or fatty acid metabolism or Ca^{2+} signaling?

Our results with BKO mice provide evidence that ABHD6-accessible MAG, which is produced during nutrient metabolism, synergizes with other cellular signals arising from fuel and some non-fuel stimuli to potentiate insulin secretion and that MAG activates the KATP-independent pathway and second phase of secretion. ABHD6-deletion in β cells does not alter glucose and fatty acid metabolism or Ca^{2+} influx. The data highlight the importance of ABHD6 and MAG in regulating insulin secretion in response to all stimuli to control glucose homeostasis, and thus ABHD6 is a potential candidate for developing drugs against type 2 diabetes.

2. MATERIALS AND METHODS

2.1. Animals

The use of animals for the experiments in this study was approved by the Institutional Committee for the Protection of Animals. C57BL/6N mice were housed at room temperature (22°C) with 12-h light/dark cycling, with free access to water and standard chow diet (11% fat by energy).

2.2. Generation of BKO mice.

The generation of inducible BKO mice where ABHD6 is deleted specifically in the ß cell has been described before (Zhao et al., 2014). In our previous report, we have made detailed comparison among wild type (WT), MIP-cre/ERT, and ABHD6 Flox/Flox (Flox) mice for many parameters. We found that WT, MIP-cre/ERT and Flox mice behaved similarly in terms of body weight gain and food intake over 5 weeks following *i.p.* tamoxifen injection, fed and fasting glycemia, islet morphology and β cell mass, oral glucose tolerance test (OGTT) and *ex vivo* GSIS. Based on this observation, in the present study we employed only Flox mice as control mice (Zhao et al., 2014). Flox mice were bred with Flox/Flox; Mip*cre*$^{+}$ (BKO) mice to obtain 50% littermates as Flox mice and 50% BKO mice. Flox and BKO mice at 8 weeks of age received daily tamoxifen injections (50mg/kg BW), for 5 consecutive days. Two weeks later, the mice were used for islet isolation.

2.3. Islet isolation

Pancreatic islets from Flox and BKO mice were isolated as described previously (Peyot et al., 2009c). The isolated islets were handpicked and let to recover by incubation overnight in RPMI 1640, supplemented with 10% FBS and 11 mM glucose (recovery medium).

2.4. MAG, DAG and TG hydrolysis activity

Procedures for measuring MAG, DAG and TG hydrolysis activities have been described earlier (Iglesias et al., 2015). Briefly, immediately after isolation, islets were washed twice with cold PBS, and then were homogenized in cold PBS. Assays for MAG, DAG and TG

hydrolysis using corresponding specific substrates were done with 0.5 μg, 0.5 μg or 10 μg protein, respectively, per assay. MAG hydrolysis was assayed in 96-well plates, with 1-S-arachidonoylthioglycerol (Cayman Chemical Co) as the substrate, and the released 1-thioglycerol was measured by reaction with ThioGlo-1 (Corvallis, OR) to form a fluorescent adduct, measured in a FLUOstar microplate reader instrument (BMG Labtech, Germany). DAG hydrolysis activity was assayed in 96-well plates using p-nitrophenylbutyrate (Sigma Aldrich) as the substrate by monitoring the reaction at 507 nm, in a plate reader. TG hydrolysis activity was measured using EnzChek lipase substrate (Life technologies) and fluorescence (excitation 485 nm; emission 510 nm) was monitored every 30 sec for 90 min. Enzyme specific inhibitors were employed in the assays for ascertaining the activity of the enzyme that was being measured. Thus for ABHD6 catalyzed MAG hydrolysis assay, 1 μM WWL70 (Cayman Chemical), an ABHD6 inhibitor (Zhao et al., 2014) was included; for total DAG hydrolysis assay, 1 μM orlistat as DAGL inhibitor since at this low concentration, orlistat inhibits mainly DAGL (Iglesias et al., 2015); and for TG hydrolysis assay, we employed 1 μM Cay10499 as TG hydrolysis inhibitor (Iglesias et al., 2015).

2.5. Ex-vivo Insulin secretion

The procedure for insulin secretion using isolated islets has been described (Zhao et al., 2014). Briefly, after overnight culture in recovery medium, the islets were starved in RPMI 1640 with 10% FBS and 2 mM glucose for 2h. After starvation, the islets were washed twice with 'enriched' KRBH, which contained 0.5% defatted BSA, 50 μM carnitine, 2 mM Gln and 4 mM glucose. This enriched KRBH, which matches better physiological milieu (Prentki et al., 2013b) was used in order to prevent fuel-depleted conditions that may arise with the commonly used KRBH, which contained only 2.8 mM glucose. Then the islets were pre-incubated in this enriched KRBH for 45 min, followed by incubation with different concentrations of glucose and in the presence or absence of different fuel and non-fuel stimuli (0.15 mM oleate plus 0.15 mM palmitate, 10 mM α-ketoisocaproate (Kic), 5 mM glutamine plus leucine (Gln plus Leu), 20 nM glucagon-like peptide 1 (GLP1), 35 mM KCl, 200 μM carbamylcholine (Carb) for 1 h. For the experiment regarding the effect of exogenous MAG in the presence of various stimuli, dispersed Wistar rat islet cells were used because MAG is lipophilic and may not access all islet cells within an intact islet but only cells at the periphery. The islets were dispersed into single islet cells by trypsin digestion (Peyot et al., 2010), and the cells were plated into 48-well plates at a density of $1x10^5$ cells per well. After 2 days culture in RPMI medium, insulin secretion experiments were performed. Following similar starvation and preincubation conditions as described above for islets, the dispersed islet cells were incubated at 6 mM glucose with or without 20 nM GLP-1, 200 μM Carb and 10 mM Kic in the absence or presence of 100 μM 1-palmitolglycerol (1-PG) for 1h. At the end of the experiments incubation media were collected for insulin release analysis. Total insulin content was measured after islets or isolated islet cells extraction by a mixture of ethanol and HCl (75%: 1.5%). Insulin was measured using Alphalisa (Perkin Elmer, Waltham, *Massachusetts*) (Zhao et al., 2014).

2.6. Glucose and fatty acid metabolism

Glucose oxidation and utilization and fatty acid oxidation were measured as described before (Kim-Muller et al., 2014) with minor modifications. Briefly, for glucose metabolism, the islets

were cultured in recovery medium overnight. Then, the islets were starved in RPMI 1640 with 2 mM glucose for 2 h. Batches of 20 islets were preincubated in enriched KRBH for 45 min, and then incubated in KRBH containing 0.5 μCi of [5-^{3}H] D-glucose (16 Ci/mmol) and 1 μCi/ml [U-^{14}C] D-glucose (250 mCi/mmol) at 4, 10, and 16 mM glucose. Then the incubation was stopped by adding citrate/NaOH buffer (400 mM, pH 4.9) containing antimycin-A (10 μM), rotenone (10 μM), and KCN (5 mM). Glucose oxidation was followed by measuring the generated $^{14}CO_2$ after 60 min in KOH trap. Glucose utilization was determined by measuring the $^{3}H_2O$ produced. For fatty acid oxidation, after a first starvation in RPMI 1640 with 2 mM glucose for 2 h, batches of 50 islets were preincubated in enriched KRBH for 45 min, and then incubated for 2 h in KRBH containing 0.25% BSA, 0.1 mM palmitate and 0.2 μCi/ml [9,10(n)-^{3}H]-palmitate (74 kBq/ml) at 4 and 16 mM glucose. The supernatant was collected to separate $^{3}H_2O$ from radioactive fatty acids and fatty acid oxidation was calculated by measuring $^{3}H_2O$ produced.

2.7. Intracellular $Ca2^{+}$ measurement

After overnight recovery of islets as above, the islets were dispersed into single cells by trypsin digestion (Peyot et al., 2010). The dispersed cells were placed in 96-well black plates with clear bottom at a density of 80,000 cells per well. After overnight culture in RPMI1640 plus 10% FBS, the cell were pre-loaded in enriched KRBH with 2.5 mM probenicid, 0.2 mM sulfinpyrazone, 0.1 mM 3-isobutyl-1-methylxanthine (IBMX), equal volume of Fura-2 AM (Life technologies) (6 μM) and Pluronic F-127 for 75 min. Then the cells were washed once with enriched KRBH, and incubated in enriched KRBH with 2.5 mM probenicid and 0.2 mM sulfinpyrazone for 30 min. Then the cells were monitored using a plate reader (FLUOstar) with two different excitation filters of 340 nm and 380 nm and with emission at 510 nm. High glucose was added manually to reach final concentration of 16 mM and KCl was injected by the machine to reach a final concentration of 35 mM. The intracellular Ca^{2+} was calculated as ratio of fluorescence outputs at 340 nm and 380 nm (F340/F380).

2.8. Perifusion experiments

Overnight recovered Flox and BKO islets were starved in RPMI 1640 medium at 2 mM glucose for 2 h. Then batches of 30 islets were placed in the perifusion chambers and perifused at a flow rate of 0.5 ml/min for 45 min in enriched KRBH, followed by perifusion with 16 mM glucose for 30 min, and then with 35 mM KCl for another 30 min. At different time points indicated in the figure legend, 0.5 ml samples were collected and centrifuged for insulin analysis. After the perifusion, the islets were removed from the chamber and extracted with a mixture of ethanol and HCl (75%: 1.5%) to release total insulin for normalization. Insulin was measured by Alphalisa analysis.

2.9. MAG species analysis

MAG species analysis was done as described before (Zhao et al., 2014). Briefly, overnight recovered islets were starved in RPMI 1640 with 2 mM glucose for 2 h, and then pre-incubated in enriched KRBH for 45 min, followed by incubation with low (4 mM) and high (16 mM) glucose in the absence and presence of different stimuli for 1 h. For each condition, 250 islets were used. After the treatment, the islets were collected for lipid extraction in Folch

reagent. After lipid extraction, the dried lipids were dissolved in a small volume of chloroform and loaded on silica gel thin layer chromatography plates and developed in the solvent system (Chloroform: acetone: acetic acid= 60:40:1, v/v) to separate 1-MAG and 2-MAG. Then the bands corresponding to 1-MAG and 2-MAG were scraped and saponified and the released FFA were extracted by Dole's procedure and measured by HPLC. The molar quantity of different FFA species corresponds to the amount of corresponding particular species of 1-MAG and 2-MAG and the total 1-MAG and 2-MAG were calculated by the sum of these individual MAG species.

2.10. Statistical Analysis

Statistical analyses were performed by Graphpad Prism software. Values were expressed as mean ± SEM. Student's t test and one way and two ANOVA were used for inter-group comparisons.

3. RESULTS

3.1. BKO islets display reduced MAG hydrolysis activity

ABHD6 is known to hydrolyze MAG to glycerol and FFA in various tissues, such as brain, liver, adipocytes and islets (Blankman et al., 2007a; Thomas et al., 2013; Zhao et al., 2014). We confirmed (Zhao et al., 2014) that ABHD6 protein levels are reduced in BKO islets by >90% (Figure 1A). However, it is not known whether deletion of ABHD6 has any compensatory effects on DAG or TG hydrolysis. Since it has been shown that suppression of DAG hydrolyzing HSL or TG hydrolyzing ATGL hampered insulin secretion (Fex et al., 2009; Peyot et al., 2009c; Peyot et al., 2004), it is necessary to ascertain that ABHD6 deletion in β cells has no secondary or compensatory effects on DAG or TG hydrolysis. In order to examine this we measured the activities of total hydrolysis of MAG, 1,2-DAG and TG in extracts of Flox and BKO mouse islets. ABHD6-specific activity was assayed by measuring the hydrolysis of 1-S-thioarachidonylglycerol in the presence and absence of WWL70, an ABHD6-specific inhibitor. MAG hydrolysis was reduced by 20% in Flox mouse islets in the presence of WWL70 and was similarly reduced by 20% in BKO vs Flox islets. The addition of WWL70 to BKO islet extracts did not further reduce the residual MAG hydrolysis, indicating complete deletion of ABHD6 activity in islet β cells (Figure 1B). Orlistat has been reported to inhibit *sn*1-DAG lipases at low micromolar concentrations (Bisogno et al., 2003) while higher concentrations are needed to inhibit HSL, which also hydrolyzes DAG (Mulder et al., 2004). Total DAG hydrolysis activity was similar in Flox and BKO islet extracts as well as the orlistat sensitive and the residual activity (Figure 1C). Similarly, there were no differences in TG hydrolysis activity between Flox and BKO islets and in both the cases TG hydrolysis could be equally inhibited by the lipase inhibitor Cay10499 (Figure 1D). The results ascertain that deletion of ABHD6 activity in islet β cells does not alter DAG and TG hydrolysis.

3.2. Insulin secretion in response to various fuel and non-fuel stimuli in BKO islets

We have earlier shown that isolated islets from global or β cell specific ABHD6-KO mice show enhanced GSIS (Zhao et al., 2014). However, the effect of ABHD6 deletion on insulin secretion in response to other fuels and non-fuel stimuli is not known. As noticed earlier (Zhao

et al., 2014), deletion of ABHD6 in islets did not affect islet morphology or β cell mass, but increasing glucose concentration to 16 mM resulted in much higher level of insulin secretion in the BKO islets than that in Flox islets (Figure 2A). The presence of palmitate and oleate (0.15 mM each) elevated insulin secretion at both 4 and 16 mM glucose in control and BKO islets to the same extent (Figure 2A). ABHD6 deletion had no further enhancing effect on fatty acid-augmented GSIS, in addition to what was noticed at 16 mM glucose alone in the Flox control (Figure 2E). Besides glucose, a combination of glutamine and leucine is known to stimulate insulin secretion at low glucose concentration (Li et al., 2003). At 4 mM glucose, Gln plus Leu also stimulated insulin secretion in control as well as in BKO islets (Figure 2B). Interestingly, similar to what was seen with high glucose concentration, there was nearly 3-fold higher secretion with Gln plus Leu in BKO islets than in Flox islets, indicating that ABHD6 deletion also enhanced amino acid stimulated insulin secretion (Figure 2B).

We noticed earlier using islets from whole body ABHD6-KO mice that besides GSIS, even KCl-stimulated insulin secretion (at 2.8 mM glucose) is also slightly elevated (Zhao et al., 2014). We now further examined the involvement of KATP-independent amplification mechanism(s) (Gembal et al., 1992) in the elevated insulin secretion seen due to ABHD6 deletion, using BKO mouse islets. The combined use of diazoxide plus an elevated concentration of KCl is a classical way to study the so-called amplifying KATP-independent pathways (Gembal et al., 1992) when β cell [Ca^{2+}] is elevated maximally and clamped by a depolarizing elevated concentration of KCl in the presence of diazoxide (KATP channels are held open to exclude an effect on these channels). The results indicated that KCl-induced insulin secretion (at 4 mM glucose) was strongly potentiated in BKO islets, compared to Flox islets. Similar observation was made when KATP channels were by-passed, in the presence of elevated KCl, with the use of diazoxide (Figure 2C) (Yajima et al., 1999). Thus, ABHD6 deletion caused augmentation of the KATP-independent amplification pathways of glucose signaling for secretion. *Kic, which* is actively metabolized in the ß cell and promotes insulin secretion (Heissig et al., 2005), was found to augment insulin release in both control and BKO islets at 4 mM glucose and this Kic augmented secretion was much higher in BKO islets than in control islets (Figure 2D). We then examined whether ABHD6 deletion influences GSIS stimulated by GLP1, which acts via Gs-coupled G-protein coupled receptor (GPCR) (MacDonald et al., 2002) and by the muscarinic receptor agonist carbamylcholine, which acts via Gq-coupled GPCR (Peter-Riesch et al., 1988). GLP1 considerably augmented GSIS in control and BKO islets and its effect was markedly amplified in BKO islets reaching a very elevated 6% of total insulin content being secreted (Figure 2D,E). Carb also amplified GSIS in control islets. There was a clear trend of enhancement of its effect in BKO islets (calculated as the difference of Carb effect on the top of 16 mM glucose in BKO vs control islets) but it did not reach statistical significance ($p<0.1$) (Figure 2E). The results indicate that a signal generated by ABHD6 deletion synergizes with those produced by the non-fuel stimulus GLP1 and possibly with those produced by Carb as well.

Insulin secretion in response to glucose by isolated islets or cultured β cells follows a biphasic process. In order to understand which of these phase(s) of insulin secretion is affected by ABHD6 deletion, we performed perifusion experiments using islets from Flox and BKO mice. Perifusion with 16 mM glucose induced a transient first phase insulin secretion in both control and BKO islets, and there were no differences between Flox and BKO islets in either the

amplitude or the time course of first phase secretion peak (Figure 3A,B). The second phase insulin secretion, was very minor in control islets consistent with previous reports that used mouse islets (Ferdaoussi et al., 2012; Peyot et al., 2010), while it was significantly elevated in BKO islets (Figure 3A,C), indicating that ABHD6 deletion enhances GSIS mainly by affecting the second phase. BKO islets also exhibited increased insulin secretion during perifusion with 35 mM KCl that followed 16 mM glucose, as compared to control islets, similar to what was observed in static incubations (Figure 3A,D).

3.3 Intracellular Ca^{2+} in Flox and BKO mouse islets

In order to determine whether ABHD6 deletion changes cytosolic Ca^{2+} levels and that such effect could contribute to the enhanced secretion in BKO islets, we measured intracellular Ca^{2+} in Flox and BKO islets in the presence of high glucose or 35 mM KCl. In both control and BKO islets, following glucose addition, cytosolic Ca^{2+} started to increase by 3 min and reached a peak by 10 min and thereafter, intracellular Ca^{2+} started to decrease slowly (Figure 4A). There were no differences between Flox and BKO islets in the glucose stimulated elevation in cytosolic Ca^{2+}. Elevated glucose caused an initial small reduction of cytosolic Ca^{2+} in control but not BKO islets. The reason for the difference in this slight initial reduction in Ca^{2+} between control and BKO islets is not known. This initial reduction in cytosolic Ca^{2+} upon a rise in glucose concentration has been reported before in some islet studies (Lund et al., 1989) but its reason has not been elucidated. It may be related to an accelerated Ca^{2+} uptake by the endoplasmic reticulum due to a rise in the ATP/ADP ratio promoting activation of the Ca^{2+} ATPase transporter. As expected, KCl induced a rapid Ca^{2+} rise in both Flox and BKO islets and there was no difference between these islets in their Ca^{2+} response (Figure 4B). These results indicate that ABHD6 deletion mediated increase in GSIS response by islets is not due to altered Ca^{2+} influx or mobilization form endogenous stores or cytosolic Ca^{2+} concentrations.

3.4. Glucose and fatty acid metabolism in β cells with ABHD6 deletion

Inasmuch as ABHD6 is a metabolic enzyme and its deletion greatly enhances glucose responsiveness of pancreatic islets to secrete insulin, it is important to ascertain whether deletion of ABHD6, a MAG hydrolase, has any effect on glucose or fatty acid metabolism in the β cells. In both control and BKO islets, there was significant level of glucose utilization and oxidation at 4 mM glucose, which increased further with increasing glucose concentration. However, there were no differences between Flox and BKO islets (Figure 5A,B). Fatty acid oxidation negatively correlates with insulin secretion (Prentki et al., 2013b). In the present study also we noticed that with increasing glucose concentration, fatty acid oxidation was significantly decreased, however, there were no differences between Flox and BKO islets (Figure 5C).

3.5. MAG levels in BKO islets

We previously reported that total and 1-MAG levels are elevated in glucose concentration-dependent manner in whole body ABHD6-KO mouse islets (Zhao et al., 2014). However, in order to eliminate the problems and uncertainties associated with global deletion, where ABHD6 is absent right from embryo stage as this might affect the expression and activities of

other enzymes and factors, we analyzed MAG levels in BKO islets, where ABHD6 was deleted in β cells at adult stage. In order to directly correlate 1-MAG levels with insulin secretion, we measured both 1-MAG and 2-MAG levels in islets incubated with low (4 mM) and high glucose (16 mM) concentration in the presence or absence of 35 mM KCl and 20 nM GLP-1. Islets were incubated under conditions similar to those employed for insulin secretion measurement. The results indicated increased total and 1-MAG levels in BKO islets at basal conditions, and at 16 mM glucose, compared to Flox islets (Figure 6A, C). 2-MAG levels were only increased at low glucose (Figure 6B). Addition of GLP1 or KCl had no additional effect on 1-MAG, 2-MAG and total MAG levels (Figure 6A-C). In agreement with our previous report in whole body ABHD6 KO islets (Zhao et al., 2014), compared to low glucose, elevated glucose increased the levels of the long chain saturated 1-stearoylglycerol (1-SG) and 1-palmitoylglycerol (1-PG) and the levels of these MAG species were much higher in BKO islets (Figure 6D,E). The level of the monounsaturated 1-oleoylglycerol (1-OG) was not significantly changed in BKO islets in comparison to control islets under all tested conditions (Figure 6F). There were no significant changes in 2-SG, 2-PG and 2-OG levels in BKO islets except for a rise at low glucose in 2-SG and 2-PG (Figure 6G-I). Addition of KCl and GLP-1 did not significantly change either 1-MAG or 2-MAG levels under all tested conditions in Flox and BKO islets (Figure 6D-I)). Most of the other 1-MAG and 2-MAG species were too low to be detected, and some unidentified MAG peaks in the HPLC analysis were not considered in the analysis. Thus, ABHD6 deletion that results in enhanced insulin secretion in response to various fuel and non-fuel stimuli is associated with increased levels of long chain saturated 1-MAG species, consistent with their postulated role as signalling molecules for insulin secretion (Zhao et al., 2014).

3.6. 1-MAG amplifies fuel and non-fuel induced insulin secretion

If the increased in 1-MAG in BKO islets is causally implicated in amplifying the secretory response of various insulinotropic agents, then exogenously added 1-MAG should mimic the effect of ABHD6 deletion. This prediction was verified as indicated in Figure 7. As the potentiating effects of GLP-1 and Carb on insulin secretion require a glucose concentration higher than basal levels, we performed this experiment using 6 mM instead of 4 mM glucose. Our result indicated that 1-palmitoylglycerol amplified the secretion of insulin at 6 mM glucose, and the effect of the nutrient stimulus Kic as well as those of the neurohormonal agonists GLP-1 and Carb.

4. DISCUSSION

This study reveals that ABHD6 and MAG play a general role in insulin secretion as they regulate the process not only in response to glucose but also to amino acids (Gln plus Leu) and Kic acting as fuels stimuli, and in response to various non-fuel stimuli (GLP-1, carbamylcholine and a depolarizing concentration of KCl). It gives also additional information about the mechanisms implicated in this process. Thus, the data indicate that: a) the elevated insulin secretion response of β cells upon ABHD6 deletion is not related to altered DAG or TG hydrolysis; b) ABHD6 deletion enhances insulin secretion promoted by elevated glucose but does not potentiate fatty acid stimulated secretion; c) β cell specific deletion of ABHD6 increases total MAG and 1-MAG in islets at both low and high glucose and this is specifically due to increased level of saturated long chain 1-MAG species; d) Enhanced GSIS caused by

ABHD6 deletion is mediated by KATP/Ca^{2+} independent mechanisms of insulin secretion; e) Augmented insulin secretion in islet deficient in ABHD6 occurs independently of mitochondrial energy metabolism as glucose and fatty acid oxidation remained unchanged in BKO islets.

We have ruled out before (Zhao et al., 2014) the possibility that endocannabinoid receptors that bind 2-arachidonoylglycerol (2-AG), but not saturated MAG, are involved in the MAG-mediated effects on insulin secretion. Thus, a specific antagonist of the CB1 receptor (AM251) and an inverse agonist (AM630) of the CB2 receptor did not alter GSIS. Also 2-AG levels even at high glucose were <1% of the total β cell MAG, whereas the saturated MAG that rose in the presence of glucose was 100-fold higher as compared to 2-AG and stimulated insulin secretion. Noteworthy, only 2-AG, but not saturated MAG, can bind CB receptors and act as their ligand.

In our earlier study, we showed that global ABHD6 suppression leads to elevated 1-MAG in islets and that 1-MAG activates the exocytosis facilitating protein Munc13-1, thus promoting enhanced insulin secretion (Zhao et al., 2014). We now show that the effect of ABHD6 deletion occurs on second but not first phase insulin secretion after stimulation by glucose. This is in accordance with a previous study in islets from Munc13-1 deficient mice where only second phase GSIS was reduced (Kang et al., 2006). However, another study in haplodeficient Munc13-1 mice (Kwan et al., 2006a) observed alterations in both phases of secretion, and β cell capacitance determinations in these mice showed reduced exocytosis of both the ready releasable and refilling pools of secretory granules (Zhao et al., 2014). The reason for the discrepancy among these studies with respect to first phase only and not second phase GSIS is not known. The possibility exists that second phase GSIS is more sensitive to an elevation in 1-MAG than first phase, and that islet MAG levels were different in the two Munc13-1 deficient islets studies, and that exogenous 1-MAG at a high concentration stimulated both phases in the β cell capacitance study. The fact that ABHD6 deletion does not amplify the glucose induced Ca^{2+} rise and enhances KATP-independent pathways of insulin secretion that are thought to be implicated primarily in second phase of GSIS (Gembal et al., 1992), is consistent with the observation that second phase is enhanced.

What is the possible mechanism whereby second phase GSIS is amplified by ABHD6-accessible MAG in the β cell? It has been suggested that Ca^{2+} binds to synaptotagmin-7, the major Ca^{2+} sensor in β cells for insulin exocytosis (Gauthier and Wollheim, 2008; Wu et al., 2015), to facilitate loosening of cortical actin beneath the plasma membrane and fusion of insulin granule membrane with the plasma membrane. On the other hand, 1-MAG that accumulates in ABHD6 deleted β cells activates Munc13-1 (Zhao et al., 2014), which is essential for forming the SNARE exocytosis complex, by direct interaction with syntaxin-2 (Xie et al., 2012) and with Rab3 interacting molecule 2 (Kwan et al., 2007). Thus, we propose that the elevated Ca^{2+} and 1-MAG signals in response to various stimuli synergize for insulin secretion because 1-MAG via its activation of Munc13-1 will promote the formation of novel granules associated to the plasma membrane (enhancement of the readily–releasable pool of granules) that can be fused when the Ca^{2+} signal occurs.

We observed that insulin secretion in response to all tested fuel and non-fuel agents was enhanced in BKO islets except for fatty acids. What is the reason for this observation that appears surprising at first sight? A likely explanation lies in the fact that glucose and fatty acid signaling for secretion share common pathways. Both glucose and FFA activate the GL/FFA cycle that generates MAG. FFA also acts via the receptor FFAR1 but a recent study documented that FFAR1 stimulation by FFA enhances the GL/FFA cycle in INS-1 β cells (El-Azzouny et al., 2014). Thus, unlike the other stimuli (for example GLP1 that acts via cAMP and Ca^{2+} signaling), there may not be a possibility of synergy among glucose and FFA signaling pathways for secretion. Both glucose and FFA converge to signaling MAG that would reach maximal levels for secretion at elevated glucose plus FFA already in control Flox islets, such that secretion cannot be further enhanced in BKO islets.

ABHD6 deletion further augmented GSIS enhanced by both GLP1 and elevated KCl. GLP1 enhances secretion only at high glucose concentration and we earlier observed that GLP1 does not alter lipolysis in islet β cells (Peyot et al., 2009a). Consistent with this we now show that GLP1 does not changes MAG levels in islets. How deletion of ABHD6, which causes MAG buildup, further amplifies GLP1 action on insulin secretion? Recent studies showed that GLP1 signaling leads to protein kinase A mediated activation of the Ca^{2+} sensor synaptotagmin-7 in β cells leading to more efficient GSIS (Wu et al., 2015). It is possible that the signals generated by GLP1 receptor via protein kinase-A converge with 1-MAG signaling and have synergistic effect on insulin exocytosis. Depolarizing concentrations of KCl markedly increase Ca^{2+} in β cells and likely the amplification of its effect on secretion in BKO islets is due to a synergy between Ca^{2+} and MAG signaling pathways. Similarly 1-MAG signaling may amplify the inositol trisphosphate/Ca^{2+} and DAG signaling cascades generated by the Gq receptor agonist carbamylcholine. Figure 8 shows a model proposing how the ABHD6/1-MAG/ Munc13-1 network regulates insulin secretion in response to various classes of insulin secretagogues.

5. CONCLUSION

MAG mediated GSIS enhancement is a second phase event during insulin secretion and is a KATP and Ca^{2+} influx independent process. The importance of ABHD6 accessible MAG as a signal for insulin secretion is recognized under conditions of fuel stimuli at large and also when secretion is stimulated by various neurohormonal GPCR agonists. The data highlight the importance of ABHD6 and MAG as candidates for developing antidiabetic drugs.

ACKNOWLEDGMENTS

This study was supported by grants from the Canadian Institutes of Health Research to MP and SRMM. M.P. holds the Canada Research Chair in Diabetes and Metabolism. SZ is supported by the fellowship from Université de Montréal and the Montreal Diabetes Research Center; YM and KV are supported by a fellowship from Fond de Recherche Santé Québec (FRQS); CA is supported by a fellowship from the Canadian Diabetes Association.

CONFLICT OF INTEREST

None declared.

References

[1] Prentki M, Matschinsky FM, Madiraju SR. Metabolic signaling in fuel-induced insulin secretion. Cell metabolism 2013;18:162-85.
[2] Bratanova-Tochkova TK, Cheng H, Daniel S, Gunawardana S, Liu YJ, Mulvaney-Musa J, et al. Triggering and augmentation mechanisms, granule pools, and biphasic insulin secretion. Diabetes 2002;51 Suppl 1:S83-90.
[3] Ashcroft FM, Rorsman P. K(ATP) channels and islet hormone secretion: new insights and controversies. Nature reviews Endocrinology 2013;9:660-9.
[4] Ivarsson R, Quintens R, Dejonghe S, Tsukamoto K, in 't Veld P, Renstrom E, et al. Redox control of exocytosis: regulatory role of NADPH, thioredoxin, and glutaredoxin. Diabetes 2005;54:2132-42.
[5] Pi J, Bai Y, Zhang Q, Wong V, Floering LM, Daniel K, et al. Reactive oxygen species as a signal in glucose-stimulated insulin secretion. Diabetes 2007;56:1783-91.
[6] Maechler P, Wollheim CB. Mitochondrial glutamate acts as a messenger in glucose-induced insulin exocytosis. Nature 1999;402:685-9.
[7] Prentki M, Vischer S, Glennon MC, Regazzi R, Deeney JT, Corkey BE. Malonyl-CoA and long chain acyl-CoA esters as metabolic coupling factors in nutrient-induced insulin secretion. The Journal of biological chemistry 1992;267:5802-10.
[8] Brun T, Roche E, Assimacopoulos-Jeannet F, Corkey BE, Kim KH, Prentki M. Evidence for an anaplerotic/malonyl-CoA pathway in pancreatic beta-cell nutrient signaling. Diabetes 1996;45:190-8.
[9] Kaneko YK, Ishikawa T. Diacylglycerol Signaling Pathway in Pancreatic beta-Cells: An Essential Role of Diacylglycerol Kinase in the Regulation of Insulin Secretion. Biological & pharmaceutical bulletin 2015;38:669-73.
[10] Peyot ML, Guay C, Latour MG, Lamontagne J, Lussier R, Pineda M, et al. Adipose triglyceride lipase is implicated in fuel- and non-fuel-stimulated insulin secretion. The Journal of biological chemistry 2009;284:16848-59.
[11] Peyot ML, Nolan CJ, Soni K, Joly E, Lussier R, Corkey BE, et al. Hormone-sensitive lipase has a role in lipid signaling for insulin secretion but is nonessential for the incretin action of glucagon-like peptide 1. Diabetes 2004;53:1733-42.
[12] Nolan CJ, Leahy JL, Delghingaro-Augusto V, Moibi J, Soni K, Peyot ML, et al. Beta cell compensation for insulin resistance in Zucker fatty rats: increased lipolysis and fatty acid signalling. Diabetologia 2006;49:2120-30.
[13] Roduit R, Masiello P, Wang SP, Li H, Mitchell GA, Prentki M. A role for hormone-sensitive lipase in glucose-stimulated insulin secretion: a study in hormone-sensitive lipase-deficient mice. Diabetes 2001;50:1970-5.
[14] Mulder H, Yang S, Winzell MS, Holm C, Ahren B. Inhibition of lipase activity and lipolysis in rat islets reduces insulin secretion. Diabetes 2004;53:122-8.
[15] Fex M, Haemmerle G, Wierup N, Dekker-Nitert M, Rehn M, Ristow M, et al. A beta cell-specific knockout of hormone-sensitive lipase in mice results in hyperglycaemia and disruption of exocytosis. Diabetologia 2009;52:271-80.

[16] Zhao S, Mugabo Y, Iglesias J, Xie L, Delghingaro-Augusto V, Lussier R, et al. alpha/beta-Hydrolase domain-6-accessible monoacylglycerol controls glucose-stimulated insulin secretion. Cell metabolism 2014;19:993-1007.
[17] Iglesias J, Lamontagne J, Erb H, Gezzar S, Zhao S, Joly E, et al. Simplified assays of lipolysis enzymes for drug discovery and specificity assessment of of known inhibitors. Journal of lipid research 2015.
[18] Peyot ML, Pepin E, Lamontagne J, Latour MG, Zarrouki B, Lussier R, et al. Beta-cell failure in diet-induced obese mice stratified according to body weight gain: secretory dysfunction and altered islet lipid metabolism without steatosis or reduced beta-cell mass. Diabetes 2010;59:2178-87.
[19] Kim-Muller JY, Zhao S, Srivastava S, Mugabo Y, Noh HL, Kim YR, et al. Metabolic inflexibility impairs insulin secretion and results in MODY-like diabetes in triple FoxO-deficient mice. Cell metabolism 2014;20:593-602.
[20] Blankman JL, Simon GM, Cravatt BF. A comprehensive profile of brain enzymes that hydrolyze the endocannabinoid 2-arachidonoylglycerol. Chemistry & biology 2007;14:1347-56.
[21] Thomas G, Betters JL, Lord CC, Brown AL, Marshall S, Ferguson D, et al. The serine hydrolase ABHD6 Is a critical regulator of the metabolic syndrome. Cell reports 2013;5:508-20.
[22] Bisogno T, Howell F, Williams G, Minassi A, Cascio MG, Ligresti A, et al. Cloning of the first sn1-DAG lipases points to the spatial and temporal regulation of endocannabinoid signaling in the brain. The Journal of cell biology 2003;163:463-8.
[23] Li C, Najafi H, Daikhin Y, Nissim IB, Collins HW, Yudkoff M, et al. Regulation of leucine-stimulated insulin secretion and glutamine metabolism in isolated rat islets. The Journal of biological chemistry 2003;278:2853-8.
[24] Gembal M, Gilon P, Henquin JC. Evidence that glucose can control insulin release independently from its action on ATP-sensitive K+ channels in mouse B cells. The Journal of clinical investigation 1992;89:1288-95.
[25] Yajima H, Komatsu M, Schermerhorn T, Aizawa T, Kaneko T, Nagai M, et al. cAMP enhances insulin secretion by an action on the ATP-sensitive K+ channel-independent pathway of glucose signaling in rat pancreatic islets. Diabetes 1999;48:1006-12.
[26] Heissig H, Urban KA, Hastedt K, Zunkler BJ, Panten U. Mechanism of the insulin-releasing action of alpha-ketoisocaproate and related alpha-keto acid anions. Molecular pharmacology 2005;68:1097-105.
[27] MacDonald PE, El-Kholy W, Riedel MJ, Salapatek AM, Light PE, Wheeler MB. The multiple actions of GLP-1 on the process of glucose-stimulated insulin secretion. Diabetes 2002;51 Suppl 3:S434-42.
[28] Peter-Riesch B, Fathi M, Schlegel W, Wollheim CB. Glucose and carbachol generate 1,2-diacylglycerols by different mechanisms in pancreatic islets. The Journal of clinical investigation 1988;81:1154-61.
[29] Ferdaoussi M, Bergeron V, Zarrouki B, Kolic J, Cantley J, Fielitz J, et al. G protein-coupled receptor (GPR)40-dependent potentiation of insulin secretion in mouse islets is mediated by protein kinase D1. Diabetologia 2012;55:2682-92.
[30] Lund PE, Gylfe E, Hellman B. Leucine induces initial lowering of cytoplasmic Ca2+ in pancreatic beta-cells without concomitant inhibition of insulin release. Biochemistry international 1989;19:83-7.

[31] Kang L, He Z, Xu P, Fan J, Betz A, Brose N, et al. Munc13-1 is required for the sustained release of insulin from pancreatic beta cells. Cell metabolism 2006;3:463-8.
[32] Kwan EP, Xie L, Sheu L, Nolan CJ, Prentki M, Betz A, et al. Munc13-1 deficiency reduces insulin secretion and causes abnormal glucose tolerance. Diabetes 2006;55:1421-9.
[33] Wu B, Wei S, Petersen N, Ali Y, Wang X, Bacaj T, et al. Synaptotagmin-7 phosphorylation mediates GLP-1-dependent potentiation of insulin secretion from beta-cells. Proceedings of the National Academy of Sciences of the United States of America 2015;112:9996-10001.
[34] Gauthier BR, Wollheim CB. Synaptotagmins bind calcium to release insulin. American journal of physiology Endocrinology and metabolism 2008;295:E1279-86.
[35] Xie L, Zhu D, Gaisano HY. Role of mammalian homologue of Caenorhabditis elegans unc-13-1 (Munc13-1) in the recruitment of newcomer insulin granules in both first and second phases of glucose-stimulated insulin secretion in mouse islets. Diabetologia 2012;55:2693-702.
[36] Kwan EP, Xie L, Sheu L, Ohtsuka T, Gaisano HY. Interaction between Munc13-1 and RIM is critical for glucagon-like peptide-1 mediated rescue of exocytotic defects in Munc13-1 deficient pancreatic beta-cells. Diabetes 2007;56:2579-88.
[37] El-Azzouny M, Evans CR, Treutelaar MK, Kennedy RT, Burant CF. Increased glucose metabolism and glycerolipid formation by fatty acids and GPR40 receptor signaling underlies the fatty acid potentiation of insulin secretion. The Journal of biological chemistry 2014;289:13575-88.
[38] Peyot ML, Gray JP, Lamontagne J, Smith PJ, Holz GG, Madiraju SR, et al. Glucagon-like peptide-1 induced signaling and insulin secretion do not drive fuel and energy metabolism in primary rodent pancreatic beta-cells. PloS one 2009;4:e6221.

Figure legends

Figure 1. BKO islets show reduced MAG hydrolysis activity. (A) Western blot analysis of ABHD6 protein level in Flox and BKO islets. (B) Total MAG hydrolysis activity was measured in the absence and presence of 1μM WWL70. (C) DAG hydrolysis activity was measured in the absence and presence of 1 μM orlistat. (D) TG hydrolysis activity was measured in the absence and presence of 1 μM Cay10499. Results are Mean ± SEM from three different experiments with pooled islets from 6-9 mice in each group. *p≤0.05 vs Flox mice; # p < 0.05 versus BKO mice.

Figure 2. Enhanced insulin secretion in response to various fuel and non-fuel stimuli in ABHD6-BKO islets. (A) The effect of glucose and fatty acids (palmitate plus oleate (P/O)) on insulin secretion. Insulin secretion was measured in Flox and BKO islets at basal (4 mM), and high (16 mM) glucose in the absence or presence of 0.15 mM palmitate and 0.15 mM oleate. (B) Effect of glutamine plus leucine on insulin secretion. Insulin secretion was measured at 4 mM glucose in the absence or presence of 5 mM glutamine plus 5 mM leucine. (C) The effect of KCl and diazoxide (DZ) on insulin secretion. Insulin secretion was measured at 4 mM glucose in the absence or presence of 35 mM KCl and 0.1 mM diazoxide. (D) The effect of Kic, GLP1 and Carb on insulin secretion. Insulin secretion was measured at 4 and 16 mM glucose. The effect of Kic was tested at 4 mM glucose, whereas the effect of 20 nM GLP1 and 200 μM Carb were tested at 16 mM glucose. (E) The net calculated effect of fatty acids (P/O), GLP-1 and Kic on the top of 16 mM glucose on insulin secretion. The results show the calculated difference in panel A of insulin secretion at 16 mM glucose in the presence of P/O minus the secretion at 16 mM glucose only, and similar calculation for the true GLP1 and Carb effects on the top of 16 mM glucose in panel D. Mean ± SEM are from three different experiments with totally 9 mice in each groups. *p < 0.05; **p < 0.01; ***p < 0.001 versus Flox group.

Figure 3. Enhanced second phase and KCl-induced insulin secretion in perifused ABHD6-BKO islets. Batches of 30 islets were perifused in enriched KRBH with 4 mM glucose for 45 min, and then followed by KRBH with 16 mM glucose for 30 min and then with 35 mM KCl for another 30 min. Results are Mean ± SEM from 4 different experiments with 8 control mice and 10 BKO mice. (A) The original trace of perifusion study. (B) First phase insulin secretion, calculated area under curve (AUC) between 0 to 10 min ($AUC_{0\text{-}10min}$); (C) Second phase insulin secretion, calculated AUC between 10 to 30 min ($AUC_{10\text{-}30min}$); (D) KCl-stimulated insulin secretion, calculated AUC between 30 to 35 min ($AUC_{30\text{-}35min}$); *p≤0.05 vs control islets.

Figure 4. Cytosolic Ca^{2+} measurements in Flox and BKO islet ß cells. Dispersed cells from islets from Flox and BKO mice were used for cytosolic free calcium measurement using a fluorescence plate-reader. (A) The effect of high glucose in control and BKO islets. 4G, 4 mM glucose; 16G, 16 mM glucose. (B) Effect of 35 mM KCl on cytosolic Ca^{2+}. Mean ± SEM are of 6 different measurements with 10-15 mice per group. Results are expressed as fluorescence ratios (F340/F380).

Figure 5. Glucose and fatty acid metabolism in Flox and BKO islets. (A) Glucose oxidation. (B) Glucose utilization. (C) Fatty acid oxidation. Each experiment was performed with pooled islets from 8 mice per group. Mean ± SEM of 6-10 determinations.

Figure 6. MAG species levels in Flox and BKO islets. Islets were incubated for 1h in enriched KRBH at 4 and 16 mM glucose in the presence or absence of 35 mM KCl and 20 nM GLP-1, and then the islets were extracted for lipid analysis. (A) Total 1-MAG levels; (B) Total 2-MAG; (C) Total MAG. (D). 1-stearoylglycerol (1-SG); (E) 1-palmitoylglycerol (1-PG); (F) 1-oleoylglycerol (1-OG); (G) 2-stearoylglycerol (2-SG); (H) 2-palmitoylglycerol (2-PG); (I) 2-oleoylglycerol (2-OG). Mean ± SEM of 5-6 different measurements with 14 mice per group. *$p < 0.05$; **$p < 0.01$; ***$p < 0.001$ versus corresponding Flox group. # $p < 0.05$ versus Flox at 4 mM glucose (4G).

Figure 7. Synergic effect on insulin secretion of 1-MAG with other stimuli in dispersed rat islet cells. Insulin secretion was measured at 6 mM glucose (6G) with or without 20 nM GLP-1, 200 μM Carb and 10 mM Kic in the absence or presence of 100 μM 1-palmitolglycerol (1-PG). Mean ± SEM from 3 different experiments, using 13 rats in total. *$p < 0.01$ versus control-6G; #$p < 0.05$; ##$p < 0.01$; ###$p < 0.001$ versus corresponding 6G group.

Figure 8. Model illustrating how the ABHD6/1-MAG/Munc13-1 network regulates insulin secretion in response to various classes of insulin secretagogues. Glucose and fatty acids enter the glycerolipid/fatty acid (GL/FA) cycle in its lipogenesis arm via the esterification of glucose-derived glycerol-3-phosphate with fatty acyl-CoA. Subsequent lipolysis produces long chain saturated 1-monoacylglycerol that act as a metabolic coupling factor causing insulin secretion via binding and activation of the exocytosis coordinator Munc13-1. Glucose and other fuel stimuli, including Gln, Leu and 2-ketoisocaproate (Kic), produce additional coupling factors (eg ATP, NADPH, ROS, Glutamate, short chain acyl-CoAs) that activate insulin secretion via other mechanisms that synergize, together with an elevation in cytosolic Ca^{2+}, with the 1-MAG signal. Non-fuel neurohormonal stimuli, such as glucagon-like peptide 1 and acetylcholine, activate Gs and Gq protein coupled receptors that signal via cAMP and inositol-1,4,5 trisphosphate and diacylglycerol, respectively. These second messengers also synergize with the 1-MAG signal for insulin secretion

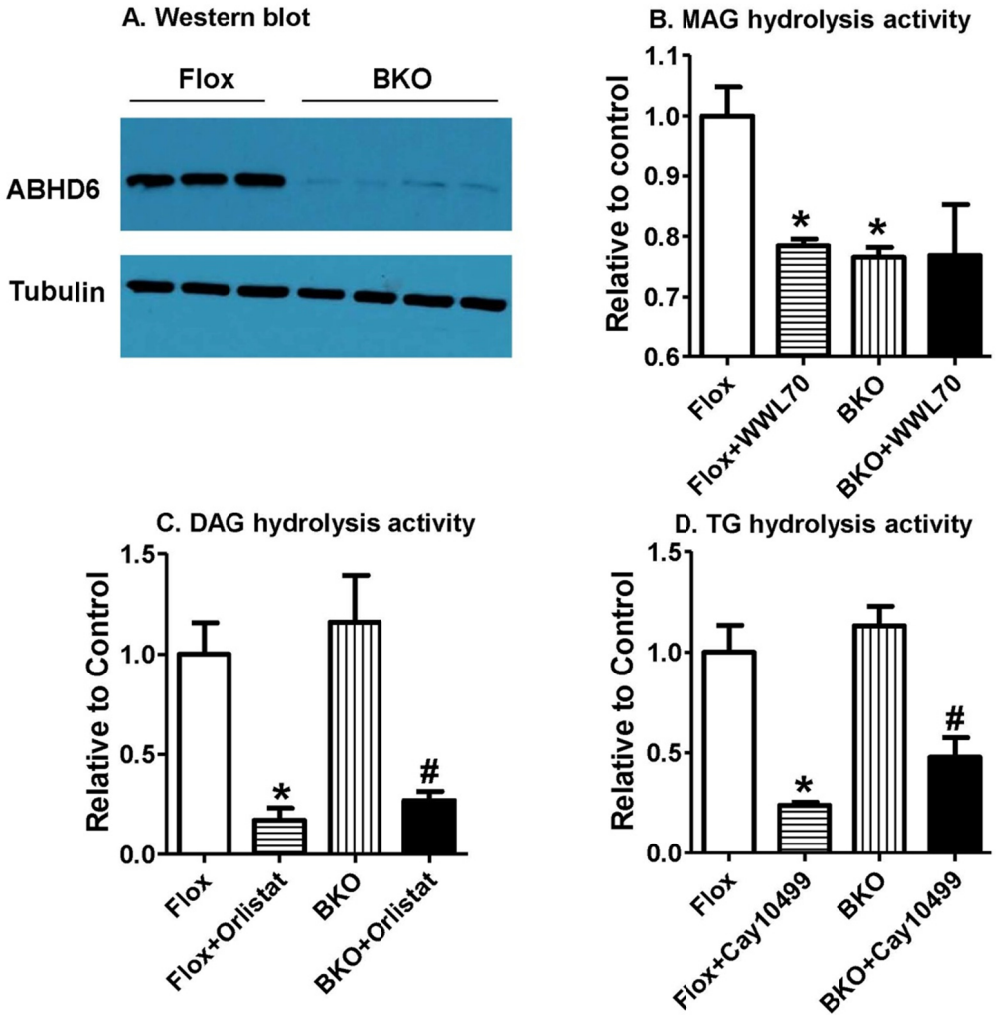
A. Western blot
Flox
BKO
ABHD6
Tubulin
B. MAG hydrolysis activity
Relative to control
1.1
1.0
0.9
0.8
0.7
0.6
*
*
Flox
Flox+WWL70
BKO
BKO+WWL70
C. DAG hydrolysis activity
Relative to Control
1.5
1.0
0.5
0.0
*
#
Flox
Flox+Orlistat
BKO
BKO+Orlistat
D. TG hydrolysis activity
Relative to Control
1.5
1.0
0.5
0.0
*
#
Flox
Flox+Cay10499
BKO
BKO+Cay10499

Figure 1

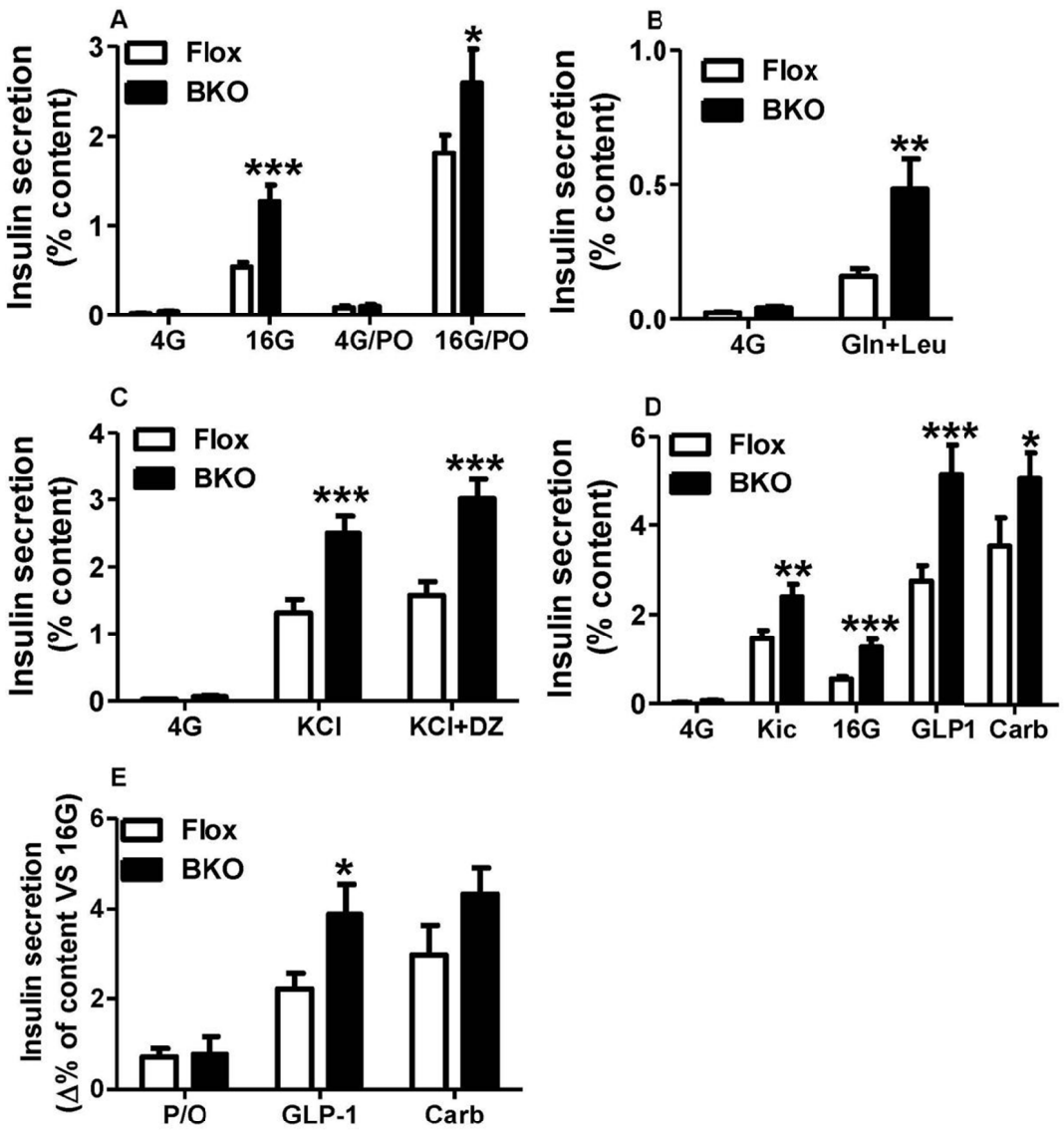
A
Insulin secretion (% content)
Flox
BKO
***
*
4G
16G
4G/PO
16G/PO
B
Insulin secretion (% content)
Flox
BKO
**
4G
Gln+Leu
C
Insulin secretion (% content)
Flox
BKO
***
***
4G
KCl
KCl+DZ
D
Insulin secretion (% content)
Flox
BKO
**
***
***
*
4G
Kic
16G
GLP1
Carb
E
Insulin secretion (Δ% of content VS 16G)
Flox
BKO
*
P/O
GLP-1
Carb

Figure 2

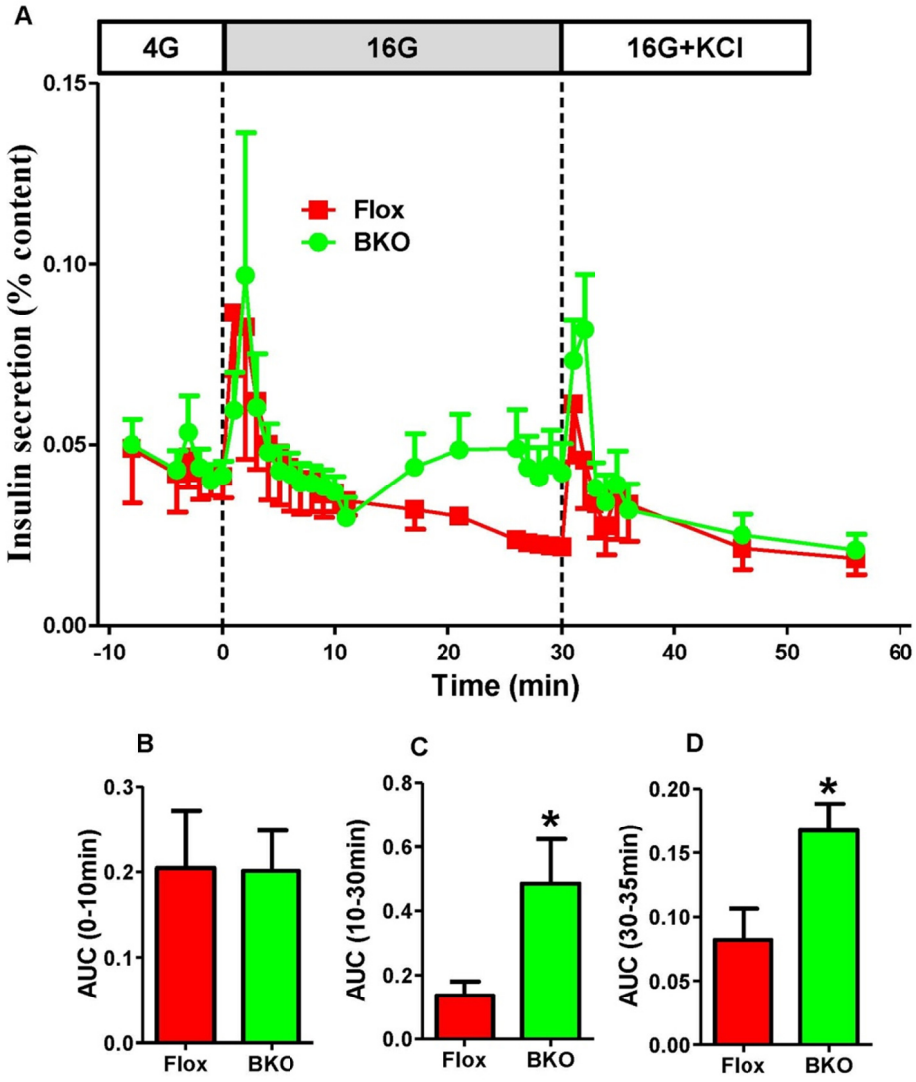
A
4G
16G
16G+KCl
Insulin secretion (% content)
0.15
0.10
0.05
0.00
Flox
BKO
-10
0
10
20
30
40
50
60
Time (min)
B
AUC (0-10min)
0.3
0.2
0.1
0.0
Flox
BKO
C
AUC (10-30min)
0.8
0.6
0.4
0.2
0.0
*
Flox
BKO
D
AUC (30-35min)
0.20
0.15
0.10
0.05
0.00
*
Flox
BKO

Figure 3

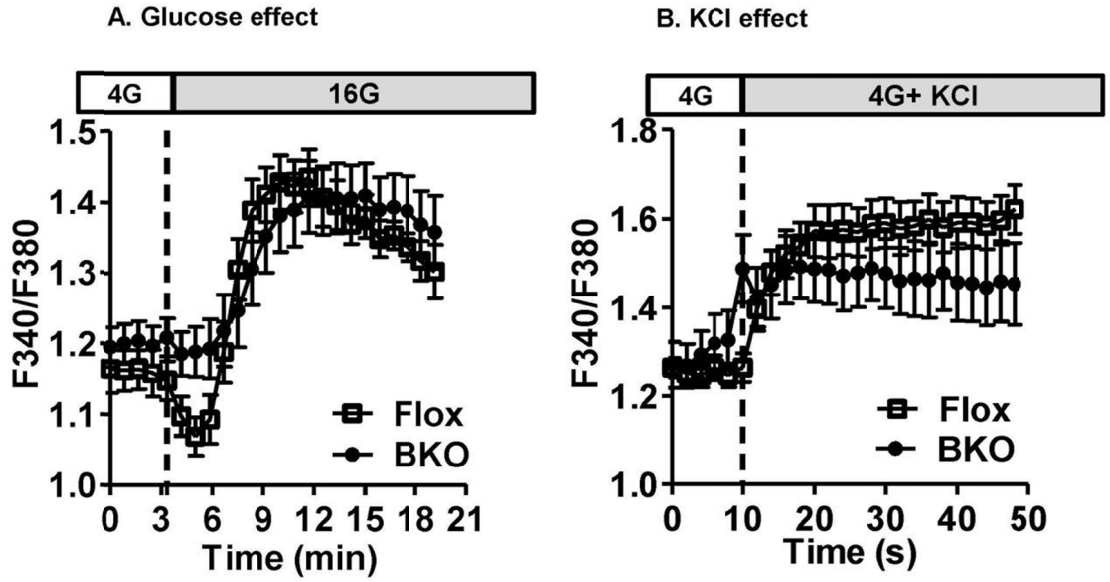
A. Glucose effect
4G
16G
F340/F380
1.5
1.4
1.3
1.2
1.1
1.0
0 3 6 9 12 15 18 21
Time (min)
Flox
BKO
B. KCl effect
4G
4G+ KCl
F340/F380
1.8
1.6
1.4
1.2
1.0
0 10 20 30 40 50
Time (s)
Flox
BKO

Figure 4

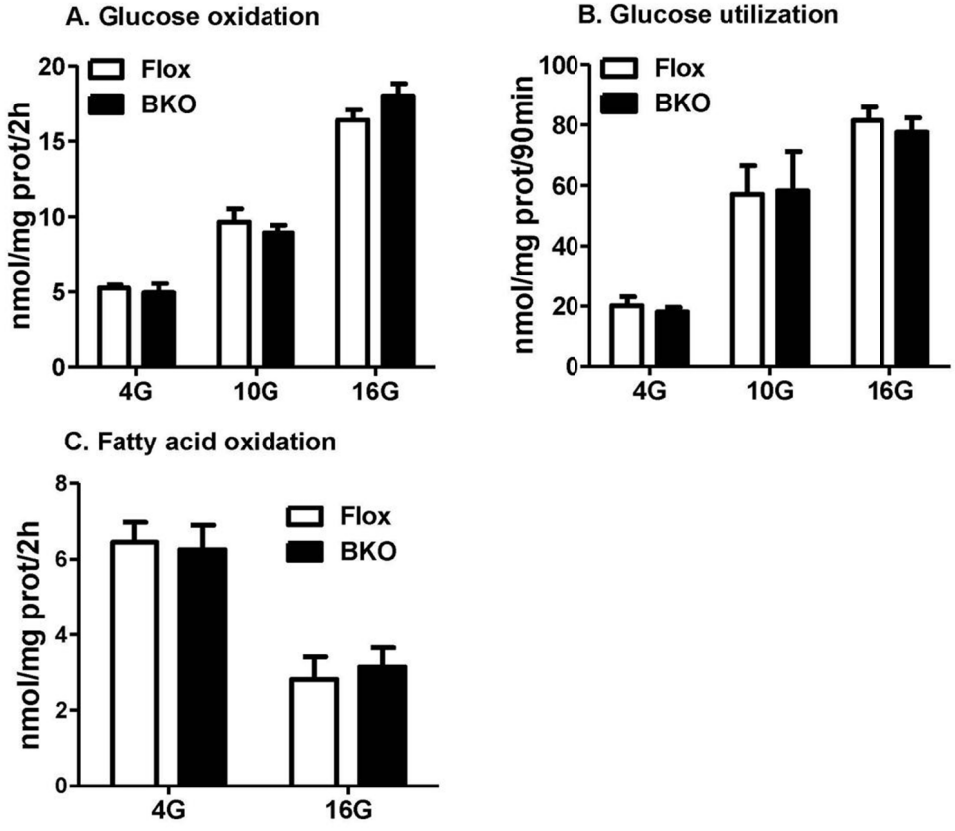
A. Glucose oxidation
nmol/mg prot/2h
20
15
10
5
0
Flox
BKO
4G
10G
16G
B. Glucose utilization
nmol/mg prot/90min
100
80
60
40
20
0
Flox
BKO
4G
10G
16G
C. Fatty acid oxidation
nmol/mg prot/2h
8
6
4
2
0
Flox
BKO
4G
16G

Figure 5

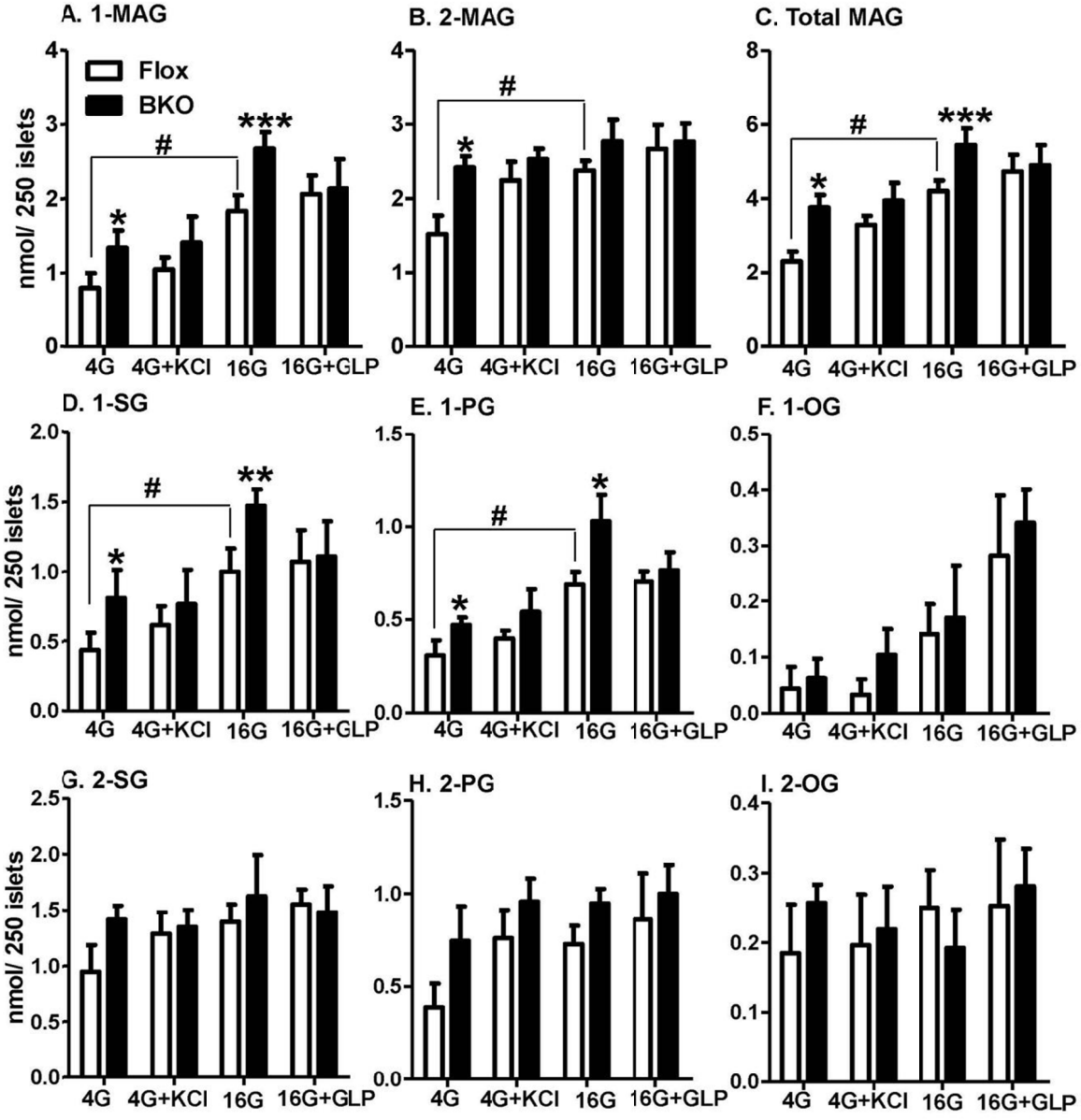
A. 1-MAG
B. 2-MAG
C. Total MAG
Flox
BKO
nmol/ 250 islets
4G
4G+KCl
16G
16G+GLP
D. 1-SG
E. 1-PG
F. 1-OG
G. 2-SG
H. 2-PG
I. 2-OG

Figure 6

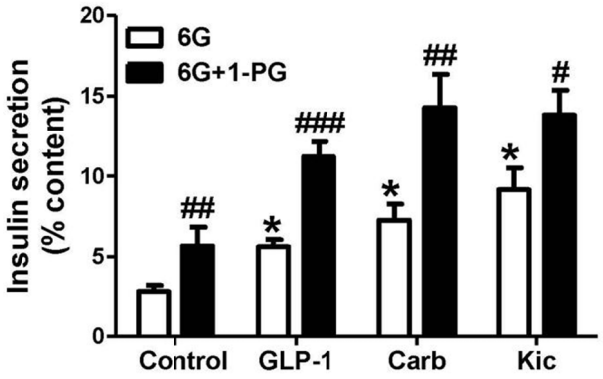
Insulin secretion
(% content)
20
15
10
5
0
6G
6G+1-PG
##
*
###
*
##
*
#
Control
GLP-1
Carb
Kic

Figure 7

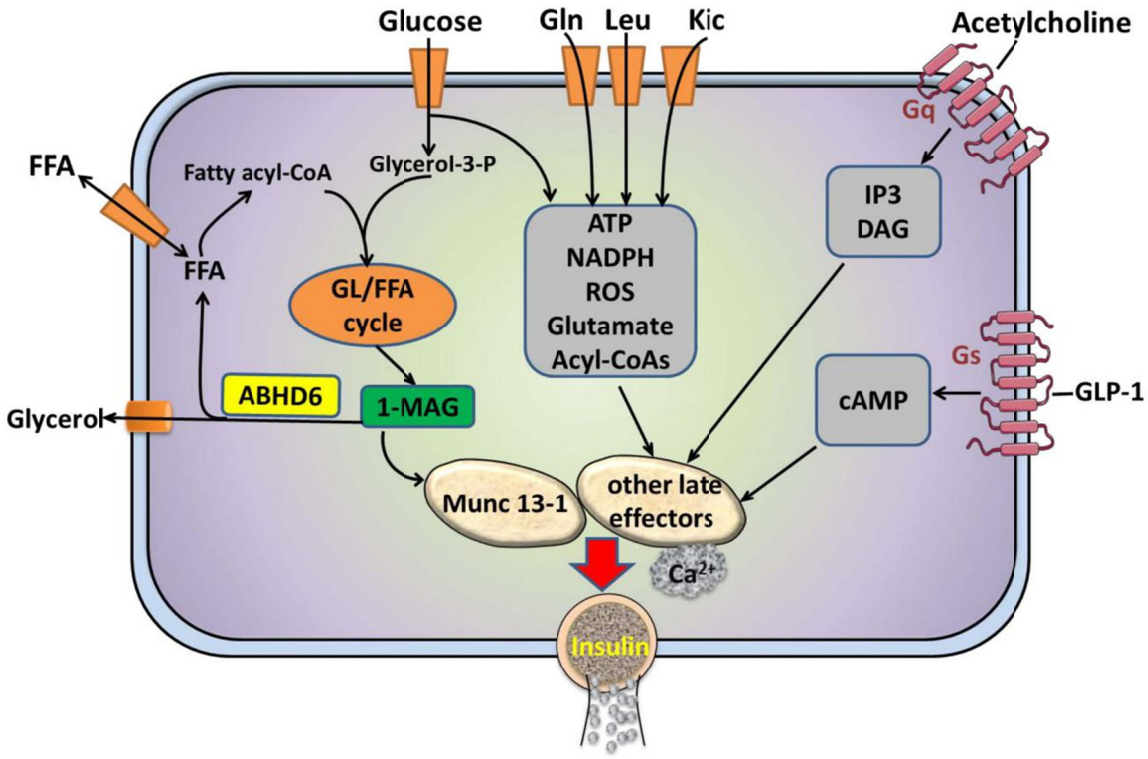
Glucose
Gln
Leu
Kic
Acetylcholine
Gq
FFA
Fatty acyl-CoA
Glycerol-3-P
IP3
DAG
ATP
NADPH
ROS
Glutamate
Acyl-CoAs
FFA
GL/FFA
cycle
Gs
GLP-1
cAMP
ABHD6
1-MAG
Glycerol
Munc 13-1
other late
effectors
Ca2+
Insulin

Figure 8

Article 3

α/β-Hydrolase domain-6 deletion induces adipose browning and prevents obesity and type-2 diabetes

Shangang Zhao[1], Yves Mugabo[1], Gwyn Thomas[2], Camille Attane[1], Jose Iglesias[1], Pegah Pourshaifi[1], Dongwei Zhang[1,4], Thuy Anne Nguyen[1], Raphael Prentki[1], Marie-line Peyot[1], Erik Joly[1], Stephanie Tobin[1], Stephanie Fulton[1], J. Mark Brown[3], S.R. Murthy Madiraju[1*] and Marc Prentki[1*]

[1]Departments of Nutrition and Biochemistry and Montreal Diabetes Research Center, CRCHUM and Université de Montréal, Montréal, QC, Canada; [2]Section on Lipid Sciences, Department of Pathology, Wake Forest University School of Medicine, Medical Center Boulevard, Winston-Salem, NC 27157, USA.; [3]Cleveland Clinic Lerner Research Institute, Department of Cellular and Molecular Medicine, Case Western Reserve University, Cleveland Clinic Lerner College of Medicine, Cleveland, Ohio 44195; [4]Current address: Department of Endocrinology and Diabetes, Beijing University of Chinese Medicine, Beijing, China

Running title: ABHD6 regulates fuel homeostasis, WAT browning and BAT function

Submitted to: Cell Reports on 29.06.2015, currently in revision.

***Correspondence to:**

Dr. Marc Prentki, Montreal Diabetes Research Center, CRCHUM, 900 St-Denis (Viger Tower), Rm R08-412, Montreal, QC H1W 4A4, Canada.

Dr. S.R. Murthy Madiraju, Montreal Diabetes Research Center, CRCHUM, 900 St-Denis (Viger Tower), Rm R08-414, Montreal, QC H1W 4A4, Canada

Detailed contribution of authors in this work:

Shangang Zhao was responsible for most of the work present in this chapter, the overall contribution to work was more than 65%. Under supervision of Dr. Madiraju and Dr. Prentki, Shangang Zhao was involved in characterizing HFD-fed whole body ABHD6 KO mice and assessing the role of ABHD6 in browning and its associated mechnisms, as well as participating in writing of the manuscript.

Yve Mugabo, Camille Attane and Jose Iglesias performed in vivo and ex vivo experiments. Jose Iglesias also performed MAG hydrolysis activity in visceral fat (Fig 5A).

Gwyn Thomas and J. Mark Brown designed and performed the WWL70 and ABHD6-ASO in vivo experiments. The detailed figures included Fig 4 and Fig S10.

Pegah Pourshaifi, Dongwei Zhang, Thuy Anne Nguyen and Raphael Prentki participated in genotyping, in vitro and respiration experiments.

Marie-line Peyot and Erik Joly participated in the design of in vivo experiments and interpretation of the data.

Stephanie Tobin and Stephanie Fulton designed and performed the behavior tests and interpreted the results. The detailed figure included Fig S6.

SR Murthy Madiraju and Marc Prentki designed and supervised the project, interpreted the data and wrote the manuscript.

Abstract

Suppression of α/β-domain hydrolase-6 (ABHD6), a monoacylglycerol (MAG) hydrolase, promotes glucose stimulated insulin secretion by pancreatic β-cells. We report here that high fat diet fed ABHD6-KO mice show modestly reduced food intake, decreased body weight gain and glycemia, improved glucose tolerance and insulin sensitivity, and enhanced locomotor activity. ABHD6-KO mice also show increased energy expenditure, cold induced thermogenesis, brown adipose UCP1 expression and fatty acid oxidation and white adipose browning. Adipose browning and cold induced thermogenesis are replicated by the ABHD6 inhibitor WWL70 and by antisense oligonucleotides against ABHD6. Evidence indicates that lipolysis derived 1-MAG signals intrinsic and cell autonomous adipose browning via PPARα and PPARγ activation, and that ABHD6 regulates adipose browning by controlling signal competent 1-MAG levels. Thus, ABHD6 regulates energy homeostasis brown adipose tissue function and white adipose tissue browning and is a potential therapeutic target for obesity and type-2 diabetes.

Introduction

Glycerolipid/ free fatty acid cycle, which generates signaling molecules within its lipolysis and lipogenesis segments, plays a role in the regulation of fat storage and mobilization, insulin secretion and action, non-shivering thermogenesis and energy homeostasis (Prentki and Madiraju, 2008). Lipolysis of triglycerides to diacylglycerol, monoacylglycerol (MAG) and glycerol plus fatty acids is catalyzed by the sequential action of adipose triglyceride lipase, hormone sensitive lipase and MAG lipase (Prentki and Madiraju, 2008; Zechner et al., 2012). Although MAG lipase is thought to be the major MAG hydrolyzing enzyme in many tissues, intracellular breakdown of MAG can also be catalyzed by membrane bound α/β-hydrolase domain-6 (ABHD6) (Blankman et al., 2007a). Whole-body deletion of MAG lipase in mice enhances insulin sensitivity and glucose tolerance without affecting body weight gain or food intake under high fat diet (HFD) condition (Taschler et al., 2011). We recently reported that ABHD6 is the major MAG hydrolase in pancreatic β-cells and that suppression of ABHD6 results in elevated islet MAG levels with enhanced glucose stimulated insulin secretion (Zhao et al., 2014). Our results identified ABHD6 as a negative modulator of insulin secretion, as this enzyme hydrolyzes the signal molecule 1-MAG that activates the exocytosis facilitating protein Munc13-1. A recent study showed that male mice fed a HFD treated with antisense oligonuleotides (ASO) against ABHD6 protects from HFD-induced obesity, hepatic steatosis and systemic insulin resistance (Thomas et al., 2013). However, female mice were not studied and the biochemical basis of these beneficial actions needs to be determined

Although an imbalance between energy intake and expenditure and the resulting obesity is a major contributor of type-2 diabetes (T2D), the current pharmacological approaches for treating obesity and diabetes target different pathways. Several studies showed altered expression of a specific gene, either by knockout or overexpression, to offer protection against diet induced obesity (DIO), but none of these genes were shown to control both insulin secretion and sensitivity directly (Dirkx et al., 2014; Koh et al., 2013; Liew et al., 2010; Liu et al., 2014; Sumara et al., 2009). However, it is desirable to identify a metabolic step/ pathway that can influence both insulin secretion and action in conjunction with additional beneficial effects on energy homeostasis, such that a single target can be addressed for diabetes and obesity.

Increased energy expenditure via fat oxidation and non-shivering thermogenesis by classical brown adipose tissue (BAT) and also by the stimulation of beige adipocytes may provide a novel avenue to alleviate the effects of obesity and prevent T2D (Wu et al., 2013). Several recent reports indicated that augmented BAT function and browning of white adipose tissue (WAT) enhance glucose tolerance, insulin sensitivity and protect from DIO and obesity-related diabetes (Cereijo et al., 2014; Pfeifer and Hoffmann, 2015; Richard et al., 2010; Rosen and Spiegelman, 2014). Signaling via peroxisomal proliferator activated receptors (PPAR) is important for the beige adipocyte formation (Wu et al., 2012) and the stimulation of BAT(Rosen and Spiegelman, 2014). PPARα itself plays a role in maintaining brown adipocyte phenotype and in the browning process of white adipose (Hondares et al., 2011b; Roberts et al., 2014). The endogenous activators of BAT activation and WAT browning are unknown and recent studies suggested that certain lipolytic products may activate PPARs (Badin et al., 2012; Haemmerle et al., 2011; Mottillo et al., 2012).

In order to understand the role of ABHD6 and monoacylglycerol in energy homeostasis we studied whole body ABHD6-KO mice and DIO mice treated with ABHD6-ASO or an ABHD6 inhibitor. When fed a high fat diet ABHD6-KO mice show a unique phenotype that implicates ABHD6 in obesity, metabolic syndrome and diabetes. They display a modest reduction of appetite, are protected from obesity, glucose intolerance, insulin resistance, hyperinsulinemia and hepatic steatosis, and also show enhanced locomotor activity, BAT activity and WAT browning. The mechanism of adipose browning appears to be, at least in part, intrinsic to adipose tissue and involves 1-monoacylglycerol accumulation causing PPARα and PPARγ activation. DIO mice treated with an ABHD6 inhibitor or with ASO also show adipose browning.

RESULTS

Improved glucose tolerance in female but not male ABHD6-KO mice on chow-diet

Six-weeks old male ABHD6-KO mice on pure C57Bl6N genetic background(Zhao et al., 2014) when placed on chow diet, showed no differences in their glucose tolerance in comparison to wild-type (WT) mice (**Supplementary Fig. 1a**) during oral glucose tolerance test (OGTT),

despite increased insulin secretion (**Supplementary Fig. 1b**). Insulin sensitivity was unaltered in these male KO mice (**Supplementary Fig. 1c**) as revealed by insulin tolerance test (ITT). This confirms our earlier results showing unaltered insulin sensitivity in 26 week old male ABHD6-KO mice (Zhao et al., 2014). Unlike male KO mice, female ABHD6-KO mice displayed better glucose tolerance than WT mice but with reduced insulin secretion (**Supplementary Fig. 1d, e**), during OGTT, indicating that female KO mice are more insulin sensitive, which was confirmed by ITT (**Supplementary Fig. 1f**). Body weight gain up to 24 weeks and cumulative food intake did not change significantly in male KO mice on chow diet (**Supplementary Fig. 1g, h**), but were slightly reduced in female ABHD6-KO mice (**Supplementary Fig. 1i, j**). Overall, female ABHD6-KO mice show stronger phenotype than the males on chow diet.

ABHD6-KO mice on high fat diet show reduced weight gain and improved glucose tolerance and insulin sensitivity

Both male and female ABHD6-KO mice after 60% HFD for 8 weeks showed improved glucose tolerance but much lower insulinemia during OGTT and also enhanced insulin sensitivity in ITT (**Fig. 1a-f**). Heterozygous mice showed intermediate response, more notably for insulinemia. The low insulinemia response in KO mice during OGTT (**Fig. 1b, e**) was suggestive of enhanced insulin sensitivity, which was confirmed by ITT (**Fig. 1c, f**) and also by hyperinsulinemic-euglycemic clamp (**Fig. 1g, h**). Glucose infusion rate (index of insulin sensitivity) in HFD fed male KO mice was higher as compared to WT mice, with heterozygous mice showing intermediate effect (**Fig. 1h**). During HFD feeding, both male and female ABHD6-KO mice showed less body weight gain (**Fig. 1i, k**) and reduced cumulative food intake (**Fig. 1j, l**). The decrease in body weight gain was more pronounced in female KO mice (~30% at week 8) as compared to male KO mice (~12 % at week 8), whereas the significant reduction in cumulative food intake (~7 % at weeks 6-8) in both sexes was modest, as compared to WT mice.

Ex-vivo analysis indicated that visceral fat and soleus muscle from ABHD6-KO mice show enhanced glucose uptake under basal and insulin stimulated conditions (**Supplementary Fig. 2**). These effects were more pronounced in female mice. Thus, ABHD6 deficiency is

associated with enhanced insulin independent glucose uptake by muscle and adipose tissues that likely contributes to the better glucose disposal in the KO mice.

Reduced fat mass and liver steatosis in ABHD6-KO mice

Echo-MRI of ABHD6-KO mice revealed no difference in lean mass (**Supplementary Fig. 3a, e**). The fat mass (**Supplementary Fig. 3b, f**) was markedly decreased in female KO mice, but modestly in males. Liver weight showed significant reduction in the KO mice as compared to WT mice in both males (**Supplementary Fig. 3c**) and females (**Supplementary Fig. 3g**) and this may be related to decreased fat content, as noticed in liver histology, showing more fat accumulation in the WT than KO mice (**Supplementary Fig. 3i**). There was no change in visceral fat weight in male KO mice (**Supplementary Fig. 3d**) while in female KO mice this was reduced by ~40% (**Supplementary Fig. 3h**) and this was also evident physically (**Supplementary Fig. 3j**).

Blood chemistry and additional parameters of ABHD6-KO mice

ABHD6-KO mice on HFD showed reduced glycemia and insulinemia. On normal diet, neither glycemia nor insulinemia of the KO mice were different from WT mice (**Supplementary Table 1**). There were no differences in chow or HFD fed KO vs WT mice in their plasma glycerol, triglyceride, free fatty acids, free and total cholesterol levels in fed states (**Supplementary Table 1**). Rectal temperature of female KO mice was slightly (not significant) higher than WT mice, suggestive of elevated energy expenditure (see below). The growth characteristics of ABHD6-KO mice were not altered as indicated by their body and tail length in comparison to WT mice. Fur appearance was also not different (**Supplementary Fig. 3j**). We measured various adipokines, cytokines and hormones in plasma by "protein array" in HFD mice and only 6 of them showed significant changes (**Supplementary Fig. 4**). FGF21 and FGF, which are implicated in protection from obesity mediated complications (Kharitonenkov and Adams, 2014; Owen et al., 2014), were elevated in the KO mice, whereas plasma proteins related to insulin resistance, including ICAM-1, IGFBP-1 and resistin were decreased. RAGE that is indicative of inflammation was also reduced.

Elevated respiration, energy expenditure and locomotor activity in ABHD6-KO mice

ABHD6-KO mice were acclimatized for 48h in metabolic cages, separately, at room temperature and at 30ºC (thermoneutral conditions). Respiratory measurements made on the third day indicated elevated VO_2 during light and dark phases (**Supplementary Fig. 5a**) and during the last 24h period (**Fig. 2a**), both in male and female mice at both room temperature and at 30ºC. VCO_2 and respiratory exchange ratio (RER) were not affected (**Fig. 2b, c; Supplementary Fig. 5b, c**). Energy expenditure as a function of metabolic mass (lean mass + 0.2× fat mass) was higher in both female and male ABHD6-KO mice, in both the dark and light phases, last 24 h and at both temperatures (**Fig. 2d, Supplementary Fig. 5d**).

ABHD6-KO mice show increased locomotor activity over a 24 h time period **(Fig. 2e)** and during dark phase and this increase was more marked in females (**Fig. 2e, Supplementary Fig. 5e**). In order to examine whether the enhanced locomotor activity is related to depressive behavior, anxiety, or stress we performed the forced swimming, open field and elevated platform tests, which revealed no differences between WT and KO mice (**Supplementary Fig. 6a-c**), suggesting that the enhanced locomotor activity of KO mice is due to voluntary exercise.

Enhanced BAT function and white adipose 'browning' in ABHD6-KO mice

As ABHD6-KO mice on HFD show enhanced energy expenditure, we examined whether BAT function is elevated in these mice and if there is white adipose 'browning'. We measured in female ABHD6-KO mice thermogenic gene expression in BAT and genes associated with adipose browning in visceral and inguinal WAT. UCP1, PGC1α, PRDM16, PPARα and CD36 mRNA levels (**Fig. 3a-e**) were elevated in visceral and inguinal WAT and in BAT. Expression of other browning related genes (TBX1, CD37, TREM26, Cox8b, Cox7a1, CIDEA) (**Supplementary Fig. 7a-i**) showed moderate or no changes. Expression of PPARα, that controls UCP1 transcription (Xue et al., 2005), was elevated in WAT and BAT (**Fig. 3e**) but no significant changes were seen in PPARβ or PPARγ, although there was a trend for higher expression in WAT and BAT of the KO mice (**Supplementary Fig. 7f, g**). PPARα target genes CD36 and CPT-1 showed increased expression in the KO mice (**Fig. 3e, Supplementary Fig. 7h**). Histology revealed smaller adipocytes in the visceral and inguinal adipose tissues and smaller adipocytes with much less lipid deposits in the BAT of the ABHD6-KO mice (**Fig. 3f**). UCP1 protein staining was higher in visceral, inguinal and brown

adipose tissues (**Fig. 3g**). Cold (4°C) induced thermogenesis for 3 h revealed higher ability of the KO mice to maintain their body temperature than WT mice (**Fig. 3h**). Similar gene expression changes were noticed in WAT and BAT from ABHD6-KO mice after 3-day acclimatization at 30ºC, except that PPARγ induction was more apparent (**Supplementary Fig. 8**). BAT from KO mice showed nearly 2-fold increase in palmitate β-oxidation (**Supplementary Fig. 9a-d**). Thus, there is increased thermogenic program and function in BAT and induction of browning related genes in visceral and subcutaneous adipose tissues of the KO mice.

Pharmacological inhibition or ASO knockdown of ABHD6 triggers adipose browning

Daily administration of the ABHD6 inhibitor WWL70 or treatment with ABHD6-ASO was shown to protect mice from HFD induced obesity (Thomas et al., 2013). In order to examine whether pharmacological inhibition of ABHD6 induces adipose browning as seen in the gene-deleted mice, C57Bl6N mice were fed a high fat diet (40% calories from fat) for 8 weeks with daily treatment with WWL70. Administration of WWL70 led to more UCP1 staining (**Fig. 4a**) and induction of browning related genes (**Fig. 4b**) in the visceral adipose. Expression of Cidea and Cox7a1 showed marginal increases whereas UCP2, PPARα and PPARγ expression were unaltered in WWL70 treated mice (**Supplementary Fig. 10a**).

ABHD6-ASO treated mice on HFD showed markedly reduced ABHD6 expression in visceral adipose in association with induction of UCP1, PRDM16, PPARα and PPARγ (**Fig. 4c-g**). Expression of Cox7a1, Elovl3, TBX1 and TREM26 were also elevated in the ASO treated mice (**Supplementary Fig. 10b**). Similar to ABHD6-KO mice, ASO treated mice could better maintain their body temperature in cold than control mice (**Fig. 4h**). Thus, *in vivo* pharmacological inhibition of ABHD6 or ABHD6 knockdown causes WAT browning as observed in the KO mice.

ABHD6 inhibition and 1-MAG cause adipose browning via PPARα and PPARγ in a cell autonomous manner

To gain insight into the mechanism by which ABHD6 inhibition causes WAT browning we first verified if 1-MAG hydrolase activity is lowered in the adipose tissue of ABHD6 deficient mice, which also contains the classical MAG lipase(Taschler et al., 2011). Total 1-MAG

hydrolase activity in extracts of visceral adipose from the KO mice was markedly decreased (~50%) (**Fig. 5a**), indicating that ABHD6 contribution to MAG hydrolysis in adipose is significant. This decrease is reflected in elevated 1-MAG species in both visceral and brown adipose tissues (**Fig. 5b,c)**. Changes in 2-MAG levels were modest (**Supplementary Fig. 11a, b**), similar to what we noticed earlier in ABHD6-KO mouse islets(Zhao et al., 2014).

We examined if the effects of ABHD6 suppression are cell-autonomous and intrinsic to adipocyte and if 1-MAG itself acts as a signal for browning. Incubation of differentiated 3T3-L1 mouse adipocytes with WWL70, 1-oleoylglycerol or 1-palmitoylglycerol increased expression of the browning marker UCP1 and PPARα (**Supplementary Fig. 12a**)**.** Similar changes were noticed with WWL70 and 1-oleoylglycerol in differentiated human primary preadipocytes (**Fig. 5d**). Addition of the PPARα antagonist GW6471 completely abrogated the WWL70 and 1-oleoylglycerol induced increases in UCP1 and PPARα expression (**Fig. 5d**), suggesting that the browning changes seen in WAT by ABHD6 suppression are mediated via 1-MAG activation of PPARα in a cell autonomous manner. Respiration was elevated in 3T3-L1 adipocytes (**Supplementary Fig. 12b-d)** and human preadipocytes (**Supplementary Fig. 13**) after incubation with WWL70 or 1-oleoylglycerol, likely because of increased uncoupled O_2 consumption due to elevated UCP1 expression (**Fig. 5e, Supplementary Fig. 12e, Supplementary Fig. 13a**). Similar to UCP1 expression, this increased O_2 consumption was curtailed by the PPARα antagonist GW6471 (**Fig. 5e, Supplementary Fig. 12b, e**).

Transactivation experiments revealed that 1-oleoylglycerol and 1-palmitoylglycerol could activate luciferase gene expression driven by PPARα, even better than the PPARα agonist WY16427, in the case of 1-OG (**Fig. 5f**). There was also significant transactivation of PPARγ, but not PPARβ, by 1-MAG (**Fig. 5f**). Finally, preadipocytes from ABHD6-KO mice expressed high levels of UCP1 and PPARα after differentiation as compared to WT mouse preadipocytes, and this increased expression in the KO adipocytes was abrogated by PPARα antagonist GW6471 (**Fig. 5g**).

We further examined the contribution of PPARγ to 1-MAG mediated browning. PPARγ antagonist T0070907 led to suppression of WWL70 or 1-OG mediated elevation in the expression of UCP1 and other browning related genes in human differentiated preadipocytes

(**Supplementary Fig. 14a-e**). Overall the data support the view that 1-MAG activation of PPARα and PPARγ mediates the adipocyte browning induced by ABHD6 suppression, in a cell autonomous manner.

Pair feeding does not prevent male ABHD6-KO mediated protection from HFD-induced obesity, glucose intolerance and insulin resistance

Since ABHD6-KO male mice on HFD exhibited slightly reduced food intake, we verified if this was the reason for the observed effects on body weight gain, glucose tolerance and insulin sensitivity. After ABHD6-KO and WT mice were pair-fed for 2 weeks, body weight gain was still lower in ABHD6-KO mice (**Supplementary Fig. 15a**). Similarly, OGTT revealed improved glucose tolerance and ITT showed better insulin sensitivity (**Supplementary Fig. 15c-e**) in the ABHD6-KO mice compared to the pair-fed WT mice.

PPARα antagonism *in vivo* counteracts beneficial metabolic effects in ABHD6-KO mice

Treatment of HFD fed ABHD6-KO male mice with the PPARα antagonist GW6471, slightly elevated their body weight gain (**Fig. 6a**), without altering cumulative food intake (**Fig. 6b**). Even though glycemia during OGTT was not changed (**Fig. 6c**), insulinemia showed a tendency to increase (**Fig. 6d**), revealing lower insulin sensitivity and this was confirmed in ITT (**Fig. 6e**). PPARα antagonism lowered oxygen consumption and VCO_2 in the ABHD6-KO mice, without change in RER (**Supplementary Fig. 16a-c)**. The elevated energy expenditure, measured at 30ºC was reduced in GW6471 treated ABHD6-KO mice compared to vehicle treated ABHD6-KO mice (**Fig. 6f**). This decreased energy expenditure was associated with curtailed expression of UCP1 (**Fig. 6g**) and other browning related genes in BAT and WAT (**Supplementary Fig. 17**), indicating that PPARα mediates adipose browning and thermogenic program at least partially in ABHD6-KO mice. Interestingly, the increased locomotor activity seen in ABHD6-KO mice, was also curtailed by PPARα antagonism (**Supplementary Fig. 16d**).

DISCUSSION

The results indicate that ABHD6-KO mice show a unique phenotype of interest for obesity and cardiometabolic disorders. When fed HFD these mice show: (1) reduced body weight gain; (2) protection from hepatic steatosis; (3) a modest lowering of food intake; (4) improved glucose tolerance; (5) increased insulin sensitivity and protection from hyperinsulinemia; (6) enhanced insulin-independent glucose uptake in adipose and muscle; (7) increased locomotor activity, females being more responsive; (8) elevated energy expenditure; (9) augmented fatty acid oxidation in BAT; (10) increased cold-induced thermogenesis; (11) browning of WAT; and (12) increased plasma FGF21, which antagonizes metabolic syndrome related defects and activates BAT and beige adipocytes(Hondares et al., 2011a; Owen et al., 2014). Interestingly, heterozygous mice deficient in ABHD6 showed an intermediate phenotype between WT and KO mice for many parameters, revealing a gene dosage effect. Also several of these effects, in particular, adipose browning and cold induced thermogenesis, were replicated *in vivo* by the ABHD6 inhibitor WWL70 and by ABHD6-ASO. Thus, the results demonstrate that ABHD6 is a new player in the control of energy homeostasis and in the regulation of BAT function and white adipose browning.

What is the mechanism whereby ABHD6 suppression exerts beneficiary metabolic effects? It is likely multifactorial. The slight reduction of food intake alone cannot quantitatively explain all metabolic improvements. Thus, food intake was similarly reduced by ~8% in male and female mice yet the phenotype in females for glucose tolerance, body weight gain, fat mass and insulin sensitivity was quantitatively more important. In addition the protective effects of ABHD6-KO are persistent even after pair-feeding, indicating the slightly lowered food intake is not primarily responsible for the observed effects in ABHD6-KO mice. The underlying causes for the modestly lowered food intake in the KO mice are not clear. Central involvement is a possibility; however, a decrease in ABHD6 activity is expected to increase endocannabinoid 2-arachidonoylglycerol that in fact enhances appetite (Di Marzo and Matias, 2005), which is not the case in the KO mice. Besides, CNS effects do not fully explain the reduced appetite and metabolic effects since ABHD6-ASO, which has no effects on brain ABHD6 levels, caused similar metabolic effects (Thomas et al., 2013). At least part of the beneficiary effects of ABHD6-KO on glycemia could be due to the enhanced insulin-

independent glucose uptake both in skeletal muscle and adipose tissues and this in turn could contribute to decreased body demand for insulin and thus to reduced hyperinsulinemia that drives obesity(Wiernsperger, 2005a, b). However, an important contributor to the beneficiary effect of ABHD6 deletion is likely enhanced BAT function and also WAT browning. Thus, energy expenditure was increased in KO mice during the light phase when the animals did not show any difference in locomotor activity. Besides, energy expenditure was elevated at 30ºC thermoneutral conditions, indicating that these effects are not because of room temperature mediated stimulation of BAT and also not due to any skin or fur defects as pointed out recently(Nedergaard and Cannon, 2014). In addition, cold induced thermogenesis was enhanced in both ABHD6-KO and ABHD6 ASO treated mice.

Little is known about the biochemical basis of WAT browning. Several transcriptional regulators including PPARs and co-activators PRDM16 and PGC1α are known to be involved in the conversion of WAT to brite adipose (Richard et al., 2010; Rosen and Spiegelman, 2014). However, whether metabolic pathways or signals play a role in this process is unknown. The results support the view that 1-MAG signaling can drive intrinsic and cell autonomous adipose browning via PPARα and PPARγ activation and that ABHD6 regulates adipose browning by controlling the signal competent 1-MAG levels. The evidence is as follows. a) Various 1-MAG species are increased in visceral adipose of ABHD6-KO mice; b) 1-MAG and WWL70 induce UCP1 and PPARα in differentiated 3T3L1 preadipocytes and human preadipocytes; c) PPARα and PPARγ antagonists abrogate UCP1 induction by 1-MAG and ABHD6 inhibition in adipocytes; d) UCP1 expression is dramatically induced during differentiation of preadipocytes from ABHD6-KO WAT and this is completely abolished by PPARα antagonism; e) 1-MAG can activate PPARα and PPARγ directly; f) PPARα and PPARγ target genes are induced in ABHD6-deficient WAT; g) 1-MAG and WWL70 increase uncoupled respiration in 3T3L1 preadipocytes and human adipocytes and this is blocked by a PPARα antagonist; h) PPARα antagonist treatment of ABHD6-KO mice prevents the browning phenomenon and associated metabolic changes; and i) treatment of mice with ABHD6-ASO or WWL70 induces WAT browning similar to ABHD6-KO.

ABHD6 and 1-MAG also appear to play a role in BAT function, which is important considering that the thermogenic contribution of classical BAT is likely predominant, even under conditions of 'WAT browning' (Shabalina et al., 2013). Thus, ABHD6-KO mice showed elevated levels of various 1-MAG species in BAT whereas 2-MAG did not rise significantly. BAT of the KO mice showed higher fat oxidation and induction of many of the BAT marker genes including PRDM16, PPARα, CD36, PGC1α and CIDEA. Also UCP1 level was markedly increased in BAT of the KO mice in association with better cold tolerance despite they were leaner. Similar to WAT browning, 1-MAG appears to activate BAT function at least in part through PPARα. This inference supported by the counteracting effect of PPARα antagonist on UCP1 induction in ABHD6-KO mice.

The phenotype of male and female ABHD6-KO mice was qualitatively similar even though it was quantitatively more marked in females. The reason for this is uncertain but estrogens are well known to be protective against metabolic syndrome and diabetes(Mauvais-Jarvis et al., 2013; Zhu et al., 2014). Also BAT in female mice is more efficient in its mitochondrial organization (Nadal-Casellas et al., 2013; Nookaew et al., 2013), which may also contribute to their increased responsiveness to ABHD6 deletion.

Mechanism underlying the elevated locomotor function seen in the ABHD6-KO mice and in mice with suppressed ABHD6 observed earlier (Thomas et al., 2013) is not clear. Since there is no associated stress or anxiety in the ABHD6-KO mice, and as the elevated locomotor activity is seen mostly during dark phase, when the rodents are more active, it can be inferred that ABHD6 suppression promotes voluntary exercise. The effects on locomotor function may also be dependent on PPAR activation, as these effects could be abrogated by PPARα antagonist. Involvement of altered centrally mediated effects cannot be ruled out.

Lipolytic products are important physiological activators of both PPARα and PPARγ (Badin et al., 2012; Haemmerle et al., 2011; Mottillo et al., 2012). Several reports indicate the role of PPARγ in WAT browning and BAT function (Ohno et al., 2012; Spiegelman, 2013). Indeed, we noticed that 1-MAG can also activate PPARγ in addition to PPARα, but not PPARβ/δ. Inasmuch as PPARγ antagonist could lower the effectiveness of WWL70 and 1-oleoylglycerol in inducing browning related gene expression in differentiated human preadipocytes, it

appears that PPARγ also plays a role in controlling ABHD6/ 1-MAG mediated adipose browning.

Collectively, our results demonstrate that ABHD6 regulates fuel homeostasis, WAT browning and BAT function. The mechanism of adipose browning appears to involve 1-monoacylglycerol acting as an intrinsic cell autonomous signal that causes PPARα and PPARγ activation in adipose tissues. ABHD6 inhibition may provide a unique approach for both lean and obese T2D. Thus, we observed before that ABHD6 inhibition in the low dose streptozotocin lean model of T2D restores normal glucose tolerance via enhanced insulin secretion(Zhao et al., 2014). Here we show in obese mice with hyperglycemia and marked glucose intolerance that ABHD6 deficiency reduces body weight gain, improves glucose homeostasis and insulin action together with mild reduction in appetite and enhanced locomotor activity. Targeting ABHD6 offers a novel avenue to develop both anti-obesity and T2D drugs.

ONLINE METHODS

Generation and maintenance of whole body ABHD6-KO mice. All procedures involving animal studies were approved by the Institutional Committee for the Protection of Animals. Generation of whole body ABHD6-KO mice (pure C57Bl6N background) was described before (Zhao et al., 2014). The mice were maintained individually caged on a standard chow diet (Teklad Global 18% protein rodent diet; Harlan Teklad, Madison, WI, 15% fat by energy) and 12-h dark/light cycle at 21°C with free access to water.

Metabolic studies on high fat diet fed mice. Male and female wild-type (WT), homozygous ABHD6-KO (KO) and heterozygous (HZ) mice at 5 weeks age were placed on chow diet or high fat diet (HFD; Bio-Ser Diet #F3282, Frenchtown, NJ, 60% fat by energy) for 8 weeks(Peyot et al., 2010). Body weight and food intake were monitored each week. At the end of feeding regimen, mice were placed in metabolic cages (CLAMS) (Comprehensive Laboratory Animal Monitoring System, Columbus Instruments, Columbus, OH) individually, for three days and oxygen consumption (VO_2), carbon dioxide production (VCO_2), respiratory exchange ratio (RER), locomotor activity and energy expenditure by indirect calorimetry were monitored. Energy expenditure was expressed as a function of metabolic mass (lean mass + 0.2 × fat mass) as suggested before (Even and Nadkarni, 2012). Results from the last 24 h (after 48 h acclimatization) were used for calculations. The mice were allowed to recover for 2 days following CLAMS studies and lean and fat mass were determined by Echo Magnetic Resonance Imaging (EchoMRI™-700; EchoMRI LLC, Houston, TX). Then oral glucose tolerance test was performed on these mice as described below.

Hyperinsulinemic euglycemic clamp (HIEC), oral glucose tolerance test (OGTT) and insulin tolerance test (ITT). Male and female WT, ABHD6-KO and HZ mice on chow diet or HFD were used for OGTT and ITT as described before (Zhao et al., 2014). HIEC was done on male mice after 10 weeks of HFD feeding (Zhao et al., 2014). During HIEC, mice were given a bolus insulin infusion (0.75U insulin/ kg body weight), followed by insulin infusion at 5 mU/ kg/ min and the glycemia was clamped at 8 mM. Glycemia measurements were made every 30 min for 2h and glucose infusion rate (GIR) was calculated as an index of insulin sensitivity during the last 30 min of the clamp. For OGTT, food was withdrawn in the morning from 7:00 to 13:00, and the mice were given 2 g glucose/ kg body weight orally and blood

collected from tail was analyzed for glucose and insulin levels at indicated time points. Intraperitoneal insulin tolerance test (IP-ITT) was performed in conscious mice in the afternoon under fed conditions. Insulin was administered intraperitoneally at a dose of 0.75U/ kg BW. Blood was collected from tail at 0, 15, 30, 45, 60 and 90 min and glycemia was monitored.

Cold-induced thermogenesis. Female ABHD6-KO and WT mice were maintained on HFD for 12 weeks. Then the mice were placed in individual cages (temperature equilibrated) in the cold room (4°C). Rectal temperature was monitored with a probe prior to cold exposure and at indicated time points during cold exposure for 3h.

Pair-feeding experiments. Male ABHD6-KO and WT mice were kept in individual cages and fed HFD for 2 weeks. In order to examine the influence of food intake on glucose homeostasis, WT mice were pair-fed with ABHD6-KO mice. Daily food intake was measured and the WT mice were given each day the same amount (average) of food consumed by ABHD6-KO mice on the previous day. Body weights were monitored each day, and after two weeks OGTT and ITT were performed and the mice sacrificed. Metabolic measurements in CLAMS could not be done as the system does not allow for pair-feeding when mice are in metabolic cages.

PPARα antagonist treatment of mice. Female ABHD6-KO and WT mice (5 wk old) were kept on HFD ad libitum, for 8 weeks and given during this period PPARα antagonist GW6471 once every two days (1mg/ kg BW; dissolved in ethanol: Tween 80: saline = 1:1:8) or vehicle, intraperitoneally. Mice were then placed in metabolic cages at 30ºC. Two days after acclimatization, respiratory exchange ratio, energy expenditure and locomotor activity were recorded at this thermoneutral condition. Then the mice were removed from metabolic cages and their lean and fat mass were measured by EchoMRI, and after acclimatization (2 days) to normal room temperature, their glucose tolerance and insulin sensitivity were assessed by OGTT and ITT, respectively. Then the mice were sacrificed and visceral, inguinal and brown fat tissues were isolated and analyzed for browning gene expression.

Behavior tests. Tests for assessing anxiety (elevated plus maze and open field) and depression (forced swimming) were conducted on both male and female ABHD6-KO and WT mice (8-10 weeks old), on normal chow diet, as described before(Sharma and Fulton, 2013). These tests

were conducted in three consecutive days on the same group of mice. First, elevated plus maze test was done followed by open field test on the second day, and forced swimming test on the third.

Treatment of high fat diet fed mice with an ABHD6 inhibitor. Male mice (6-8 wk old) were fed 45% fat diet (~45% of energy as lard; contains fatty acids: 16:0 = 23.3%, 18:0 = 15.9%, 18:1 = 34.8%, 18:2 = 18.7%), for 8 weeks. One group of mice received WWL70 at 10 mg/kg BW/day intraperitoneally and the control mice were given vehicle. At the end of the feeding period mice were sacrificed and visceral fat was removed and processed for UCP1 immunohistochemistry. Visceral fat tissue was also processed for measuring the expression of adipose browning related genes by RT-PCR, as described below.

Treatment of high fat diet fed mice with ABHD6 antisense oligonucleotide. A 20-mer phosphorothioate antisense oligonucleotide (ASO) against ABHD6 was designed to contain 2'-0-methoxyethyl groups at positions 1 to 5 and 15 to 20, and was synthesized, screened, purified and supplied by ISIS Pharmaceuticals, Inc. (Carlsbad, CA) (Thomas et al., 2013). Male mice (6-8 wk old) were fed a 45% fat diet for 8 weeks. One group of mice was simultaneously injected with murine-specific ABHD6 ASO biweekly (25 mg/kg BW) and another group of mice was given control ASO. At the end of feeding period, mice were examined for cold-induced thermogenesis by housing the mice at 4ºC for 4h, as described above. Then the mice were sacrificed, and visceral fat was removed and processed for UCP1 immunohistochemistry. Visceral fat tissue was also processed for measuring the expression of adipose browning related genes by RT-PCR, as described below.

Blood/ plasma analyses. Glycerol, non-esterified fatty acids (NEFA), triglycerides (TG) and cholesterol ester (CE) were measured using commercially available kits in plasma from chow diet or HFD-fed mice in fed state. Plasma adipokines were measured using Mouse Adipokine Antibody Array (Catalog# ARY013; R & D Systems, Minneapolis, MN).

RNA extraction and RT-PCR. Total RNA was extracted using a kit from Invitrogen and after quantification, 2 μg RNA was used for cDNA synthesis. Primers for different genes are described in Supplementary Table 2.

Glucose uptake and fatty acid oxidation. Glucose uptake was measured in visceral fat and soleus muscle and palmitate oxidation was measured in inguinal fat, visceral fat, brown fat and soleus muscle, isolated from ABHD6-KO and WT mice on HFD for 14 weeks. The isolated tissues were rinsed and weighed (~150 mg per condition) and pre-incubated at 37ºC in Krebs–Henseleit (KH) buffer, pH 7.4, containing 2 mM sodium pyruvate, 3.5% fatty acid-free BSA (w/v) in the presence or absence of 100 nM insulin for 45 min as described previously(Attane et al., 2011), for studying insulin dependent and independent glucose uptake. Following pre-incubation, 0.1 mM 2-deoxyglucose (2-DG) and 5µCi [^{3}H]-D-2-DG (PerkinElmer) were added and incubations continued for 10 min. At the end of the incubation, explants were washed with PBS, lysed in 500µl 1M NaOH at 50ºC for 30 min and neutralized by 1M 500 µl HCl. This lysate (100µl) was used to quantify 2-DG uptake by liquid scintillation counting. For palmitate oxidation, the tissues were incubated at 30°C in modified KH buffer containing 5% fatty acid-free BSA, 5 mM glucose, 1 mM palmitate, and 1 µCi/mL [1-^{14}C]-palmitate (PerkinElmer) for 1h (soleus muscle) or 2h (adipose tissue). After the incubation, complete oxidation was determined by acidifying the incubation medium with 1 ml of 1 M sulfuric acid, and measuring the released $^{14}CO_2$ (Attane et al., 2012).

PPAR transactivation assay. In a 24-well plate, 293T cells were transfected with plasmids expressing PPARα, PPARβ or PPARγ (400ng DNA/ well), PPAR response element (PPRE)-directed luciferase expression plasmid (PPRE X3-TK-luc, Addgene; 800ng DNA/ well) and Renilla luciferase internal control plasmid (25 ng DNA/ well) using lipofectamine 2000 (Life Technologies). After 24h, the transfected cells were starved overnight in DMEM without FBS. Then the cells were incubated in DMEM without FBS in the presence or absence of 10µM WWL70, 100µM 1-palmitoylglycerol (1-PG), 100µM 1-oleoylglycerol (1-OG), 50µM WY14643 (PPARα agonist), 100nM GW501516 (PPARβ agonist), or 50µM pioglitazone (PPARγ agonist) for another 24h. After washing twice with PBS, the cells were scraped, lysed and stored at -80°C for further analysis. Luciferase assay was done with 2 µl of cell lysate using a kit (Promega). PPRE-directed luciferase expression was normalized with Renilla luciferase activity (internal control) in the same sample.

Analysis of monoacylglycerol species. Analysis of different species of MAG (both 1- and 2-MAG) was done as described before (Zhao et al., 2014). Briefly, total lipids were extracted by

Folch extraction from visceral and brown fat (20 mg each), isolated from ABHD6 WT and KO mice. The extracted lipids were dried under nitrogen and dissolved in 50 μl chloroform and spotted on thin layer chromatography plates, pre-coated with 2.3% boric acid. Lipids and 1- and 2-MAGs were separated using a solvent system (chloroform: acetone: acetic acid in a ratio of 60:40:1). The plates were exposed to iodine vapor and the spots corresponding 1-MAG and 2-MAG were scraped and saponified, followed by analysis of the released FFA by HPLC.

Histology and UCP1 immunohistochemistry. Inguinal fat, visceral fat, brown fat and liver were isolated from female ABHD6-KO and WT mice on HFD. After washing twice in cold PBS, the tissues were fixed in 10% paraformaldehyde and the tissue sections were processed for hematoxylin-eosin staining for assessing tissue morphology and for UCP1 immunostaining using anti-UCP1 antibody (Abcam). The stained sections were examined using a Nikon microscope.

Monoacylglycerol hydrolysis activity. ABHD6-KO and WT mice were fed HFD for 10 weeks, and then the mice were sacrificed, and visceral fat was quickly removed and washed in cold PBS and homogenized in KRBH. Adipose tissue total MAG hydrolysis activity was measured in the homogenates as described before (Zhao et al., 2014). The assay system, in a final volume of 100 μl, contained 50 mM potassium phosphate, pH 7.2, 1 μg of tissue extract protein and 13 μM ThioGlo-1 (Covalent Associates, Corvallis, OR). Reactions were started with the addition of 5 μM 1-S-arachidonoylthioglycerol substrate after a pre-incubation of 15 min at 37°C. 1-S-arachidonoylthioglycerol hydrolysis was followed by the reaction of released thioglycerol with ThioGlo-1 to form a fluorescent adduct, which is measured continuously for 30 min at 380 nm excitation and 510 nm emission.

Effect of PPARα and PPARγ antagonists, *in vitro,* on the expression of genes related to adipose browning. Fully differentiated 3T3-L1 cells(Kohanski et al., 1986) and human primary adipocytes(Ahfeldt et al., 2012) were prepared as described before. Preadipocytes from ABHD6-KO and WT mice were prepared (Liu et al., 2010) by rapidly dissecting out the fat pads (visceral, subcutaneous or brown), washing away all the blood and then cutting the tissue into small fragments followed by collagenase (1 mg/ ml) treatment. After complete

digestion for 1 h at 37°C, the homogenate was filtered and then centrifuged at 300xg for 5 min, and the sedimented preadipocytes were suspended in an erythrocyte lysis buffer (154 mM NH_4Cl, 10 mM $KHCO_3$ and 0.1 mM EDTA, pH 7.4). After 10 min, the preadipocytes were collected by centrifugation at 300xg for 5 min. The differentiated adipocytes were treated with 10μM WWL70, 100μM 1-oleoylglycerol in the absence or presence of 1 μM PPARα antagonist GW6471 (Wang et al., 2013d) or 1 μM PPARγ antagonist T0070907 (Lee et al., 2002) for 24h, and then the cells were used for mRNA analysis of genes related to adipose browning.

Oxygen consumption rates in adipocytes. Fully differentiated mouse 3T3-L1 cells and human adipocytes derived from subcutaneous fat were treated overnight in DMEM medium with DMSO, 100 μM 1-oleoylglycerol, or 10 μM WWL70, without and with 1μM GW6471 (PPARα antagonist). Next day, the incubation medium was replaced with the specially formulated unbuffered DMEM-based medium provided (Seahorse) with 25 mM glucose with or without various inhibitors. Cells were incubated for 1h, and then the oxygen consumption rate was measured using XF analyzer (Seahorse Bioscience) following supplier's procedures.

Statistical analysis. Statistical analysis was performed using one-way ANOVA with Dunnett's post-test for multiple comparisons or two-way ANOVA with Bonferroni's post-test for multiple comparisons using GraphPad Prism. For browning gene expression results, comparisons were made by unpaired two-tailed Student's *t* test. Values are expressed as means ± SEM.

REFERENCES

1. Prentki, M. & Madiraju, S.R. Glycerolipid metabolism and signaling in health and disease. *Endocr Rev* **29**, 647-676 (2008).
2. Zechner, R.*, et al.* FAT SIGNALS--lipases and lipolysis in lipid metabolism and signaling. *Cell metabolism* **15**, 279-291 (2012).
3. Blankman, J.L., Simon, G.M. & Cravatt, B.F. A comprehensive profile of brain enzymes that hydrolyze the endocannabinoid 2-arachidonoylglycerol. *Chemistry & biology* **14**, 1347-1356 (2007).
4. Taschler, U.*, et al.* Monoglyceride lipase deficiency in mice impairs lipolysis and attenuates diet-induced insulin resistance. *The Journal of biological chemistry* **286**, 17467-17477 (2011).
5. Zhao, S.*, et al.* alpha/beta-Hydrolase domain-6-accessible monoacylglycerol controls glucose-stimulated insulin secretion. *Cell metabolism* **19**, 993-1007 (2014).
6. Thomas, G.*, et al.* The serine hydrolase ABHD6 Is a critical regulator of the metabolic syndrome. *Cell reports* **5**, 508-520 (2013).
7. Dirkx, E.*, et al.* Protein kinase-D1 overexpression prevents lipid-induced cardiac insulin resistance. *Journal of molecular and cellular cardiology* **76**, 208-217 (2014).
8. Koh, H.J.*, et al.* Tribbles 3 mediates endoplasmic reticulum stress-induced insulin resistance in skeletal muscle. *Nature communications* **4**, 1871 (2013).
9. Liew, C.W.*, et al.* The pseudokinase tribbles homolog 3 interacts with ATF4 to negatively regulate insulin exocytosis in human and mouse beta cells. *The Journal of clinical investigation* **120**, 2876-2888 (2010).
10. Liu, S.*, et al.* Disruption of protein-tyrosine phosphatase 1B expression in the pancreas affects beta-cell function. *Endocrinology* **155**, 3329-3338 (2014).
11. Sumara, G.*, et al.* Regulation of PKD by the MAPK p38delta in insulin secretion and glucose homeostasis. *Cell* **136**, 235-248 (2009).
12. Wu, J., Cohen, P. & Spiegelman, B.M. Adaptive thermogenesis in adipocytes: is beige the new brown? *Genes & development* **27**, 234-250 (2013).
13. Cereijo, R., Giralt, M. & Villarroya, F. Thermogenic brown and beige/brite adipogenesis in humans. *Annals of medicine*, 1-9 (2014).
14. Pfeifer, A. & Hoffmann, L.S. Brown, beige, and white: the new color code of fat and its pharmacological implications. *Annual review of pharmacology and toxicology* **55**, 207-227 (2015).
15. Richard, D., Carpentier, A.C., Dore, G., Ouellet, V. & Picard, F. Determinants of brown adipocyte development and thermogenesis. *Int J Obes (Lond)* **34 Suppl 2**, S59-66 (2010).

16. Rosen, E.D. & Spiegelman, B.M. What we talk about when we talk about fat. *Cell* **156**, 20-44 (2014).

17. Wu, J.*, et al.* Beige adipocytes are a distinct type of thermogenic fat cell in mouse and human. *Cell* **150**, 366-376 (2012).

18. Hondares, E.*, et al.* Peroxisome proliferator-activated receptor alpha (PPARalpha) induces PPARgamma coactivator 1alpha (PGC-1alpha) gene expression and contributes to thermogenic activation of brown fat: involvement of PRDM16. *The Journal of biological chemistry* **286**, 43112-43122 (2011).

19. Roberts, L.D.*, et al.* beta-Aminoisobutyric acid induces browning of white fat and hepatic beta-oxidation and is inversely correlated with cardiometabolic risk factors. *Cell metabolism* **19**, 96-108 (2014).

20. Badin, P.M.*, et al.* Regulation of skeletal muscle lipolysis and oxidative metabolism by the co-lipase CGI-58. *Journal of lipid research* **53**, 839-848 (2012).

21. Mottillo, E.P., Bloch, A.E., Leff, T. & Granneman, J.G. Lipolytic products activate peroxisome proliferator-activated receptor (PPAR) alpha and delta in brown adipocytes to match fatty acid oxidation with supply. *The Journal of biological chemistry* **287**, 25038-25048 (2012).

22. Haemmerle, G.*, et al.* ATGL-mediated fat catabolism regulates cardiac mitochondrial function via PPAR-alpha and PGC-1. *Nature medicine* **17**, 1076-1085 (2011).

23. Kharitonenkov, A. & Adams, A.C. Inventing new medicines: The FGF21 story. *Molecular metabolism* **3**, 221-229 (2014).

24. Owen, B.M.*, et al.* FGF21 acts centrally to induce sympathetic nerve activity, energy expenditure, and weight loss. *Cell metabolism* **20**, 670-677 (2014).

25. Xue, B., Coulter, A., Rim, J.S., Koza, R.A. & Kozak, L.P. Transcriptional synergy and the regulation of Ucp1 during brown adipocyte induction in white fat depots. *Molecular and cellular biology* **25**, 8311-8322 (2005).

26. Hondares, E.*, et al.* Thermogenic activation induces FGF21 expression and release in brown adipose tissue. *The Journal of biological chemistry* **286**, 12983-12990 (2011).

27. Di Marzo, V. & Matias, I. Endocannabinoid control of food intake and energy balance. *Nature neuroscience* **8**, 585-589 (2005).

28. Wiernsperger, N.F. Is non-insulin dependent glucose uptake a therapeutic alternative? Part 2: Do such mechanisms fulfil the required combination of power and tolerability? *Diabetes & metabolism* **31**, 521-525 (2005).

29. Wiernsperger, N.F. Is non-insulin dependent glucose uptake a therapeutic alternative? Part 1: physiology, mechanisms and role of non insulin-dependent glucose uptake in type 2 diabetes. *Diabetes & metabolism* **31**, 415-426 (2005).

30. Nedergaard, J. & Cannon, B. The browning of white adipose tissue: some burning issues. *Cell metabolism* **20**, 396-407 (2014).

31. Shabalina, I.G.*, et al.* UCP1 in brite/beige adipose tissue mitochondria is functionally thermogenic. *Cell reports* **5**, 1196-1203 (2013).

32. Mauvais-Jarvis, F., Clegg, D.J. & Hevener, A.L. The role of estrogens in control of energy balance and glucose homeostasis. *Endocr Rev* **34**, 309-338 (2013).

33. Zhu, L., Martinez, M.N., Emfinger, C.H., Palmisano, B.T. & Stafford, J.M. Estrogen signaling prevents diet-induced hepatic insulin resistance in male mice with obesity. *American journal of physiology. Endocrinology and metabolism* **306**, E1188-1197 (2014).

34. Nadal-Casellas, A., Bauza-Thorbrugge, M., Proenza, A.M., Gianotti, M. & Llado, I. Sex-dependent differences in rat brown adipose tissue mitochondrial biogenesis and insulin signaling parameters in response to an obesogenic diet. *Molecular and cellular biochemistry* **373**, 125-135 (2013).

35. Nookaew, I.*, et al.* Adipose tissue resting energy expenditure and expression of genes involved in mitochondrial function are higher in women than in men. *The Journal of clinical endocrinology and metabolism* **98**, E370-378 (2013).

36. Spiegelman, B.M. Banting Lecture 2012: Regulation of adipogenesis: toward new therapeutics for metabolic disease. *Diabetes* **62**, 1774-1782 (2013).

37. Ohno, H., Shinoda, K., Spiegelman, B.M. & Kajimura, S. PPARgamma agonists induce a white-to-brown fat conversion through stabilization of PRDM16 protein. *Cell metabolism* **15**, 395-404 (2012).

38. Peyot, M.L.*, et al.* Beta-cell failure in diet-induced obese mice stratified according to body weight gain: secretory dysfunction and altered islet lipid metabolism without steatosis or reduced beta-cell mass. *Diabetes* **59**, 2178-2187 (2010).

39. Even, P.C. & Nadkarni, N.A. Indirect calorimetry in laboratory mice and rats: principles, practical considerations, interpretation and perspectives. *American journal of physiology. Regulatory, integrative and comparative physiology* **303**, R459-476 (2012).

40. Sharma, S. & Fulton, S. Diet-induced obesity promotes depressive-like behaviour that is associated with neural adaptations in brain reward circuitry. *Int J Obes (Lond)* **37**, 382-389 (2013).

41. Attane, C.*, et al.* Apelin stimulates glucose uptake but not lipolysis in human adipose tissue ex vivo. *Journal of molecular endocrinology* **46**, 21-28 (2011).

42. Attane, C.*, et al.* Apelin treatment increases complete Fatty Acid oxidation, mitochondrial oxidative capacity, and biogenesis in muscle of insulin-resistant mice. *Diabetes* **61**, 310-320 (2012).

43. Kohanski, R.A., Frost, S.C. & Lane, M.D. Insulin-dependent phosphorylation of the insulin receptor-protein kinase and activation of glucose transport in 3T3-L1 adipocytes. *The Journal of biological chemistry* **261**, 12272-12281 (1986).

44. Ahfeldt, T.*, et al.* Programming human pluripotent stem cells into white and brown adipocytes. *Nature cell biology* **14**, 209-219 (2012).

45. Liu, Q., Gauthier, M.S., Sun, L., Ruderman, N. & Lodish, H. Activation of AMP-activated protein kinase signaling pathway by adiponectin and insulin in mouse adipocytes: requirement of acyl-CoA synthetases FATP1 and Acsl1 and association with an elevation in AMP/ATP ratio. *FASEB journal : official publication of the Federation of American Societies for Experimental Biology* **24**, 4229-4239 (2010).

46. Wang, W.*, et al.* PPARalpha agonist fenofibrate attenuates TNF-alpha-induced CD40 expression in 3T3-L1 adipocytes via the SIRT1-dependent signaling pathway. *Experimental cell research* **319**, 1523-1533 (2013).

47. Lee, G.*, et al.* T0070907, a selective ligand for peroxisome proliferator-activated receptor gamma, functions as an antagonist of biochemical and cellular activities. *The Journal of biological chemistry* **277**, 19649-19657 (2002).

Supplementary Table 1. Blood chemistry, body length and rectal temperature of male and female ABHD6-KO mice fed normal and high fat diet.

Values are means ± SEM of 11 - 12 mice per group. *P<0.05. NM, Not measured

		Male		Female	
		ND	**HFD**	**ND**	**HFD**
Glycemia (mM)	WT	7.96±0.54	12.5±0.74	7.50±0.31	8.53±0.48
	KO	7.43±0.24	10.2±0.63*	7.86±0.45	7.50±0.37*
Insulinemia (ng/ml)	WT	0.76±0.21	5.69±0.66	0.50±0.13	1.92±0.41
	KO	0.90±0.14	3.29±0.48*	0.51±0.15	1.02±0.13*
CE (mM)	WT	34.5±12.7	44.2±5.54	40.6± 10.7	38.2±8.20
	KO	39.9±7.72	42.7±4.10	35.8± 15.9	40.9±7.50
TG (mM)	WT	0.21±0.14	0.25±0.14	0.25±0.20	0.13±0.10
	KO	0.25±0.03	0.23±0.08	0.27±0.18	0.13±0.08
FFA (mM)	WT	1.22±0.42	1.27±0.26	1.44±0.52	1.18±0.33
	KO	1.32±0.34	1.29±0.33	1.46±0.28	0.99±0.40
Glycerol (mM)	WT	0.31±0.03	0.25±0.04	0.34±0.19	0.26±0.05
	KO	0.32±0.02	0.23±0.04	0.33±0.11	0.30±0.08
Body length (cm)	WT	9.10±0.14	9.00±0.18	8.90±0.20	9.10±0.14
	KO	9.00±0.24	9.10±0.21	9.20±0.24	9.00±0.16

Rectal temperature (°C)	WT	NM	NM	NM	38.7±0.55
	KO	NM	NM	NM	39.1±0.64

Supplementary Table 2. Primer sequences used for RT-PCR

Gene Name		Primer Sequence
Beta actin	Forward	CAT GGA TGA CGA TAT CGA TCG
	Reverse	GTA CGA CCA GAG GCA TAC AGG
h-ABHD6	Forward	TGT GGT CAA GTT CCT TCC AAA
	Reverse	TTG TTC AGC TTC AGG CAT TCT
mCOX8b	Forward	GAA CCA TGA AGC CAA CGA CT
	Reverse	GCG AAG TTC ACA GTG GTT CC
mCOX7a1	Forward	CAG CGT CAT GGT CAG TCT GT
	Reverse	AGA AAA CCG TGT GGC AGA GA
mPRDM16	Forward	CAG CAC GGT GAA GCC ATT C
	Reverse	GCG TGC ATC CGC TTG TG
mCD37	Forward	CGT GCA GAA CTC CTG TGA TAA C
	Reverse	GTC CAC CTA TGC TGG AGA AGG
mCidea	Forward	TGC TCT TCT GTA TCG CCC AGT
	Reverse	GCC GTG TTA AGG AAT CTG CTG
mCOX7b1	Forward	CAG CGT CAT GGT CAG TCT GT
	Reverse	AGA AAA CCG TGT GGC AGA GA

mTBX1	Forward	GGC AGG CAG ACG AAT GTT C
	Reverse	TTG TCA TCT ACG GGC ACA AAG
mTmem26	Forward	ACC CTG TCA TCC CAC AGA G
	Reverse	TGT TTG GTG GAG TCC TAA GGT C
18s	Forward	CTG AGA AAC GGC TAG CAC ATC
	Reverse	GGC CTC GAA AGA GTC CTG TAT
hTBX1	Forward	CCT CGG CAT ATT TCT CGC TAT CT
	Reverse	ACG ACA ACG GCC ACA TTA TTC
hPRDM16	Forward	CCT TCA TGG CTG CAA AGC TC
	Reverse	CAG CAG GGT AGA AAA GCA GA
hPGC1α	Forward	AAG GGA GAA TTT CGG TGC GT
	Reverse	AAG GAT GCG CTC TCG TTC AA
mAP2	Forward	CCA TCT AGG GTT ATG ATG CTC TTC
	Reverse	ACA CCG AGA TTT CCT TCA AAC TG
hUCP1	Forward	GCG GTG ATT GTT CCC AGG A
	Reverse	AGG TCC AAG GTG AAT GCC C
mPPARγ	Forward	GGT CAG CTC TTG TGA ATG GAA
	Reverse	ATC AGC TCT GTG GAC CTC TCC
mPPARα	Forward	GGC CAT ACA CAA GGT CTC CAT
	Reverse	AGA GAA TCC ACG AAG CCT ACC
mUCP1	Forward	ACT GCC ACA CCT CCA GTC ATT
	Reverse	CTT TGC CTC ACT CAG GAT TGG
mPPARβ	Forward	CGGCAGCCTCAACATG

	Reverse	AGATCCGATCGCACTTCTCATA
hPPARβ	Forward	CACATCTACAATGCCTACCT
	Reverse	CTTCTCTGCCTGCCACAATGTCT
hPPARγ	Forward	AGCCTGCATCTCCACCTTATT
	Reverse	TCCTTCACAAGCATGAACTCC
hPPARα	Forward	AGTGGAGCATTGAACATCGAA
	Reverse	GTCGCACTTGTCATACACCAG
mABHD6	Forward	ACTTGGTCTGTGTGGACATGC
	Reverse	GTGCCTATAAGGTGAAAGGGC
mPGC1α	Forward	TAG AGT GTG CTG CTC TGG TTG
	Reverse	GAT TGG TCG CTA CAC CAC TTC
mCD36	Forward	AGG TCT ATC TAC GCT GTG TTC G
	Reverse	CAA TGG TTG TCT GGA TTC TGG
mCPT1	Forward	GGT TCA AGC TGT TCA AGA TAG C
	Reverse	ACC ACA TAG AGG CAG AAG AGG

FIGURE LEGENDS

Figure 1. Improved glucose tolerance, insulin sensitivity and reduced food intake and body weight gain in ABHD6-KO mice on high fat diet. . Male and female ABHD6-KO (homozygous), heterozygous (HZ) and wild-type (WT) mice were on HFD for 8 weeks, and food intake and body weight gain were monitored. Oral glucose tolerance test (OGTT) was performed after 8 weeks, after a 6 h food withdrawal. Tail blood was collected at indicated times and analyzed for glucose and insulin by ELISA. Insulin tolerance test (ITT) and hyperinsulinemic euglycemic clamp (HIEC) were performed after 10 weeks on HFD. (**a**) Glycemia during OGTT on male WT, HZ and KO mice (n=9). Inset depicts area under the curve (AUC) for glycemia. (**b**) Insulinemia during OGTT in male mice. Inset, area under the curve. (**c**) Glycemia during ITT on male mice (n=6). Inset depicts area above the curve (AAC). (**d**) Glycemia during OGTT on female mice (n=8). Inset depicts area under the curve. * $P<0.05$ vs WT. (**e**) Corresponding plasma insulin levels for female mice. (**f**) Blood glucose levels during ITT on female mice (n=8). Inset depicts area above the curve for insulinemia. (**g**) Blood glucose levels during HIEC on male WT (n=8), HZ (n=9) and KO (n=10) mice. (**h**) Glucose infusion rate (GIR) during HIEC on male mice. (**i**) Body weight gain of male WT, HZ and KO mice (n=9). (**j**) Cumulative food intake of male mice over 7 weeks. (**k**) Body weight gain in female mice (n=9). (**l**) Cumulative food intake in female mice over 7 weeks. * $P<0.05$; ** $P<0.01$ vs WT.

Figure 2. Increased energy expenditure and locomotor activity in high fat diet-fed ABHD6-KO mice. Male and female ABHD6-KO, HZ and WT (n=10) mice were fed HFD for 6 weeks, and at the end of feeding period the mice were placed in metabolic cages at room temperature for 3 days. After acclimatization for the first two days, volume of O_2, CO_2 as well as locomotor activity measurements were made on the 3rd day and based on these parameters, respiration exchange ratio (RER) and energy expenditure (EE) were calculated. In parallel, metabolic cage measurements were also made with HFD fed male ABHD6-KO and WT mice under thermoneutral (30°C) conditions. Results shown were calculated for 24h period on the 3rd day. (**a**) Volume O_2,; (**b**) Volume CO_2 (expressed as liters/kg body weight/ h); (**c**) RER; (**d**) Energy expenditure (expressed as kcal/kg metabolic mass/h); (**e**) Locomotor activity (arbitrary

units). Metabolic mass was calculated as lean mass + 0.2 × fat mass for each mouse. * $P<0.05$ vs WT.

Figure 3. Increased expression of UCP1 and other adipose browning related genes and cold-induced thermogenesis in HFD-fed ABHD6-KO mice. Female ABHD6-KO (n=7) and WT (n=7) mice fed HFD for 10 weeks, were sacrificed, and visceral, inguinal and brown fat tissues were removed for analysis. Total RNA was extracted and the expression of various browning marker genes was assessed by RT-PCR (**a-e**). All gene expressions are normalized to 18S RNA expression. Histological (hematoxylin-eosin staining) and immunochemical (for UCP1 expression) examination was also done on the adipose tissues (**f**, **g**). Also, another batch of HFD fed ABHD6-KO and WT mice were placed in cold room (4ºC) for 3h, and rectal temperature was monitored every 30 min (**h**). Gene expressions (mRNA) in visceral, inguinal and brown adipose tissues: (**a**) UCP1 expression; (**b**) PGC1α; (**c**) PRDM16; (**d**) PPARα; (**e**) CD36. Histochemistry of visceral, inguinal and brown adipose tissues: (**f**) H-E staining; (**g**) UCP1 immunohistochemical staining. (**h**) Cold–induced thermogenesis. *$P<0.05$ vs WT.

Figure 4. Suppression of ABHD6 by WWL70 or antisense-oligonucleotide (ASO) increases cold induced thermogenesis and expression of browning related genes in white adipose tissue in HFD fed mice. Wild-type C57Bl6N mice fed high fat diet for 8 weeks were treated with WWL-70 (10 mg/kg/ day, i.p.) or vehicle (n= 9 for each group) or ABHD6-ASO (25mg/kg/ two weeks) or control ASO (n=9 for each group), during the feeding period. Cold-induced thermogenesis was assessed in ABHD6-ASO treated mice at the end of the 8 weeks period. After the feeding period, mice were sacrificed and visceral fat was removed and processed for measuring the expression of UCP1 and browning related genes normalized to 18S RNA. (**a**) UCP1 immunohistochemical staining in visceral adipose from control and WWL70 treated mice. (**b**) Browning related genes (UCP1, PRDM16, Trem26 and TBX1) expression in visceral adipose from WWL70 treated and Control mice. (**c-g**) Browning related gene expression in visceral adipose from Control-ASO and ABHD6-ASO treated mice: (**c**) ABHD6; (**d**) UCP1; (**e**) PRDM16; (**f**) PPARα; (**g**) PPARγ. (**h**) Cold induced thermogenesis in ABHD6-ASO treated vs control mice (n=10 for each group). * $P<0.05$.

Figure 5. Accumulation of 1-MAG in ABHD6-KO mouse adipose tissues and PPARα-dependence of elevated browning gene expression by 1-MAG and WWL70 in human

adipocytes or in ABHD6-KO mouse adipocytes. (**a**) MAG hydrolase activity in visceral adipose from ABHD6 WT and KO mice. Visceral adipose tissues were employed for assaying MAG hydrolysis activity using 1-S-arachidonoylglycerol, as described in Methods. * P<0.05 vs WT (n=7, each). (**b, c**) Visceral and brown adipose tissues were processed for MAG species analysis, as described in Methods. (**b**) Increased levels of long chain 1-MAG species in visceral adipose isolated from HFD fed female ABHD6-KO mice. * P<0.05 vs WT mice (n=7, each). (**c**) Increased levels of long chain 1-MAG species in brown adipose isolated from HFD fed female ABHD6-KO mice (n=7, each). * P<0.05 vs WT. (**d**) PPARα-dependence of elevated browning gene (UCP1, PGC1α, PRDM16 and PPARα) expression by 1-oleoylglycerol (1-OG) or WWL70 (W) in human adipocytes. Fully differentiated human adipocytes were incubated overnight with either DMSO vehicle, 10 μM WWL70 or 100 μM 1-OG, in the presence and absence of PPARα antagonist 1 μM GW6471 (G), and the cells were collected for mRNA analysis. Results were normalized to 18S RNA (n = 5). * P<0.05 vs control (DMSO); # P<0.05 vs GW6471. (**e**) Stimulation of uncoupled oxygen consumption rate (OCR) in differentiated human adipocytes by 1-OG and WWL70 and this increase is curtailed by PPARα antagonist GW6471 (n = 5). * P<0.05 vs DMSO control; # P<0.05 vs GW6471. For further details see Supplementary Figure 13. (**f**) Transactivation of PPARα and PPARγ by 1-MAG. PPAR transactivation assay was done in 293T cells, transfected with plasmids expressing PPARα, PPARβ or PPARγ, using dual luciferase PPRE reporter assay. WY16427, GW501516 and pioglitazone were used as positive controls for the activation of PPARα, PPARβ and PPARγ, respectively (n = 6). * P<0.05, ** P<0.01, ** P<0.001 vs DMSO. (**g**) PPARα antagonist GW6471 suppresses the expression of browning related genes UCP1, PGC1α, PRDM16 and PPARα in adipocytes differentiated *ex vivo* from pre-adipocytes isolated from ABHD6-KO and WT mice (n = 5). * P<0.05; *** P<0.001 vs WT-DMSO; # P<0.05 vs KO-DMSO.

Figure 6. Reversal of ABHD6-KO mediated effects on obesity, glucose tolerance, insulin sensitivity, energy expenditure and adipose tissue UCP1 expression by PPARα antagonist. Female ABHD6-KO and WT mice were fed HFD for 8 weeks without or with PPARα antagonist GW6471 treatment (1mg/ kg BW; once every two days, i.p.). Daily body weight gain and food intake were monitored and at the end of feeding period energy

expenditure, lean and fat mass were assessed and OGTT and ITT were performed. Then the mice were sacrificed and adipose tissues were isolated for measuring browning related gene expression. (**a**) Body weight; (**b**) Food intake; (**c**) Glycemia during OGTT. Inset depicts area under the curve (AUC); (**d**) Insulinemia during OGTT. Inset depicts AUC; (**e**) ITT. Glycemia with time is shown as percentage of basal 0 min value; (**f**) Energy expenditure under thermoneutrality (30ºC) conditions (expressed as kcal/kg metabolic mass), during light and dark phases and complete 24h; (**g**) UCP1 expression in visceral, inguinal and brown adipose tissues. (n=6, each group). * P<0.05, ** P<0.01, *** P<0.001 vs WT-Vehicle; # P<0.05 vs KO-Vehicle.

Supplementary Figure 1. Characterization of ABHD6-KO mice on chow diet. Male and female ABHD6-KO, HZ and WT mice were fed chow diet over 24 weeks and food intake and body weight gain were measured each week. OGTT was performed on 6-week old mice following a 6h food withdrawal and ITT was performed on 12-week old mice. (**a**) Glycemia of male mice during OGTT. Inset depicts area under the curve for glycemia. (**b**) Corresponding plasma insulin levels of male mice during OGTT. Inset depicts area under the curve for insulinemia. * P<0.05 vs WT. (**c**) Glycemia during ITT on male mice. Inset depicts area above the curve (AAC). (**d**) Glycemia during OGTT on female mice. Inset depicts area under the curve for glycemia. * P<0.05 vs WT. (**e**) Corresponding plasma levels for female mice. * P<0.05 vs WT. (**f**) Blood glucose levels during ITT on female mice. Inset depicts area above the curve (AAC) for insulinemia. * P<0.05 vs WT. (**g**) Body weight gain of male mice over 24 weeks. (**h**) Cumulative weekly food intake of male mice over 16 weeks. (**i**) Body weight gain of female mice. (**j**) Cumulative weekly food intake of female mice. * P<0.05 vs WT. For all the studies on male and female mice, each group has 6-9 mice.

Supplementary Figure 2. Increased glucose uptake in soleus muscle and visceral fat from HFD fed ABHD6-KO mice. ABHD6-KO and WT mice were fed HFD for 12 weeks. Then the mice were sacrificed, and soleus muscle and visceral fat were removed, and used for measuring glucose uptake with [^{3}H]-2-deoxy-glucose (2DG), in the absence or presence of insulin (100 nM), as detailed in Methods. (**a**) Glucose uptake in visceral fat of male mice. (**b**) Glucose uptake in soleus muscle of male mice. (**c**) Glucose uptake in visceral fat of female mice. (**d**) Glucose uptake in soleus muscle of female mice. * P<0.05 vs WT.

Supplementary Figure 3. Body composition, tissues weights and liver histology of HFD-fed ABHD6-KO mice. After 10 weeks of HFD, body composition of male and female ABHD6-KO, HZ and WT mice was analyzed by Echo-MRI, and then the mice were sacrificed and fat and liver tissues were removed for further analysis. (**a**) Lean mass of male mice. (**b**) Fat mass of male mice. (**c**) Liver weight of male mice. (**d**) Visceral fat weight of male mice. (**e**) Lean mass of female mice. (**f**) Fat mass of female mice. (**g**) Liver weight of female mice. (**h**) Visceral fat weight of female mice. (**i**) H-E staining of female liver. Black arrows indicate lipid droplets. (**j**) Appearance of female ABHD6-KO and WT mice. * P<0.05 vs WT (n= 7-10 mice).

Supplementary Figure 4. Plasma adipokine profile in HFD-fed female ABHD6-KO and WT mice. Female ABHD6-KO and WT mice (n=8, each) were fed HFD and sacrificed. Blood was collected by heart puncture and plasma was used for analysis. Plasma adipokines were measured using Mouse Adipokine Antibody Array and adipokine levels were expressed as relative expression compared to the control provided by the supplier. (**a**) Adipokines with significant changes. (**b**) Adipokine levels with no significant difference. * P<0.05, ** P<0.01 vs WT (n= 6 mice).

Supplementary Figure 5. Increased energy expenditure and locomotor activity in HFD-fed ABHD6-KO and WT mice during dark and light phases. Male and female ABHD6-KO, HZ and WT mice (n=10, each) were fed HFD for 6 weeks, and at the end of the feeding period mice were placed in metabolic cages at room temperature (RT) for 3 days. After acclimatization for the first two days, volume of O_2, CO_2 as well as locomotor activity measurements were made on the 3rd day and based on these parameters, respiration exchange ratio (RER) and energy expenditure (EE) were calculated. In parallel, metabolic cage measurements were also made with HFD fed male ABHD6-KO and WT mice under thermoneutral (30°C) conditions. Results shown were calculated for light and dark phases separately, during the 3rd day. (**a**) Volume O_2 and (**b**) Volume CO_2 (expressed as liters /kg body weight/ h); (**c**) RER; (**d**) Energy expenditure (expressed as kcal/ kg metabolic mass/h); (**e**) Locomotor activity (arbitrary units). Metabolic mass was calculated as lean mass + 0.2 × fat mass for each mouse. * P<0.05 vs WT.

Supplementary Figure 6. Lack of difference between ABHD6-KO and WT mice in their response to anxiety and depression tests. Male and female ABHD6-KO and WT mice (8-10 wk old) on normal chow diet were subjected to anxiety (elevated plus maze and open field) and depression (forced swimming) tests, as described in Methods. (**a**) Elevated plus maze. (**b**) Open field. (**c**) Forced swimming.

Supplementary Figure 7. Expression of different adipose browning related genes in visceral, inguinal and brown adipose tissues from HFD-fed ABHD6-KO mice. Female ABHD6-KO and WT mice (n=7, each) fed HFD for 10 weeks were sacrificed, and visceral, inguinal and brown fat tissues were removed and total RNA was extracted and the expression of various browning related genes was assessed by real-time PCR. All gene expressions in visceral, inguinal and brown adipose tissues are normalized to 18S mRNA. (**a**) TBX1. (**b**) CD37. (**c**) TREM26. (**d**) Cox8b. (**e**) Cox7a1. (**f**) PPARβ. (**g**) PPARγ. (**h**) CPT1. (**i**) CIDEA. * $P<0.05$ vs WT.

Supplementary Figure 8. Increased expression of UCP1 and other adipose browning related genes in HFD-fed male ABHD6-KO mice under thermoneutrality conditions. ABHD6-KO and WT mice (5 weeks age) were fed HFD for 8 weeks, and then the mice were placed under thermoneutrality conditions (30ºC) for 3 days, and sacrificed. Visceral, inguinal and brown fat were isolated and expression of various adipose browning related genes was measured by RT-PCR. All gene expressions are normalized to 18S mRNA. (**a**) UCP1. (**b**) PGC1α. (**c**) PRDM16. (**d**) PPARα. (**e**) PPARγ. (**f**) AP2. * $P<0.05$ vs WT.

Supplementary Figure 9. Increased fatty acid oxidation in brown fat of HFD fed ABHD6-KO female mice. ABHD6-KO and WT mice were fed HFD for 12 weeks. Then the mice were sacrificed, and soleus muscle and visceral fat were removed, and used for measuring fatty acid oxidation using [1-^{14}C]-palmitate. Incubations were at 30ºC in modified Krebs-Henseleit buffer containing 5% fatty acid-free BSA, 5 mM glucose, 1 mM [1-^{14}C]-palmitate for 1h (soleus muscle) or 2h (adipose tissues). After the incubation, complete oxidation was determined by acidifying the incubation medium and measuring the released $^{14}CO_2$. Palmitate oxidation is expressed as nmol/ mg tissue. (**a**) Inguinal fat. (**b**) Visceral fat. (**c**) Brown fat. (**d**) Soleus muscle. * $P<0.05$ vs WT.

Supplementary Figure 10. Expression of additional browning related genes in visceral adipose from HFD-fed mice treated with WWL70 or ABHD6 ASO. Treatment of mice with WWL70 or ABHD6 ASO was as described under Figure 4. Additional browning related gene expression was examined by RT-PCR in visceral adipose and the results were normalized to 18S RNA. (**a**) Expression of UCP2, Cidea, Cox7a1, PPARα and PPARγ in vehicle and WWL70 treated mice. (**b**) Expression of Cidea, Cox7a1, UCP2, ELOVL3, TBX1 and TREM26 in control ASO and ABHD6 ASO treated mice. * P<0.05 vs WT.

Supplementary Figure 11. 2-MAG species levels in visceral and brown adipose tissues isolated from HFD-fed female ABHD6-KO and WT mice. Visceral and brown adipose tissues were processed for MAG species quantification as in Figure 5**b, c**. Levels of different species of 2-MAG are expressed per total tissue weight. (**a**) 2-MAG profile in visceral adipose. (**b**) 2-MAG profile in brown adipose.

Supplementary Figure 12. WWL70 and 1-MAG induce browning related gene expression and increase oxygen consumption rate in mouse 3T3-L1 adipocytes in a PPARα dependent manner. (**a**) Browning related gene expression in 3T3-L1 cells. Fully differentiated 3T3-L1 cells were incubated in the presence of 10 μM WWL70, 100 μM 1-oleoylglycerol (1-OG), 100 μM 1-palmitoylglycerol (1-PG) or DMSO (control) for 24h and then the cells were processed for gene expression analysis by RT-PCR. The results are normalized to 18S RNA. n= 3 experiments with triplicate observations in each group. * P<0.05 vs DMSO. (**b**) Oxygen consumption rate (OCR) in fully differentiated 3T3-L1 cells incubated for 24h with 10 μM WWL70 or 100 μM 1-OG in the absence or presence of 1 μM PPARα antagonist GW6471. OCR in these cells was monitored with different mitochondrial inhibitors (n=4 experiments with quadruplicate observations in each group). From these traces (**c**) basal, (**d**) maximal and (**e**) uncoupled oxygen consumption were calculated.

Supplementary Figure 13. WWL70 and 1-oleoylglycerol increase oxygen consumption rate in human differentiated adipocytes in a PPARα dependent manner. (**a**) Original traces (in a representative experiment) of oxygen consumption rate (OCR) in differentiated human adipocytes, incubated overnight with 10 μM WWL70 or 100 μM 1-oleoylglycerol (1-

OG) in the absence or presence of 1 μM PPARα antagonist GW6471. (**b**) Basal respiration. (**c**) Maximal respiration. n= 3 experiments with quadruplicate observations in each group).

Supplementary Figure 14. WWL70 and 1-oleoylglycerol induced browning-related gene expression in differentiated human adipocytes is inhibited by a PPARγ antagonist. Fully differentiated human adipocytes, were treated overnight with 10 μM WWL70 or 100 μM 1-oleoyglycerol (1-OG) in the absence or presence of 1 μM PPARγ antagonist T0070907. Then the adipocytes were harvested and mRNA expression of browning-related genes was assessed by RT-PCR. Gene expressions were normalized to 18S RNA. (**a**) UCP1; (**b**) PGC1α; (**c**) PRDM16; (**d**) PPARα and (**e**) PPARγ. (n=5). * P<0.05 vs control; # P<0.05 vs corresponding WWL70 or 1-OG without T0070907 treatment.

Supplementary Figure 15. Pair-fed ABHD6-KO mice on HFD also show reduced body weight, improved glucose tolerance and insulin sensitivity. Male ABHD6-KO and WT mice (6-week old) were pair-fed HFD every day. Daily body weight gain was monitored and OGTT and ITT were performed at the end of the feeding period. (**a**) Body weight. (**b**) Daily food intake. (**c**) Glycemia during OGTT. Inset depicts AUC. (**d**) Insulinemia during OGTT. Inset depicts AUC. (**e**) ITT. Results of ITT were calculated as percentage of basal (0 min) glycemia. * P<0.05 vs WT.

Supplementary Figure 16. Reversal of ABHD6-KO mediated effects on metabolic parameters and locomotor activity by a PPARα antagonist. Female ABHD6-KO and WT mice were fed HFD and treated with PPARα antagonist GW6471 for 8 weeks, as described in Figure 6. After the feeding period, the mice were placed in metabolic cages under thermoneutrality (30ºC) condition for 3 consecutive days. After two days of acclimatization, on the third day VO_2, VCO_2 and locomotor activity were monitored, and RER was calculated for light and dark phases and for the complete 24 h period. (**a**) VO_2. (**b**) VCO_2. (**c**) RER. (**d**) Locomotor activity. (n=6, each group) * P<0.05 vs WT-vehicle; # P<0.05 vs KO-vehicle.

Supplementary Figure 17. Reversal of ABHD6-KO mediated effects on adipose tissue browning related gene expression by PPARα antagonist. Female ABHD6-KO and WT mice were fed HFD and treated with the PPARα antagonist GW6471 for 8 weeks, as described

under Figure 6. After the feeding period the mice were sacrificed and visceral, inguinal and brown adipose tissues were isolated to measure the expression of browning related genes. Liver and sloeus muscle were also isolated and palmitate oxidation was measured in liver, brown adipose, visceral adipose and muscle. Gene expressions are normalized to 18S RNA. (**a**) PGC1α. (**b**) PRDM16. (**c**) PPARα. (**d**) Palmitate oxidation in visceral adipose, brown adipose, liver, and muscle. (n=6, each group) * $P<0.05$ vs WT-vehicle; # $P<0.05$ vs KO-vehicle.

ACKNOWLEDGMENTS

This study was supported by funds from Canadian Institutes of Health Research grants to MP and SRMM and by a start-up package to JMB. M.P. holds the Canada Research Chair in Diabetes and Metabolism. SZ is supported by a fellowship from Montreal Diabetes Research Center and Université de Montreal. YM is supported by a fellowship from Fond de recherche Santé Québec (FRSQ).

COMPETING FINANCIAL INTEREST

The authors do not declare any competing financial interests.

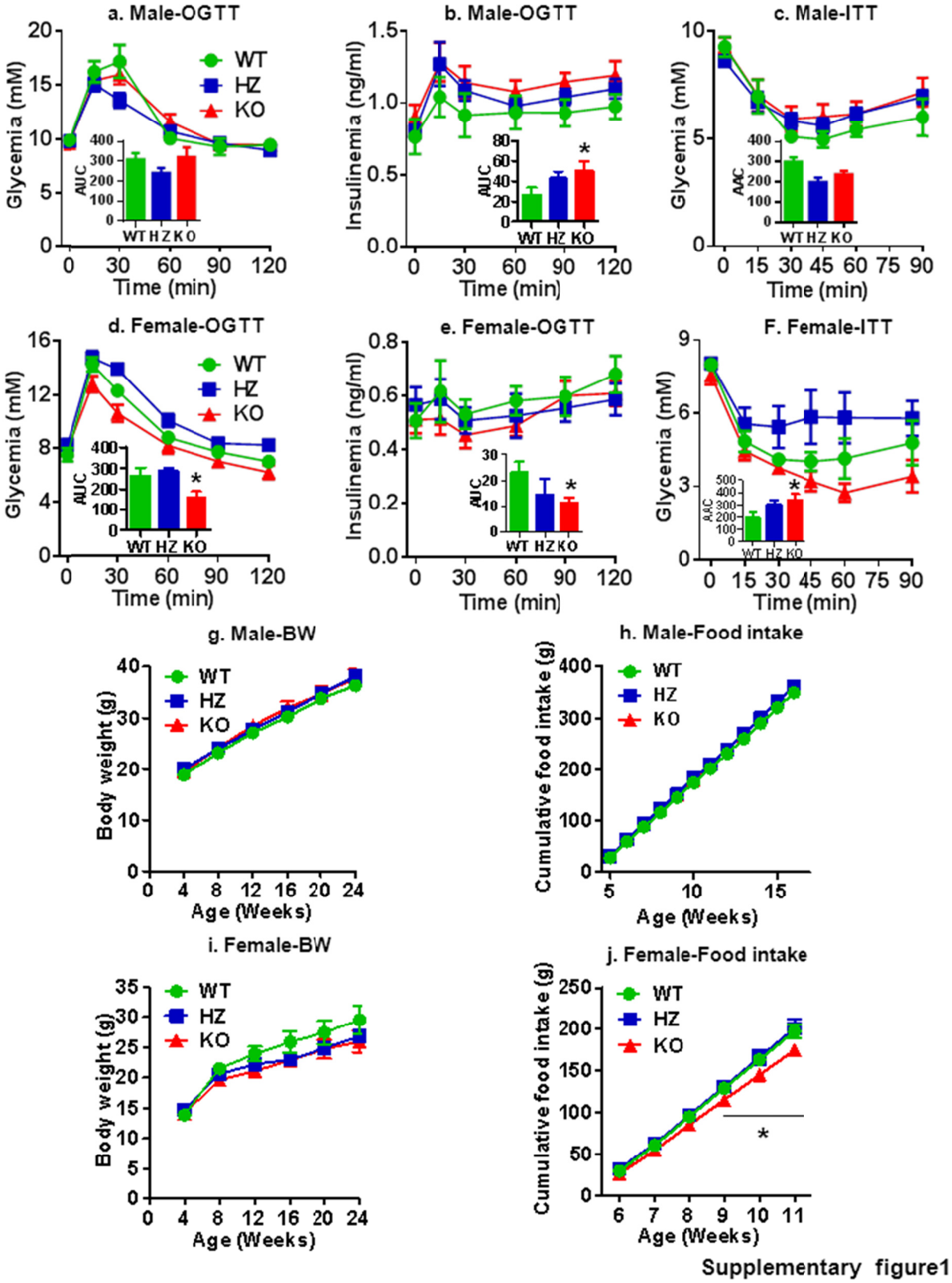

Supplementary figure1

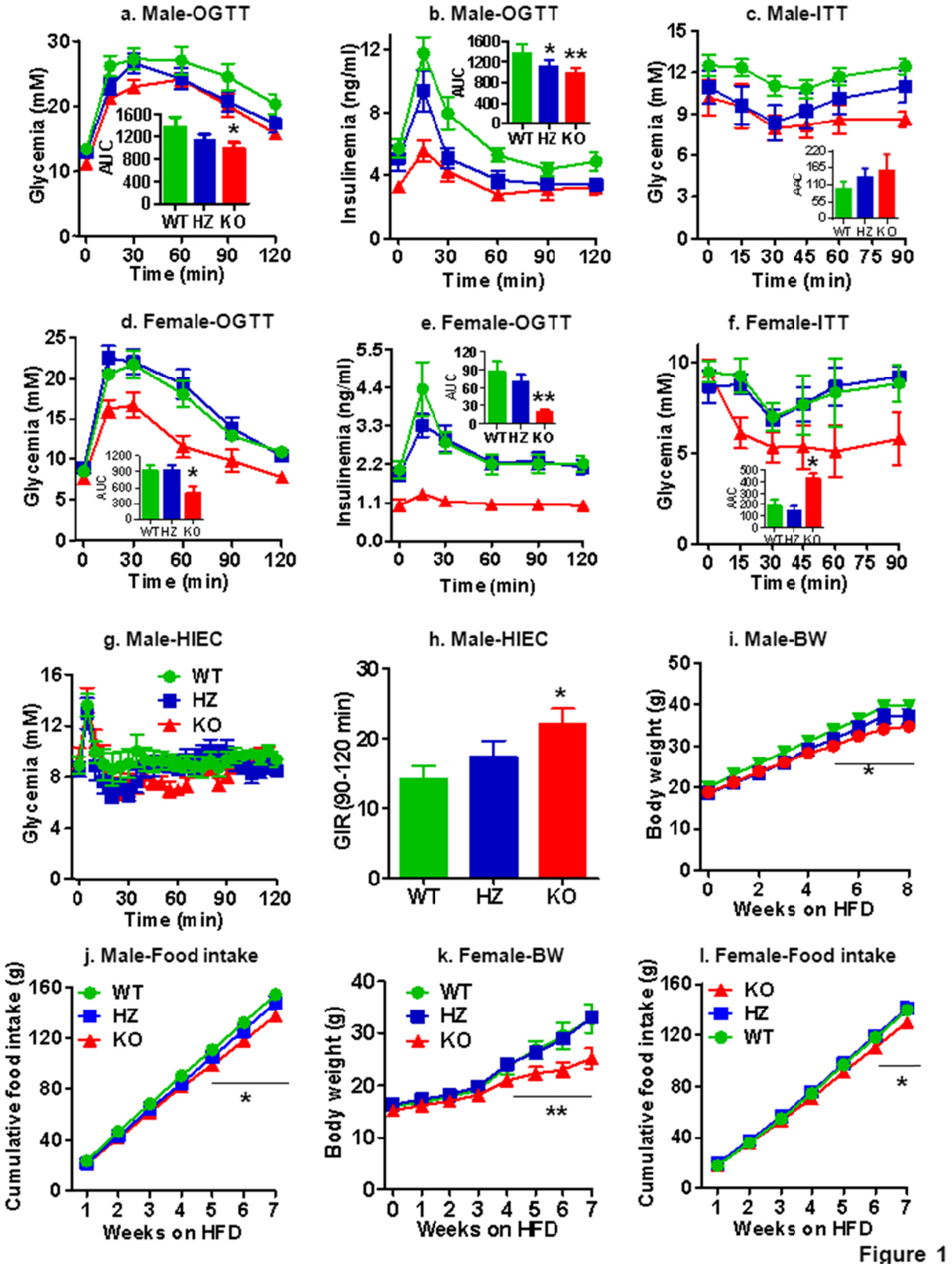
a. Male-OGTT
Glycemia (mM)
Time (min)
AUC
WT HZ KO
b. Male-OGTT
Insulinemia (ng/ml)
Time (min)
c. Male-ITT
Glycemia (mM)
Time (min)
d. Female-OGTT
Glycemia (mM)
Time (min)
e. Female-OGTT
Insulinemia (ng/ml)
Time (min)
f. Female-ITT
Glycemia (mM)
Time (min)
g. Male-HIEC
WT
HZ
KO
Glycemia (mM)
Time (min)
h. Male-HIEC
GIR(90-120 min)
i. Male-BW
Body weight (g)
Weeks on HFD
j. Male-Food intake
Cumulative food intake (g)
Weeks on HFD
k. Female-BW
Body weight (g)
Weeks on HFD
l. Female-Food intake
Cumulative food intake (g)
Weeks on HFD

Figure 1

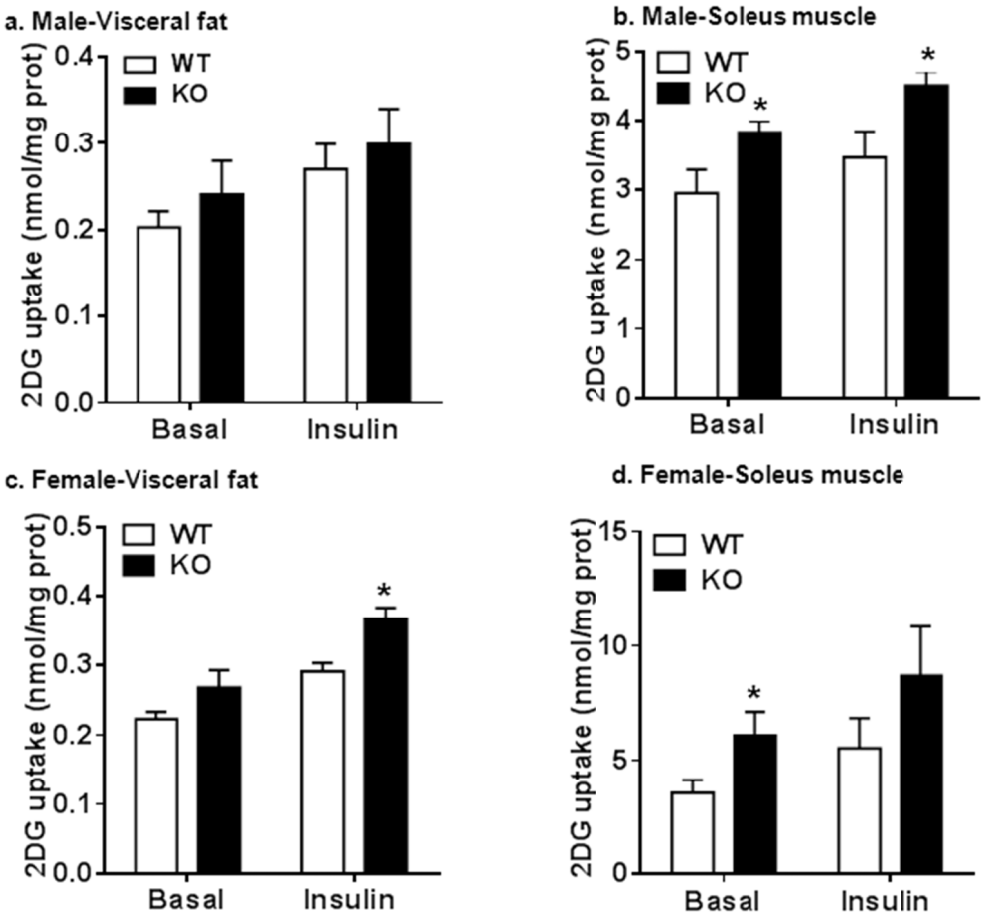

Supplementary figure 2

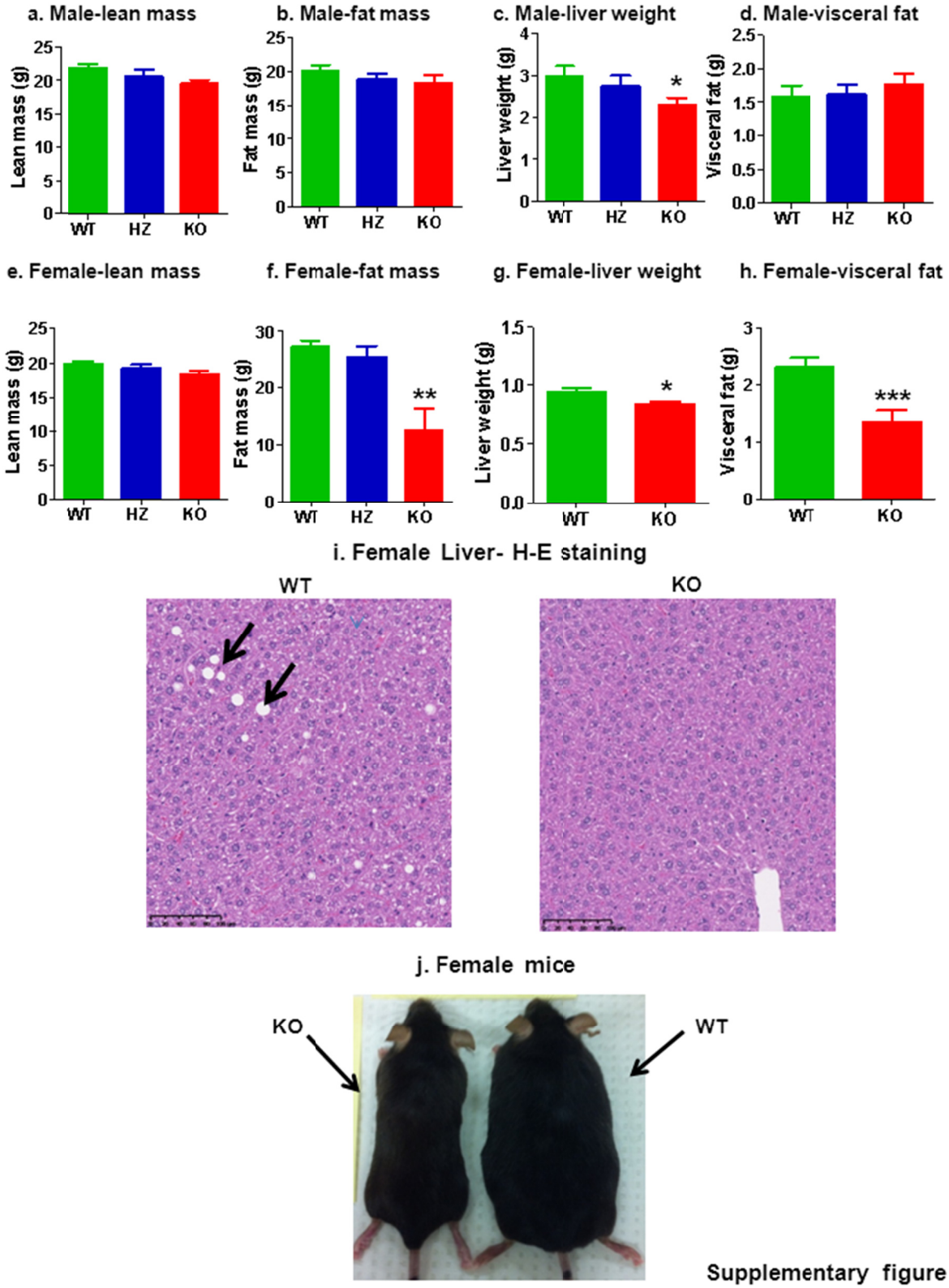

Supplementary figure 3

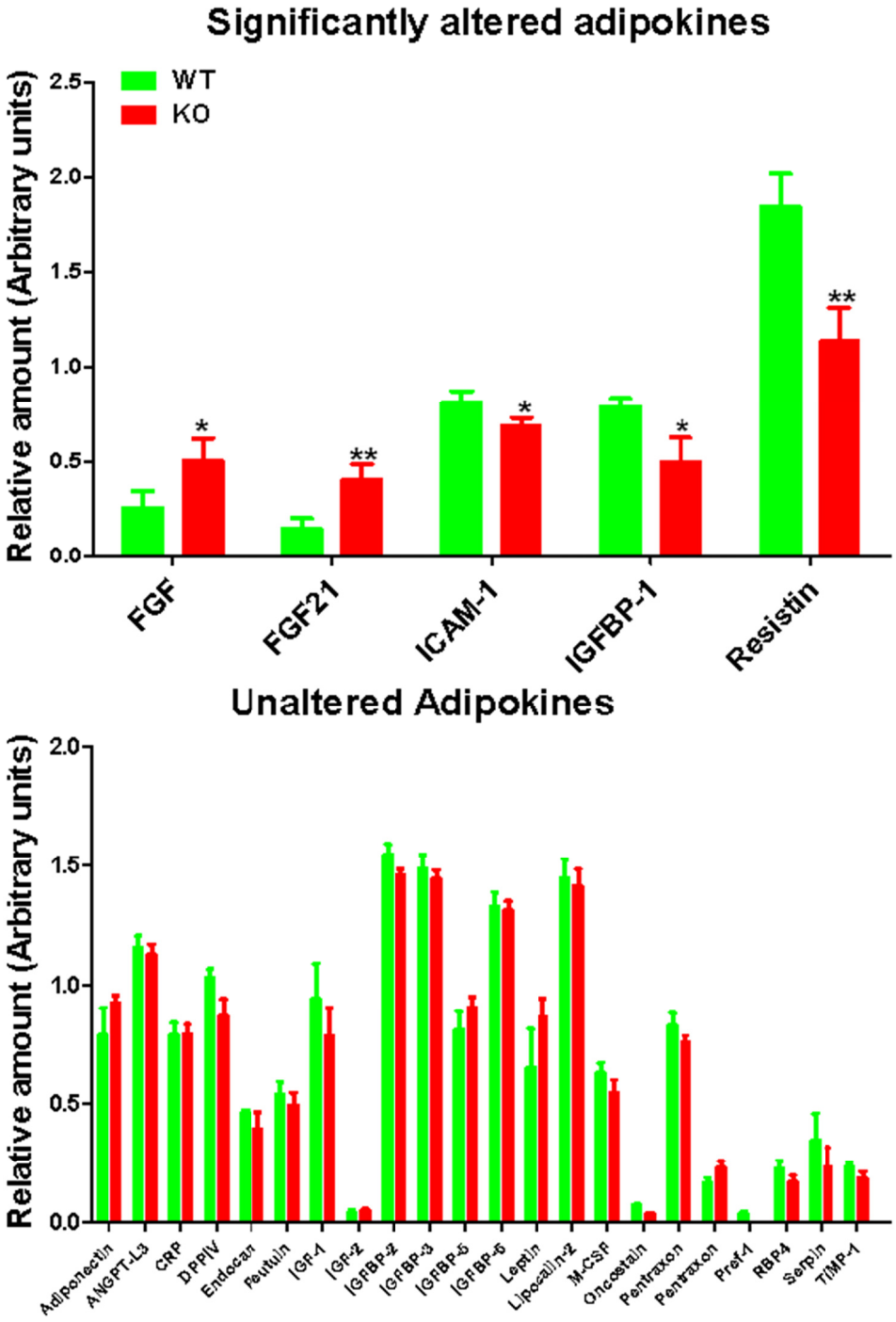

Supplementary figure 4

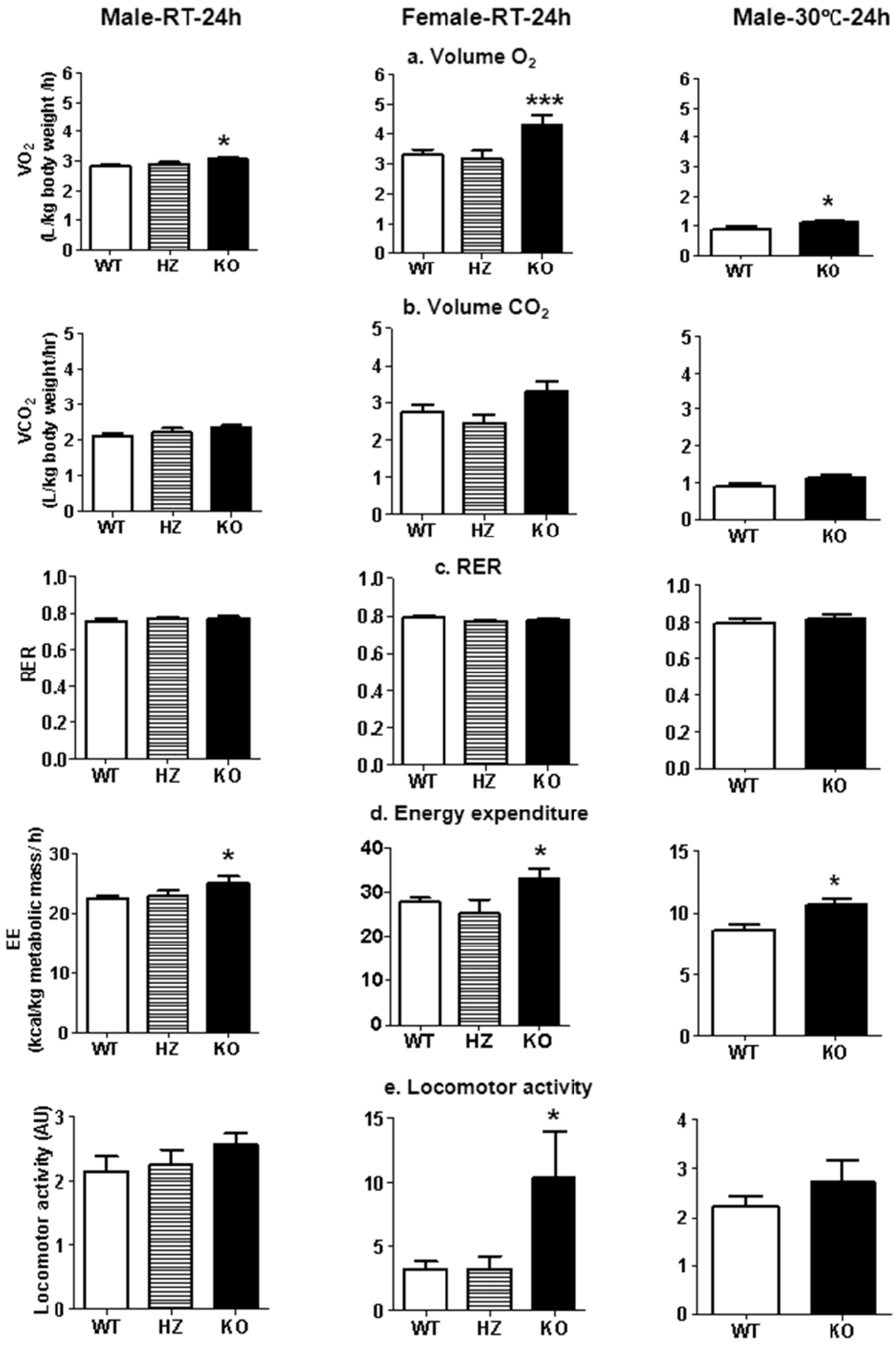
Male-RT-24h
Female-RT-24h
Male-30℃-24h
a. Volume O_2
VO_2 (L/kg body weight /h)
b. Volume CO_2
VCO_2 (L/kg body weight/hr)
c. RER
RER
d. Energy expenditure
EE (kcal/kg metabolic mass/ h)
e. Locomotor activity
Locomotor activity (AU)
WT
HZ
KO
*
***

Figure 2

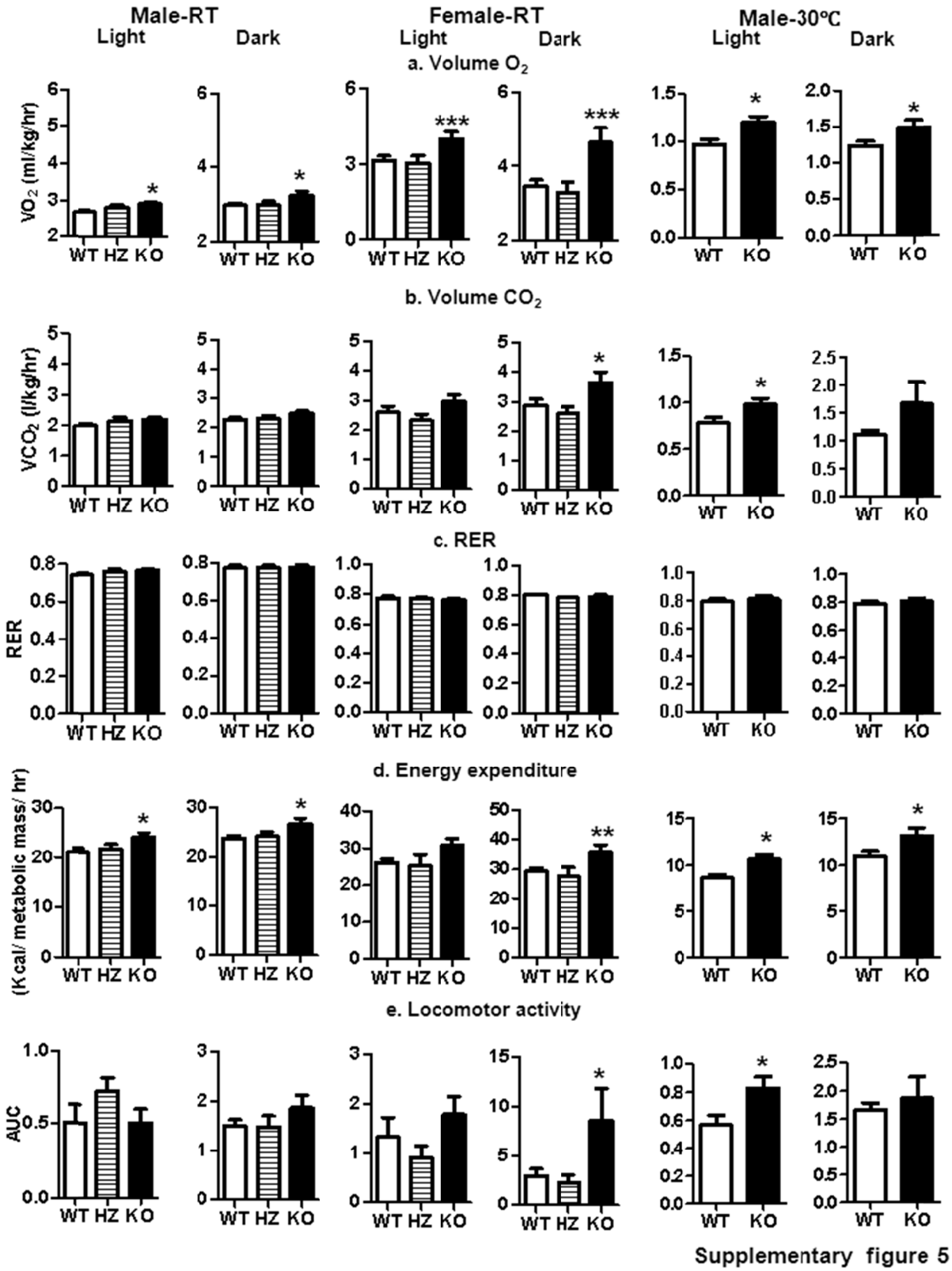

Supplementary figure 5

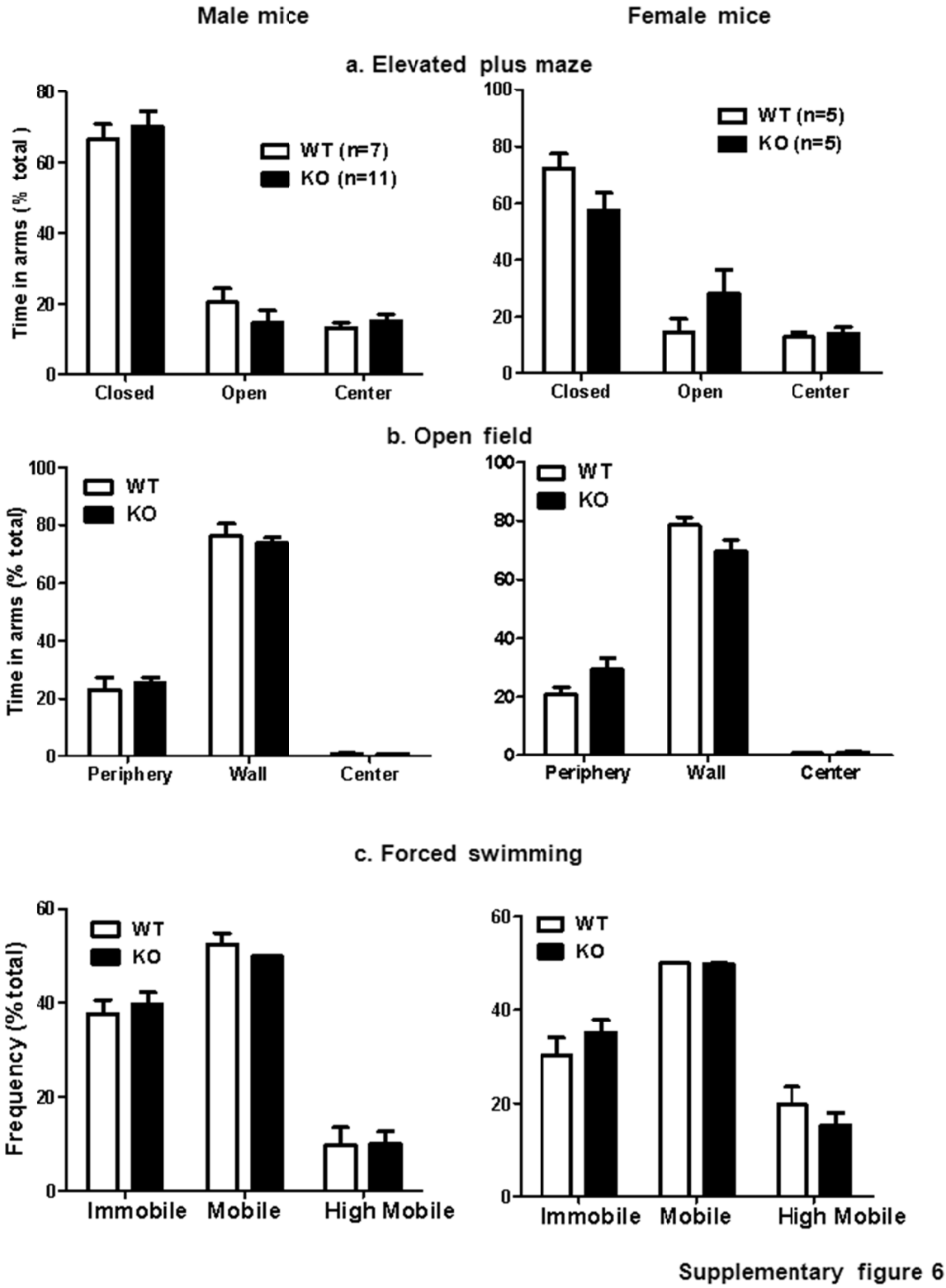

Supplementary figure 6

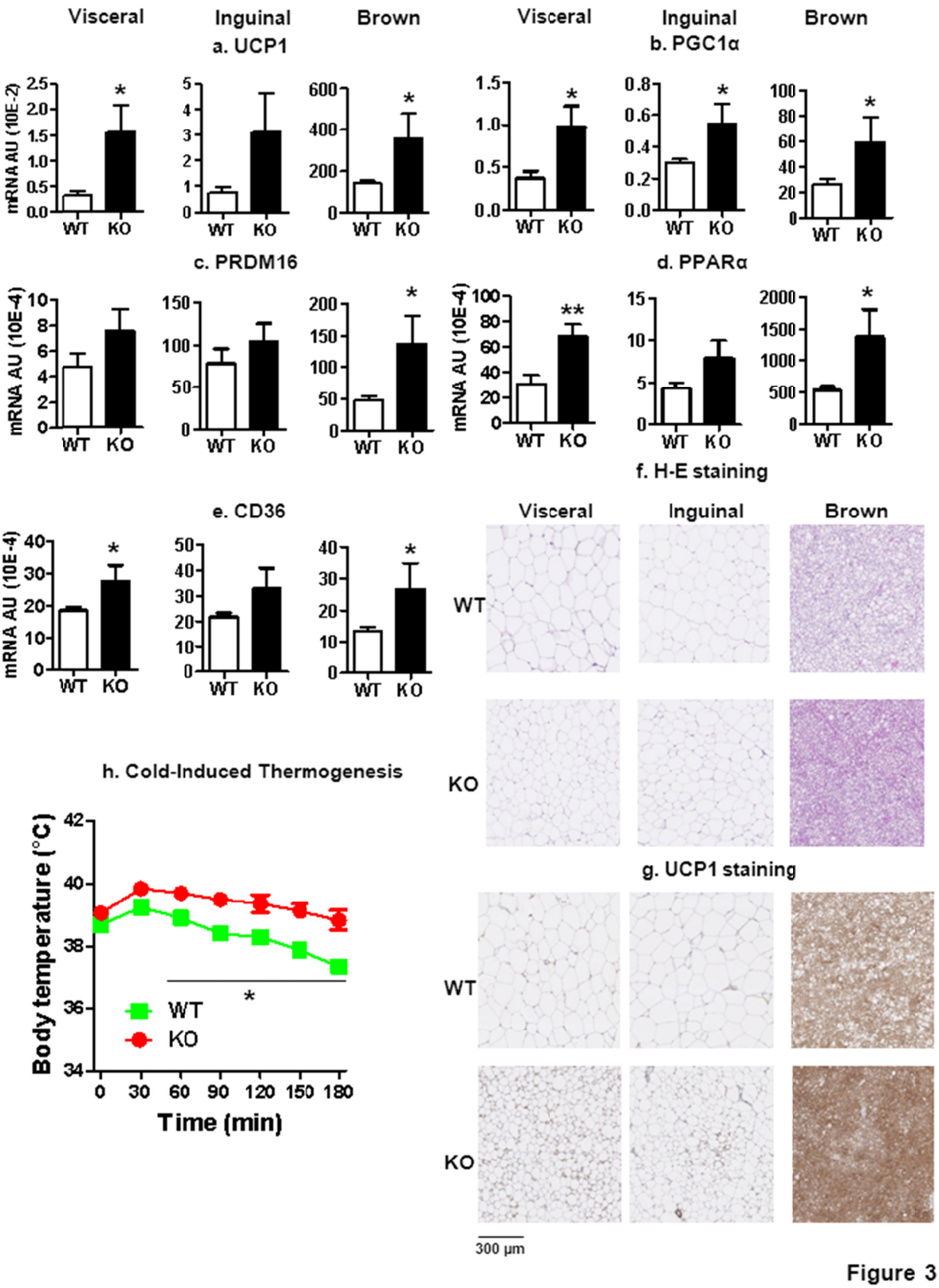
Visceral
Inguinal
Brown
a. UCP1
b. PGC1α
c. PRDM16
d. PPARα
e. CD36
f. H-E staining
g. UCP1 staining
h. Cold-Induced Thermogenesis
mRNA AU (10E-2)
mRNA AU (10E-4)
WT
KO
Body temperature (°C)
Time (min)
0 30 60 90 120 150 180
34 36 38 40 42
300 µm

Figure 3

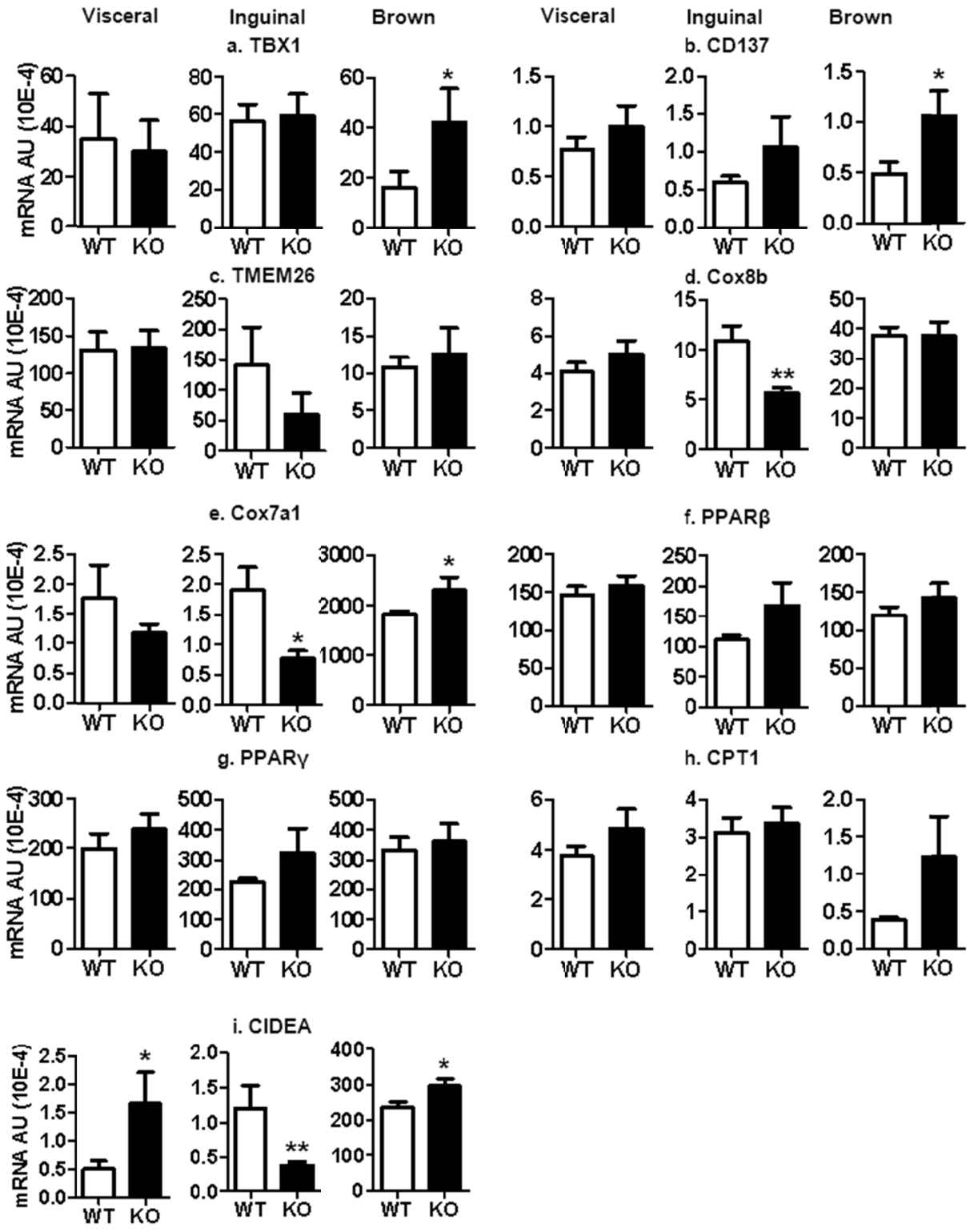

Supplementary figure 7

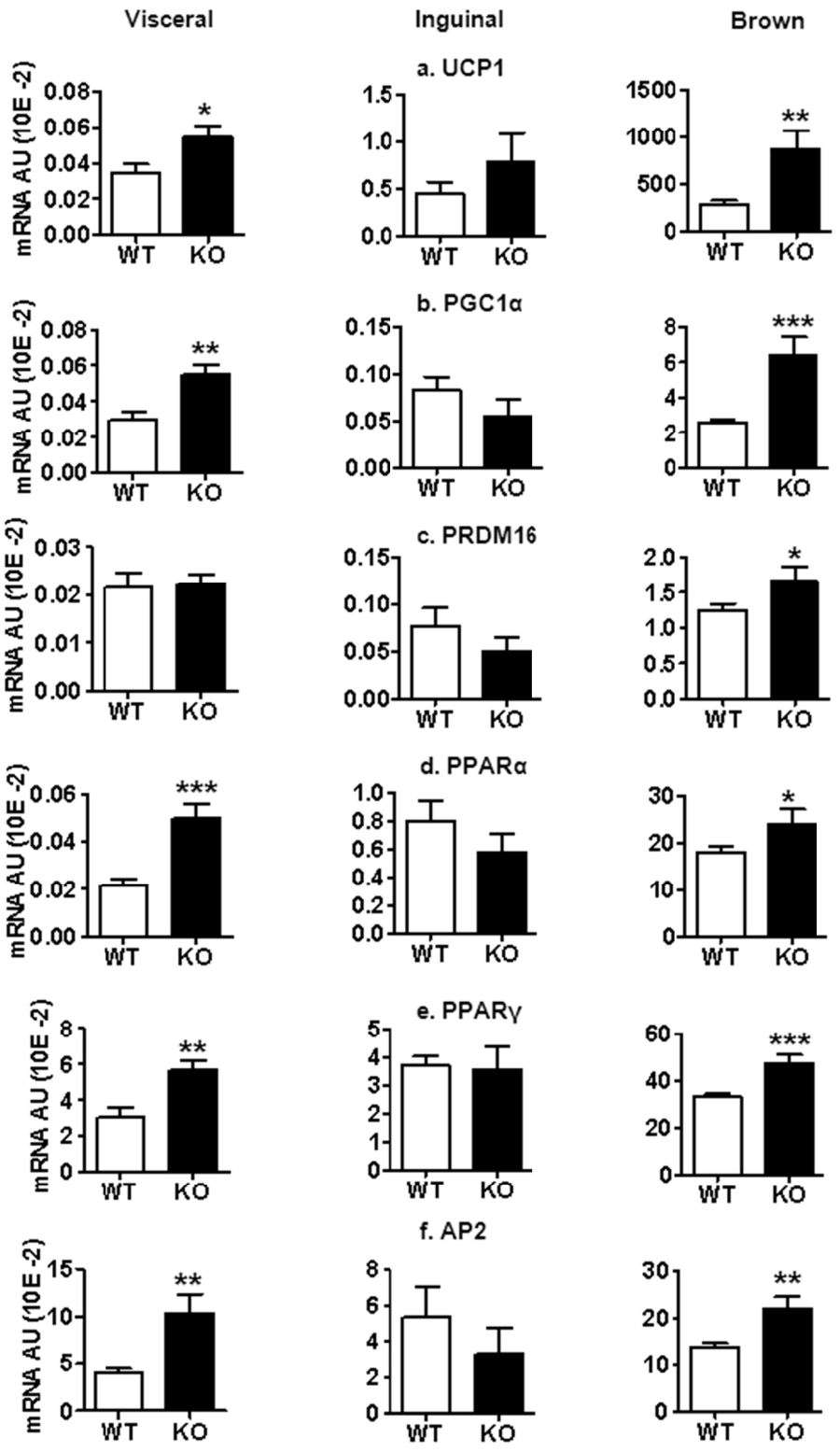

Supplementary figure 8

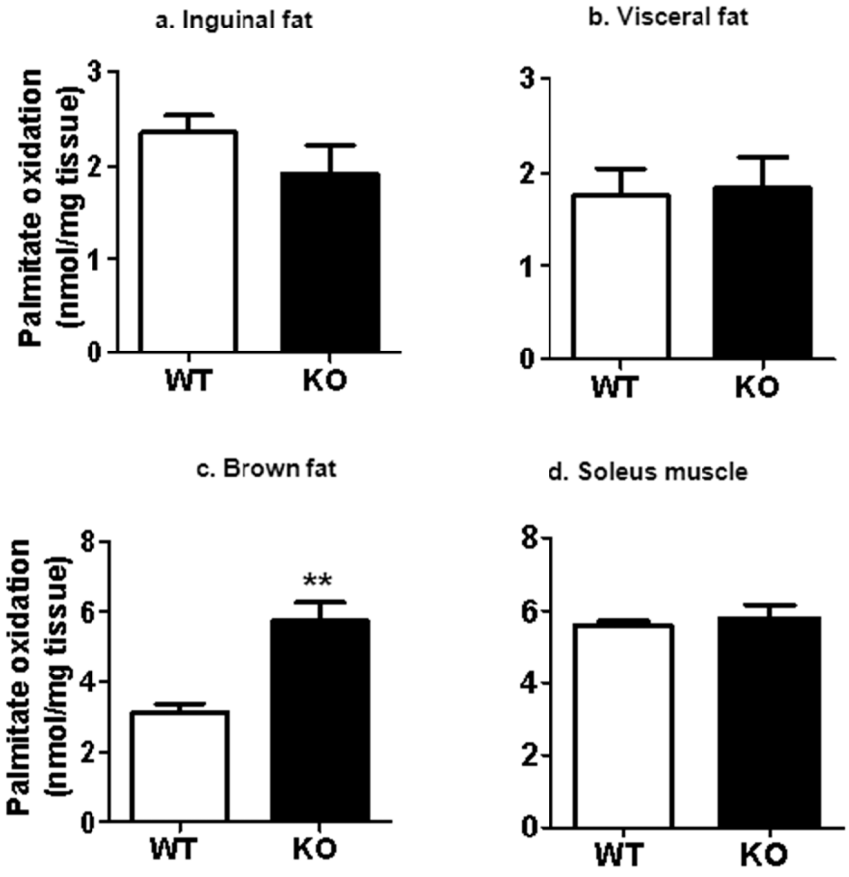

Supplementary figure 9

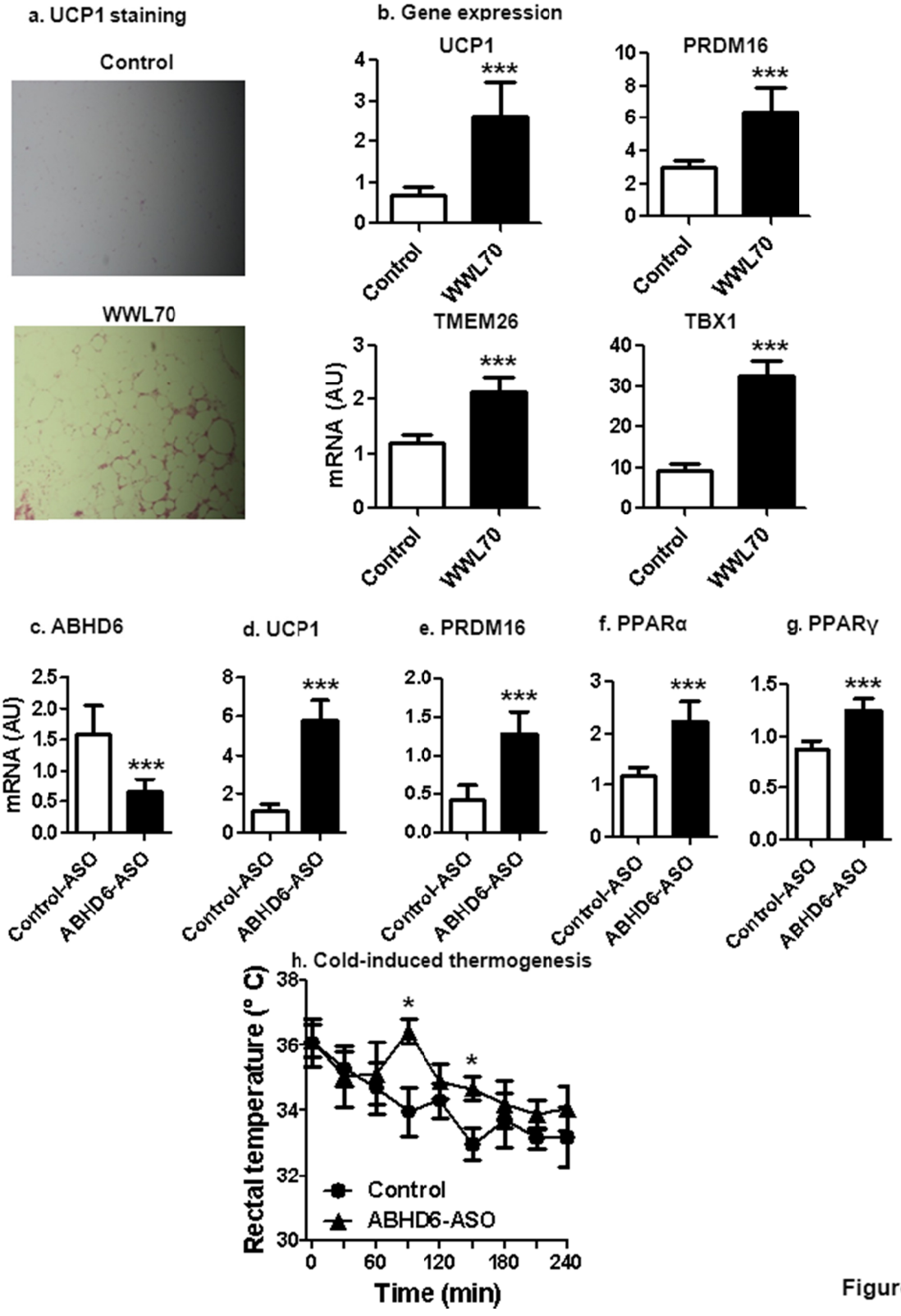
a. UCP1 staining
Control
WWL70
b. Gene expression
UCP1
PRDM16
TMEM26
TBX1
mRNA (AU)
***
Control
WWL70
c. ABHD6
d. UCP1
e. PRDM16
f. PPARα
g. PPARγ
Control-ASO
ABHD6-ASO
h. Cold-induced thermogenesis
Rectal temperature (° C)
Time (min)
*
Control
ABHD6-ASO

Figure 4

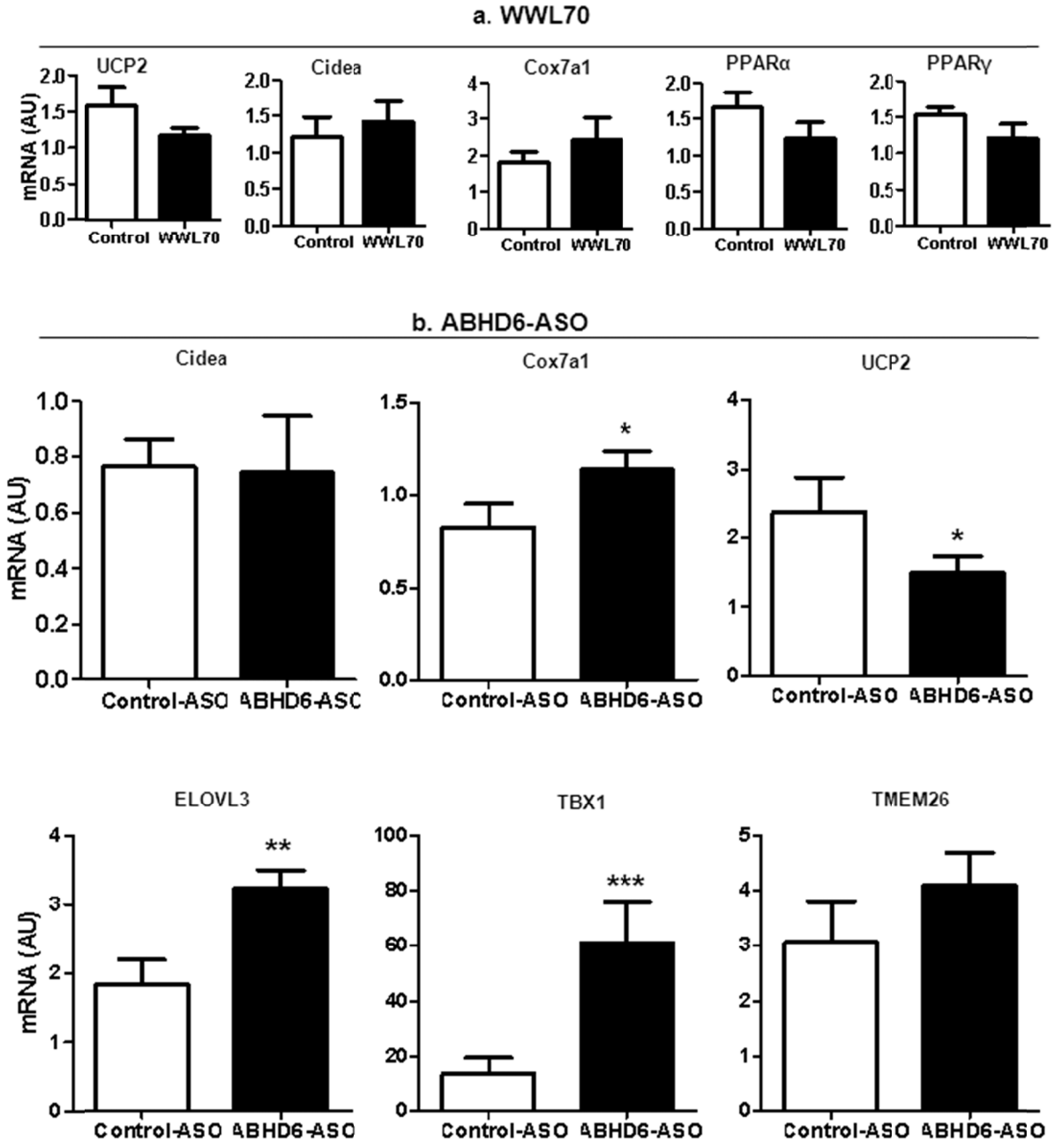

Supplementary figure 10

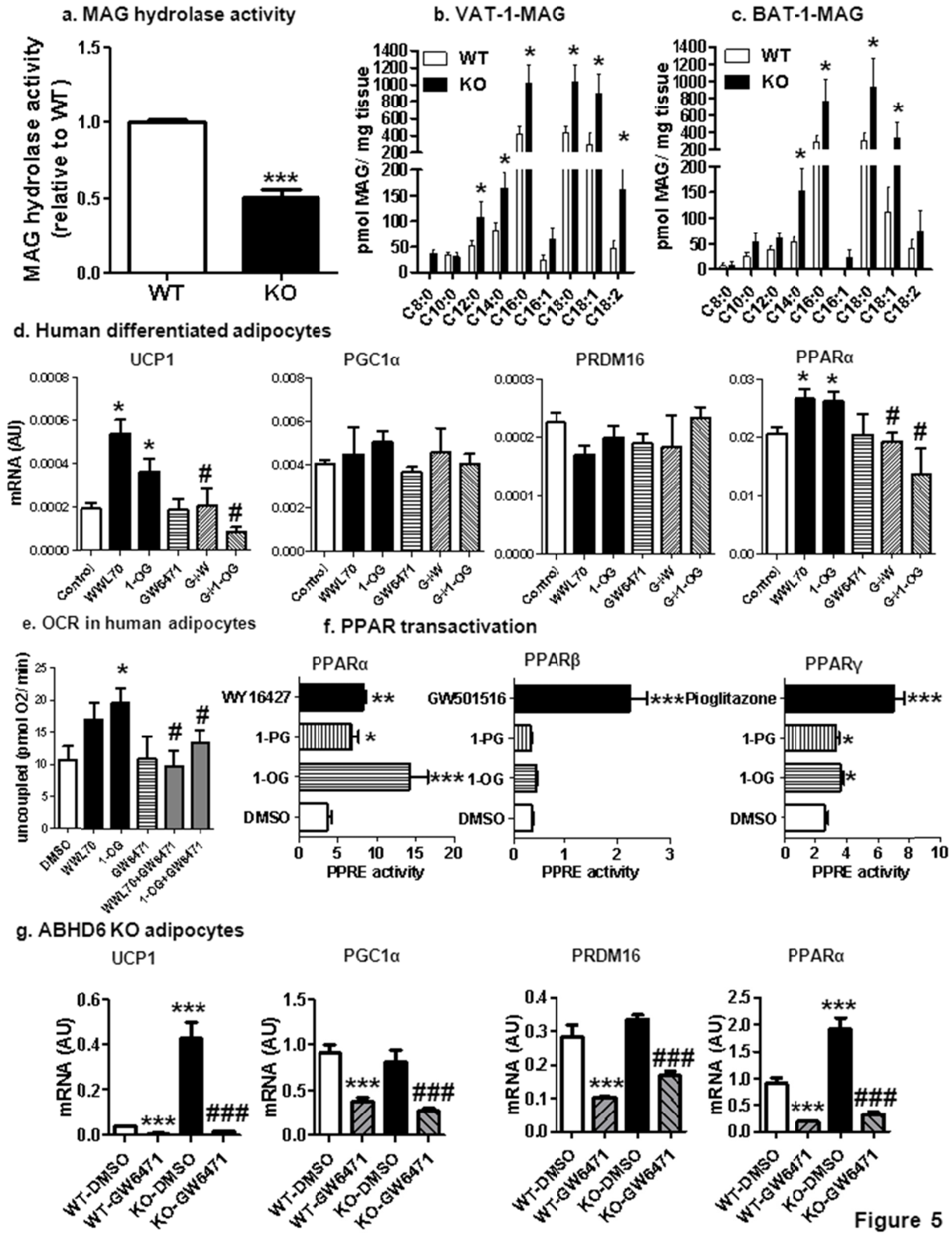
a. MAG hydrolase activity
MAG hydrolase activity (relative to WT)
WT
KO
b. VAT-1-MAG
c. BAT-1-MAG
pmol MAG/ mg tissue
C8:0
C10:0
C12:0
C14:0
C16:0
C16:1
C18:0
C18:1
C18:2
d. Human differentiated adipocytes
UCP1
PGC1α
PRDM16
PPARα
mRNA (AU)
Control
WWL70
1-OG
GW6471
G+W
G+1-OG
e. OCR in human adipocytes
uncoupled (pmol O2/ min)
DMSO
WWL70
1-OG
GW6471
WWL70+GW6471
1-OG+GW6471
f. PPAR transactivation
PPARα
PPARβ
PPARγ
WY16427
GW501516
Pioglitazone
1-PG
1-OG
DMSO
PPRE activity
g. ABHD6 KO adipocytes
UCP1
PGC1α
PRDM16
PPARα
mRNA (AU)
WT-DMSO
WT-GW6471
KO-DMSO
KO-GW6471

Figure 5

a. 2-MAG in visceral adipocytes

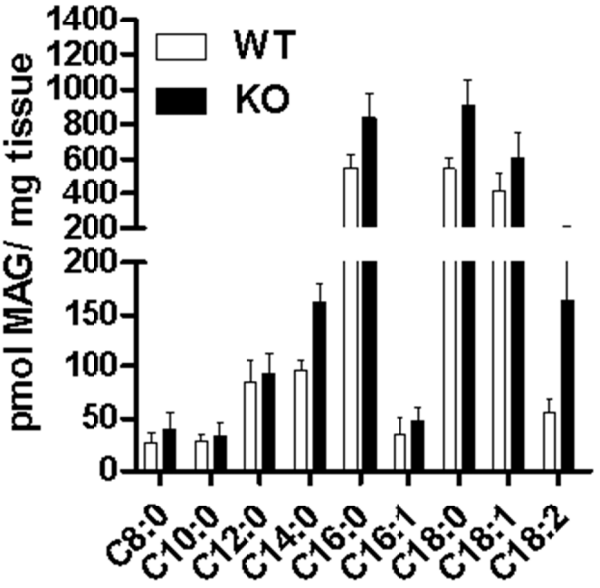

b. 2-MAG in brown adipocytes

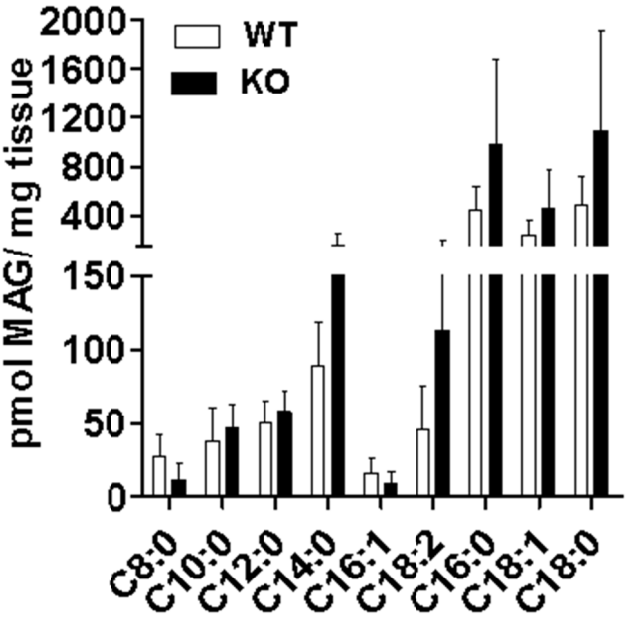

Supplementary figure 11

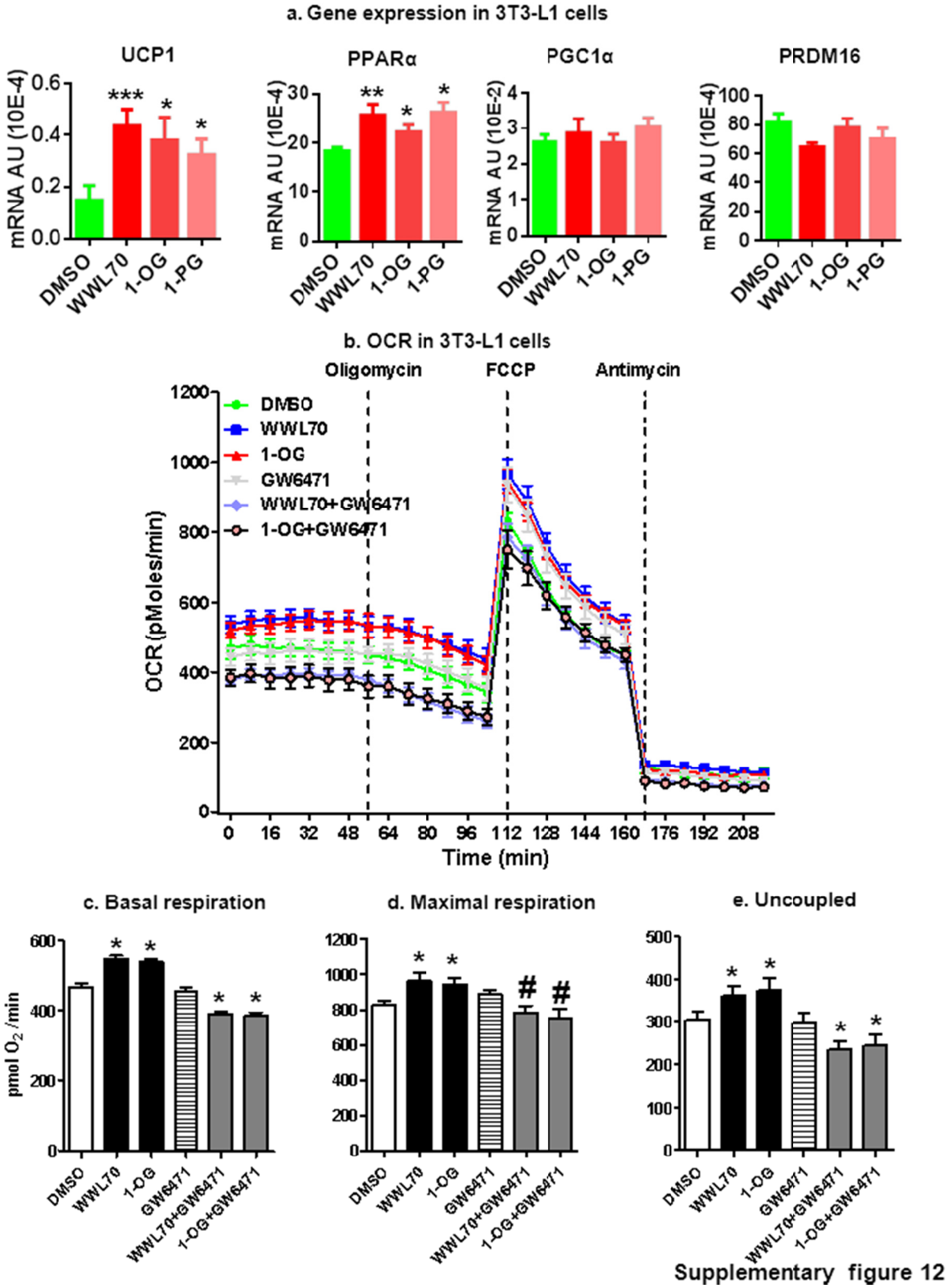

Supplementary figure 12

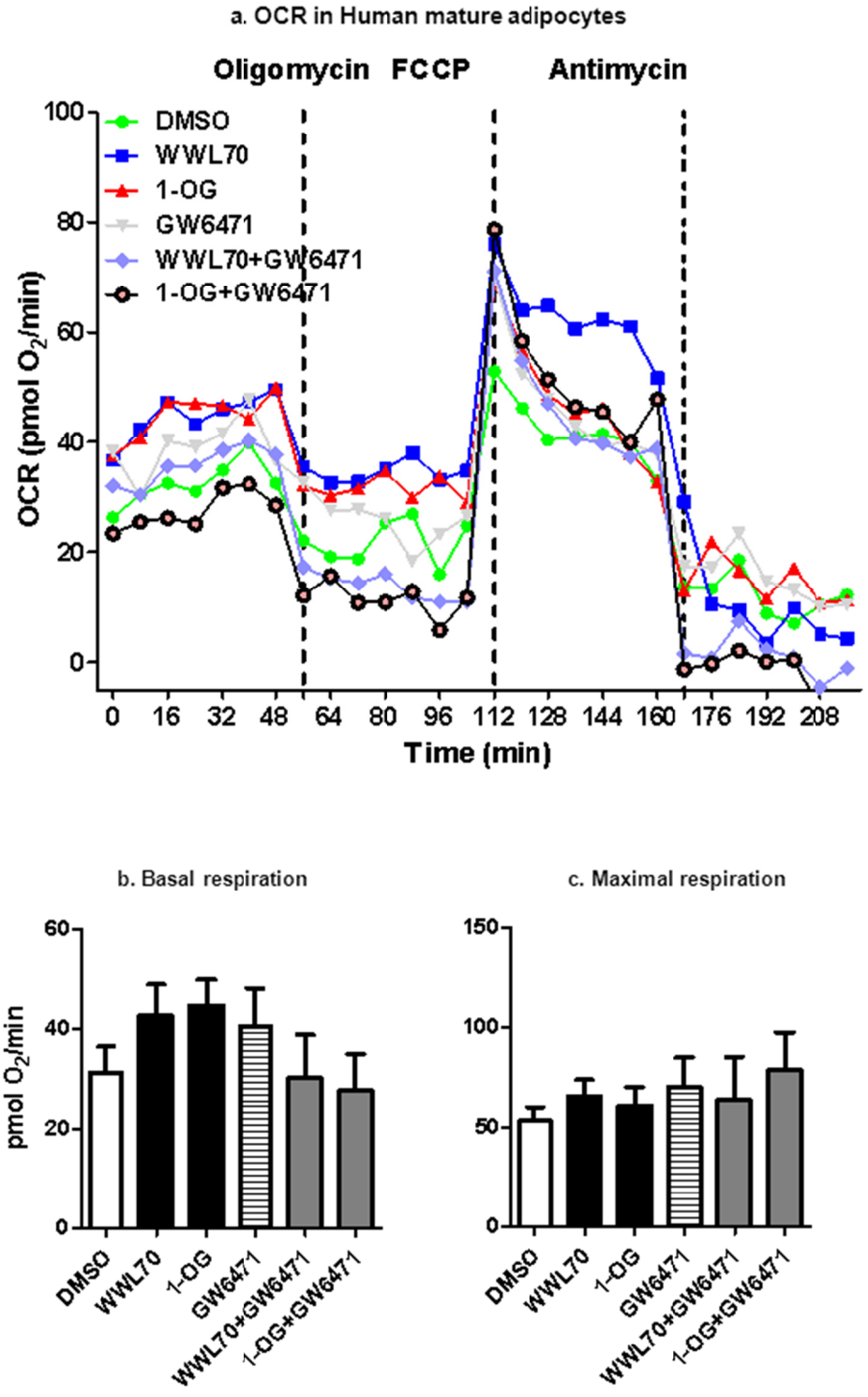

Supplementary figure 13

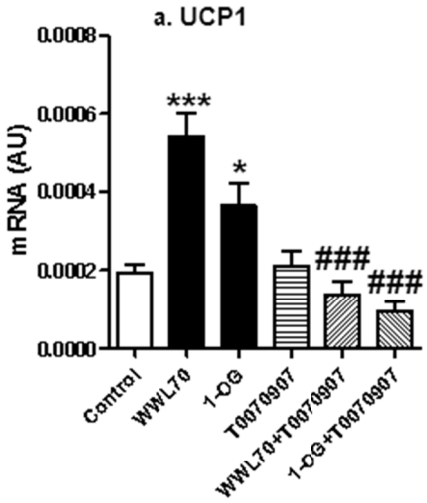

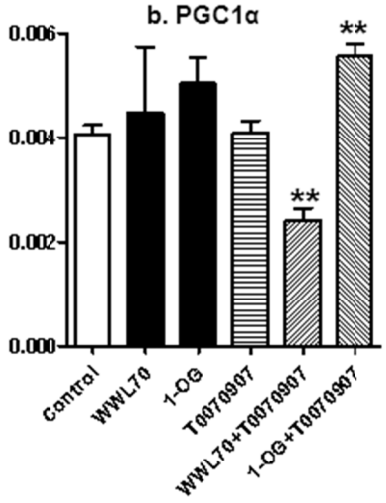

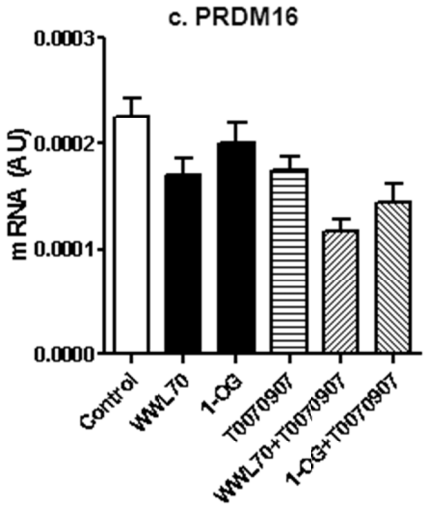

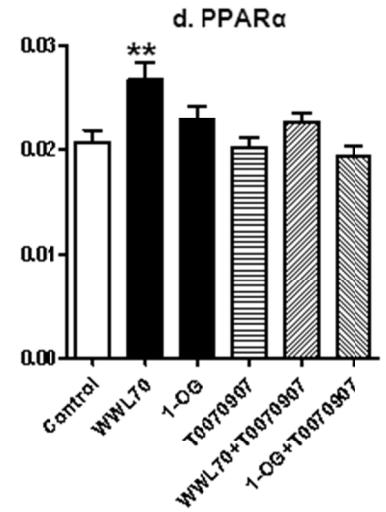

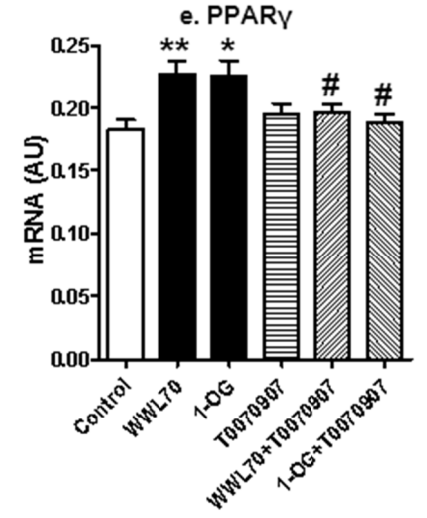

WWL70: ABHD6 inhibitor

1-OG: 1-oleoyl-rac-glycerol

T0070907: PPARγ antagonist

Supplementary figure 14

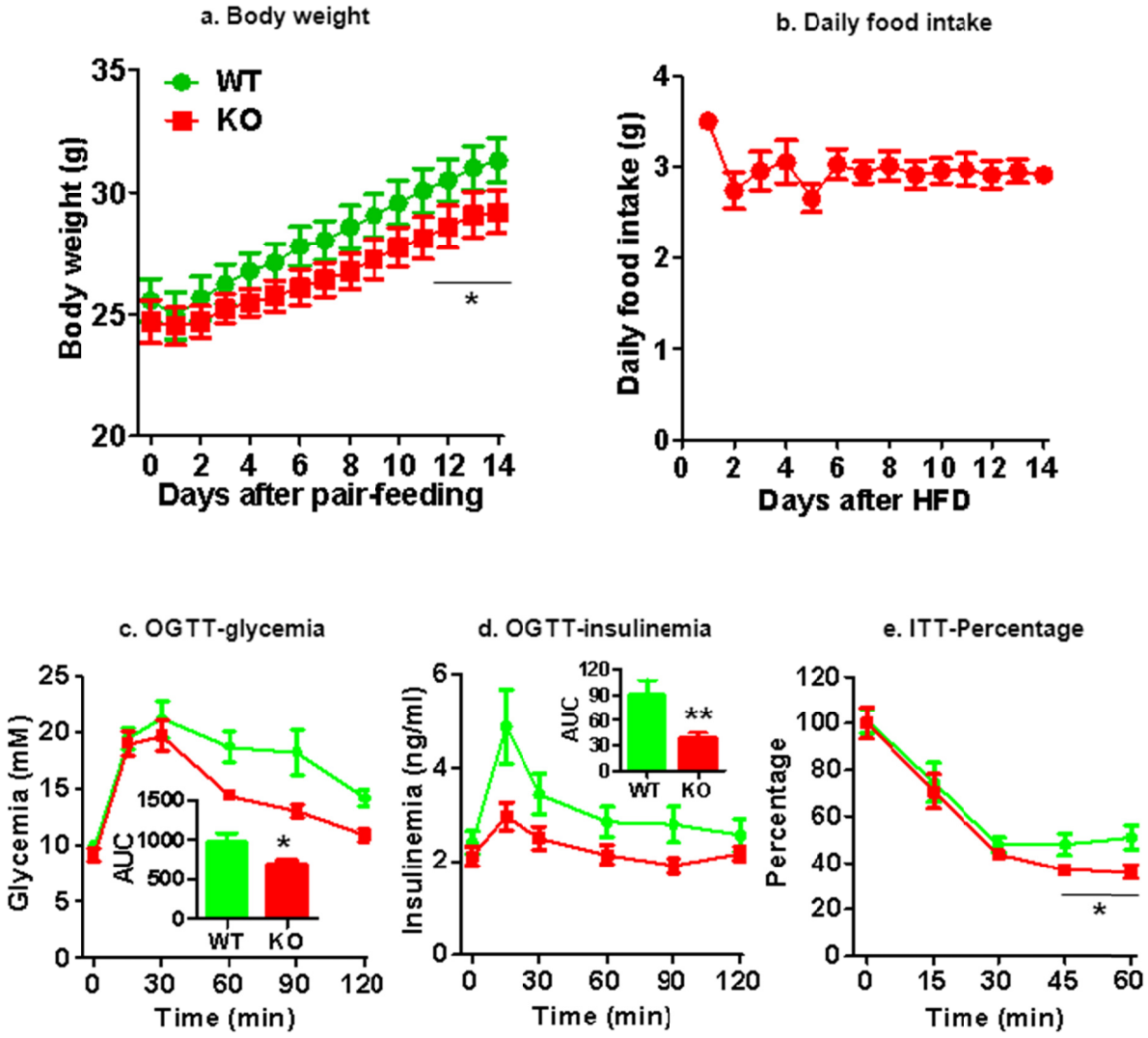

Supplementary figure 15

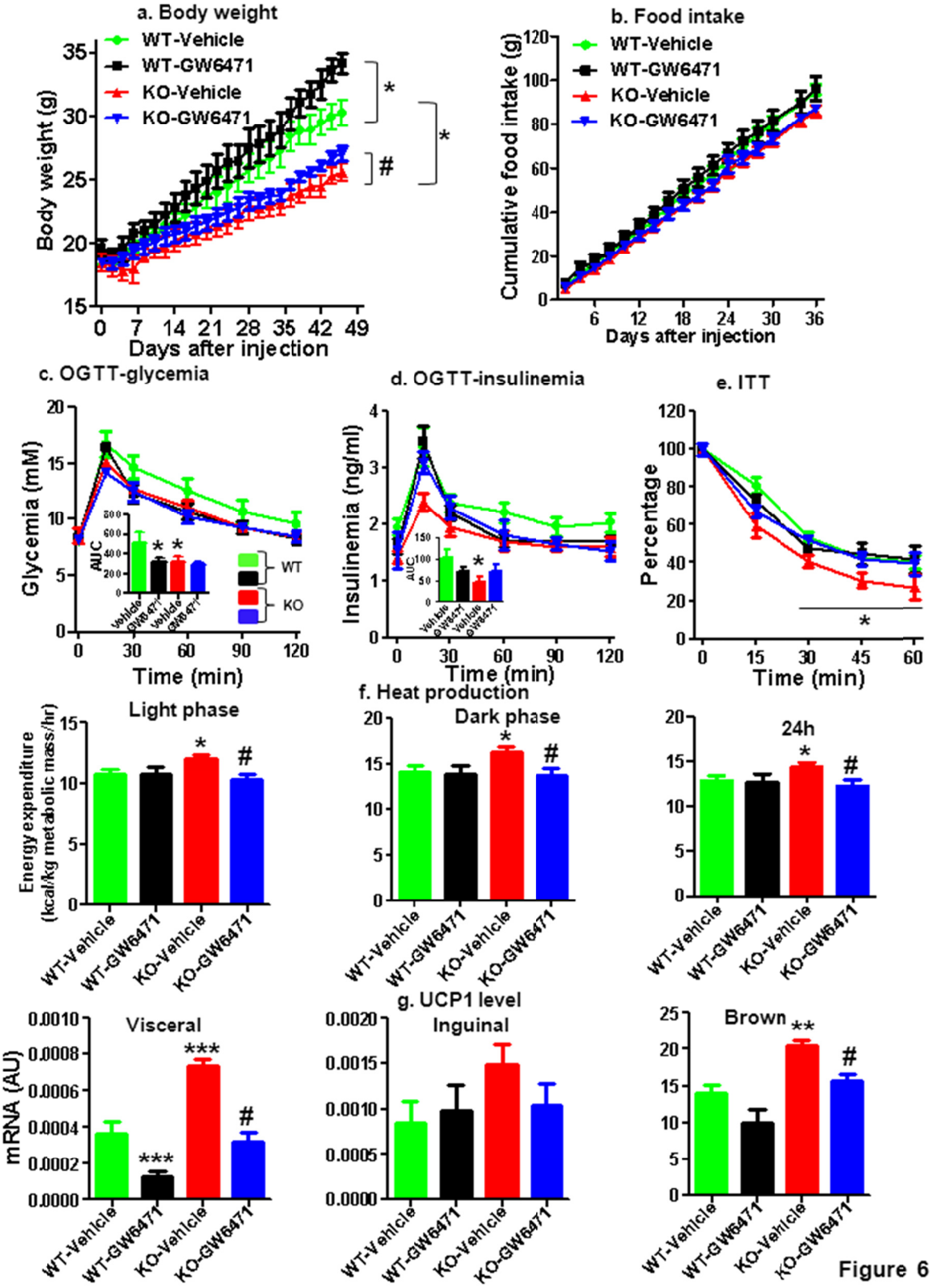
a. Body weight
WT-Vehicle
WT-GW6471
KO-Vehicle
KO-GW6471
Body weight (g)
Days after injection
b. Food intake
Cumulative food intake (g)
Days after injection
c. OGTT-glycemia
Glycemia (mM)
Time (min)
AUC
WT
KO
d. OGTT-insulinemia
Insulinemia (ng/ml)
Time (min)
e. ITT
Percentage
Time (min)
f. Heat production
Light phase
Dark phase
24h
Energy expenditure (kcal/kg metabolic mass/hr)
g. UCP1 level
Visceral
Inguinal
Brown
mRNA (AU)

Figure 6

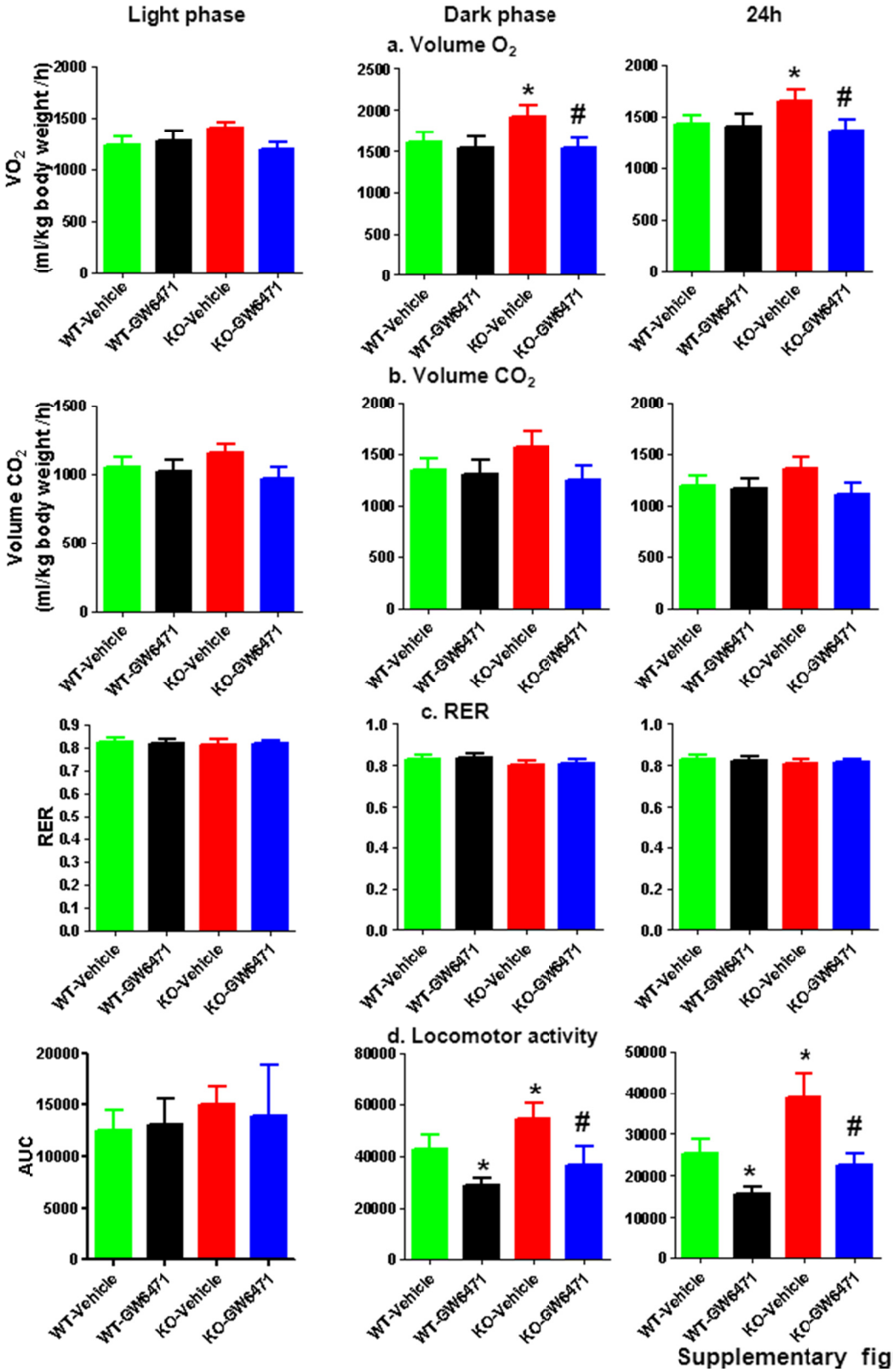

Supplementary figure 16

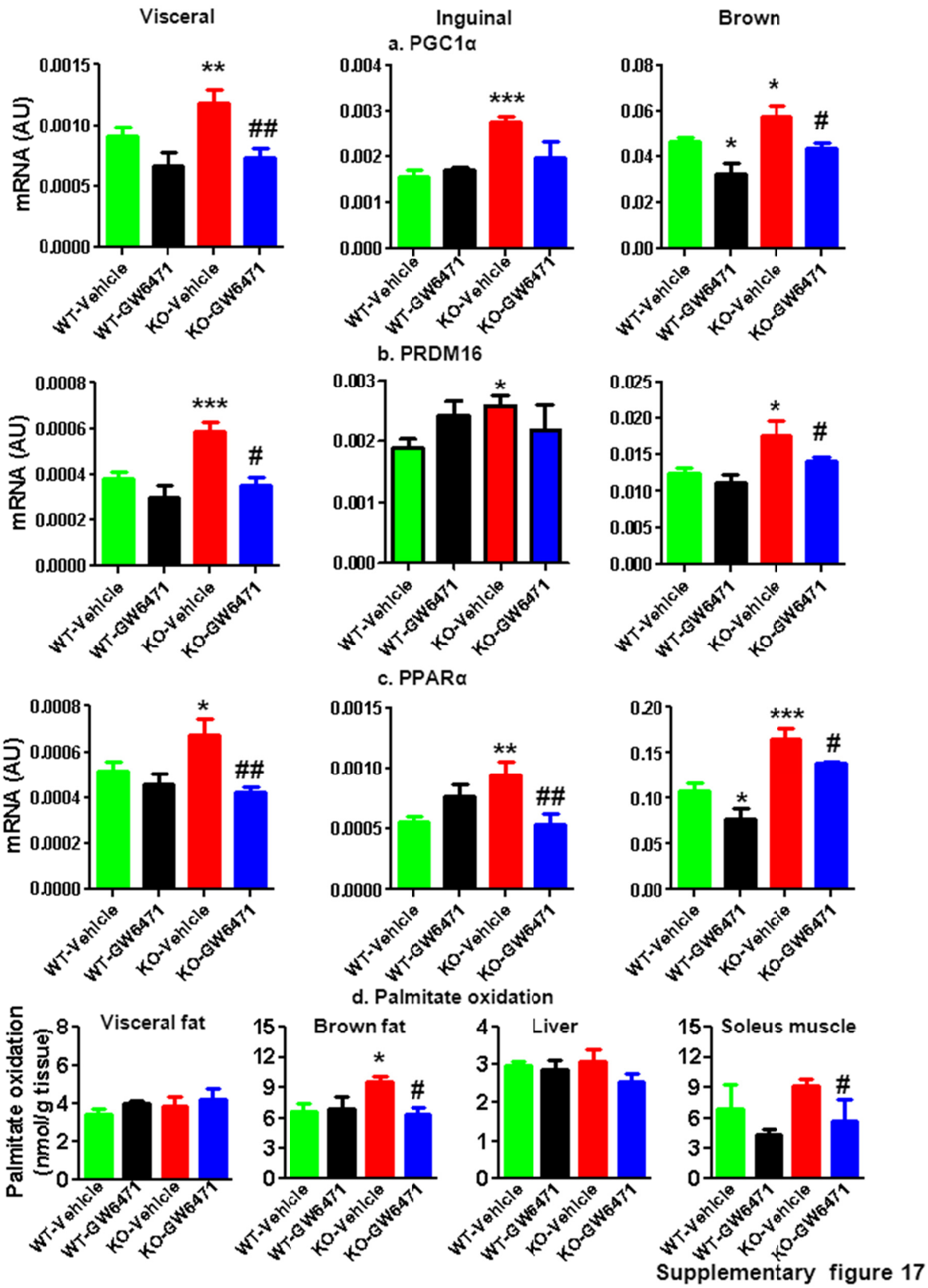

Supplementary figure 17

2. Discussion

GL/FFA cycling plays an important role in different biological processes, such as glucose-stimulated insulin secretion, and non-shivering thermogenesis. However, the involved lipid species are poorly identified. Here, by using whole body and beta cell specific ABHD6 KO mice, we have revealed the important role of ABHD6-accessible 1-MAG in regulating glucose homeostasis and energy metabolism (Figure 12). In pancreatic beta cells, ABHD6-accessible 1-MAG regulates both fuel and non-fuel stimulated insulin secretion via activation of Munc13-1 (Article 1 and 2); in the adipose tissue, ABHD6-accessible 1-MAG regulates energy metabolism by inducing browning of white adipose tissue and stimulation of brown adipose tissue via activation PPARα and PPARγ (Article 3). Our work indicates that ABHD6 is a *bona fide* MAG lipase under physiological conditions in islets as well as adipose tissues and we identified 1-MAG as a novel lipid signal generated in the lipolysis process. 1-MAG acts as a metabolic coupling factor in fuel and non-fuel induced insulin secretion and as a physiological ligand for PPARα. Thus 1-MAG is likely to be another important second messenger in regulating various biological processes in different tissues.

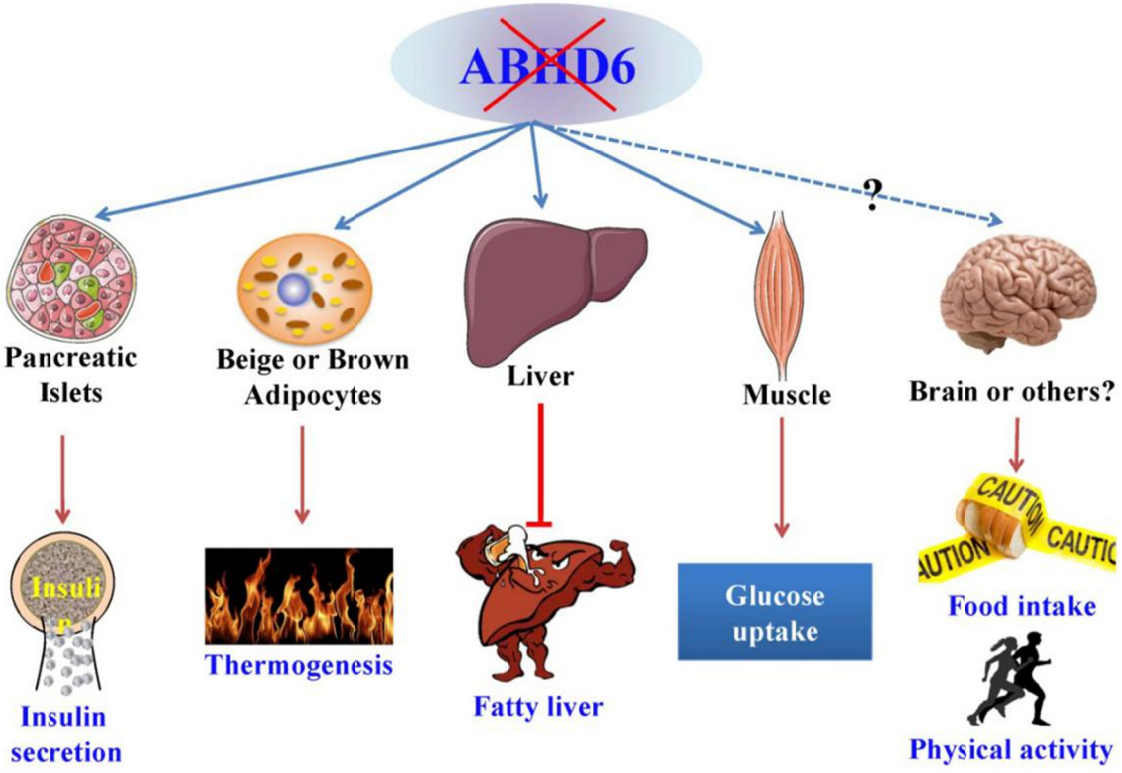

Figure 12. Beneficial effects of deletion of ABHD6 in different tissues. The detailed beneficial effects are presented in the thesis.

Lipid metabolism involving lipogenesis and lipolysis, two essential parts of glycerolipid/ free fatty acid cycle (GL/FFA cycle), produces many lipids and other metabolic signals to regulate cell function (Prentki and Madiraju, 2008, 2012). GL/FFA cycling is a continuous process of synthesis and breakdown of TG, DAG, MAG and several phospholipids. Some of the intermediates derived from the cycling, such as LPA and DAG (Eichmann and Lass, 2015; Lin et al., 2010), are well-known for their roles in regulating many biological processes. Except for 2-arachidonoylglycerol (2-AG) (Piomelli, 2003), other MAGs are not considered to mediate any signaling functions in cells. The reason for this is probably because DAG has been considered since several decades as the key neutral complex lipid with cell signaling properties and also perhaps because MAGs are short-lived lipid intermediates and their turnover inside the cells is quite rapid (Taschler et al., 2011). Moreover, even though there are two distinct isoforms of MAG, 1-MAG and 2-MAG, 2-MAG goes through rapid transformation to 1-MAG, probably non-enzymatically, making it difficult for precise quantification of each isoform. However, 1-MAG and 2-MAG exert totally different activities toward specific targets. For example, 2-AG is a strong agonist to CB1 and CB2 receptors (Jung et al., 2012), while 1-AG barely shows agonistic effects on these receptors. In addition, the relative amount of MAGs is quantitatively low and advanced technology is needed for their measurement. So far, LC/MS/MS is the most efficient way for lipid quantification, but the major problem is that this technique cannot differentiate the two different isoforms of MAG, unless it is associated with a specific chiral column to separate the two types of MAG.

Based on previous work, we have developed a method to effectively separate and measure 1-MAG and 2-MAG, by combination of thin layer chromatography (TLC) and high performance lipid chromatography (HPLC) (Zhao et al., 2014). We first separate 1-MAG and 2-MAG by TLC and then scrape the bands corresponding to 1-MAG and 2-MAG, and then perform saponification of 1-MAG and 2-MAG to release FFA, and finally use HPLC to quantify different fatty acid species. We could calculate the quantity of different MAG species based on the released fatty acids in both types of isoforms (1- and 2-MAGs). Even though this technique needs larger amount of sample as compared to LC/MS/MS, this developed method

is efficient and gives reliable and reproducible quantitative data in the absence of specialized chiral column-equipped LC/MS/MS availability. By using this method, we have successfully measured different MAG species and total MAG in INS832/13 ß-cell line and mouse islets as well as in white and brown adipose tissues. The newly developed method to quantify 1-MAG and 2-MAG is very important, as only 1-MAG was found to functions as a competent lipid signal, while 2-MAG had less or no such function. As the quantity of 1-MAG and 2-MAG is similar and 2-MAG does not response well to various treatments, measurement of total MAG would mask the changes in 1-MAG. Based on the results presented in this thesis, we provide evidence that MAGs, in particular long chain saturated 1-MAG species generated in the lipolysis process play important role in regulating insulin secretion in ß-cells, white, beige and brown adipocyte function and whole body energy homeostasis (Figure 12).

As a new comer in the class of the lipid signals, many questions related to 1-MAG are yet to be answered: how is MAG regulated inside the cells? What are possible and established roles of MAG, and how MAG mediates these functions? In the following parts, we will discuss these questions in detail.

Regulation of cellular MAG levels

As short-lived lipid intermediates, MAGs are mainly derived from hydrolysis of phospholipids or TG and partially through intestinal absorption during food digestion. The levels of MAG within cells are regulated by different synthesizing and degrading enzymes and it has been shown that MAG levels vary in pancreatic islets isolated from different diabetic mouse models , and this may be closely associated with variation in different metabolic enzymes (Delghingaro-Augusto et al., 2012; Tiano et al., 2011). However, in these initial studies, the importance of MAG as a signal was not realized. The most known enzymes implicated in MAG metabolism are the classical monoacylglycerol lipase (MAGL), ABHD6, ABHD12 and acyl CoA: monoacylglycerol acyltransferase (MGAT). We will discuss the relative contribution of different enzymes in MAG levels control and their implications in our study (Figure13).

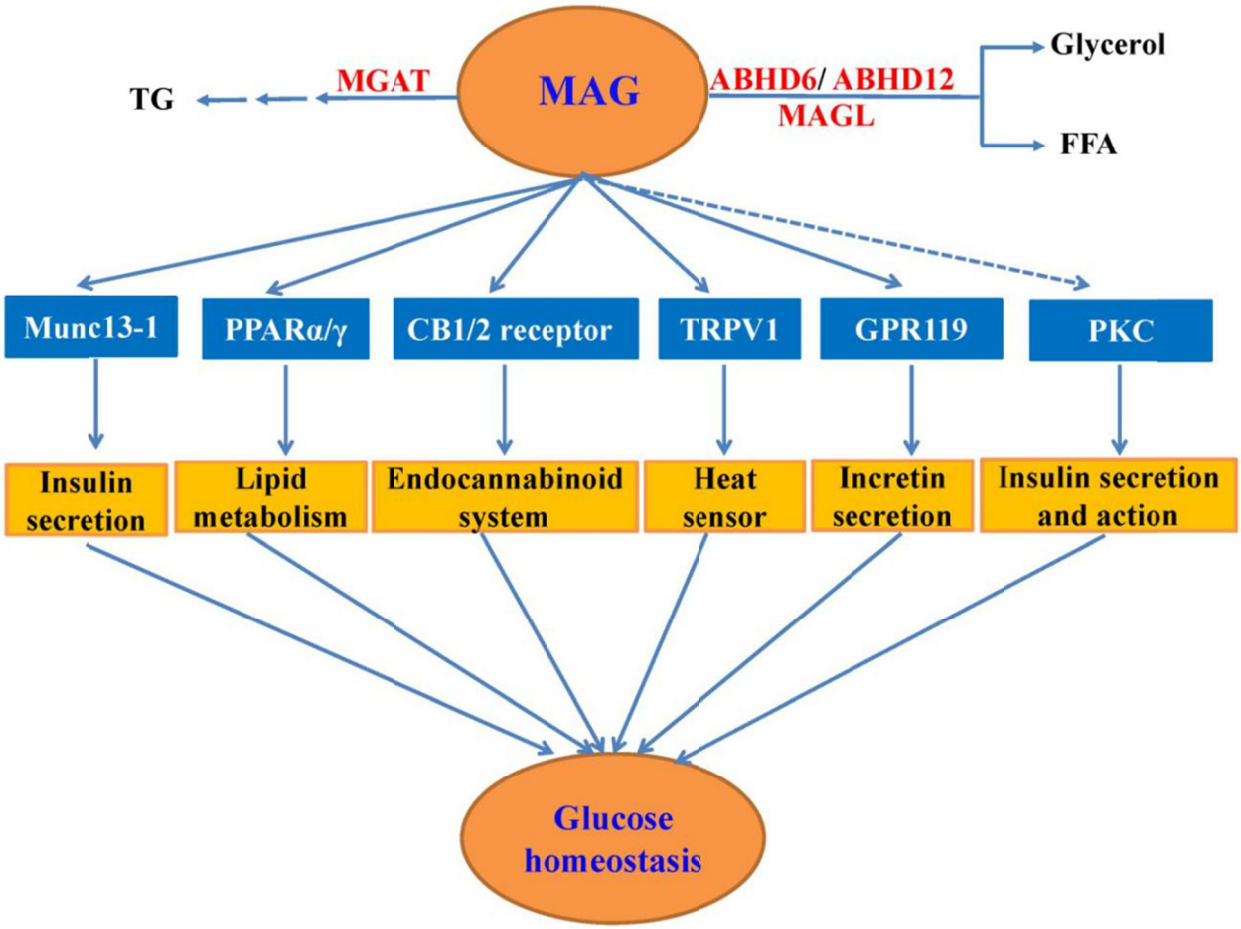

Figure 13: The proposed working model for MAG in glucose homeostasis. MAG could bind with various known or unknown receptors to regulate glucose homeostasis. The detailed decription of this figure could be found in the text.

Role of ABHD6, MAGL and ABHD12.

ABHD6 is first identified as a MAG lipase by Cravatt group in brain in 2007. After that, many aspects of ABHD6 biology are being revealed by our lab and others. In the present work, we found a wide tissue distribution of ABHD6, including rodent and human islets, brain, liver and adipocytes, and to lesser extent in the skeletal muscle (Zhao et al., 2014). We have shown that ABHD6 contributes to more than 80% of total MAG hydrolysis activity in the ß-cell line INS832/13 and islets, and around 50% of activity in adipocytes (Article 1-3). Inhibition of ABHD6 by WWL70 in INS832/13 cells and rat islets decreases FFA and glycerol release, and leads to MAG accumulation, and similar observation was made in white and brown adipose

tissues. All these evidences clearly indicate that ABHD6 is a *bona fide* MAG hydrolyzing enzyme. Besides its role in hydrolyzing MAG, a recent report has proposed that ABHD6 also functions as a physiological lysophospholipase in mouse liver; however, compared to MAG hydrolysis activity, the lysophospholipase activity of ABHD6 is quantitively much lower (Thomas et al., 2013). Considering that both in beta cells and in white adipocytes, the observed effects of ABHD6-KO, i.e., elevated glucose stimulated insulin secretion and browning phenomena, respectively, could be reproduced by exogenous MAG addition to isolated cells, the phenotype we observed in our ABHD6-KO mice is possibly contributed by MAG accumulation rather than LPA or LPC accumulation. Also LPA inhibits GSIS rather than stimulating as MAG does (Rancoule et al., 2013). However, we cannot rule out the possibility that the observed effects upon ABHD6 inhibition or suppression are in part mediated by other lipids than MAG and in particular that LPA or LPC may have some effects on insulin secretion or browning of white adipocytes.

As a MAG lipase, the preferable substrate for ABHD6 is MAG with long-chain saturated fatty acid at sn-1 position. We have compared activity of ABHD6 with several MAG species, and we found that hydrolysis of 1-palmitoylglycerol (1-PG) by ABHD6 is higher than hydrolysis of 1-OG (Article 1, Fig 1E). Also, this may be the reason why the MAGs with long chain saturated FFAs accumulate after inhibition or deletion of ABHD6. Besides, existing evidence suggests that TG hydrolysis by ATGL in the absence of co-activator ABHD5 produces 1,3-DAG (Eichmann et al., 2012), which could be further hydrolyzed by HSL to generate 1-MAG, which is the major substrate for ABHD6.

Compared to ABHD6, MAG lipase (MAGL) is the classical MAG lipase and highly expressed in different tissues, especially in adipocytes, liver, muscle and brain. To our surprise, MAGL is not expressed in beta cell lines, rat and human islets, and weakly expressed in mouse islets (Zhao et al., 2014). Some reports indicate that this enzyme is mainly located in the cytoplasm and is regarded as the rate-limiting step in MAG hydrolysis (Zechner et al., 2012). Mice deficient in MAGL show modestly reduced glycerol and FFA circulating levels. Also it has been shown that MAG accumulates in adipocytes, liver and brain of these mice (Taschler et al., 2011). However, the adipocytes isolated from MAGL KO mice do not show any variation in glycerol release in basal conditions, and the decrease in glycerol and FFA release is only

observed when stimulated with isopropanol, a classical activator of lipolysis. This observation suggests that MAGL may mainly contributes to stimulated lipolysis rather than basal lipolysis, while ABHD6 contributes to basal and also stimulated lipolysis. Presently we do not know why such difference exists in the contribution of these enzymes to basal and stimulated lipolysis. Basal lipolysis much slower compared to stimulated lipolysis. However, which process is responsible for the generation of signaling lipid molecule(s) is currently unknown. In our Article 3, we have shown that exposure of fully differentiated adipocytes to WWL70 induces browning of white adipocytes, while the MAGL inhibitor JZL184 has limited effect. This raises an interesting topic regarding the different roles of basal and stimulated lipolysis in the browning of white adipocytes, and perhaps only lipid signals produced from basal lipolysis contribute to the browning of white adipocytes, and stimulated lipolysis may only contribute to provide FFA for energy supply.

The differences in the contribution to lipolysis by ABHD6 and MGAL may help explain the different phenotypes of the corresopnding KO mice in response to HFD. In the present work, we have shown that mice deficient in ABHD6 are resistant to diet-induced obesity with greatly increased thermogenesis, while there have been discrepant results with respect to the effect of MAGL KO in DIO mice. One report indicates that MAGL-KO mice fed 74% fat diet, are not protected from obesity as compared to control mice (Taschler et al., 2011). However, recent report shows that whole body MAGL-KO mice gain less body weight when fed 45% high fat diet, due to reduced intestinal fat absorption (Douglass et al., 2015). In either case, MAGL-KO does not appear to increase non-shivering thermogenesis, as in the case of ABHD6-KO mice, even though MAG accumulation is observed in white adipocytes in both the KO mice. It is possible that the intracellular MAG elevated in ABHD6-KO mice is functionally more capable of inducing the observed metabolic changes, probably because of its compartmentalization in the cells whereas MAG that builds-up in MAGL-KO mice is not capable of this metabolic function as it likely accumulates in an intracellular location that is not relevant for signaling. Thus, ABHD6 is thought to be a plasma membrane protein (Blankman et al., 2007a). Besides, it seems that deletion of MAGL leads to accumulation of MAG with unsaturated FFA, while deletion of ABHD6 leads to the accumulation of MAG with long-chain saturated FFAs. Whether these differences could explain observed phenotypes is currently unknown.

Besides the possible roles in basal and stimulated lipolysis, MAGL and ABHD6 may have different roles in hydrolyzing different MAG species. While both MAGL and ABHD6 can hydrolyze the two isomers of MAG, ABHD6 shows preferential activity towards 1-MAG and MAGL uses both 1-MAG and 2-MAG with equal efficiency (Navia-Paldanius et al., 2012b). In the studies that described MAGL-KO mice (Douglass et al., 2015) even though an increase in cellular MAG was demonstrated, whether 1-MAG or 2-MAG or both increased, was not shown. In our study, we observed a specific elevation in 1-MAG species in pancreatic islets and in both white and brown adipocytes. Our results also have shown that 1-MAGs possess higher activity than 2-MAGs in inducing insulin secretion (Article 1). In addition, MAGL is a cytosolic enzyme and therefore the MAG accumulation by MAGL inhibition is probably largely limited to cytosol. MAG localized in cytosol, probably has no access to the downstream targets we have studied, such as plasma membrane Munc13-1 or nuclear PPARs. In contrast, ABHD6 is a membrane-associated protein, and it locates predominantly in the plasma membrane and to a lesser extent in nuclear membrane. Thus when ABHD6 is suppressed, it is likely that MAG accumulates at plasma or nuclear membranes, where it efficiently binds and activates Munc13-1 or PPARs, respectively as we observed. It has been recently suggested that in neuronal nuclei, a DAGL dependent pathway for the generation of 2-AG exists and that MAGL does not participate in controlling the levels of 2-AG produced intra-nuclearly, and that the nuclear 2-AG participates in the activation of PPARγ (Garcia Del Cano et al., 2014).

Besides ABHD6 and MAGL, ABHD12 is also reported as a MAG lipase by Cravatt group. It has been shown that loss of function of ABHD12 leads to a neurodegenerative disease in humans called polyneuropathy, hearing loss, ataxia, retinitis pigmentosa and cataract (PHARC) (Blankman et al., 2013). Similar to ABHD6, ABHD12 is also shown to be located in the plasma membrane but with its catalytic domain facing outside the cell. Thus the substrates of ABHD12, including MAG, likely build up on the outer surface of the cell but not inside the cells.

Role of acyl coenzyme A: monoacylglycerol acyltransferase.

MGAT is believed to be an essential and rate-limiting step for the absorption of fat in the small intestine. MGAT converts MAG into DAG, an important precursor of TG and

phospholipid synthesis. So far, three isoforms of MGAT have been identified: MGAT1, MGAT2 and MGAT3. These isoforms show different tissue distributions, degrees of MGAT acyltransferase activity, and to a lesser extent, some DGAT activity. MGAT1 (Yen et al., 2002) was first identified and it is expressed mainly in stomach, liver, kidney, white and brown adipose tissue. However, MGAT1 was not identified in the small intestine, indicating other MGAT isoforms exist in this tissue. MGAT2 is highly expressed in the small intestine and shows high activity toward the two MAG isoforms (sn-1 and sn-2). Overexpression of MGAT2 in AV-12, COS-7, and Caco-2 cells led to a more than 70-, 30-, and 35-fold increase in the synthesis of diacylglycerol, respectively (Yen and Farese, 2003). MGAT3 encodes a 36-kDa transmembrane protein that is highly homologous to MGAT1 and -2. It is also highly expressed in the small intestine (Cheng et al., 2003), and it specifically recognizes 2-MAG as substrate. 2-MAG is formed during intestinal fat breakdown and absorbed into enterocytes, where it is reacylated to TG, packed into chylomicrons and released into blood. All the MGAT isoforms share some degree of sequence homology with acyl-coenzyme A: diacylglycerol acyltransferase 2 (DGAT2), and they display some DGAT activity also. MGAT3 possesses higher DGAT activity compared to MGAT1 and MGAT2 (Cao et al., 2007). So far, several reports implicate MGAT in intestine and liver TG synthesis but no direct evidence has been shown indicating that MGAT activity is negatively correlated with MAG levels inside the cells. However, we can speculate that alteration of MGAT activity is associated with change in MAG levels in tissues where it is expressed. MGAT is very poorly expressed in islet and adipose tissues (Zhao et al., 2014), the two tissues that we have primarily studied; it is unlikely that it plays significant role in the regulation of insulin secretion and PPAR activation and adipose browning under normal conditions. However, it may be interesting to assess the relative expression level of MGAT in ABHD6 KO mice or MAGL-KO mice, to see if there is some compensatory increase in this enzyme to utilize the accumulating MAG in beta cells and adipose tissues.

The identified and emerging roles of MAG in regulating biological processes

MAGs and the endocannabinoid system

Among the MAG species, 2-arachidonoylglycerol is identified as an endocannabinoid, an endogenous agonist of the CB1 and CB2 receptors. The endocannabinoid system regulates

food intake, body weight gain (Battista et al., 2012), nausea and vomiting(Parker et al., 2014), and this is of special interest under conditions of obesity. It is an important target to treat obesity since CB1 receptor blockers reduce food intake (Di Marzo and Matias, 2005). 2-AG is a CB1 and CB2 receptor agonist, and its level within cells is controlled by MAGL and ABHD6. Inhibition of MAGL by JZL184 raises 2-AG levels, and produces cannabinoid behavioral effects, such as analgesia, hypothermia and hypomotility (Long et al., 2009a). However, mice deficient in MAGL show about 40 fold increase in 2-AG levels in the brain without any cannabinoid-like effects on food intake and body weight gain, and this may be explained by desensitization of CB1 and CB2 receptors (Taschler et al., 2011). ABHD6 also contributes to MAG hydrolysis in the brain, and selective blockade of ABHD6 by a specific inhibitor induces CB1-dependent long-term depression in specific neurons. ABHD6 is regarded as a member of the endocannabinoid signaling system (Marrs et al., 2010). However, we noticed that whole body ABHD6 KO mice do not display any endocannabinoid-like mediated effects. For example, these KO mice do not show elevated food intake or body weight gain, which is to be expected under conditions of endocannabinoid build-up and in stead, these KO mice show reduced food intake and body weight gain on high fat diet (Article 1). Even though these findings may be partially explained by the desentizition of CB1 and CB2 receptors as brain 2-AG levels would be increased since the birth of the mice, such is not likely the case as these mice do not show any changes in pain sensitivity, which is to be expected under chronic desensitization of cannabinoid receptors. In addition to 2-AG, other MAGs levels are also elevated in islets and adipose tissues of whole body ABHD6 KO mice. It has been reported that a PPARα agonist, oleoylethanolamide, reduces food intake when administered either peripherally or intra-lateral hypothalamically (Soria-Gomez et al., 2010). We have observed that 1-oleoyl-glycerol, which accumulates in the adipose tissue of ABHD6-KO mice, in fact activates PPARα very potently in *in vitro* transactivation assays. Thus, a possible increase in 1-oleoyl-glycerol or other MAG species in hypothalamic or other brain areas controlling food consumption in ABHD6-KO mice may be responsible for the reduced food intake in ABHD6-KO mice via PPARα activation. The role of ABHD6, 2-AG and additional MAG species in key brain areas controlling energy homeostasis remains to be

assessed and this aspect is currently being studied by collaborators of the Prentki group in various hypothalamic and brain reward areas.

MAGs and insulin secretion

The involvement of lipolysis-derived lipid signals in glucose stimulated insulin secretion is well-accepted, as inhibition of lipolysis by the pan-lipase inhibitor orlistat, or genetic manipulation of adipose triacylglycerol lipase (Peyot et al., 2009c), hormone sensitive lipase (Fex et al., 2009; Peyot et al., 2004; Roduit et al., 2001) reduce glucose stimulated insulin secretion. It has been speculated for a long time that DAG derived from lipolysis may be the lipid signal, as increasing 1,2-DAG levels by exogenous administration increases insulin secretion. However, the evidence from HSL KO mice does not support this hypothesis. Also, hydrolysis of TG produces 2,3-DAG or 1,3-DAG, other than 1,2-DAG. Therefore, other lipid species, generated in the lipolysis process, act as a metabolic coupling factor to promote insulin secretion. Comprehensive biochemical, pharmacological, cell and molecular biology, and genetic work during this thesis (Article 1) showed that MAG, especially 1-MAG species with long chain saturated fatty acids, is a lipid signal that contributes to glucose-signaling for insulin secretion. In the beta cells, ABHD6, rather than MAGL, is the main MAG hydrolase. Some of the key evidences in favor for a role of ABHD6-accessible MAG in GSIS was that decreasing activity of ABHD6 with a specific inhibitor or genetic manipulation, leads to increased MAG levels in ß-cells, and this is associated with enhanced GSIS. In contrast, increasing ABHD6 activity by overexpression, decreased glucose induced insulin secretion.

Overall our results have identified MAG as a novel signaling metabolic coupling factor both for fuel and non-fuel induced insulin secretion in the ß-cell and that ABHD6 by regulating MAG levels, negatively controls insulin secretion (Article 1 and 2).

MAGs and insulin sensitivity

Elevated circulating levels of FFA is a major risk factor for insulin resistance, and there is much evidence for the view that activation of the DAG-Protein kinase C pathway contributes to FFA-induced insulin resistance in liver and muscle (Samuel and Shulman, 2012). However, the view that DAG accumulation in tissues is causally linked to insulin resistance is currently debated (Amati, 2012). As DAG and MAG have highly similar structures, whether MAG

participates in regulates insulin signaling pathway is not well elucidated. The major MAG lipases MAGL and ABDH6 are well-expressed in peripheral tissues, such as skeletal muscle, adipose and liver. Previous studies in MAGL-KO mice (Taschler et al., 2011) and the present work on ABHD6-KO mice suggest that these enzymes may regulate insulin sensitivity. Thus, deletion of MAGL in mice, increased MAG levels in various tissues and enhanced glucose tolerance and insulin sensitivity and protects from diet-induced obesity after a high fat diet (Douglass et al., 2015; Taschler et al., 2011). The authors suggested that the observed modest decrease in circulating FFA levels contributes to this process in MAGL-deficient mice. However, it does not rule out the possibility that MAG accumulation inside the tissues was in fact the main contributor to the improved insulin sensitivity of these mice. We speculate that MAG directly acts via the insulin signaling pathway to enhance insulin sensitivity because: (a) we observed that ABHD6 expression is increased with obesity and this may be a compensation phenomenon to limit insulin resistance; (b) decreasing ABHD6 activity by genetic deletion (Article 3) or by ABHD6-antisense oligonucleotides (ASO), or by the specific inhibitor WWL70 protects mice from high fat diet-induced insulin resistance (Thomas et al., 2013); and (c) MAG accumulation in peripheral tissues is well-correlated to improved insulin sensitivity (Okuma et al., 2015). Thus, it would be of interest to test the view that MAG is a lipolysis-derived signal that controls insulin action and to determine the mechanisms involved.

MGAT enzymes and activity are found to be induced in diet-induced obesity and *ob/ob* mice and in insulin-resistant human subjects with nonalcoholic fatty liver disease (Hall et al., 2012). In liver, MGAT1 expression is regulated by the nuclear receptor PPARγ and is responsible for the lipid accumulation in diet-induced hepatic steatosis (Lee et al., 2012b). Knockdown of MAGT1 by ASO in mouse liver, caused reduced hepatic MGAT activity, greatly increased glucose tolerance and hepatic insulin signaling, even though this is accompanied with increased membrane and cytosolic DAG levels (Hall et al., 2014). MGAT2 is a tetrameric enzyme that heterodimerizes with DGAT1 (Zhang et al., 2014a) or DGAT2 (Jin et al., 2014), two essential enzymes of the last step in TG synthesis. Whole body and intestine specific deletion of MGAT2 reduces food intake, protects against diet-induced obesity, increases glucose tolerance, and reduces hypercholesterolemia and fatty liver (Nelson et al., 2011; Nelson et al., 2014; Yen et al., 2009). Mice deficient in MGAT2 also show increased energy

expenditure and higher body temperature, and a trend to elevated locomotor activity in light phase. These beneficial effects in whole body-MGAT2-KO mice are only partly reproduced in intestine-specific deletion of MGAT2, indicating that MGAT2 in other tissues, such as liver and adipocyte, may also contribute to regulate energy metabolism (Gao et al., 2013; Nelson et al., 2011). Liver specific MGAT2 KO mice also show increased insulin sensitivity. Overall, these MGAT KO studies in which MAG levels are elevated in various tissues, strongly support the view for a role of MAG in the control of insulin sensitivity and energy homeostasis, in accordance with the results in this thesis.

In sum, reducing the activity of the MAG hydrolyzing or utilizing enzymes in mice (MAGL, ABHD6 and MGAT) results in beneficial effects on energy metabolism and increased insulin signaling and these effects cannot be explained exclusively by reduced circulating levels of FFA or tissue DAG levels, as knockout of either ABHD6 or MGAT do not affect FFA levels and MGAT1 suppression in liver actually increases membrane DAG content (Taschler et al., 2011) (Article 3). All these evidences suggest that MAG is probably responsible for the increased insulin sensitivity, seen in these models. In accordance with this view, the ABHD6 inhibitor WWL70 increased Akt phosphorylation levels in traumatic brain injury (TBI) mouse brain (Tchantchou and Zhang, 2013). In conclusion, MAG may directly regulate the insulin signaling pathway and direct testing of this hypothesis using *in vitro* and *in vivo* models are warranted.

MAG and adipose browning

Non-shivering thermogenesis is mainly conducted by brown and beige adipocytes (Cohen and Spiegelman, 2015). In the process of formation of beige adipocytes, dramatic change in the lipid droplet-associated proteins occurs in order to facilitate the process of lipolysis. Multiple evidences support the notion that increased lipolysis is associated with increased browning of white adipocytes. Some physiological stimuli, such as cold exposure and exercise, increase browning of white adipocytes as well as lipolysis (Hao et al., 2015). However, it is still unclear whether lipolysis is a causing factor or a consequence of browning of white adipocytes. Studies of various browning agents reveal that lipolysis is a driving force to induce browning of white adipocytes. Adrenergic stimulation is a classical stimulation for increasing lipolysis by increasing cyclic AMP levels and hence the protein kinase A-mediated phosphorylation of

HSL and perilipin. Consistent with this, adrenergic stimulation also greatly increases browning of adipocytes (Bonet et al., 2013); Adenosine is well-known to induce browning of human adipocytes, and acute exposure of human adipocytes to adenosine increases lipolysis, which precedes the formation of beige adipocytes (Rines et al., 2015). In contrast, RFamide peptide QRFP 43 (Mulumba et al., 2015) inhibits lipolysis, decreases non-shivering thermogenesis by decreasing browning of white adipose tissue and thus causes obesity in mice. α-Lipoic acid treatment increases lipolysis in adipocytes and promotes beige adipose features in subcutaneous adipocytes from overweight/obese subjects (Fernandez-Galilea et al., 2015). All these evidences imply that lipolysis is not a consequence of browning of white adipocytes and more likely a cause for the browning process. However, the specific lipid species involving in this process is poorly identified.

Based on the observations made on MGAT-KO and ABHD6 KO mice, we propose that lipolysis generated MAG may directly induce browning of white adipocytes and regulate energy homeostasis. It has been observed in our and other laboratories that mice deficient in MGAT2 (Nelson et al., 2011) and ABHD6 show greatly increased energy expenditure and slightly higher body temperature with browning of white adipocytes. We observed that MAG induces browning of mouse and human adipocytes in a cell-autonomous manner. Exposure of fully differentiated mouse and human adipocytes to 1-oleoylglycerol elevated UCP1 level, a marker for browning of white adipocytes. In agreement with this, increasing MAG levels by 1-oleoylglycerol addition or by specific ABHD6 inhibitor WWL70 increased oxygen consumption rate (OCR), particularly the uncoupled respiration, in 3T3-L1 mouse cells and fully differentiated human adipocytes, indicating that increased MAG levels induce browning of white adipocytes and that the elevated UCP1 protein is indeed fully functional in uncoupling mitochondrial respiration and probably in heat production. Furthermore, MAG-induced white adipose browning is not dependent on signals from the central nervous system, as similar browning effect is observed in ABHD6-ASO mice on high fat diet. It is well-accepted that ASO cannot enter the brain, and thus it will not affect ABHD6 in the brain (Thomas et al., 2013). Thus, overall our results indicate that ABHD6 is a new player in adipose browning and strongly support the view that lipolysis derived MAG is a signal for adipose browning.

MAG, cell growth and tumorigenesis

A potential link between obesity and several cancers is established and it is well-accepted that tumor cells display dysregulated lipid metabolism to provide large amounts of FFA for membrane synthesis and signaling molecules (Benjamin et al., 2012). Alteration in the level of enzymes involved in lipid metabolism and transport are associated with tumorigenesis. Some reports have already shown that increased levels of MAGL and ABHD6 are observed in some cancers, such as Ewing tumors (Li et al., 2009; Max et al., 2009). MAGL is regarded as a biomarker for several cancers and inhibition of MAGL by genetic deletion decreases cancer growth, and overexpression of MAGL in nonaggressive cancer cells increases tumor growth (Nomura et al., 2010). This effect of MAGL on tumor growth is largely ascribed to the change of FFA levels. However, overexpression or deletion of MAGL not only modulates FFA but also MAG levels. Whether endogenous MAG can directly regulate tumorigenesis is still unknown. Some reports indicate that 2-AG can have direct anticancer effect, suggesting that various MAG species may play a role in tumorigenesis (Massi et al., 2013). More experimental results are warranted to directly test this hypothesis and to determine if ABHD6 plays a role in the control of cell growth at large.

Possible downstream targets for MAG in regulating cell function

As described above, MAG can regulate many cell functions, such as insulin secretion and browning of white adipocytes. Based on the work done in our other laboratories, MAGs can function as agonists for CB receptors, the exocytotic regulator Munc13-1, the non-selective calcium channel TRPV1, and the GPR119 receptor. Also, MAGs may also be implicated in activating nuclear receptor of the PPAR family and specific PKC enzymes.

MAG and CB1 and CB2 receptors

The endocannabinoid system, consisting of endocannabinoids (2-arachidonoylglycerol and anandamide), and associated synthesizing and degrading enzymes, together with cannabinoid receptors (predominately CB1 and CB2), functions both centrally and peripherally to regulate satiety and energy metabolism, and over-activation of this system is associated with obesity (Boyd, 2006). The CB1 receptor is widely distributed, and is expressed not only in the central nervous system, but also in peripheral tissues, such as adipocytes, skeletal muscles,

gastrointestinal tract, liver and the pancreas, while the CB2 receptor is expressed in immune cells, spleen and tonsils. One of the MAG species, 2-arachidonoylglycerol (2-AG) was first identified as an endocannabinoid in 1995, and it is shown to be present in the bloodstream with high affinity for CB1 and CB2 receptors (Sugiura et al., 1995). Manipulation of 2-AG levels by pharmacological inhibitors or genetic mouse models with deletion in the synthesizing or degrading enzymes, established the endocannabinoid role of 2-AG. Except 2-AG, other MAG species do not show any effect on CB1 and CB2 receptors. Our data show that changes in insulin secretion in response to glucose in ß-cells and its modulation by variations in ABHD6 expression levels, best correlate with long chain saturated 1-MAG species and not with 2-MAG species or 2-AG itself, which discounts a role of 2-AG as a metabolic coupling factor in GSIS. Similarly adipose tissue of ABHD6-KO mice show increased levels of 1-MAG species and minor changes in 2-MAGs levels, which does not favor the view that 2-AG controls adipose browning. However, we cannot discount the possibility that variations in 2-AG levels in critical brain areas contribute to phenotypic characteristics of ABHD6 KO mice that show slightly reduced appetite, a protection from high fat diet body weight increase and enhanced physical activity.

MAG and transient receptor potential vanilloid subfamily, member 1 (TRPV1)

TRPV1, a molecular integrator of inflammatory mediators, plays crucial roles in initiating neurogenic inflammatory response and transducing the pain in conjunction with emerging roles in energy metabolism (Szallasi et al., 2007). TRPV1 was the first protein to be cloned in the large TRP family and similar to other TRP channels, TRPV1 has a putative six-transmembrane-spanning protein, and its pore region is localized between transmembrane domains 5 and 6. TRPV1 is a non-selective calcium channel, which accounts for many functions within the cells.

TRPV1 can be activated by many agents, such as capsaicin and anandamide. Among all the activators, MAG, especially the ones with unsaturated fatty acid chain, can activate TRPV1 with about half of the affinity of capsaicin. Feeding mice with a combination of MAGs with mono- and poly-unsaturated fatty acid side chains was shown to increase UCP1 levels in brown adipocytes and prevent diet-induced obesity (Iwasaki et al., 2011), and it was suggested that TRPV1 mediates this effect. However, there was no direct evidence for this claim and this

does not contradict our data indicating that MAG induced browning is mediated by PPARα and PPARγ.

In our own studies, we noticed that the stimulating effect of MAG on insulin secretion in INS832/13 cells is antagonized by a specific TRPV1 antagonist AMG9810, indicating the MAG partially acts via TRPV1 to promote insulin secretion in INS cells. INS832/13 cell line is a cancer cell line, derived from tumors of rat pancreatic islets and thus does not truly represent normal beta cells, with respect to the expression several genes. Also, the effect of the inhibitor on GSIS may be non-specific. We tested GSIS in TRPV1 KO mice and found it to be unaltered *in vivo* and *ex-vivo*. Thus, even though TRPV1 function is discernable in INS cells, it is very poorly expressed in the beta cells of mouse and rat islets, and because of this the above drug effects are not seen in mouse and rat islets. Hence, MAG and ABHD6 suppression effects in normal ß-cells are not mediated by TRPV1 but rather via munc13-1. Consistent with this view we report that the glucose induced rise in cytosolic Ca2+ is unaltered in islet from beta-cell specific KO mice.

MAG and G protein-coupled receptor 119 (GPR119)

As a novel endocannabinoid receptor, GPR119 is regarded as a promising drug target for treating obesity and T2D. It is predominantly expressed in the gastrointestinal tract and in the endocrine pancreas, to a lesser extent, in the brain (Godlewski et al., 2009). Activation of GPR119 reduces food intake and body weight gain possibly through changes in incretin and insulin secretion (Overton et al., 2006). Some endogenous lipid ligands, such as oleoyl-lysophosphatidylcholine and oleoylethanolamide (OEA), have been shown to activate GPR119, and promote insulin secretion in the islets (Ning et al., 2008). Recently, some MAG species such as 2-oleoylglycerol, 1-oleoylglycerol, 2-palmitoylglycerol and 2-linoleoylglycerol were shown to act as ligands of GPR119, and administration of 2-oleoylglycerol to humans was found to increase incretin secretion (Hansen et al., 2011). Whether GPR119 activation contributes to insulin secretion changes and benefic effects on energy homeostasis in ABHD6-KO mice is a possibility to consider.

MAG and Munc13-1

Exocytosis processes in different cells, such as neurotransmitter release, insulin secretion and catecholamine release, are regulated by the core of membrane fusion machinery. This machinery consists of "SNARE complex", including syntaxin-1, SNAP-25 and synaptobrevin (Leung et al., 2007). Munc13-1 is a synaptic protein that regulates the SNARE complex assembly and it is regarded as the major protein that determines the priming of synaptic vesicles (Guan et al., 2008). Munc13-1 is essential for fusion competence of neurotransmitter and insulin granules (Augustin et al., 1999; Sheu et al., 2003). It was suggested that Munc13-1 functions as a DAG receptor, and is responsible for DAG-induced augmentation of transmitter release (Rhee et al., 2002). However, unlike the DAG binding site C1-domain seen in classical PKC enzymes, the C1 domain of Munc13-1 is occluded by a conserved tryptophan side chain and requires a considerable conformational change for DAG binding. As a consequence, DAG binds Munc13-1 C1 domain with lower affinity compared to PKC, and possibly other lipid ligands are more important for Munc13-1 function (Shen et al., 2005). We proposed that since MAG has a similar structure as DAG and of special importance, it possesses only one fatty acid chain and thus may have easier access to Munc13-1 C1 domain, then MAG is more important than DAG for Munc13-1 regulation. Our *in vitro* assays supported this hypothesis and MAG shows better affinity than DAG to C1-domain of Munc13-1, and thus Munc13-1 is also a MAG receptor and likely responsible for MAG-induced increased insulin secretion in INS cells, and rodent and human islets (Zhao et al., 2014). Moreover, MAG can induce the translocation of Munc13-1 from cytosol to plasma membrane. However, there is little evidence regarding the role of MAG in neurotransmitter release. We speculate that increasing MAG levels by specific inhibitors or by genetic manipulation of MAG degrading enzymes may also play crucial roles in regulating neurotransmitter release.

MAG and protein kinase C

PKC belongs to a super family of protein kinase enzymes that function in signal transduction through phosphorylation of serine and threonine residues on target proteins. PKC enzymes are divided into 3 subgroups, classical PKC, novel PKC and atypical PKC (Quest, 1996). It is well accepted that DAG can activate classical and novel PKC by binding to their C1 domains. DAG-activated PKC in muscle and liver are thought to be responsible for insulin resistance seen in obesity and T2D (Samuel and Shulman, 2012). Our results showed that MAG can bind

to the C1 domain of Munc13-1; however, whether MAG also binds to PKC C1-domain and affect PKC activity is still unknown. This is an interesting avenue of research to pursue to enhance our understanding of the biochemical basis of insulin resistance.

MAG and the peroxisome proliferator-activated receptors

PPARs are a group of nuclear receptors that control cell functions through regulating other gene expressions. Among all three PPAR, PPARα and PPARγ are already shown to be drug targets, as PPARα and PPARγ agonists are already in the drug market. However, great concerns with their use in humans have recently being raised (Cariou et al., 2012). Recent studies have shown that agonists of PPARα and PPARγ can trigger browning of white adipocytes (Wang et al., 2013b). To better understand how PPARs act within cells, the identification of the endogenous ligands is of special importance. Besides FFA, more endogenous ligands exist in the lipolysis process, as decreasing ATGL activity in the heart, brown adipocytes and islets greatly reduced PPARα and PPARγ activity, indicating the existence of some endogenous ligands produced downstream of TG hydrolysis (Mottillo et al., 2012). Still we do not know whether other specific lipid based metabolites, other than FFA, could function as physiological ligands of PPARs. With luciferase gene reporter assay in 293T cells, we have shown that MAG can transactivate PPARα and PPARγ, but not PPARβ, indicating that MAG produced in the lipolysis process may be a novel ligand for PPARs (Article 3). Furthermore, using PPAR-Gal4 assay, we have confirmed direct binding effect of 1-MAG and PPARα and PPARγ (Article 3). Of special interest, it seems that MAG could function as the natural/ physiological PPARα and PPARγ dual agonist. In the adipocytes from HFD-fed ABHD6 KO mice, PPARα and PPARγ levels and also MAG levels are elevated, resulting in increased UCP1 expression and browning of white adipocytes. PPARα and PPARγ antagonism by specific inhibitors curtails the browning effects induced by 1-oleoylglycerol and the ABHD6 inhibitor WWL70. *In vivo* administration of PPARα antagonist to female whole body ABHD6-KO mice completely diminishes the browning effect in adipocytes and decreased non-shivering thermogenesis and partially restored body weight gain (Article 3). All this data strongly supports the view that lipolysis-derived MAG controls adipose tissue browning via PPARα and PPARγ.

Conclusion and therapeutic implication

The results presented in this thesis clearly indicate that ABHD6-accessible 1-MAG plays important roles in regulating insulin secretion by activation of Munc13-1 in beta-cells and regulates adipose tissues function as related to thermogenesis.

Thus, collectively our results demonstrate that ABHD6 regulates fuel homeostasis, white adipose browning and brown adipose function. The mechanism of adipose tissue browning appears to involve 1-MAG acting as an intrinsic cell autonomous signal that causes PPARα and PPARγ activation in adipose tissues. ABHD6 inhibition may provide a unique therapeutic approach for both lean and obese T2D. Indeed, we have shown that ABHD6 inhibition in the low dose streptozotocin lean model of T2D restores normal glucose tolerance via enhanced insulin secretion (Zhao et al., 2014). Subsequently we have shown in obese mice with hyperglycemia and marked glucose intolerance that ABHD6 deficiency reduces body weight gain, improves glucose homeostasis and insulin action together with mild reduction in appetite and enhanced locomotor activity. Targeting ABHD6 offers a novel avenue to develop both anti-obesity and T2D drugs.

3. Perspectives

The exciting observations made from whole body and tissue specific ABHD6 KO mice place 1-MAG as a crucial regulator of glucose and insulin homeostasis and energy metabolism via binding with some receptors, such as PPARα, PPARγ and Munc13-1 (Figure 12 and 13) to exert its functions. Much is still unknown regarding the role of ABHD6-accessible MAG and further work is required in this regard.

As MAG is a key metabolic coupling factor in fuel and non-fuel-induced insulin secretion, whether increasing MAG levels in pancreatic islets could reverse the insulin secretion defects observed in T2D? It is well-known that the islets isolated from type 2 diabetes models secrete less insulin in response to both fuel and non-fuel stimulation. Under situations of T2D, the MAG levels in these islets are likely decreased, as impaired GL/FFA cycling occurs in these islets and increased intracelluar TG leves. Also, ABHD6 level in these islets may be increased similar as in muscle, liver and adipose in response to high fat diet feeding (Article 3). Based on these observations, we hypothesize that decreased MAG level is at least partially

responsible for the insulin secretion defect in islets from diabetic animals and thus restoration of MAG levels by decreasing ABHD6 activity may be a valuable avenue to treat T2D. In order to directly test this hypothesis, we will place inducible beta cell specific ABHD6 KO mice on HFD, and we will induce ABHD6 deletion by tamoxifen injection only when hyperglycemia occurs in both control and beta cell specific KO mice. 8 weeks after tamoxifen injection, we will assess insulin secretion and MAG levels as well as specific MAG species. We expect to see that beta cell specific ABHD6 mice could reverse the insulin secretion defect and restore normal glycemia after deletion of ABHD6.

Besides the role in beta cells, we will use adipose tissue specific ABHD6 KO mice to further explore the browning mechanisms. In order to focus on the browning aspect, we will employ adiponectin-cre to generate adipose tissue specific KO mice. And we will characterize the phenotype of these mice and role of PPARs in the browning process. Of special importance, we will measure brown fat mass in control and adipose tissue specific ABHD6 KO mice. Moreover, in the adipose tissue isolated from whole body ABHD6 KO mice, we have noticed greatly increased browning effect, while there is no significant increase in fatty acid oxidation. However, these measurements were made using tissue explants and need to be verified by using isolated adipocytes to avoid uneven distribution of substrates. We also need to verify if there is any change in mitochondrial content in the beige adipocytes from ABHD6-KO mice. Besides this, we will also use positron emission tomography, which has been successfully applied to human studies to quantify the FFA flux (Noll et al., 2015). We will also assess the involvement of ABHD6-assessible MAG in adipokine secretion. Adipose tissues communicate with other organs in large part by adipokines. Since adipokines regulate insulin sensitivity and inflammation it is important to understand the role of ABHD6 and MAG in this process as these factors alter the phenotype of white adipocyte. Our results indicated that whole body ABHD6 KO mice do show altered plasma FGF21, resistin and IGFBP1, suggesting altered adipokine secretion (Article 3).

Furthermore, as we have shown direct binding effect of MAG with PPARα, it will be highly interesting to investigate its role in liver, as high PPARα activity is observed in the liver. It has been reported that decreased fatty acid oxidation is one of the reported mechanisms for fatty liver (Reddy and Rao, 2006). As increasing MAG levels activate PPARα to increase fatty acid

oxidation, liver specific ABHD6 KO mice are likely protected from fatty liver and insulin resistance by the elevated MAG.

Also, increasing locomotor activity is an efficient way to increase energy expenditure, and in female ABHD6 KO mice, locomotor activity is increased. What is relative contribution of increased locomotor activity to energy expenditure? At present we did not test this hypothesis directly. As locomotor activity is largely regulated by CNS, we examined if these KO mice suffer from anxiety or depressive behavior and found such is not to be the case. It has been reported that increased exercise is associated with elevated irisin secretion, and irisin is reported as a strong browning agent at least in rodent models (Bostrom et al., 2012). So whether increased irisin levels could be causing the observed browning effects in ABHD6 KO mice needs to be examined. However, we speculate that irisin may play minor, if any, effect on browning effect. The reason for this is that increased heat production in male ABHD6 KO mice is not associated with elevated locomotor activity In order to directly examine this we will measure irisin levels in both male and female ABHD6-KO mice in light and dark phases.

Besides the role of ABHD6 in MAG hydrolysis, MAGL and MGAT also contribute to total MAG metabolism. Thus, it will be interesting to assess the relative contribution of different enzymes in MAG depletion in various cell types, and how this affects the physiological functionality of the corresponding cell, its insulin sensitivity.

The fact that ABHD6 KO mice show reduced food intake suggests a possible CNS role of this enzyme in energy homeostasis. It will be of interest to assess the role of this enzyme in various brain areas regulating food intake and reward in particular the arcuate and ventromedial nuclei of the hypothalamus and the nucleus acumbens. We are currently studying this in collaboration with neurophysiologists.

Considering the beneficial effects in inhibiting of ABHD6 in glucose and energy metabolism, search for more specific and powerful inhibitor for this enzyme may provide novel choices to develop different class of drugs against obesity and T2D. Currently, our lab is screening for more specific and potent inhibitors of ABHD6 with the possible development of these inhibitors as anti-diabetic drugs.

4. References

(1998). Tight blood pressure control and risk of macrovascular and microvascular complications in type 2 diabetes: UKPDS 38. UK Prospective Diabetes Study Group. Bmj *317*, 703-713.

Agarwal, A.K., Sukumaran, S., Cortes, V.A., Tunison, K., Mizrachi, D., Sankella, S., Gerard, R.D., Horton, J.D., and Garg, A. (2011). Human 1-acylglycerol-3-phosphate O-acyltransferase isoforms 1 and 2: biochemical characterization and inability to rescue hepatic steatosis in Agpat2(-/-) gene lipodystrophic mice. The Journal of biological chemistry *286*, 37676-37691.

Ahfeldt, T., Schinzel, R.T., Lee, Y.K., Hendrickson, D., Kaplan, A., Lum, D.H., Camahort, R., Xia, F., Shay, J., Rhee, E.P., et al. (2012). Programming human pluripotent stem cells into white and brown adipocytes. Nature cell biology *14*, 209-219.

Ahmadian, M., Abbott, M.J., Tang, T., Hudak, C.S., Kim, Y., Bruss, M., Hellerstein, M.K., Lee, H.Y., Samuel, V.T., Shulman, G.I., et al. (2011). Desnutrin/ATGL is regulated by AMPK and is required for a brown adipose phenotype. Cell metabolism *13*, 739-748.

Alappat, L., and Awad, A.B. (2010). Curcumin and obesity: evidence and mechanisms. Nutrition reviews *68*, 729-738.

Alberti, K.G., Christensen, N.J., Christensen, S.E., Hansen, A.P., Iversen, J., Lundbaek, K., Seyer-Hansen, K., and Orskov, H. (1973). Inhibition of insulin secretion by somatostatin. Lancet *2*, 1299-1301.

Alfadda, A.A., and Sallam, R.M. (2012). Reactive oxygen species in health and disease. Journal of biomedicine & biotechnology *2012*, 936486.

Alhouayek, M., Masquelier, J., Cani, P.D., Lambert, D.M., and Muccioli, G.G. (2013). Implication of the anti-inflammatory bioactive lipid prostaglandin D2-glycerol ester in the control of macrophage activation and inflammation by ABHD6. Proceedings of the National Academy of Sciences of the United States of America *110*, 17558-17563.

Amati, F. (2012). Revisiting the diacylglycerol-induced insulin resistance hypothesis. Obesity reviews : an official journal of the International Association for the Study of Obesity *13 Suppl 2*, 40-50.

Amos, A.F., McCarty, D.J., and Zimmet, P. (1997). The rising global burden of diabetes and its complications: estimates and projections to the year 2010. Diabetic medicine : a journal of the British Diabetic Association *14 Suppl 5*, S1-85.

Anis, A.H., Zhang, W., Bansback, N., Guh, D.P., Amarsi, Z., and Birmingham, C.L. (2010). Obesity and overweight in Canada: an updated cost-of-illness study. Obesity reviews : an official journal of the International Association for the Study of Obesity *11*, 31-40.

Apovian, C.M., Bigornia, S., Mott, M., Meyers, M.R., Ulloor, J., Gagua, M., McDonnell, M., Hess, D., Joseph, L., and Gokce, N. (2008). Adipose macrophage infiltration is associated with insulin resistance and vascular endothelial dysfunction in obese subjects. Arteriosclerosis, thrombosis, and vascular biology *28*, 1654-1659.

Arkan, M.C., Hevener, A.L., Greten, F.R., Maeda, S., Li, Z.W., Long, J.M., Wynshaw-Boris, A., Poli, G., Olefsky, J., and Karin, M. (2005). IKK-beta links inflammation to obesity-induced insulin resistance. Nature medicine *11*, 191-198.

Arner, P., and Langin, D. (2014). Lipolysis in lipid turnover, cancer cachexia, and obesity-induced insulin resistance. Trends in endocrinology and metabolism: TEM *25*, 255-262.
Ashcroft, F.M., and Rorsman, P. (2012). Diabetes mellitus and the beta cell: the last ten years. Cell *148*, 1160-1171.
Ashcroft, F.M., and Rorsman, P. (2013). K(ATP) channels and islet hormone secretion: new insights and controversies. Nature reviews. Endocrinology *9*, 660-669.
Astrup, A., and Finer, N. (2000). Redefining type 2 diabetes: 'diabesity' or 'obesity dependent diabetes mellitus'? Obesity reviews : an official journal of the International Association for the Study of Obesity *1*, 57-59.
Attane, C., Daviaud, D., Dray, C., Dusaulcy, R., Masseboeuf, M., Prevot, D., Carpene, C., Castan-Laurell, I., and Valet, P. (2011). Apelin stimulates glucose uptake but not lipolysis in human adipose tissue ex vivo. Journal of molecular endocrinology *46*, 21-28.
Attane, C., Foussal, C., Le Gonidec, S., Benani, A., Daviaud, D., Wanecq, E., Guzman-Ruiz, R., Dray, C., Bezaire, V., Rancoule, C., et al. (2012). Apelin treatment increases complete Fatty Acid oxidation, mitochondrial oxidative capacity, and biogenesis in muscle of insulin-resistant mice. Diabetes *61*, 310-320.
Auboeuf, D., Rieusset, J., Fajas, L., Vallier, P., Frering, V., Riou, J.P., Staels, B., Auwerx, J., Laville, M., and Vidal, H. (1997). Tissue distribution and quantification of the expression of mRNAs of peroxisome proliferator-activated receptors and liver X receptor-alpha in humans: no alteration in adipose tissue of obese and NIDDM patients. Diabetes *46*, 1319-1327.
Augustin, I., Rosenmund, C., Sudhof, T.C., and Brose, N. (1999). Munc13-1 is essential for fusion competence of glutamatergic synaptic vesicles. Nature *400*, 457-461.
Bachovchin, D.A., Ji, T., Li, W., Simon, G.M., Blankman, J.L., Adibekian, A., Hoover, H., Niessen, S., and Cravatt, B.F. (2010). Superfamily-wide portrait of serine hydrolase inhibition achieved by library-versus-library screening. Proceedings of the National Academy of Sciences of the United States of America *107*, 20941-20946.
Badin, P.M., Loubiere, C., Coonen, M., Louche, K., Tavernier, G., Bourlier, V., Mairal, A., Rustan, A.C., Smith, S.R., Langin, D., et al. (2012). Regulation of skeletal muscle lipolysis and oxidative metabolism by the co-lipase CGI-58. Journal of lipid research *53*, 839-848.
Badman, M.K., Pissios, P., Kennedy, A.R., Koukos, G., Flier, J.S., and Maratos-Flier, E. (2007). Hepatic fibroblast growth factor 21 is regulated by PPARalpha and is a key mediator of hepatic lipid metabolism in ketotic states. Cell metabolism *5*, 426-437.
Bagchi, M., Kim, L.A., Boucher, J., Walshe, T.E., Kahn, C.R., and D'Amore, P.A. (2013). Vascular endothelial growth factor is important for brown adipose tissue development and maintenance. FASEB journal : official publication of the Federation of American Societies for Experimental Biology *27*, 3257-3271.
Baillot, A., Pelletier, C., Dunbar, P., Geiss, L., Johnson, J.A., Leiter, L.A., and Langlois, M.F. (2014). Profile of adults with type 2 diabetes and uptake of clinical care best practices: results from the 2011 Survey on Living with Chronic Diseases in Canada - Diabetes component. Diabetes research and clinical practice *103*, 11-19.
Balthasar, N., Coppari, R., McMinn, J., Liu, S.M., Lee, C.E., Tang, V., Kenny, C.D., McGovern, R.A., Chua, S.C., Jr., Elmquist, J.K., et al. (2004). Leptin receptor signaling in POMC neurons is required for normal body weight homeostasis. Neuron *42*, 983-991.

Barker, C.J., Illies, C., Fiume, R., Gaboardi, G.C., Yu, J., and Berggren, P.O. (2009). Diphosphoinositol pentakisphosphate as a novel mediator of insulin exocytosis. Advances in enzyme regulation *49*, 168-173.
Barneda, D., Frontini, A., Cinti, S., and Christian, M. (2013). Dynamic changes in lipid droplet-associated proteins in the "browning" of white adipose tissues. Biochimica et biophysica acta *1831*, 924-933.
Bates, S.H., Stearns, W.H., Dundon, T.A., Schubert, M., Tso, A.W., Wang, Y., Banks, A.S., Lavery, H.J., Haq, A.K., Maratos-Flier, E., et al. (2003). STAT3 signalling is required for leptin regulation of energy balance but not reproduction. Nature *421*, 856-859.
Battista, N., Di Tommaso, M., Bari, M., and Maccarrone, M. (2012). The endocannabinoid system: an overview. Frontiers in behavioral neuroscience *6*, 9.
Begriche, K., Massart, J., and Fromenty, B. (2010). Effects of beta-aminoisobutyric acid on leptin production and lipid homeostasis: mechanisms and possible relevance for the prevention of obesity. Fundamental & clinical pharmacology *24*, 269-282.
Ben-Shabat, S., Fride, E., Sheskin, T., Tamiri, T., Rhee, M.H., Vogel, Z., Bisogno, T., De Petrocellis, L., Di Marzo, V., and Mechoulam, R. (1998). An entourage effect: inactive endogenous fatty acid glycerol esters enhance 2-arachidonoyl-glycerol cannabinoid activity. European journal of pharmacology *353*, 23-31.
Benjamin, D.I., Cravatt, B.F., and Nomura, D.K. (2012). Global profiling strategies for mapping dysregulated metabolic pathways in cancer. Cell metabolism *16*, 565-577.
Berggren, P.O., and Barker, C.J. (2008). A key role for phosphorylated inositol compounds in pancreatic beta-cell stimulus-secretion coupling. Advances in enzyme regulation *48*, 276-294.
Berry, R., and Rodeheffer, M.S. (2013). Characterization of the adipocyte cellular lineage in vivo. Nature cell biology *15*, 302-308.
Bisogno, T., Howell, F., Williams, G., Minassi, A., Cascio, M.G., Ligresti, A., Matias, I., Schiano-Moriello, A., Paul, P., Williams, E.J., et al. (2003). Cloning of the first sn1-DAG lipases points to the spatial and temporal regulation of endocannabinoid signaling in the brain. The Journal of cell biology *163*, 463-468.
Blankman, J.L., Long, J.Z., Trauger, S.A., Siuzdak, G., and Cravatt, B.F. (2013). ABHD12 controls brain lysophosphatidylserine pathways that are deregulated in a murine model of the neurodegenerative disease PHARC. Proceedings of the National Academy of Sciences of the United States of America *110*, 1500-1505.
Blankman, J.L., Simon, G.M., and Cravatt, B.F. (2007a). A comprehensive profile of brain enzymes that hydrolyze the endocannabinoid 2-arachidonoylglycerol. Chemistry & biology *14*, 1347-1356.
Blankman, J.L., Simon, G.M., and Cravatt, B.F. (2007b). A comprehensive profile of brain enzymes that hydrolyze the endocannabinoid 2-arachidonoylglycerol. Chemistry and Biology *14*, 1347-1356.
Blondin, D.P., Labbe, S.M., Noll, C., Kunach, M., Phoenix, S., Guerin, B., Turcotte, E.E., Haman, F., Richard, D., and Carpentier, A.C. (2015). Selective impairment of glucose, but not fatty acid or oxidative metabolism in brown adipose tissue of subjects with type 2 diabetes. Diabetes.

Bonet, M.L., Oliver, P., and Palou, A. (2013). Pharmacological and nutritional agents promoting browning of white adipose tissue. Biochimica et biophysica acta *1831*, 969-985.
Bonet, M.L., Ribot, J., and Palou, A. (2012). Lipid metabolism in mammalian tissues and its control by retinoic acid. Biochimica et biophysica acta *1821*, 177-189.
Boni-Schnetzler, M., Thorne, J., Parnaud, G., Marselli, L., Ehses, J.A., Kerr-Conte, J., Pattou, F., Halban, P.A., Weir, G.C., and Donath, M.Y. (2008). Increased interleukin (IL)-1beta messenger ribonucleic acid expression in beta -cells of individuals with type 2 diabetes and regulation of IL-1beta in human islets by glucose and autostimulation. The Journal of clinical endocrinology and metabolism *93*, 4065-4074.
Bordicchia, M., Liu, D., Amri, E.Z., Ailhaud, G., Dessi-Fulgheri, P., Zhang, C., Takahashi, N., Sarzani, R., and Collins, S. (2012). Cardiac natriuretic peptides act via p38 MAPK to induce the brown fat thermogenic program in mouse and human adipocytes. The Journal of clinical investigation *122*, 1022-1036.
Borghouts, L.B., and Keizer, H.A. (2000). Exercise and insulin sensitivity: a review. International journal of sports medicine *21*, 1-12.
Bostrom, P., Wu, J., Jedrychowski, M.P., Korde, A., Ye, L., Lo, J.C., Rasbach, K.A., Bostrom, E.A., Choi, J.H., Long, J.Z., et al. (2012). A PGC1-alpha-dependent myokine that drives brown-fat-like development of white fat and thermogenesis. Nature *481*, 463-468.
Boyd, A.E., 3rd, and Moss, L.G. (1993). When sugar is not so sweet: glucose toxicity. The Journal of clinical investigation *92*, 2.
Boyd, S.T. (2006). The endocannabinoid system. Pharmacotherapy *26*, 218S-221S.
Bozza, P.T., Bakker-Abreu, I., Navarro-Xavier, R.A., and Bandeira-Melo, C. (2011). Lipid body function in eicosanoid synthesis: an update. Prostaglandins, leukotrienes, and essential fatty acids *85*, 205-213.
Braissant, O., Foufelle, F., Scotto, C., Dauca, M., and Wahli, W. (1996). Differential expression of peroxisome proliferator-activated receptors (PPARs): tissue distribution of PPAR-alpha, -beta, and -gamma in the adult rat. Endocrinology *137*, 354-366.
Bratanova-Tochkova, T.K., Cheng, H., Daniel, S., Gunawardana, S., Liu, Y.J., Mulvaney-Musa, J., Schermerhorn, T., Straub, S.G., Yajima, H., and Sharp, G.W. (2002). Triggering and augmentation mechanisms, granule pools, and biphasic insulin secretion. Diabetes *51 Suppl 1*, S83-90.
Briaud, I., Rouault, C., Reach, G., and Poitout, V. (1999). Long-term exposure of isolated rat islets of Langerhans to supraphysiologic glucose concentrations decreases insulin mRNA levels. Metabolism: clinical and experimental *48*, 319-323.
Brooks, G.A. (2009). Cell-cell and intracellular lactate shuttles. The Journal of physiology *587*, 5591-5600.
Brun, T., Roche, E., Assimacopoulos-Jeannet, F., Corkey, B.E., Kim, K.H., and Prentki, M. (1996). Evidence for an anaplerotic/malonyl-CoA pathway in pancreatic beta-cell nutrient signaling. Diabetes *45*, 190-198.
Buteau, J., El-Assaad, W., Rhodes, C.J., Rosenberg, L., Joly, E., and Prentki, M. (2004). Glucagon-like peptide-1 prevents beta cell glucolipotoxicity. Diabetologia *47*, 806-815.

Calkin, A.C., and Tontonoz, P. (2012). Transcriptional integration of metabolism by the nuclear sterol-activated receptors LXR and FXR. Nature reviews. Molecular cell biology *13*, 213-224.
Cannon, B., and Nedergaard, J. (2004). Brown adipose tissue: function and physiological significance. Physiological reviews *84*, 277-359.
Cao, J., Cheng, L., and Shi, Y. (2007). Catalytic properties of MGAT3, a putative triacylglycerol synthase. Journal of lipid research *48*, 583-591.
Capurso, C., and Capurso, A. (2012). From excess adiposity to insulin resistance: the role of free fatty acids. Vascular pharmacology *57*, 91-97.
Cariou, B., Charbonnel, B., and Staels, B. (2012). Thiazolidinediones and PPARgamma agonists: time for a reassessment. Trends in endocrinology and metabolism: TEM *23*, 205-215.
Caro, J.F., Kolaczynski, J.W., Nyce, M.R., Ohannesian, J.P., Opentanova, I., Goldman, W.H., Lynn, R.B., Zhang, P.L., Sinha, M.K., and Considine, R.V. (1996). Decreased cerebrospinal-fluid/serum leptin ratio in obesity: a possible mechanism for leptin resistance. Lancet *348*, 159-161.
Carpentier, A., Mittelman, S.D., Lamarche, B., Bergman, R.N., Giacca, A., and Lewis, G.F. (1999). Acute enhancement of insulin secretion by FFA in humans is lost with prolonged FFA elevation. The American journal of physiology *276*, E1055-1066.
Carriere, A., Jeanson, Y., Berger-Muller, S., Andre, M., Chenouard, V., Arnaud, E., Barreau, C., Walther, R., Galinier, A., Wdziekonski, B., et al. (2014). Browning of white adipose cells by intermediate metabolites: an adaptive mechanism to alleviate redox pressure. Diabetes *63*, 3253-3265.
Cederberg, A., Gronning, L.M., Ahren, B., Tasken, K., Carlsson, P., and Enerback, S. (2001). FOXC2 is a winged helix gene that counteracts obesity, hypertriglyceridemia, and diet-induced insulin resistance. Cell *106*, 563-573.
Cereijo, R., Giralt, M., and Villarroya, F. (2014). Thermogenic brown and beige/brite adipogenesis in humans. Annals of medicine, 1-9.
Cerk, I.K., Salzburger, B., Boeszoermenyi, A., Heier, C., Pillip, C., Romauch, M., Schweiger, M., Cornaciu, I., Lass, A., Zimmermann, R., et al. (2014). A peptide derived from G0/G1 switch gene 2 acts as noncompetitive inhibitor of adipose triglyceride lipase. The Journal of biological chemistry *289*, 32559-32570.
Chechi, K., Carpentier, A.C., and Richard, D. (2013). Understanding the brown adipocyte as a contributor to energy homeostasis. Trends in endocrinology and metabolism: TEM *24*, 408-420.
Cheng, D., Nelson, T.C., Chen, J., Walker, S.G., Wardwell-Swanson, J., Meegalla, R., Taub, R., Billheimer, J.T., Ramaker, M., and Feder, J.N. (2003). Identification of acyl coenzyme A:monoacylglycerol acyltransferase 3, an intestinal specific enzyme implicated in dietary fat absorption. The Journal of biological chemistry *278*, 13611-13614.
Cheon, H.G., and Cho, Y.S. (2014). Protection of palmitic acid-mediated lipotoxicity by arachidonic acid via channeling of palmitic acid into triglycerides in C2C12. Journal of biomedical science *21*, 13.

Chimen, M., Kennedy, A., Nirantharakumar, K., Pang, T.T., Andrews, R., and Narendran, P. (2012). What are the health benefits of physical activity in type 1 diabetes mellitus? A literature review. Diabetologia *55*, 542-551.
Choi, Y.K., Kim, M.K., Bae, K.H., Seo, H.A., Jeong, J.Y., Lee, W.K., Kim, J.G., Lee, I.K., and Park, K.G. (2013). Serum irisin levels in new-onset type 2 diabetes. Diabetes research and clinical practice *100*, 96-101.
Cnop, M., Hannaert, J.C., Hoorens, A., Eizirik, D.L., and Pipeleers, D.G. (2001). Inverse relationship between cytotoxicity of free fatty acids in pancreatic islet cells and cellular triglyceride accumulation. Diabetes *50*, 1771-1777.
Cohen, P., Levy, J.D., Zhang, Y., Frontini, A., Kolodin, D.P., Svensson, K.J., Lo, J.C., Zeng, X., Ye, L., Khandekar, M.J., et al. (2014). Ablation of PRDM16 and beige adipose causes metabolic dysfunction and a subcutaneous to visceral fat switch. Cell *156*, 304-316.
Cohen, P., and Spiegelman, B.M. (2015). Brown and Beige Fat: Molecular Parts of a Thermogenic Machine. Diabetes *64*, 2346-2351.
Cortes, V.A., Curtis, D.E., Sukumaran, S., Shao, X., Parameswara, V., Rashid, S., Smith, A.R., Ren, J., Esser, V., Hammer, R.E., et al. (2009). Molecular mechanisms of hepatic steatosis and insulin resistance in the AGPAT2-deficient mouse model of congenital generalized lipodystrophy. Cell metabolism *9*, 165-176.
Cypess, A.M., Chen, Y.C., Sze, C., Wang, K., English, J., Chan, O., Holman, A.R., Tal, I., Palmer, M.R., Kolodny, G.M., et al. (2012). Cold but not sympathomimetics activates human brown adipose tissue in vivo. Proceedings of the National Academy of Sciences of the United States of America *109*, 10001-10005.
Cypess, A.M., Lehman, S., Williams, G., Tal, I., Rodman, D., Goldfine, A.B., Kuo, F.C., Palmer, E.L., Tseng, Y.H., Doria, A., et al. (2009). Identification and importance of brown adipose tissue in adult humans. The New England journal of medicine *360*, 1509-1517.
Dandona, P., Aljada, A., and Bandyopadhyay, A. (2004). Inflammation: the link between insulin resistance, obesity and diabetes. Trends in immunology *25*, 4-7.
Delghingaro-Augusto, V., Decary, S., Peyot, M.L., Latour, M.G., Lamontagne, J., Paradis-Isler, N., Lacharite-Lemieux, M., Akakpo, H., Birot, O., Nolan, C.J., et al. (2012). Voluntary running exercise prevents beta-cell failure in susceptible islets of the Zucker diabetic fatty rat. American journal of physiology. Endocrinology and metabolism *302*, E254-264.
Di Marzo, V., and Matias, I. (2005). Endocannabinoid control of food intake and energy balance. Nature neuroscience *8*, 585-589.
Diakogiannaki, E., Welters, H.J., and Morgan, N.G. (2008). Differential regulation of the endoplasmic reticulum stress response in pancreatic beta-cells exposed to long-chain saturated and monounsaturated fatty acids. The Journal of endocrinology *197*, 553-563.
Dirkx, E., van Eys, G.J., Schwenk, R.W., Steinbusch, L.K., Hoebers, N., Coumans, W.A., Peters, T., Janssen, B.J., Brans, B., Vogg, A.T., et al. (2014). Protein kinase-D1 overexpression prevents lipid-induced cardiac insulin resistance. Journal of molecular and cellular cardiology *76*, 208-217.
Dodd, G.T., Decherf, S., Loh, K., Simonds, S.E., Wiede, F., Balland, E., Merry, T.L., Munzberg, H., Zhang, Z.Y., Kahn, B.B., et al. (2015). Leptin and insulin act on POMC neurons to promote the browning of white fat. Cell *160*, 88-104.

Donath, M.Y. (2013). Targeting inflammation in the treatment of type 2 diabetes. Diabetes, obesity & metabolism *15 Suppl 3*, 193-196.
Douglass, J.D., Zhou, Y.X., Wu, A., Zadrogra, J.A., Gajda, A.M., Lackey, A.I., Lang, W., Chevalier, K.M., Sutton, S.W., Zhang, S.P., et al. (2015). Global deletion of MGL in mice delays lipid absorption and alters energy homeostasis and diet-induced obesity. Journal of lipid research *56*, 1153-1171.
Dowler, S., Kular, G., and Alessi, D.R. (2002). Protein lipid overlay assay. Sci STKE *2002*, pl6.
Dumortier, O., Hinault, C., Gautier, N., Patouraux, S., Casamento, V., and Van Obberghen, E. (2014). Maternal protein restriction leads to pancreatic failure in offspring: role of misexpressed microRNA-375. Diabetes *63*, 3416-3427.
Duttaroy, A., Zimliki, C.L., Gautam, D., Cui, Y., Mears, D., and Wess, J. (2004). Muscarinic stimulation of pancreatic insulin and glucagon release is abolished in m3 muscarinic acetylcholine receptor-deficient mice. Diabetes *53*, 1714-1720.
Ebbeling, C.B., Swain, J.F., Feldman, H.A., Wong, W.W., Hachey, D.L., Garcia-Lago, E., and Ludwig, D.S. (2012). Effects of dietary composition on energy expenditure during weight-loss maintenance. Jama *307*, 2627-2634.
Eichmann, T.O., Kumari, M., Haas, J.T., Farese, R.V., Jr., Zimmermann, R., Lass, A., and Zechner, R. (2012). Studies on the substrate and stereo/regioselectivity of adipose triglyceride lipase, hormone-sensitive lipase, and diacylglycerol-O-acyltransferases. The Journal of biological chemistry *287*, 41446-41457.
Eichmann, T.O., and Lass, A. (2015). DAG tales: the multiple faces of diacylglycerol-stereochemistry, metabolism, and signaling. Cellular and molecular life sciences : CMLS *72*, 3931-3952.
Eizirik, D.L., and Cnop, M. (2010). ER stress in pancreatic beta cells: the thin red line between adaptation and failure. Science signaling *3*, pe7.
Eizirik, D.L., and Darville, M.I. (2001). beta-cell apoptosis and defense mechanisms: lessons from type 1 diabetes. Diabetes *50 Suppl 1*, S64-69.
El-Assaad, W., Buteau, J., Peyot, M.L., Nolan, C., Roduit, R., Hardy, S., Joly, E., Dbaibo, G., Rosenberg, L., and Prentki, M. (2003). Saturated fatty acids synergize with elevated glucose to cause pancreatic beta-cell death. Endocrinology *144*, 4154-4163.
El-Assaad, W., El-Kouhen, K., Mohammad, A.H., Yang, J., Morita, M., Gamache, I., Mamer, O., Avizonis, D., Hermance, N., Kersten, S., et al. (2015). Deletion of the gene encoding G0/G 1 switch protein 2 (G0s2) alleviates high-fat-diet-induced weight gain and insulin resistance, and promotes browning of white adipose tissue in mice. Diabetologia *58*, 149-157.
El-Assaad, W., Joly, E., Barbeau, A., Sladek, R., Buteau, J., Maestre, I., Pepin, E., Zhao, S., Iglesias, J., Roche, E., et al. (2010). Glucolipotoxicity alters lipid partitioning and causes mitochondrial dysfunction, cholesterol, and ceramide deposition and reactive oxygen species production in INS832/13 ss-cells. Endocrinology *151*, 3061-3073.
El-Azzouny, M., Evans, C.R., Treutelaar, M.K., Kennedy, R.T., and Burant, C.F. (2014). Increased glucose metabolism and glycerolipid formation by fatty acids and GPR40 receptor signaling underlies the fatty acid potentiation of insulin secretion. The Journal of biological chemistry *289*, 13575-13588.

Eliasson, L., Abdulkader, F., Braun, M., Galvanovskis, J., Hoppa, M.B., and Rorsman, P. (2008). Novel aspects of the molecular mechanisms controlling insulin secretion. The Journal of physiology *586*, 3313-3324.
Enerback, S. (2010). Human brown adipose tissue. Cell metabolism *11*, 248-252.
Enerback, S., Jacobsson, A., Simpson, E.M., Guerra, C., Yamashita, H., Harper, M.E., and Kozak, L.P. (1997). Mice lacking mitochondrial uncoupling protein are cold-sensitive but not obese. Nature *387*, 90-94.
Eto, H., Kato, H., Suga, H., Aoi, N., Doi, K., Kuno, S., and Yoshimura, K. (2012). The fate of adipocytes after nonvascularized fat grafting: evidence of early death and replacement of adipocytes. Plastic and reconstructive surgery *129*, 1081-1092.
Even, P.C., and Nadkarni, N.A. (2012). Indirect calorimetry in laboratory mice and rats: principles, practical considerations, interpretation and perspectives. American journal of physiology. Regulatory, integrative and comparative physiology *303*, R459-476.
Fajans, S.S., Floyd, J.C., Jr., Knopf, R.F., and Conn, F.W. (1967). Effect of amino acids and proteins on insulin secretion in man. Recent progress in hormone research *23*, 617-662.
Fang, P., Bo, P., Shi, M., Yu, M., and Zhang, Z. (2013). Circulating galanin levels are increased in patients with gestational diabetes mellitus. Clinical biochemistry *46*, 831-833.
Farfari, S., Schulz, V., Corkey, B., and Prentki, M. (2000). Glucose-regulated anaplerosis and cataplerosis in pancreatic beta-cells: possible implication of a pyruvate/citrate shuttle in insulin secretion. Diabetes *49*, 718-726.
Fedorenko, A., Lishko, P.V., and Kirichok, Y. (2012). Mechanism of fatty-acid-dependent UCP1 uncoupling in brown fat mitochondria. Cell *151*, 400-413.
Fei, H., Zhao, B., Zhao, S., and Wang, Q. (2008). Requirements of calcium fluxes and ERK kinase activation for glucose- and interleukin-1beta-induced beta-cell apoptosis. Molecular and cellular biochemistry *315*, 75-84.
Feldmann, H.M., Golozoubova, V., Cannon, B., and Nedergaard, J. (2009). UCP1 ablation induces obesity and abolishes diet-induced thermogenesis in mice exempt from thermal stress by living at thermoneutrality. Cell metabolism *9*, 203-209.
Ferdaoussi, M., Bergeron, V., Zarrouki, B., Kolic, J., Cantley, J., Fielitz, J., Olson, E.N., Prentki, M., Biden, T., MacDonald, P.E., et al. (2012). G protein-coupled receptor (GPR)40-dependent potentiation of insulin secretion in mouse islets is mediated by protein kinase D1. Diabetologia *55*, 2682-2692.
Fernandez-Galilea, M., Perez-Matute, P., Prieto-Hontoria, P.L., Houssier, M., Burrell, M.A., Langin, D., Martinez, J.A., and Moreno-Aliaga, M.J. (2015). alpha-Lipoic acid treatment increases mitochondrial biogenesis and promotes beige adipose features in subcutaneous adipocytes from overweight/obese subjects. Biochimica et biophysica acta *1851*, 273-281.
Ferrara, N., Gerber, H.P., and LeCouter, J. (2003). The biology of VEGF and its receptors. Nature medicine *9*, 669-676.
Fex, M., Haemmerle, G., Wierup, N., Dekker-Nitert, M., Rehn, M., Ristow, M., Zechner, R., Sundler, F., Holm, C., Eliasson, L., et al. (2009). A beta cell-specific knockout of hormone-sensitive lipase in mice results in hyperglycaemia and disruption of exocytosis. Diabetologia *52*, 271-280.

Fisher, F.M., Kleiner, S., Douris, N., Fox, E.C., Mepani, R.J., Verdeguer, F., Wu, J., Kharitonenkov, A., Flier, J.S., Maratos-Flier, E., et al. (2012). FGF21 regulates PGC-1alpha and browning of white adipose tissues in adaptive thermogenesis. Genes & development *26*, 271-281.
Fontes, G., Zarrouki, B., Hagman, D.K., Latour, M.G., Semache, M., Roskens, V., Moore, P.C., Prentki, M., Rhodes, C.J., Jetton, T.L., et al. (2010). Glucolipotoxicity age-dependently impairs beta cell function in rats despite a marked increase in beta cell mass. Diabetologia *53*, 2369-2379.
Fredrikson, G., Stralfors, P., Nilsson, N.O., and Belfrage, P. (1981). Hormone-sensitive lipase of rat adipose tissue. Purification and some properties. The Journal of biological chemistry *256*, 6311-6320.
Fredrikson, G., Tornqvist, H., and Belfrage, P. (1986). Hormone-sensitive lipase and monoacylglycerol lipase are both required for complete degradation of adipocyte triacylglycerol. Biochimica et biophysica acta *876*, 288-293.
Fruchart, J.C., Duriez, P., and Staels, B. (1999). Peroxisome proliferator-activated receptor-alpha activators regulate genes governing lipoprotein metabolism, vascular inflammation and atherosclerosis. Current opinion in lipidology *10*, 245-257.
Fujioka, S., Matsuzawa, Y., Tokunaga, K., and Tarui, S. (1987). Contribution of intra-abdominal fat accumulation to the impairment of glucose and lipid metabolism in human obesity. Metabolism: clinical and experimental *36*, 54-59.
Fukami, A., Seino, Y., Ozaki, N., Yamamoto, M., Sugiyama, C., Sakamoto-Miura, E., Himeno, T., Takagishi, Y., Tsunekawa, S., Ali, S., et al. (2013). Ectopic expression of GIP in pancreatic beta-cells maintains enhanced insulin secretion in mice with complete absence of proglucagon-derived peptides. Diabetes *62*, 510-518.
Gao, M., Zhang, C., Ma, Y., and Liu, D. (2015). Cold Exposure Improves the Anti-diabetic Effect of T0901317 in Streptozotocin-Induced Diabetic Mice. The AAPS journal.
Gao, Y., Nelson, D.W., Banh, T., Yen, M.I., and Yen, C.L. (2013). Intestine-specific expression of MOGAT2 partially restores metabolic efficiency in Mogat2-deficient mice. Journal of lipid research *54*, 1644-1652.
Garcia Del Cano, G., Aretxabala, X., Gonzalez-Burguera, I., Montana, M., Lopez de Jesus, M., Barrondo, S., Barrio, R.J., Sampedro, C., Goicolea, M.A., and Salles, J. (2014). Nuclear diacylglycerol lipase-alpha in rat brain cortical neurons: evidence of 2-arachidonoylglycerol production in concert with phospholipase C-beta activity. Journal of neurochemistry.
Gauthier, B.R., and Wollheim, C.B. (2008). Synaptotagmins bind calcium to release insulin. American journal of physiology. Endocrinology and metabolism *295*, E1279-1286.
Gauthier, M.S., O'Brien, E.L., Bigornia, S., Mott, M., Cacicedo, J.M., Xu, X.J., Gokce, N., Apovian, C., and Ruderman, N. (2011). Decreased AMP-activated protein kinase activity is associated with increased inflammation in visceral adipose tissue and with whole-body insulin resistance in morbidly obese humans. Biochemical and biophysical research communications *404*, 382-387.
Gembal, M., Gilon, P., and Henquin, J.C. (1992). Evidence that glucose can control insulin release independently from its action on ATP-sensitive K+ channels in mouse B cells. The Journal of clinical investigation *89*, 1288-1295.

Ghosh, A., Ronner, P., Cheong, E., Khalid, P., and Matschinsky, F.M. (1991). The role of ATP and free ADP in metabolic coupling during fuel-stimulated insulin release from islet beta-cells in the isolated perfused rat pancreas. The Journal of biological chemistry *266*, 22887-22892.
Gillis, K.D., Mossner, R., and Neher, E. (1996). Protein kinase C enhances exocytosis from chromaffin cells by increasing the size of the readily releasable pool of secretory granules. Neuron *16*, 1209-1220.
Godlewski, G., Offertaler, L., Wagner, J.A., and Kunos, G. (2009). Receptors for acylethanolamides-GPR55 and GPR119. Prostaglandins & other lipid mediators *89*, 105-111.
Gopel, S., Kanno, T., Barg, S., Galvanovskis, J., and Rorsman, P. (1999). Voltage-gated and resting membrane currents recorded from B-cells in intact mouse pancreatic islets. The Journal of physiology *521 Pt 3*, 717-728.
Green, C.D., Jump, D.B., and Olson, L.K. (2009). Elevated insulin secretion from liver X receptor-activated pancreatic beta-cells involves increased de novo lipid synthesis and triacylglyceride turnover. Endocrinology *150*, 2637-2645.
Gremlich, S., Bonny, C., Waeber, G., and Thorens, B. (1997). Fatty acids decrease IDX-1 expression in rat pancreatic islets and reduce GLUT2, glucokinase, insulin, and somatostatin levels. The Journal of biological chemistry *272*, 30261-30269.
Grundlingh, J., Dargan, P.I., El-Zanfaly, M., and Wood, D.M. (2011). 2,4-dinitrophenol (DNP): a weight loss agent with significant acute toxicity and risk of death. Journal of medical toxicology : official journal of the American College of Medical Toxicology *7*, 205-212.
Guan, R., Dai, H., and Rizo, J. (2008). Binding of the Munc13-1 MUN domain to membrane-anchored SNARE complexes. Biochemistry *47*, 1474-1481.
Guariguata, L., Whiting, D.R., Hambleton, I., Beagley, J., Linnenkamp, U., and Shaw, J.E. (2014). Global estimates of diabetes prevalence for 2013 and projections for 2035. Diabetes research and clinical practice *103*, 137-149.
Guay, C., Madiraju, S.R., Aumais, A., Joly, E., and Prentki, M. (2007). A role for ATP-citrate lyase, malic enzyme, and pyruvate/citrate cycling in glucose-induced insulin secretion. The Journal of biological chemistry *282*, 35657-35665.
Guay, C., and Regazzi, R. (2013). Circulating microRNAs as novel biomarkers for diabetes mellitus. Nature reviews. Endocrinology *9*, 513-521.
Guenifi, A., Simonsson, E., Karlsson, S., Ahren, B., and Abdel-Halim, S.M. (2001). Carbachol restores insulin release in diabetic GK rat islets by mechanisms largely involving hydrolysis of diacylglycerol and direct interaction with the exocytotic machinery. Pancreas *22*, 164-171.
Gunawardana, S.C., and Piston, D.W. (2012). Reversal of type 1 diabetes in mice by brown adipose tissue transplant. Diabetes *61*, 674-682.
Gunawardana, S.C., and Piston, D.W. (2015). Insulin-independent reversal of type 1 diabetes in non-obese diabetic mice with brown adipose tissue transplant. American journal of physiology. Endocrinology and metabolism, ajpendo 00570 02014.
Guo, S. (2014). Insulin signaling, resistance, and the metabolic syndrome: insights from mouse models into disease mechanisms. The Journal of endocrinology *220*, T1-T23.

Gurgul, E., Lortz, S., Tiedge, M., Jorns, A., and Lenzen, S. (2004). Mitochondrial catalase overexpression protects insulin-producing cells against toxicity of reactive oxygen species and proinflammatory cytokines. Diabetes *53*, 2271-2280.
Haemmerle, G., Lass, A., Zimmermann, R., Gorkiewicz, G., Meyer, C., Rozman, J., Heldmaier, G., Maier, R., Theussl, C., Eder, S., et al. (2006). Defective lipolysis and altered energy metabolism in mice lacking adipose triglyceride lipase. Science *312*, 734-737.
Haemmerle, G., Moustafa, T., Woelkart, G., Buttner, S., Schmidt, A., van de Weijer, T., Hesselink, M., Jaeger, D., Kienesberger, P.C., Zierler, K., et al. (2011). ATGL-mediated fat catabolism regulates cardiac mitochondrial function via PPAR-alpha and PGC-1. Nature medicine *17*, 1076-1085.
Haemmerle, G., Zimmermann, R., Hayn, M., Theussl, C., Waeg, G., Wagner, E., Sattler, W., Magin, T.M., Wagner, E.F., and Zechner, R. (2002). Hormone-sensitive lipase deficiency in mice causes diglyceride accumulation in adipose tissue, muscle, and testis. J Biol Chem *277*, 4806-4815.
Haigis, M.C., and Guarente, L.P. (2006). Mammalian sirtuins--emerging roles in physiology, aging, and calorie restriction. Genes & development *20*, 2913-2921.
Hall, A.M., Kou, K., Chen, Z., Pietka, T.A., Kumar, M., Korenblat, K.M., Lee, K., Ahn, K., Fabbrini, E., Klein, S., et al. (2012). Evidence for regulated monoacylglycerol acyltransferase expression and activity in human liver. Journal of lipid research *53*, 990-999.
Hall, A.M., Soufi, N., Chambers, K.T., Chen, Z., Schweitzer, G.G., McCommis, K.S., Erion, D.M., Graham, M.J., Su, X., and Finck, B.N. (2014). Abrogating monoacylglycerol acyltransferase activity in liver improves glucose tolerance and hepatic insulin signaling in obese mice. Diabetes *63*, 2284-2296.
Halter, J.B., Musi, N., McFarland Horne, F., Crandall, J.P., Goldberg, A., Harkless, L., Hazzard, W.R., Huang, E.S., Kirkman, M.S., Plutzky, J., et al. (2014). Diabetes and cardiovascular disease in older adults: current status and future directions. Diabetes *63*, 2578-2589.
Han, M.S., Jung, D.Y., Morel, C., Lakhani, S.A., Kim, J.K., Flavell, R.A., and Davis, R.J. (2013). JNK expression by macrophages promotes obesity-induced insulin resistance and inflammation. Science *339*, 218-222.
Hansen, K.B., Rosenkilde, M.M., Knop, F.K., Wellner, N., Diep, T.A., Rehfeld, J.F., Andersen, U.B., Holst, J.J., and Hansen, H.S. (2011). 2-Oleoyl glycerol is a GPR119 agonist and signals GLP-1 release in humans. The Journal of clinical endocrinology and metabolism *96*, E1409-1417.
Hao, Q., Yadav, R., Basse, A.L., Petersen, S., Sonne, S.B., Rasmussen, S., Zhu, Q., Lu, Z., Wang, J., Audouze, K., et al. (2015). Transcriptome profiling of brown adipose tissue during cold exposure reveals extensive regulation of glucose metabolism. American journal of physiology. Endocrinology and metabolism *308*, E380-392.
Harmon, J.S., Bogdani, M., Parazzoli, S.D., Mak, S.S., Oseid, E.A., Berghmans, M., Leboeuf, R.C., and Robertson, R.P. (2009). beta-Cell-specific overexpression of glutathione peroxidase preserves intranuclear MafA and reverses diabetes in db/db mice. Endocrinology *150*, 4855-4862.

Harmon, J.S., Gleason, C.E., Tanaka, Y., Oseid, E.A., Hunter-Berger, K.K., and Robertson, R.P. (1999). In vivo prevention of hyperglycemia also prevents glucotoxic effects on PDX-1 and insulin gene expression. Diabetes *48*, 1995-2000.
Harris, C.A., Haas, J.T., Streeper, R.S., Stone, S.J., Kumari, M., Yang, K., Han, X., Brownell, N., Gross, R.W., Zechner, R., et al. (2011). DGAT enzymes are required for triacylglycerol synthesis and lipid droplets in adipocytes. Journal of lipid research *52*, 657-667.
Hartley, T., Brumell, J., and Volchuk, A. (2009). Emerging roles for the ubiquitin-proteasome system and autophagy in pancreatic beta-cells. American journal of physiology. Endocrinology and metabolism *296*, E1-10.
Hauge-Evans, A.C., Bowe, J., Franklin, Z.J., Hassan, Z., and Jones, P.M. (2015). Inhibitory effect of somatostatin on insulin secretion is not mediated via the CNS. The Journal of endocrinology *225*, 19-26.
Haus, J.M., Kashyap, S.R., Kasumov, T., Zhang, R., Kelly, K.R., Defronzo, R.A., and Kirwan, J.P. (2009). Plasma ceramides are elevated in obese subjects with type 2 diabetes and correlate with the severity of insulin resistance. Diabetes *58*, 337-343.
Hayashi, K., Kojima, R., and Ito, M. (2006). Strain differences in the diabetogenic activity of streptozotocin in mice. Biol Pharm Bull *29*, 1110-1119.
Heissig, H., Urban, K.A., Hastedt, K., Zunkler, B.J., and Panten, U. (2005). Mechanism of the insulin-releasing action of alpha-ketoisocaproate and related alpha-keto acid anions. Molecular pharmacology *68*, 1097-1105.
Henquin, J.C. (2011). The dual control of insulin secretion by glucose involves triggering and amplifying pathways in beta-cells. Diabetes research and clinical practice *93 Suppl 1*, S27-31.
Higashiyama, H., Billin, A.N., Okamoto, Y., Kinoshita, M., and Asano, S. (2007). Expression profiling of peroxisome proliferator-activated receptor-delta (PPAR-delta) in mouse tissues using tissue microarray. Histochemistry and cell biology *127*, 485-494.
Hirosumi, J., Tuncman, G., Chang, L., Gorgun, C.Z., Uysal, K.T., Maeda, K., Karin, M., and Hotamisligil, G.S. (2002). A central role for JNK in obesity and insulin resistance. Nature *420*, 333-336.
Hla, T., and Kolesnick, R. (2014). C16:0-ceramide signals insulin resistance. Cell metabolism *20*, 703-705.
Hohmeier, H.E., Mulder, H., Chen, G., Henkel-Rieger, R., Prentki, M., and Newgard, C.B. (2000). Isolation of INS-1-derived cell lines with robust ATP-sensitive K+ channel-dependent and -independent glucose-stimulated insulin secretion. Diabetes *49*, 424-430.
Holland, W.L., Brozinick, J.T., Wang, L.P., Hawkins, E.D., Sargent, K.M., Liu, Y., Narra, K., Hoehn, K.L., Knotts, T.A., Siesky, A., et al. (2007). Inhibition of ceramide synthesis ameliorates glucocorticoid-, saturated-fat-, and obesity-induced insulin resistance. Cell metabolism *5*, 167-179.
Holloszy, J.O., and Coyle, E.F. (1984). Adaptations of skeletal muscle to endurance exercise and their metabolic consequences. Journal of applied physiology: respiratory, environmental and exercise physiology *56*, 831-838.
Hondares, E., Iglesias, R., Giralt, A., Gonzalez, F.J., Giralt, M., Mampel, T., and Villarroya, F. (2011a). Thermogenic activation induces FGF21 expression and release in brown adipose tissue. The Journal of biological chemistry *286*, 12983-12990.

Hondares, E., Rosell, M., Diaz-Delfin, J., Olmos, Y., Monsalve, M., Iglesias, R., Villarroya, F., and Giralt, M. (2011b). Peroxisome proliferator-activated receptor alpha (PPARalpha) induces PPARgamma coactivator 1alpha (PGC-1alpha) gene expression and contributes to thermogenic activation of brown fat: involvement of PRDM16. The Journal of biological chemistry *286*, 43112-43122.
Hoover, H.S., Blankman, J.L., Niessen, S., and Cravatt, B.F. (2008). Selectivity of inhibitors of endocannabinoid biosynthesis evaluated by activity-based protein profiling. Bioorganic & medicinal chemistry letters *18*, 5838-5841.
Hu, L., Deeney, J.T., Nolan, C.J., Peyot, M.L., Ao, A., Richard, A.M., Luc, E., Faergeman, N.J., Knudsen, J., Guo, W., et al. (2005). Regulation of lipolytic activity by long-chain acyl-coenzyme A in islets and adipocytes. American journal of physiology. Endocrinology and metabolism *289*, E1085-1092.
Hue, L., and Taegtmeyer, H. (2009). The Randle cycle revisited: a new head for an old hat. American journal of physiology. Endocrinology and metabolism *297*, E578-591.
Huijsman, E., van de Par, C., Economou, C., van der Poel, C., Lynch, G.S., Schoiswohl, G., Haemmerle, G., Zechner, R., and Watt, M.J. (2009). Adipose triacylglycerol lipase deletion alters whole body energy metabolism and impairs exercise performance in mice. American journal of physiology. Endocrinology and metabolism *297*, E505-513.
Iglesias, J., Barg, S., Vallois, D., Lahiri, S., Roger, C., Yessoufou, A., Pradevand, S., McDonald, A., Bonal, C., Reimann, F., et al. (2012). PPARbeta/delta affects pancreatic beta cell mass and insulin secretion in mice. The Journal of clinical investigation *122*, 4105-4117.
Iglesias, J., Lamontagne, J., Erb, H., Gezzar, S., Zhao, S., Joly, E., Truong, V.L., Skorey, K., Crane, S., Madiraju, S.R., et al. (2015). Simplified assays of lipolysis enzymes for drug discovery and specificity assessment of of known inhibitors. Journal of lipid research.
Imbeault, P., Saint-Pierre, S., Almeras, N., and Tremblay, A. (1997). Acute effects of exercise on energy intake and feeding behaviour. The British journal of nutrition *77*, 511-521.
Itoh, Y., Kawamata, Y., Harada, M., Kobayashi, M., Fujii, R., Fukusumi, S., Ogi, K., Hosoya, M., Tanaka, Y., Uejima, H., et al. (2003). Free fatty acids regulate insulin secretion from pancreatic beta cells through GPR40. Nature *422*, 173-176.
Ivarsson, R., Quintens, R., Dejonghe, S., Tsukamoto, K., in 't Veld, P., Renstrom, E., and Schuit, F.C. (2005). Redox control of exocytosis: regulatory role of NADPH, thioredoxin, and glutaredoxin. Diabetes *54*, 2132-2142.
Iwasaki, Y., Saito, O., Tanabe, M., Inayoshi, K., Kobata, K., Uno, S., Morita, A., and Watanabe, T. (2008). Monoacylglycerols activate capsaicin receptor, TRPV1. Lipids *43*, 471-483.
Iwasaki, Y., Tamura, Y., Inayoshi, K., Narukawa, M., Kobata, K., Chiba, H., Muraki, E., Tsunoda, N., and Watanabe, T. (2011). TRPV1 agonist monoacylglycerol increases UCP1 content in brown adipose tissue and suppresses accumulation of visceral fat in mice fed a high-fat and high-sucrose diet. Bioscience, biotechnology, and biochemistry *75*, 904-909.
Jacqueminet, S., Briaud, I., Rouault, C., Reach, G., and Poitout, V. (2000). Inhibition of insulin gene expression by long-term exposure of pancreatic beta cells to palmitate is dependent on the presence of a stimulatory glucose concentration. Metabolism: clinical and experimental *49*, 532-536.

Janikiewicz, J., Hanzelka, K., Kozinski, K., Kolczynska, K., and Dobrzyn, A. (2015). Islet beta-cell failure in type 2 diabetes - within the network of toxic lipids. Biochemical and biophysical research communications.
Jensen, M.V., Joseph, J.W., Ilkayeva, O., Burgess, S., Lu, D., Ronnebaum, S.M., Odegaard, M., Becker, T.C., Sherry, A.D., and Newgard, C.B. (2006). Compensatory responses to pyruvate carboxylase suppression in islet beta-cells. Preservation of glucose-stimulated insulin secretion. The Journal of biological chemistry *281*, 22342-22351.
Jewell, J.L., Luo, W., Oh, E., Wang, Z., and Thurmond, D.C. (2008). Filamentous actin regulates insulin exocytosis through direct interaction with Syntaxin 4. The Journal of biological chemistry *283*, 10716-10726.
Jin, Y., McFie, P.J., Banman, S.L., Brandt, C., and Stone, S.J. (2014). Diacylglycerol Acyltransferase-2 (DGAT2) and Monoacylglycerol Acyltransferase-2 (MGAT2) Interact to Promote Triacylglycerol Synthesis. The Journal of biological chemistry *289*, 28237-28248.
Jitrapakdee, S., Wutthisathapornchai, A., Wallace, J.C., and MacDonald, M.J. (2010). Regulation of insulin secretion: role of mitochondrial signalling. Diabetologia *53*, 1019-1032.
Jones, J.R., Barrick, C., Kim, K.A., Lindner, J., Blondeau, B., Fujimoto, Y., Shiota, M., Kesterson, R.A., Kahn, B.B., and Magnuson, M.A. (2005). Deletion of PPARgamma in adipose tissues of mice protects against high fat diet-induced obesity and insulin resistance. Proceedings of the National Academy of Sciences of the United States of America *102*, 6207-6212.
Jung, H.S., Chung, K.W., Won Kim, J., Kim, J., Komatsu, M., Tanaka, K., Nguyen, Y.H., Kang, T.M., Yoon, K.H., Kim, J.W., et al. (2008). Loss of autophagy diminishes pancreatic beta cell mass and function with resultant hyperglycemia. Cell metabolism *8*, 318-324.
Jung, K.M., Clapper, J.R., Fu, J., D'Agostino, G., Guijarro, A., Thongkham, D., Avanesian, A., Astarita, G., DiPatrizio, N.V., Frontini, A., et al. (2012). 2-arachidonoylglycerol signaling in forebrain regulates systemic energy metabolism. Cell metabolism *15*, 299-310.
Jung, S.R., Kuok, I.T., Couron, D., Rizzo, N., Margineantu, D.H., Hockenbery, D.M., Kim, F., and Sweet, I.R. (2011). Reduced cytochrome C is an essential regulator of sustained insulin secretion by pancreatic islets. The Journal of biological chemistry *286*, 17422-17434.
Jung, T.W., Hwang, H.J., Hong, H.C., Yoo, H.J., Baik, S.H., and Choi, K.M. (2015). BAIBA attenuates insulin resistance and inflammation induced by palmitate or a high fat diet via an AMPK-PPARdelta-dependent pathway in mice. Diabetologia.
Kahn, S.E. (2003). The relative contributions of insulin resistance and beta-cell dysfunction to the pathophysiology of Type 2 diabetes. Diabetologia *46*, 3-19.
Kajimura, S., Seale, P., Kubota, K., Lunsford, E., Frangioni, J.V., Gygi, S.P., and Spiegelman, B.M. (2009). Initiation of myoblast to brown fat switch by a PRDM16-C/EBP-beta transcriptional complex. Nature *460*, 1154-1158.
Kammoun, H.L., and Febbraio, M.A. (2014). Come on BAIBA light my fire. Cell metabolism *19*, 1-2.
Kaneko, Y.K., and Ishikawa, T. (2015). Diacylglycerol Signaling Pathway in Pancreatic beta-Cells: An Essential Role of Diacylglycerol Kinase in the Regulation of Insulin Secretion. Biological & pharmaceutical bulletin *38*, 669-673.

Kaneto, H., Kajimoto, Y., Miyagawa, J., Matsuoka, T., Fujitani, Y., Umayahara, Y., Hanafusa, T., Matsuzawa, Y., Yamasaki, Y., and Hori, M. (1999). Beneficial effects of antioxidants in diabetes: possible protection of pancreatic beta-cells against glucose toxicity. Diabetes *48*, 2398-2406.
Kanety, H., Hemi, R., Papa, M.Z., and Karasik, A. (1996). Sphingomyelinase and ceramide suppress insulin-induced tyrosine phosphorylation of the insulin receptor substrate-1. The Journal of biological chemistry *271*, 9895-9897.
Kang, L., He, Z., Xu, P., Fan, J., Betz, A., Brose, N., and Xu, T. (2006). Munc13-1 is required for the sustained release of insulin from pancreatic beta cells. Cell metabolism *3*, 463-468.
Kasai, K., Ohara-Imaizumi, M., Takahashi, N., Mizutani, S., Zhao, S., Kikuta, T., Kasai, H., Nagamatsu, S., Gomi, H., and Izumi, T. (2005). Rab27a mediates the tight docking of insulin granules onto the plasma membrane during glucose stimulation. The Journal of clinical investigation *115*, 388-396.
Kebede, M., Alquier, T., Latour, M.G., Semache, M., Tremblay, C., and Poitout, V. (2008). The fatty acid receptor GPR40 plays a role in insulin secretion in vivo after high-fat feeding. Diabetes *57*, 2432-2437.
Kelly, D.P. (2012). Medicine. Irisin, light my fire. Science *336*, 42-43.
Kelly, L.J., Vicario, P.P., Thompson, G.M., Candelore, M.R., Doebber, T.W., Ventre, J., Wu, M.S., Meurer, R., Forrest, M.J., Conner, M.W., et al. (1998). Peroxisome proliferator-activated receptors gamma and alpha mediate in vivo regulation of uncoupling protein (UCP-1, UCP-2, UCP-3) gene expression. Endocrinology *139*, 4920-4927.
Kharitonenkov, A., and Adams, A.C. (2014). Inventing new medicines: The FGF21 story. Molecular metabolism *3*, 221-229.
Kibbey, R.G., Pongratz, R.L., Romanelli, A.J., Wollheim, C.B., Cline, G.W., and Shulman, G.I. (2007). Mitochondrial GTP regulates glucose-stimulated insulin secretion. Cell metabolism *5*, 253-264.
Kim-Muller, J.Y., Zhao, S., Srivastava, S., Mugabo, Y., Noh, H.L., Kim, Y.R., Madiraju, S.R., Ferrante, A.W., Skolnik, E.Y., Prentki, M., et al. (2014). Metabolic inflexibility impairs insulin secretion and results in MODY-like diabetes in triple FoxO-deficient mice. Cell metabolism *20*, 593-602.
Kim, M.S., Park, J.Y., Namkoong, C., Jang, P.G., Ryu, J.W., Song, H.S., Yun, J.Y., Namgoong, I.S., Ha, J., Park, I.S., et al. (2004). Anti-obesity effects of alpha-lipoic acid mediated by suppression of hypothalamic AMP-activated protein kinase. Nature medicine *10*, 727-733.
Kim, W., Doyle, M.E., Liu, Z., Lao, Q., Shin, Y.K., Carlson, O.D., Kim, H.S., Thomas, S., Napora, J.K., Lee, E.K., et al. (2011). Cannabinoids inhibit insulin receptor signaling in pancreatic beta-cells. Diabetes *60*, 1198-1209.
Knudsen, J.G., Murholm, M., Carey, A.L., Bienso, R.S., Basse, A.L., Allen, T.L., Hidalgo, J., Kingwell, B.A., Febbraio, M.A., Hansen, J.B., et al. (2014). Role of IL-6 in exercise training- and cold-induced UCP1 expression in subcutaneous white adipose tissue. PloS one *9*, e84910.
Koh, H.J., Toyoda, T., Didesch, M.M., Lee, M.Y., Sleeman, M.W., Kulkarni, R.N., Musi, N., Hirshman, M.F., and Goodyear, L.J. (2013). Tribbles 3 mediates endoplasmic reticulum stress-induced insulin resistance in skeletal muscle. Nature communications *4*, 1871.

Kohanski, R.A., Frost, S.C., and Lane, M.D. (1986). Insulin-dependent phosphorylation of the insulin receptor-protein kinase and activation of glucose transport in 3T3-L1 adipocytes. The Journal of biological chemistry *261*, 12272-12281.
Kwan, E.P., and Gaisano, H.Y. (2009). Rescuing the subprime meltdown in insulin exocytosis in diabetes. Ann N Y Acad Sci *1152*, 154-164.
Kwan, E.P., Xie, L., Sheu, L., Nolan, C.J., Prentki, M., Betz, A., Brose, N., and Gaisano, H.Y. (2006a). Munc13-1 deficiency reduces insulin secretion and causes abnormal glucose tolerance. Diabetes *55*, 1421-1429.
Kwan, E.P., Xie, L., Sheu, L., Nolan, C.J., Prentki, M., Betz, A., Brose, N., and Gaisano, H.Y. (2006b). Munc13-1 deficiency reduces insulin secretion and causes abnormal glucose tolerance. Diabetes *55*, 1421-1429.
Kwan, E.P., Xie, L., Sheu, L., Ohtsuka, T., and Gaisano, H.Y. (2007). Interaction between Munc13-1 and RIM is critical for glucagon-like peptide-1 mediated rescue of exocytotic defects in Munc13-1 deficient pancreatic beta-cells. Diabetes *56*, 2579-2588.
Lamontagne, J., Pepin, E., Peyot, M.L., Joly, E., Ruderman, N.B., Poitout, V., Madiraju, S.R., Nolan, C.J., and Prentki, M. (2009). Pioglitazone acutely reduces insulin secretion and causes metabolic deceleration of the pancreatic beta-cell at submaximal glucose concentrations. Endocrinology *150*, 3465-3474.
Lan, R., Liu, Q., Fan, P., Lin, S., Fernando, S.R., McCallion, D., Pertwee, R., and Makriyannis, A. (1999). Structure-activity relationships of pyrazole derivatives as cannabinoid receptor antagonists. Journal of medicinal chemistry *42*, 769-776.
Lang, T., and Jahn, R. (2008). Core proteins of the secretory machinery. Handbook of experimental pharmacology, 107-127.
Lass, A., Zimmermann, R., Oberer, M., and Zechner, R. (2011). Lipolysis - a highly regulated multi-enzyme complex mediates the catabolism of cellular fat stores. Progress in lipid research *50*, 14-27.
Latour, M.G., Alquier, T., Oseid, E., Tremblay, C., Jetton, T.L., Luo, J., Lin, D.C., and Poitout, V. (2007). GPR40 is necessary but not sufficient for fatty acid stimulation of insulin secretion in vivo. Diabetes *56*, 1087-1094.
Lawal, H.O., and Krantz, D.E. (2013). SLC18: Vesicular neurotransmitter transporters for monoamines and acetylcholine. Molecular aspects of medicine *34*, 360-372.
Laybutt, D.R., Preston, A.M., Akerfeldt, M.C., Kench, J.G., Busch, A.K., Biankin, A.V., and Biden, T.J. (2007). Endoplasmic reticulum stress contributes to beta cell apoptosis in type 2 diabetes. Diabetologia *50*, 752-763.
Lecker, S.H., Zavin, A., Cao, P., Arena, R., Allsup, K., Daniels, K.M., Joseph, J., Schulze, P.C., and Forman, D.E. (2012). Expression of the irisin precursor FNDC5 in skeletal muscle correlates with aerobic exercise performance in patients with heart failure. Circulation. Heart failure *5*, 812-818.
Lee, G., Elwood, F., McNally, J., Weiszmann, J., Lindstrom, M., Amaral, K., Nakamura, M., Miao, S., Cao, P., Learned, R.M., et al. (2002). T0070907, a selective ligand for peroxisome proliferator-activated receptor gamma, functions as an antagonist of biochemical and cellular activities. The Journal of biological chemistry *277*, 19649-19657.

Lee, J.Y., Takahashi, N., Yasubuchi, M., Kim, Y.I., Hashizaki, H., Kim, M.J., Sakamoto, T., Goto, T., and Kawada, T. (2012a). Triiodothyronine induces UCP-1 expression and mitochondrial biogenesis in human adipocytes. American journal of physiology. Cell physiology *302*, C463-472.
Lee, P., Brychta, R.J., Linderman, J., Smith, S., Chen, K.Y., and Celi, F.S. (2013). Mild cold exposure modulates fibroblast growth factor 21 (FGF21) diurnal rhythm in humans: relationship between FGF21 levels, lipolysis, and cold-induced thermogenesis. The Journal of clinical endocrinology and metabolism *98*, E98-102.
Lee, P., Linderman, J.D., Smith, S., Brychta, R.J., Wang, J., Idelson, C., Perron, R.M., Werner, C.D., Phan, G.Q., Kammula, U.S., et al. (2014). Irisin and FGF21 are cold-induced endocrine activators of brown fat function in humans. Cell metabolism *19*, 302-309.
Lee, Y.H., Giraud, J., Davis, R.J., and White, M.F. (2003). c-Jun N-terminal kinase (JNK) mediates feedback inhibition of the insulin signaling cascade. The Journal of biological chemistry *278*, 2896-2902.
Lee, Y.J., Ko, E.H., Kim, J.E., Kim, E., Lee, H., Choi, H., Yu, J.H., Kim, H.J., Seong, J.K., Kim, K.S., et al. (2012b). Nuclear receptor PPARgamma-regulated monoacylglycerol O-acyltransferase 1 (MGAT1) expression is responsible for the lipid accumulation in diet-induced hepatic steatosis. Proceedings of the National Academy of Sciences of the United States of America *109*, 13656-13661.
Leloup, C., Tourrel-Cuzin, C., Magnan, C., Karaca, M., Castel, J., Carneiro, L., Colombani, A.L., Ktorza, A., Casteilla, L., and Penicaud, L. (2009). Mitochondrial reactive oxygen species are obligatory signals for glucose-induced insulin secretion. Diabetes *58*, 673-681.
Leonardsson, G., Steel, J.H., Christian, M., Pocock, V., Milligan, S., Bell, J., So, P.W., Medina-Gomez, G., Vidal-Puig, A., White, R., et al. (2004). Nuclear receptor corepressor RIP140 regulates fat accumulation. Proceedings of the National Academy of Sciences of the United States of America *101*, 8437-8442.
Leung, Y.M., Kwan, E.P., Ng, B., Kang, Y., and Gaisano, H.Y. (2007). SNAREing voltage-gated K+ and ATP-sensitive K+ channels: tuning beta-cell excitability with syntaxin-1A and other exocytotic proteins. Endocrine reviews *28*, 653-663.
Levine, B., and Klionsky, D.J. (2004). Development by self-digestion: molecular mechanisms and biological functions of autophagy. Developmental cell *6*, 463-477.
Li, C., Najafi, H., Daikhin, Y., Nissim, I.B., Collins, H.W., Yudkoff, M., Matschinsky, F.M., and Stanley, C.A. (2003). Regulation of leucine-stimulated insulin secretion and glutamine metabolism in isolated rat islets. The Journal of biological chemistry *278*, 2853-2858.
Li, C., Vilches-Flores, A., Zhao, M., Amiel, S.A., Jones, P.M., and Persaud, S.J. (2012a). Expression and function of monoacylglycerol lipase in mouse beta-cells and human islets of Langerhans. Cellular physiology and biochemistry : international journal of experimental cellular physiology, biochemistry, and pharmacology *30*, 347-358.
Li, F., Fei, X., Xu, J., and Ji, C. (2009). An unannotated alpha/beta hydrolase superfamily member, ABHD6 differentially expressed among cancer cell lines. Molecular biology reports *36*, 691-696.

Li, L.O., Hu, Y.F., Wang, L., Mitchell, M., Berger, A., and Coleman, R.A. (2010). Early hepatic insulin resistance in mice: a metabolomics analysis. Molecular endocrinology *24*, 657-666.
Li, N., Li, B., Brun, T., Deffert-Delbouille, C., Mahiout, Z., Daali, Y., Ma, X.J., Krause, K.H., and Maechler, P. (2012b). NADPH oxidase NOX2 defines a new antagonistic role for reactive oxygen species and cAMP/PKA in the regulation of insulin secretion. Diabetes *61*, 2842-2850.
Liang, H., and Ward, W.F. (2006). PGC-1alpha: a key regulator of energy metabolism. Advances in physiology education *30*, 145-151.
Liew, C.W., Bochenski, J., Kawamori, D., Hu, J., Leech, C.A., Wanic, K., Malecki, M., Warram, J.H., Qi, L., Krolewski, A.S., et al. (2010). The pseudokinase tribbles homolog 3 interacts with ATF4 to negatively regulate insulin exocytosis in human and mouse beta cells. The Journal of clinical investigation *120*, 2876-2888.
Lin, M.E., Herr, D.R., and Chun, J. (2010). Lysophosphatidic acid (LPA) receptors: signaling properties and disease relevance. Prostaglandins & other lipid mediators *91*, 130-138.
Liu, C., Wu, J., Zhu, J., Kuei, C., Yu, J., Shelton, J., Sutton, S.W., Li, X., Yun, S.J., Mirzadegan, T., et al. (2009). Lactate inhibits lipolysis in fat cells through activation of an orphan G-protein-coupled receptor, GPR81. The Journal of biological chemistry *284*, 2811-2822.
Liu, Q., Gauthier, M.S., Sun, L., Ruderman, N., and Lodish, H. (2010). Activation of AMP-activated protein kinase signaling pathway by adiponectin and insulin in mouse adipocytes: requirement of acyl-CoA synthetases FATP1 and Acsl1 and association with an elevation in AMP/ATP ratio. FASEB journal : official publication of the Federation of American Societies for Experimental Biology *24*, 4229-4239.
Liu, S., Xi, Y., Bettaieb, A., Matsuo, K., Matsuo, I., Kulkarni, R.N., and Haj, F.G. (2014). Disruption of protein-tyrosine phosphatase 1B expression in the pancreas affects beta-cell function. Endocrinology *155*, 3329-3338.
Liu, X., Zheng, Z., Zhu, X., Meng, M., Li, L., Shen, Y., Chi, Q., Wang, D., Zhang, Z., Li, C., et al. (2013). Brown adipose tissue transplantation improves whole-body energy metabolism. Cell research *23*, 851-854.
Lloyd, L.J., Langley-Evans, S.C., and McMullen, S. (2012). Childhood obesity and risk of the adult metabolic syndrome: a systematic review. International journal of obesity *36*, 1-11.
Loft, A., Forss, I., Siersbaek, M.S., Schmidt, S.F., Larsen, A.S., Madsen, J.G., Pisani, D.F., Nielsen, R., Aagaard, M.M., Mathison, A., et al. (2015). Browning of human adipocytes requires KLF11 and reprogramming of PPARgamma superenhancers. Genes & development *29*, 7-22.
Long, J.Z., Li, W., Booker, L., Burston, J.J., Kinsey, S.G., Schlosburg, J.E., Pavon, F.J., Serrano, A.M., Selley, D.E., Parsons, L.H., et al. (2009a). Selective blockade of 2-arachidonoylglycerol hydrolysis produces cannabinoid behavioral effects. Nature chemical biology *5*, 37-44.
Long, J.Z., Nomura, D.K., and Cravatt, B.F. (2009b). Characterization of monoacylglycerol lipase inhibition reveals differences in central and peripheral endocannabinoid metabolism. Chemistry & biology *16*, 744-753.

Long, J.Z., Svensson, K.J., Tsai, L., Zeng, X., Roh, H.C., Kong, X., Rao, R.R., Lou, J., Lokurkar, I., Baur, W., et al. (2014). A smooth muscle-like origin for beige adipocytes. Cell metabolism *19*, 810-820.
Loubatieres-Mariani, M.M., Chapal, J., Lignon, F., and Valette, G. (1979). Structural specificity of nucleotides for insulin secretory action from the isolated perfused rat pancreas. European journal of pharmacology *59*, 277-286.
Lu, X., Yang, X., and Liu, J. (2010). Differential control of ATGL-mediated lipid droplet degradation by CGI-58 and G0S2. Cell cycle *9*, 2719-2725.
Lund, P.E., Gylfe, E., and Hellman, B. (1989). Leucine induces initial lowering of cytoplasmic Ca2+ in pancreatic beta-cells without concomitant inhibition of insulin release. Biochemistry international *19*, 83-87.
Ma, C., Su, L., Seven, A.B., Xu, Y., and Rizo, J. (2013). Reconstitution of the vital functions of Munc18 and Munc13 in neurotransmitter release. Science *339*, 421-425.
Ma, T., Lopez-Aguiar, A.G., Li, A., Lu, Y., Sekula, D., Nattie, E.E., Freemantle, S., and Dmitrovsky, E. (2014). Mice lacking G0S2 are lean and cold-tolerant. Cancer biology & therapy *15*, 643-650.
MacDonald, M.J., Chaplen, F.W., Triplett, C.K., Gong, Q., and Drought, H. (2006). Stimulation of insulin release by glyceraldehyde may not be similar to glucose. Archives of biochemistry and biophysics *447*, 118-126.
MacDonald, P.E. (2011). Signal integration at the level of ion channel and exocytotic function in pancreatic beta-cells. American journal of physiology. Endocrinology and metabolism *301*, E1065-1069.
MacDonald, P.E., El-Kholy, W., Riedel, M.J., Salapatek, A.M., Light, P.E., and Wheeler, M.B. (2002). The multiple actions of GLP-1 on the process of glucose-stimulated insulin secretion. Diabetes *51 Suppl 3*, S434-442.
MacDonald, P.E., Joseph, J.W., Yau, D., Diao, J., Asghar, Z., Dai, F., Oudit, G.Y., Patel, M.M., Backx, P.H., and Wheeler, M.B. (2004). Impaired glucose-stimulated insulin secretion, enhanced intraperitoneal insulin tolerance, and increased beta-cell mass in mice lacking the p110gamma isoform of phosphoinositide 3-kinase. Endocrinology *145*, 4078-4083.
Mackenzie, R.W., and Elliott, B.T. (2014). Akt/PKB activation and insulin signaling: a novel insulin signaling pathway in the treatment of type 2 diabetes. Diabetes, metabolic syndrome and obesity : targets and therapy *7*, 55-64.
Maechler, P., and Wollheim, C.B. (1998). Role of mitochondria in metabolism-secretion coupling of insulin release in the pancreatic beta-cell. Biofactors *8*, 255-262.
Maechler, P., and Wollheim, C.B. (1999). Mitochondrial glutamate acts as a messenger in glucose-induced insulin exocytosis. Nature *402*, 685-689.
Maeda, N., Shimomura, I., Kishida, K., Nishizawa, H., Matsuda, M., Nagaretani, H., Furuyama, N., Kondo, H., Takahashi, M., Arita, Y., et al. (2002). Diet-induced insulin resistance in mice lacking adiponectin/ACRP30. Nature medicine *8*, 731-737.
Majka, S.M., Fox, K.E., Psilas, J.C., Helm, K.M., Childs, C.R., Acosta, A.S., Janssen, R.C., Friedman, J.E., Woessner, B.T., Shade, T.R., et al. (2010). De novo generation of white adipocytes from the myeloid lineage via mesenchymal intermediates is age, adipose depot, and

gender specific. Proceedings of the National Academy of Sciences of the United States of America *107*, 14781-14786.
Malaisse, W.J., Sener, A., Malaisse-Lagae, F., Welsh, M., Matthews, D.E., Bier, D.M., and Hellerstrom, C. (1982). The stimulus-secretion coupling of amino acid-induced insulin release. Metabolic response of pancreatic islets of L-glutamine and L-leucine. The Journal of biological chemistry *257*, 8731-8737.
Marrs, W.R., Blankman, J.L., Horne, E.A., Thomazeau, A., Lin, Y.H., Coy, J., Bodor, A.L., Muccioli, G.G., Hu, S.S., Woodruff, G., et al. (2010). The serine hydrolase ABHD6 controls the accumulation and efficacy of 2-AG at cannabinoid receptors. Nature neuroscience *13*, 951-957.
Massi, P., Solinas, M., Cinquina, V., and Parolaro, D. (2013). Cannabidiol as potential anticancer drug. British journal of clinical pharmacology *75*, 303-312.
Matias, I., Gonthier, M.P., Orlando, P., Martiadis, V., De Petrocellis, L., Cervino, C., Petrosino, S., Hoareau, L., Festy, F., Pasquali, R., et al. (2006). Regulation, function, and dysregulation of endocannabinoids in models of adipose and beta-pancreatic cells and in obesity and hyperglycemia. Journal of Clinical Endocrinology and Metabolism *91*, 3171-3180.
Matsumoto, M., Ogawa, W., Akimoto, K., Inoue, H., Miyake, K., Furukawa, K., Hayashi, Y., Iguchi, H., Matsuki, Y., Hiramatsu, R., et al. (2003). PKClambda in liver mediates insulin-induced SREBP-1c expression and determines both hepatic lipid content and overall insulin sensitivity. The Journal of clinical investigation *112*, 935-944.
Matsuzawa, Y. (2005). Adiponectin: Identification, physiology and clinical relevance in metabolic and vascular disease. Atherosclerosis. Supplements *6*, 7-14.
Mauvais-Jarvis, F., Clegg, D.J., and Hevener, A.L. (2013). The role of estrogens in control of energy balance and glucose homeostasis. Endocr Rev *34*, 309-338.
Max, D., Hesse, M., Volkmer, I., and Staege, M.S. (2009). High expression of the evolutionarily conserved alpha/beta hydrolase domain containing 6 (ABHD6) in Ewing tumors. Cancer science *100*, 2383-2389.
Mayer, N., Schweiger, M., Melcher, M.C., Fledelius, C., Zechner, R., Zimmermann, R., and Breinbauer, R. (2015). Structure-activity studies in the development of a hydrazone based inhibitor of adipose-triglyceride lipase (ATGL). Bioorganic & medicinal chemistry.
McDonald, T.J., Dupre, J., Tatemoto, K., Greenberg, G.R., Radziuk, J., and Mutt, V. (1985). Galanin inhibits insulin secretion and induces hyperglycemia in dogs. Diabetes *34*, 192-196.
Mehta, A., Oeser, A.M., and Carlson, M.G. (1998). Rapid quantitation of free fatty acids in human plasma by high-performance liquid chromatography. J Chromatogr B Biomed Sci Appl *719*, 9-23.
Meier, U., and Gressner, A.M. (2004). Endocrine regulation of energy metabolism: review of pathobiochemical and clinical chemical aspects of leptin, ghrelin, adiponectin, and resistin. Clinical chemistry *50*, 1511-1525.
Mela, D.J. (2001). Determinants of food choice: relationships with obesity and weight control. Obesity research *9 Suppl 4*, 249S-255S.
Mentis, N., Vardarli, I., Kothe, L.D., Holst, J.J., Deacon, C.F., Theodorakis, M., Meier, J.J., and Nauck, M.A. (2011). GIP does not potentiate the antidiabetic effects of GLP-1 in hyperglycemic patients with type 2 diabetes. Diabetes *60*, 1270-1276.

Mercader, J., Madsen, L., Felipe, F., Palou, A., Kristiansen, K., and Bonet, M.L. (2007). All-trans retinoic acid increases oxidative metabolism in mature adipocytes. Cellular physiology and biochemistry : international journal of experimental cellular physiology, biochemistry, and pharmacology *20*, 1061-1072.
Mercader, J., Palou, A., and Bonet, M.L. (2010). Induction of uncoupling protein-1 in mouse embryonic fibroblast-derived adipocytes by retinoic acid. Obesity *18*, 655-662.
Michaliszyn, S.F., Mari, A., Lee, S., Bacha, F., Tfayli, H., Farchoukh, L., Ferrannini, E., and Arslanian, S. (2014). beta-cell function, incretin effect, and incretin hormones in obese youth along the span of glucose tolerance from normal to prediabetes to type 2 diabetes. Diabetes *63*, 3846-3855.
Moran, O., and Phillip, M. (2003). Leptin: obesity, diabetes and other peripheral effects--a review. Pediatric diabetes *4*, 101-109.
Morris, A.P., Voight, B.F., Teslovich, T.M., Ferreira, T., Segre, A.V., Steinthorsdottir, V., Strawbridge, R.J., Khan, H., Grallert, H., Mahajan, A., et al. (2012). Large-scale association analysis provides insights into the genetic architecture and pathophysiology of type 2 diabetes. Nature genetics *44*, 981-990.
Morrison, S.F. (2011). 2010 Carl Ludwig Distinguished Lectureship of the APS Neural Control and Autonomic Regulation Section: Central neural pathways for thermoregulatory cold defense. Journal of applied physiology *110*, 1137-1149.
Mottillo, E.P., Bloch, A.E., Leff, T., and Granneman, J.G. (2012). Lipolytic products activate peroxisome proliferator-activated receptor (PPAR) alpha and delta in brown adipocytes to match fatty acid oxidation with supply. The Journal of biological chemistry *287*, 25038-25048.
Mugabo, Y., Li, L., and Renier, G. (2010). The connection between C-reactive protein (CRP) and diabetic vasculopathy. Focus on preclinical findings. Current diabetes reviews *6*, 27-34.
Mugabo, Y., Mukaneza, Y., and Renier, G. (2011). Palmitate induces C-reactive protein expression in human aortic endothelial cells. Relevance to fatty acid-induced endothelial dysfunction. Metabolism: clinical and experimental *60*, 640-648.
Mulder, H., Yang, S., Winzell, M.S., Holm, C., and Ahren, B. (2004). Inhibition of lipase activity and lipolysis in rat islets reduces insulin secretion. Diabetes *53*, 122-128.
Mulumba, M., Granata, R., Marleau, S., and Ong, H. (2015). QRFP-43 inhibits lipolysis by preventing ligand-induced complex formation between perilipin A, caveolin-1, the catalytic subunit of protein kinase and hormone-sensitive lipase in 3T3-L1 adipocytes. Biochimica et biophysica acta *1851*, 657-666.
Nadal-Casellas, A., Bauza-Thorbrugge, M., Proenza, A.M., Gianotti, M., and Llado, I. (2013). Sex-dependent differences in rat brown adipose tissue mitochondrial biogenesis and insulin signaling parameters in response to an obesogenic diet. Molecular and cellular biochemistry *373*, 125-135.
Nagasumi, K., Esaki, R., Iwachidow, K., Yasuhara, Y., Ogi, K., Tanaka, H., Nakata, M., Yano, T., Shimakawa, K., Taketomi, S., et al. (2009). Overexpression of GPR40 in pancreatic beta-cells augments glucose-stimulated insulin secretion and improves glucose tolerance in normal and diabetic mice. Diabetes *58*, 1067-1076.

Nagle, C.A., Vergnes, L., Dejong, H., Wang, S., Lewin, T.M., Reue, K., and Coleman, R.A. (2008). Identification of a novel sn-glycerol-3-phosphate acyltransferase isoform, GPAT4, as the enzyme deficient in Agpat6-/- mice. Journal of lipid research *49*, 823-831.
Navia-Paldanius, D., Savinainen, J.R., and Laitinen, J.T. (2012a). Biochemical and pharmacological characterization of human alpha/beta-hydrolase domain containing 6 (ABHD6) and 12 (ABHD12). Journal of lipid research.
Navia-Paldanius, D., Savinainen, J.R., and Laitinen, J.T. (2012b). Biochemical and pharmacological characterization of human alpha/beta-hydrolase domain containing 6 (ABHD6) and 12 (ABHD12). Journal of lipid research *53*, 2413-2424.
Nedergaard, J., and Cannon, B. (2014). The browning of white adipose tissue: some burning issues. Cell metabolism *20*, 396-407.
Neel, J.V. (1962). Diabetes mellitus: a "thrifty" genotype rendered detrimental by "progress"? American journal of human genetics *14*, 353-362.
Neel, J.V. (1999). Diabetes mellitus: a "thrifty" genotype rendered detrimental by "progress"? 1962. Bulletin of the World Health Organization *77*, 694-703; discussion 692-693.
Nelson, D.W., Gao, Y., Spencer, N.M., Banh, T., and Yen, C.L. (2011). Deficiency of MGAT2 increases energy expenditure without high-fat feeding and protects genetically obese mice from excessive weight gain. Journal of lipid research *52*, 1723-1732.
Nelson, D.W., Gao, Y., Yen, M.I., and Yen, C.L. (2014). Intestine-specific deletion of acyl-CoA:monoacylglycerol acyltransferase (MGAT) 2 protects mice from diet-induced obesity and glucose intolerance. The Journal of biological chemistry *289*, 17338-17349.
Nesca, V., Guay, C., Jacovetti, C., Menoud, V., Peyot, M.L., Laybutt, D.R., Prentki, M., and Regazzi, R. (2013). Identification of particular groups of microRNAs that positively or negatively impact on beta cell function in obese models of type 2 diabetes. Diabetologia *56*, 2203-2212.
Neschen, S., Morino, K., Hammond, L.E., Zhang, D., Liu, Z.X., Romanelli, A.J., Cline, G.W., Pongratz, R.L., Zhang, X.M., Choi, C.S., et al. (2005). Prevention of hepatic steatosis and hepatic insulin resistance in mitochondrial acyl-CoA:glycerol-sn-3-phosphate acyltransferase 1 knockout mice. Cell metabolism *2*, 55-65.
Newsholme, P., Gaudel, C., and McClenaghan, N.H. (2010). Nutrient regulation of insulin secretion and beta-cell functional integrity. Advances in experimental medicine and biology *654*, 91-114.
Nguyen, M.T., Satoh, H., Favelyukis, S., Babendure, J.L., Imamura, T., Sbodio, J.I., Zalevsky, J., Dahiyat, B.I., Chi, N.W., and Olefsky, J.M. (2005). JNK and tumor necrosis factor-alpha mediate free fatty acid-induced insulin resistance in 3T3-L1 adipocytes. The Journal of biological chemistry *280*, 35361-35371.
Nielsen, H.R., Sjolin, K.E., Nyholm, K., Baliga, B.S., Wong, R., and Borek, E. (1974). Beta-aminoisobutyric acid, a new probe for the metabolism of DNA and RNA in normal and tumorous tissue. Cancer research *34*, 1381-1384.
Ning, Y., O'Neill, K., Lan, H., Pang, L., Shan, L.X., Hawes, B.E., and Hedrick, J.A. (2008). Endogenous and synthetic agonists of GPR119 differ in signalling pathways and their effects on insulin secretion in MIN6c4 insulinoma cells. British journal of pharmacology *155*, 1056-1065.

Nishizawa, M., Nakabayashi, H., Uehara, K., Nakagawa, A., Uchida, K., and Koya, D. (2013). Intraportal GLP-1 stimulates insulin secretion predominantly through the hepatoportal-pancreatic vagal reflex pathways. American journal of physiology. Endocrinology and metabolism *305*, E376-387.
Nolan, C.J., Leahy, J.L., Delghingaro-Augusto, V., Moibi, J., Soni, K., Peyot, M.L., Fortier, M., Guay, C., Lamontagne, J., Barbeau, A., et al. (2006a). Beta cell compensation for insulin resistance in Zucker fatty rats: increased lipolysis and fatty acid signalling. Diabetologia *49*, 2120-2130.
Nolan, C.J., Leahy, J.L., Delghingaro-Augusto, V., Moibi, J., Soni, K., Peyot, M.L., Fortier, M., Guay, C., Lamontagne, J., Barbeau, A., et al. (2006b). Beta cell compensation for insulin resistance in Zucker fatty rats: increased lipolysis and fatty acid signalling. Diabetologia *49*, 2120-2130.
Nolan, C.J., Madiraju, M.S., Delghingaro-Augusto, V., Peyot, M.L., and Prentki, M. (2006c). Fatty Acid Signaling in the {beta}-Cell and Insulin Secretion. Diabetes *55 Suppl 2*, S16-23.
Nolan, C.J., Madiraju, M.S., Delghingaro-Augusto, V., Peyot, M.L., and Prentki, M. (2006d). Fatty acid signaling in the beta-cell and insulin secretion. Diabetes *55 Suppl 2*, S16-23.
Nolan, C.J., and Prentki, M. (2008). The islet beta-cell: fuel responsive and vulnerable. Trends in endocrinology and metabolism: TEM *19*, 285-291.
Nolan, C.J., Ruderman, N.B., Kahn, S.E., Pedersen, O., and Prentki, M. (2015). Insulin resistance as a physiological defense against metabolic stress: implications for the management of subsets of type 2 diabetes. Diabetes *64*, 673-686.
Noll, C., Kunach, M., Frisch, F., Bouffard, L., Dubreuil, S., Jean-Denis, F., Phoenix, S., Cunnane, S.C., Guerin, B., Turcotte, E.E., et al. (2015). Seven-Day Caloric and Saturated Fat Restriction Increases Myocardial Dietary Fatty Acid Partitioning in Impaired Glucose-Tolerant Subjects. Diabetes *64*, 3690-3699.
Nomura, D.K., Long, J.Z., Niessen, S., Hoover, H.S., Ng, S.W., and Cravatt, B.F. (2010). Monoacylglycerol lipase regulates a fatty acid network that promotes cancer pathogenesis. Cell *140*, 49-61.
Nookaew, I., Svensson, P.A., Jacobson, P., Jernas, M., Taube, M., Larsson, I., Andersson-Assarsson, J.C., Sjostrom, L., Froguel, P., Walley, A., et al. (2013). Adipose tissue resting energy expenditure and expression of genes involved in mitochondrial function are higher in women than in men. The Journal of clinical endocrinology and metabolism *98*, E370-378.
Norheim, F., Langleite, T.M., Hjorth, M., Holen, T., Kielland, A., Stadheim, H.K., Gulseth, H.L., Birkeland, K.I., Jensen, J., and Drevon, C.A. (2014). The effects of acute and chronic exercise on PGC-1alpha, irisin and browning of subcutaneous adipose tissue in humans. The FEBS journal *281*, 739-749.
O'Rahilly, S., Turner, R.C., and Matthews, D.R. (1988). Impaired pulsatile secretion of insulin in relatives of patients with non-insulin-dependent diabetes. The New England journal of medicine *318*, 1225-1230.
Obici, S., Feng, Z., Morgan, K., Stein, D., Karkanias, G., and Rossetti, L. (2002). Central administration of oleic acid inhibits glucose production and food intake. Diabetes *51*, 271-275.
Obregon, M.J. (2014). Adipose tissues and thyroid hormones. Frontiers in physiology *5*, 479.

Oh, E., Kalwat, M.A., Kim, M.J., Verhage, M., and Thurmond, D.C. (2012). Munc18-1 regulates first-phase insulin release by promoting granule docking to multiple syntaxin isoforms. The Journal of biological chemistry *287*, 25821-25833.
Ohno, H., Shinoda, K., Spiegelman, B.M., and Kajimura, S. (2012). PPARgamma agonists induce a white-to-brown fat conversion through stabilization of PRDM16 protein. Cell metabolism *15*, 395-404.
Okla, M., Ha, J.H., Temel, R.E., and Chung, S. (2015). BMP7 drives human adipogenic stem cells into metabolically active beige adipocytes. Lipids *50*, 111-120.
Okuma, C., Ohta, T., Tadaki, H., Hamada, H., Oda, T., Taniuchi, H., Yamanaka, K., Ishii, Y., Ohe, Y., Yata, S., et al. (2015). JTP-103237, a novel monoacylglycerol acyltransferase inhibitor, modulates fat absorption and prevents diet-induced obesity. European journal of pharmacology *758*, 72-81.
Olson, L.K., Redmon, J.B., Towle, H.C., and Robertson, R.P. (1993). Chronic exposure of HIT cells to high glucose concentrations paradoxically decreases insulin gene transcription and alters binding of insulin gene regulatory protein. The Journal of clinical investigation *92*, 514-519.
Ouellet, V., Labbe, S.M., Blondin, D.P., Phoenix, S., Guerin, B., Haman, F., Turcotte, E.E., Richard, D., and Carpentier, A.C. (2012). Brown adipose tissue oxidative metabolism contributes to energy expenditure during acute cold exposure in humans. The Journal of clinical investigation *122*, 545-552.
Overton, H.A., Babbs, A.J., Doel, S.M., Fyfe, M.C., Gardner, L.S., Griffin, G., Jackson, H.C., Procter, M.J., Rasamison, C.M., Tang-Christensen, M., et al. (2006). Deorphanization of a G protein-coupled receptor for oleoylethanolamide and its use in the discovery of small-molecule hypophagic agents. Cell metabolism *3*, 167-175.
Owen, B.M., Ding, X., Morgan, D.A., Coate, K.C., Bookout, A.L., Rahmouni, K., Kliewer, S.A., and Mangelsdorf, D.J. (2014). FGF21 acts centrally to induce sympathetic nerve activity, energy expenditure, and weight loss. Cell metabolism *20*, 670-677.
Pages, C., Simon, M., Valet, P., and Saulnier-Blache, J.S. (2001). Lysophosphatidic acid synthesis and release(1). Prostaglandins *64*, 1-10.
Palladino, A.A., and Stanley, C.A. (2010). The hyperinsulinism/hyperammonemia syndrome. Reviews in endocrine & metabolic disorders *11*, 171-178.
Park, K.H., Zaichenko, L., Brinkoetter, M., Thakkar, B., Sahin-Efe, A., Joung, K.E., Tsoukas, M.A., Geladari, E.V., Huh, J.Y., Dincer, F., et al. (2013a). Circulating irisin in relation to insulin resistance and the metabolic syndrome. The Journal of clinical endocrinology and metabolism *98*, 4899-4907.
Park, S., Mori, R., and Shimokawa, I. (2013b). Do sirtuins promote mammalian longevity? A critical review on its relevance to the longevity effect induced by calorie restriction. Molecules and cells *35*, 474-480.
Parker, L.A., Niphakis, M.J., Downey, R., Limebeer, C.L., Rock, E.M., Sticht, M.A., Morris, H., Abdullah, R.A., Lichtman, A.H., and Cravatt, B.F. (2014). Effect of selective inhibition of monoacylglycerol lipase (MAGL) on acute nausea, anticipatory nausea, and vomiting in rats and Suncus murinus. Psychopharmacology.

Pedersen, B.K. (2007). IL-6 signalling in exercise and disease. Biochemical Society transactions *35*, 1295-1297.
Pekkala, S., Wiklund, P.K., Hulmi, J.J., Ahtiainen, J.P., Horttanainen, M., Pollanen, E., Makela, K.A., Kainulainen, H., Hakkinen, K., Nyman, K., et al. (2013). Are skeletal muscle FNDC5 gene expression and irisin release regulated by exercise and related to health? The Journal of physiology *591*, 5393-5400.
Perciaccante, A., Fiorentini, A., Paris, A., Serra, P., and Tubani, L. (2006). Circadian rhythm of the autonomic nervous system in insulin resistant subjects with normoglycemia, impaired fasting glycemia, impaired glucose tolerance, type 2 diabetes mellitus. BMC cardiovascular disorders *6*, 19.
Perry, J.R., Voight, B.F., Yengo, L., Amin, N., Dupuis, J., Ganser, M., Grallert, H., Navarro, P., Li, M., Qi, L., et al. (2012). Stratifying type 2 diabetes cases by BMI identifies genetic risk variants in LAMA1 and enrichment for risk variants in lean compared to obese cases. PLoS genetics *8*, e1002741.
Perry, R.J., Samuel, V.T., Petersen, K.F., and Shulman, G.I. (2014). The role of hepatic lipids in hepatic insulin resistance and type 2 diabetes. Nature *510*, 84-91.
Peter-Riesch, B., Fathi, M., Schlegel, W., and Wollheim, C.B. (1988). Glucose and carbachol generate 1,2-diacylglycerols by different mechanisms in pancreatic islets. The Journal of clinical investigation *81*, 1154-1161.
Peters, J.M., Park, Y., Gonzalez, F.J., and Pariza, M.W. (2001). Influence of conjugated linoleic acid on body composition and target gene expression in peroxisome proliferator-activated receptor alpha-null mice. Biochimica et biophysica acta *1533*, 233-242.
Petrovic, N., Walden, T.B., Shabalina, I.G., Timmons, J.A., Cannon, B., and Nedergaard, J. (2010). Chronic peroxisome proliferator-activated receptor gamma (PPARgamma) activation of epididymally derived white adipocyte cultures reveals a population of thermogenically competent, UCP1-containing adipocytes molecularly distinct from classic brown adipocytes. The Journal of biological chemistry *285*, 7153-7164.
Petry, S., Ben Ali, Y., Chahinian, H., Jordan, H., Kleine, H., Muller, G., Carriere, F., and Abousalham, A. (2005). Sensitive assay for hormone-sensitive lipase using NBD-labeled monoacylglycerol to detect low activities in rat adipocytes. Journal of lipid research *46*, 603-614.
Peyot, M.L., Gray, J.P., Lamontagne, J., Smith, P.J., Holz, G.G., Madiraju, S.R., Prentki, M., and Heart, E. (2009a). Glucagon-like peptide-1 induced signaling and insulin secretion do not drive fuel and energy metabolism in primary rodent pancreatic beta-cells. PloS one *4*, e6221.
Peyot, M.L., Guay, C., Latour, M.G., Lamontagne, J., Lussier, R., Pineda, M., Ruderman, N.B., Haemmerle, G., Zechner, R., Joly, E., et al. (2009b). Adipose triglyceride lipase is implicated in fuel- and non-fuel-stimulated insulin secretion. Journal of Biological Chemistry *284*, 16848-16859.
Peyot, M.L., Guay, C., Latour, M.G., Lamontagne, J., Lussier, R., Pineda, M., Ruderman, N.B., Haemmerle, G., Zechner, R., Joly, E., et al. (2009c). Adipose triglyceride lipase is implicated in fuel- and non-fuel-stimulated insulin secretion. The Journal of biological chemistry *284*, 16848-16859.

Peyot, M.L., Nolan, C.J., Soni, K., Joly, E., Lussier, R., Corkey, B.E., Wang, S.P., Mitchell, G.A., and Prentki, M. (2004). Hormone-sensitive lipase has a role in lipid signaling for insulin secretion but is nonessential for the incretin action of glucagon-like peptide 1. Diabetes *53*, 1733-1742.
Peyot, M.L., Pepin, E., Lamontagne, J., Latour, M.G., Zarrouki, B., Lussier, R., Pineda, M., Jetton, T.L., Madiraju, S.R., Joly, E., et al. (2010). Beta-cell failure in diet-induced obese mice stratified according to body weight gain: secretory dysfunction and altered islet lipid metabolism without steatosis or reduced beta-cell mass. Diabetes *59*, 2178-2187.
Pfeifer, A., and Hoffmann, L.S. (2015). Brown, beige, and white: the new color code of fat and its pharmacological implications. Annual review of pharmacology and toxicology *55*, 207-227.
Phillips, L.K., and Prins, J.B. (2011). Update on incretin hormones. Annals of the New York Academy of Sciences *1243*, E55-74.
Pi, J., Bai, Y., Zhang, Q., Wong, V., Floering, L.M., Daniel, K., Reece, J.M., Deeney, J.T., Andersen, M.E., Corkey, B.E., et al. (2007). Reactive oxygen species as a signal in glucose-stimulated insulin secretion. Diabetes *56*, 1783-1791.
Pigeau, G.M., Kolic, J., Ball, B.J., Hoppa, M.B., Wang, Y.W., Ruckle, T., Woo, M., Manning Fox, J.E., and MacDonald, P.E. (2009). Insulin granule recruitment and exocytosis is dependent on p110gamma in insulinoma and human beta-cells. Diabetes *58*, 2084-2092.
Piomelli, D. (2003). The molecular logic of endocannabinoid signalling. Nature reviews. Neuroscience *4*, 873-884.
Plum, L., Belgardt, B.F., and Bruning, J.C. (2006). Central insulin action in energy and glucose homeostasis. The Journal of clinical investigation *116*, 1761-1766.
Poitout, V., Amyot, J., Semache, M., Zarrouki, B., Hagman, D., and Fontes, G. (2010). Glucolipotoxicity of the pancreatic beta cell. Biochimica et biophysica acta *1801*, 289-298.
Poitout, V., and Robertson, R.P. (2002). Minireview: Secondary beta-cell failure in type 2 diabetes--a convergence of glucotoxicity and lipotoxicity. Endocrinology *143*, 339-342.
Pongratz, R.L., Kibbey, R.G., Shulman, G.I., and Cline, G.W. (2007). Cytosolic and mitochondrial malic enzyme isoforms differentially control insulin secretion. The Journal of biological chemistry *282*, 200-207.
Powell, D.J., Turban, S., Gray, A., Hajduch, E., and Hundal, H.S. (2004). Intracellular ceramide synthesis and protein kinase Czeta activation play an essential role in palmitate-induced insulin resistance in rat L6 skeletal muscle cells. The Biochemical journal *382*, 619-629.
Prentki, M., Biden, T.J., Janjic, D., Irvine, R.F., Berridge, M.J., and Wollheim, C.B. (1984). Rapid mobilization of Ca2+ from rat insulinoma microsomes by inositol-1,4,5-trisphosphate. Nature *309*, 562-564.
Prentki, M., Joly, E., El-Assaad, W., and Roduit, R. (2002). Malonyl-CoA signaling, lipid partitioning, and glucolipotoxicity: role in beta-cell adaptation and failure in the etiology of diabetes. Diabetes *51 Suppl 3*, S405-413.
Prentki, M., and Madiraju, S.R. (2008). Glycerolipid metabolism and signaling in health and disease. Endocrine reviews *29*, 647-676.

Prentki, M., and Madiraju, S.R. (2012). Glycerolipid/free fatty acid cycle and islet beta-cell function in health, obesity and diabetes. Molecular and cellular endocrinology *353*, 88-100.
Prentki, M., and Matschinsky, F.M. (1987). Ca2+, cAMP, and phospholipid-derived messengers in coupling mechanisms of insulin secretion. Physiol Rev *67*, 1185-1248.
Prentki, M., Matschinsky, F.M., and Madiraju, M.S. (2013a). Metabolic Signaling in Fuel-Induced Insulin Secretion Cell Metabol *In Press*.
Prentki, M., Matschinsky, F.M., and Madiraju, S.R. (2013b). Metabolic signaling in fuel-induced insulin secretion. Cell metabolism *18*, 162-185.
Prentki, M., and Nolan, C.J. (2006). Islet beta cell failure in type 2 diabetes. The Journal of clinical investigation *116*, 1802-1812.
Prentki, M., Segall, L., Roche, E., Thumelin, S., Brun, T., McGarry, J.D., Corkey, B.E., and Assimacopoulos-Jeannet, F. (1998). [Gluco-lipotoxicity and gene expression in the pancreatic beta cell]. Journees annuelles de diabetologie de l'Hotel-Dieu, 17-27.
Prentki, M., Tornheim, K., and Corkey, B.E. (1997). Signal transduction mechanisms in nutrient-induced insulin secretion. Diabetologia *40 Suppl 2*, S32-41.
Prentki, M., Vischer, S., Glennon, M.C., Regazzi, R., Deeney, J.T., and Corkey, B.E. (1992). Malonyl-CoA and long chain acyl-CoA esters as metabolic coupling factors in nutrient-induced insulin secretion. The Journal of biological chemistry *267*, 5802-5810.
Pribasnig, M.A., Mrak, I., Grabner, G.F., Taschler, U., Knittelfelder, O., Scherz, B., Eichmann, T.O., Heier, C., Grumet, L., Kowaliuk, J., et al. (2015). alpha/beta Hydrolase Domain-Containing 6 (ABHD6) Degrades the Late Endosomal/Lysosomal Lipid Bis(monoacylglycero)phosphate. The Journal of biological chemistry.
Puigserver, P., Wu, Z., Park, C.W., Graves, R., Wright, M., and Spiegelman, B.M. (1998). A cold-inducible coactivator of nuclear receptors linked to adaptive thermogenesis. Cell *92*, 829-839.
Pulinilkunnil, T., Kienesberger, P.C., Nagendran, J., Waller, T.J., Young, M.E., Kershaw, E.E., Korbutt, G., Haemmerle, G., Zechner, R., and Dyck, J.R. (2013). Myocardial adipose triglyceride lipase overexpression protects diabetic mice from the development of lipotoxic cardiomyopathy. Diabetes *62*, 1464-1477.
Puttmann, M., Krug, H., von Ochsenstein, E., and Kattermann, R. (1993). Fast HPLC determination of serum free fatty acids in the picomole range. Clin Chem *39*, 825-832.
Qian, S.W., Tang, Y., Li, X., Liu, Y., Zhang, Y.Y., Huang, H.Y., Xue, R.D., Yu, H.Y., Guo, L., Gao, H.D., et al. (2013). BMP4-mediated brown fat-like changes in white adipose tissue alter glucose and energy homeostasis. Proceedings of the National Academy of Sciences of the United States of America *110*, E798-807.
Quest, A.F. (1996). Regulation of protein kinase C: a tale of lipids and proteins. Enzyme & protein *49*, 231-261.
Rachid, T.L., Penna-de-Carvalho, A., Bringhenti, I., Aguila, M.B., Mandarim-de-Lacerda, C.A., and Souza-Mello, V. (2015). Fenofibrate (PPARalpha agonist) induces beige cell formation in subcutaneous white adipose tissue from diet-induced male obese mice. Molecular and cellular endocrinology *402*, 86-94.

Rancoule, C., Attane, C., Gres, S., Fournel, A., Dusaulcy, R., Bertrand, C., Vinel, C., Treguer, K., Prentki, M., Valet, P., et al. (2013). Lysophosphatidic acid impairs glucose homeostasis and inhibits insulin secretion in high-fat diet obese mice. Diabetologia *56*, 1394-1402.
Raschke, S., Elsen, M., Gassenhuber, H., Sommerfeld, M., Schwahn, U., Brockmann, B., Jung, R., Wisloff, U., Tjonna, A.E., Raastad, T., et al. (2013). Evidence against a beneficial effect of irisin in humans. PloS one *8*, e73680.
Reaven, G.M. (1997). Banting Lecture 1988. Role of insulin resistance in human disease. 1988. Nutrition *13*, 65; discussion 64, 66.
Reddy, J.K., and Rao, M.S. (2006). Lipid metabolism and liver inflammation. II. Fatty liver disease and fatty acid oxidation. American journal of physiology. Gastrointestinal and liver physiology *290*, G852-858.
Reinbothe, T.M., Ivarsson, R., Li, D.Q., Niazi, O., Jing, X., Zhang, E., Stenson, L., Bryborn, U., and Renstrom, E. (2009). Glutaredoxin-1 mediates NADPH-dependent stimulation of calcium-dependent insulin secretion. Molecular endocrinology *23*, 893-900.
Relimpio, F. (2003). "The relative contributions of insulin resistance and beta-cell dysfunction to the pathophysiology of Type 2 diabetes", by Kahn SE. Diabetologia *46*, 1707.
Rhee, J.S., Betz, A., Pyott, S., Reim, K., Varoqueaux, F., Augustin, I., Hesse, D., Sudhof, T.C., Takahashi, M., Rosenmund, C., et al. (2002). Beta phorbol ester- and diacylglycerol-induced augmentation of transmitter release is mediated by Munc13s and not by PKCs. Cell *108*, 121-133.
Richard, D., Carpentier, A.C., Dore, G., Ouellet, V., and Picard, F. (2010). Determinants of brown adipocyte development and thermogenesis. Int J Obes (Lond) *34 Suppl 2*, S59-66.
Rines, A.K., Verdeguer, F., and Puigserver, P. (2015). Adenosine activates thermogenic adipocytes. Cell research *25*, 155-156.
Roberts, L.D., Bostrom, P., O'Sullivan, J.F., Schinzel, R.T., Lewis, G.D., Dejam, A., Lee, Y.K., Palma, M.J., Calhoun, S., Georgiadi, A., et al. (2014). beta-Aminoisobutyric acid induces browning of white fat and hepatic beta-oxidation and is inversely correlated with cardiometabolic risk factors. Cell metabolism *19*, 96-108.
Robertson, R.P., Harmon, J., Tran, P.O., Tanaka, Y., and Takahashi, H. (2003). Glucose toxicity in beta-cells: type 2 diabetes, good radicals gone bad, and the glutathione connection. Diabetes *52*, 581-587.
Roca-Rivada, A., Castelao, C., Senin, L.L., Landrove, M.O., Baltar, J., Belen Crujeiras, A., Seoane, L.M., Casanueva, F.F., and Pardo, M. (2013). FNDC5/irisin is not only a myokine but also an adipokine. PloS one *8*, e60563.
Rodriguez-Diaz, R., Dando, R., Jacques-Silva, M.C., Fachado, A., Molina, J., Abdulreda, M.H., Ricordi, C., Roper, S.D., Berggren, P.O., and Caicedo, A. (2011). Alpha cells secrete acetylcholine as a non-neuronal paracrine signal priming beta cell function in humans. Nature medicine *17*, 888-892.
Roduit, R., Masiello, P., Wang, S.P., Li, H., Mitchell, G.A., and Prentki, M. (2001). A role for hormone-sensitive lipase in glucose-stimulated insulin secretion: a study in hormone-sensitive lipase-deficient mice. Diabetes *50*, 1970-1975.
Roduit, R., Nolan, C., Alarcon, C., Moore, P., Barbeau, A., Delghingaro-Augusto, V., Przybykowski, E., Morin, J., Masse, F., Massie, B., et al. (2004). A role for the malonyl-

CoA/long-chain acyl-CoA pathway of lipid signaling in the regulation of insulin secretion in response to both fuel and nonfuel stimuli. Diabetes *53*, 1007-1019.
Rorsman, P., Eliasson, L., Renstrom, E., Gromada, J., Barg, S., and Gopel, S. (2000). The Cell Physiology of Biphasic Insulin Secretion. News in physiological sciences : an international journal of physiology produced jointly by the International Union of Physiological Sciences and the American Physiological Society *15*, 72-77.
Rorsman, P., and Renstrom, E. (2003). Insulin granule dynamics in pancreatic beta cells. Diabetologia *46*, 1029-1045.
Rosen, E.D., and Spiegelman, B.M. (2014). What we talk about when we talk about fat. Cell *156*, 20-44.
Ross, R.A., Brockie, H.C., Stevenson, L.A., Murphy, V.L., Templeton, F., Makriyannis, A., and Pertwee, R.G. (1999). Agonist-inverse agonist characterization at CB1 and CB2 cannabinoid receptors of L759633, L759656, and AM630. British journal of pharmacology *126*, 665-672.
Rudic, R.D., McNamara, P., Curtis, A.M., Boston, R.C., Panda, S., Hogenesch, J.B., and Fitzgerald, G.A. (2004). BMAL1 and CLOCK, two essential components of the circadian clock, are involved in glucose homeostasis. PLoS biology *2*, e377.
Sacks, H.S., Fain, J.N., Holman, B., Cheema, P., Chary, A., Parks, F., Karas, J., Optican, R., Bahouth, S.W., Garrett, E., et al. (2009). Uncoupling protein-1 and related messenger ribonucleic acids in human epicardial and other adipose tissues: epicardial fat functioning as brown fat. The Journal of clinical endocrinology and metabolism *94*, 3611-3615.
Sampath, H., Flowers, M.T., Liu, X., Paton, C.M., Sullivan, R., Chu, K., Zhao, M., and Ntambi, J.M. (2009). Skin-specific deletion of stearoyl-CoA desaturase-1 alters skin lipid composition and protects mice from high fat diet-induced obesity. The Journal of biological chemistry *284*, 19961-19973.
Samuel, V.T., and Shulman, G.I. (2012). Mechanisms for insulin resistance: common threads and missing links. Cell *148*, 852-871.
Schmitz-Peiffer, C., Laybutt, D.R., Burchfield, J.G., Gurisik, E., Narasimhan, S., Mitchell, C.J., Pedersen, D.J., Braun, U., Cooney, G.J., Leitges, M., et al. (2007). Inhibition of PKCepsilon improves glucose-stimulated insulin secretion and reduces insulin clearance. Cell metabolism *6*, 320-328.
Schrauwen, P., van Marken Lichtenbelt, W.D., and Spiegelman, B.M. (2015). The future of brown adipose tissues in the treatment of type 2 diabetes. Diabetologia.
Schuit, F., De Vos, A., Farfari, S., Moens, K., Pipeleers, D., Brun, T., and Prentki, M. (1997). Metabolic fate of glucose in purified islet cells. Glucose-regulated anaplerosis in beta cells. The Journal of biological chemistry *272*, 18572-18579.
Schuit, F.C. (1997). Is GLUT2 required for glucose sensing? Diabetologia *40*, 104-111.
Seale, P., Bjork, B., Yang, W., Kajimura, S., Chin, S., Kuang, S., Scime, A., Devarakonda, S., Conroe, H.M., Erdjument-Bromage, H., et al. (2008). PRDM16 controls a brown fat/skeletal muscle switch. Nature *454*, 961-967.
Seale, P., Conroe, H.M., Estall, J., Kajimura, S., Frontini, A., Ishibashi, J., Cohen, P., Cinti, S., and Spiegelman, B.M. (2011). Prdm16 determines the thermogenic program of subcutaneous white adipose tissue in mice. The Journal of clinical investigation *121*, 96-105.

Seifi, S., Nazifi, S., Tabandeh, M.R., and Saeb, M. (2013). AdipoR1 and AdipoR2 gene expression are regulated by thyroid hormones in adipose tissue. Molecular and cellular biochemistry *377*, 55-63.
Seifi, S., Tabandeh, M.R., Nazifi, S., Saeb, M., Shirian, S., and Sarkoohi, P. (2012). Regulation of adiponectin gene expression in adipose tissue by thyroid hormones. Journal of physiology and biochemistry *68*, 193-203.
Seki, E., Brenner, D.A., and Karin, M. (2012). A liver full of JNK: signaling in regulation of cell function and disease pathogenesis, and clinical approaches. Gastroenterology *143*, 307-320.
Severson, D.L., and Hee-Cheong, M. (1988). Monoacylglycerol lipase activity in cardiac myocytes. Biochemistry and cell biology = Biochimie et biologie cellulaire *66*, 1013-1018.
Shabalina, I.G., Petrovic, N., de Jong, J.M., Kalinovich, A.V., Cannon, B., and Nedergaard, J. (2013). UCP1 in brite/beige adipose tissue mitochondria is functionally thermogenic. Cell reports *5*, 1196-1203.
Sharara-Chami, R.I., Zhou, Y., Ebert, S., Pacak, K., Ozcan, U., and Majzoub, J.A. (2012). Epinephrine deficiency results in intact glucose counter-regulation, severe hepatic steatosis and possible defective autophagy in fasting mice. The international journal of biochemistry & cell biology *44*, 905-913.
Sharma, A., Olson, L.K., Robertson, R.P., and Stein, R. (1995). The reduction of insulin gene transcription in HIT-T15 beta cells chronically exposed to high glucose concentration is associated with the loss of RIPE3b1 and STF-1 transcription factor expression. Molecular endocrinology *9*, 1127-1134.
Sharma, S., and Fulton, S. (2013). Diet-induced obesity promotes depressive-like behaviour that is associated with neural adaptations in brain reward circuitry. Int J Obes (Lond) *37*, 382-389.
Sharp, L.Z., Shinoda, K., Ohno, H., Scheel, D.W., Tomoda, E., Ruiz, L., Hu, H., Wang, L., Pavlova, Z., Gilsanz, V., et al. (2012). Human BAT possesses molecular signatures that resemble beige/brite cells. PloS one *7*, e49452.
Shen, N., Guryev, O., and Rizo, J. (2005). Intramolecular occlusion of the diacylglycerol-binding site in the C1 domain of munc13-1. Biochemistry *44*, 1089-1096.
Sheu, L., Pasyk, E.A., Ji, J., Huang, X., Gao, X., Varoqueaux, F., Brose, N., and Gaisano, H.Y. (2003). Regulation of insulin exocytosis by Munc13-1. The Journal of biological chemistry *278*, 27556-27563.
Shi, Y., and Cheng, D. (2009). Beyond triglyceride synthesis: the dynamic functional roles of MGAT and DGAT enzymes in energy metabolism. American journal of physiology. Endocrinology and metabolism *297*, E10-18.
Shulman, G.I. (2014). Ectopic fat in insulin resistance, dyslipidemia, and cardiometabolic disease. The New England journal of medicine *371*, 1131-1141.
Sidossis, L., and Kajimura, S. (2015). Brown and beige fat in humans: thermogenic adipocytes that control energy and glucose homeostasis. The Journal of clinical investigation *125*, 478-486.

Siow, D., and Wattenberg, B. (2011). The compartmentalization and translocation of the sphingosine kinases: mechanisms and functions in cell signaling and sphingolipid metabolism. Critical reviews in biochemistry and molecular biology *46*, 365-375.
Skarnes, W.C., Rosen, B., West, A.P., Koutsourakis, M., Bushell, W., Iyer, V., Mujica, A.O., Thomas, M., Harrow, J., Cox, T., et al. (2011). A conditional knockout resource for the genome-wide study of mouse gene function. Nature *474*, 337-342.
Sladek, R., Rocheleau, G., Rung, J., Dina, C., Shen, L., Serre, D., Boutin, P., Vincent, D., Belisle, A., Hadjadj, S., et al. (2007). A genome-wide association study identifies novel risk loci for type 2 diabetes. Nature *445*, 881-885.
Smirnova, E., Goldberg, E.B., Makarova, K.S., Lin, L., Brown, W.J., and Jackson, C.L. (2006). ATGL has a key role in lipid droplet/adiposome degradation in mammalian cells. EMBO reports *7*, 106-113.
Smith, S.J., Cases, S., Jensen, D.R., Chen, H.C., Sande, E., Tow, B., Sanan, D.A., Raber, J., Eckel, R.H., and Farese, R.V., Jr. (2000). Obesity resistance and multiple mechanisms of triglyceride synthesis in mice lacking Dgat. Nature genetics *25*, 87-90.
Soria-Gomez, E., Guzman, K., Pech-Rueda, O., Montes-Rodriguez, C.J., Cisneros, M., and Prospero-Garcia, O. (2010). Oleoylethanolamide affects food intake and sleep-waking cycle through a hypothalamic modulation. Pharmacological research : the official journal of the Italian Pharmacological Society *61*, 379-384.
Spiegelman, B.M. (2013). Banting Lecture 2012: Regulation of adipogenesis: toward new therapeutics for metabolic disease. Diabetes *62*, 1774-1782.
Stanford, K.I., Middelbeek, R.J., Townsend, K.L., Lee, M.Y., Takahashi, H., So, K., Hitchcox, K.M., Markan, K.R., Hellbach, K., Hirshman, M.F., et al. (2015). A Novel Role for Subcutaneous Adipose Tissue in Exercise-Induced Improvements in Glucose Homeostasis. Diabetes.
Stanley, C.A., Lieu, Y.K., Hsu, B.Y., Burlina, A.B., Greenberg, C.R., Hopwood, N.J., Perlman, K., Rich, B.H., Zammarchi, E., and Poncz, M. (1998). Hyperinsulinism and hyperammonemia in infants with regulatory mutations of the glutamate dehydrogenase gene. The New England journal of medicine *338*, 1352-1357.
Stefl, B., Janovska, A., Hodny, Z., Rossmeisl, M., Horakova, M., Syrovy, I., Bemova, J., Bendlova, B., and Kopecky, J. (1998). Brown fat is essential for cold-induced thermogenesis but not for obesity resistance in aP2-Ucp mice. The American journal of physiology *274*, E527-533.
Straub, S.G., and Sharp, G.W. (2002). Glucose-stimulated signaling pathways in biphasic insulin secretion. Diabetes/metabolism research and reviews *18*, 451-463.
Strowski, M.Z., Parmar, R.M., Blake, A.D., and Schaeffer, J.M. (2000). Somatostatin inhibits insulin and glucagon secretion via two receptors subtypes: an in vitro study of pancreatic islets from somatostatin receptor 2 knockout mice. Endocrinology *141*, 111-117.
Stumvoll, M., Goldstein, B.J., and van Haeften, T.W. (2005). Type 2 diabetes: principles of pathogenesis and therapy. Lancet *365*, 1333-1346.
Sugiura, T., Kondo, S., Sukagawa, A., Nakane, S., Shinoda, A., Itoh, K., Yamashita, A., and Waku, K. (1995). 2-Arachidonoylglycerol: a possible endogenous cannabinoid receptor ligand in brain. Biochemical and biophysical research communications *215*, 89-97.

Sumara, G., Formentini, I., Collins, S., Sumara, I., Windak, R., Bodenmiller, B., Ramracheya, R., Caille, D., Jiang, H., Platt, K.A., et al. (2009). Regulation of PKD by the MAPK p38delta in insulin secretion and glucose homeostasis. Cell *136*, 235-248.
Sun, K., Wernstedt Asterholm, I., Kusminski, C.M., Bueno, A.C., Wang, Z.V., Pollard, J.W., Brekken, R.A., and Scherer, P.E. (2012). Dichotomous effects of VEGF-A on adipose tissue dysfunction. Proceedings of the National Academy of Sciences of the United States of America *109*, 5874-5879.
Swick, A.G., Orena, S., and O'Connor, A. (2013). Irisin levels correlate with energy expenditure in a subgroup of humans with energy expenditure greater than predicted by fat free mass. Metabolism: clinical and experimental *62*, 1070-1073.
Szallasi, A., Cortright, D.N., Blum, C.A., and Eid, S.R. (2007). The vanilloid receptor TRPV1: 10 years from channel cloning to antagonist proof-of-concept. Nature reviews. Drug discovery *6*, 357-372.
Takahashi, N., Kishimoto, T., Nemoto, T., Kadowaki, T., and Kasai, H. (2002). Fusion pore dynamics and insulin granule exocytosis in the pancreatic islet. Science *297*, 1349-1352.
Takeda, K., Noguchi, K., Shi, W., Tanaka, T., Matsumoto, M., Yoshida, N., Kishimoto, T., and Akira, S. (1997). Targeted disruption of the mouse Stat3 gene leads to early embryonic lethality. Proceedings of the National Academy of Sciences of the United States of America *94*, 3801-3804.
Takeuchi, K., and Reue, K. (2009). Biochemistry, physiology, and genetics of GPAT, AGPAT, and lipin enzymes in triglyceride synthesis. American journal of physiology. Endocrinology and metabolism *296*, E1195-1209.
Tang, G., Wang, Y., Park, S., Bajpayee, N.S., Vi, D., Nagaoka, Y., Birnbaumer, L., and Jiang, M. (2012). Go2 G protein mediates galanin inhibitory effects on insulin release from pancreatic beta cells. Proceedings of the National Academy of Sciences of the United States of America *109*, 2636-2641.
Tang, T., Abbott, M.J., Ahmadian, M., Lopes, A.B., Wang, Y., and Sul, H.S. (2013). Desnutrin/ATGL activates PPARdelta to promote mitochondrial function for insulin secretion in islet beta cells. Cell metabolism *18*, 883-895.
Tareste, D., Shen, J., Melia, T.J., and Rothman, J.E. (2008). SNAREpin/Munc18 promotes adhesion and fusion of large vesicles to giant membranes. Proceedings of the National Academy of Sciences of the United States of America *105*, 2380-2385.
Taschler, U., Radner, F.P., Heier, C., Schreiber, R., Schweiger, M., Schoiswohl, G., Preiss-Landl, K., Jaeger, D., Reiter, B., Koefeler, H.C., et al. (2011). Monoglyceride lipase deficiency in mice impairs lipolysis and attenuates diet-induced insulin resistance. The Journal of biological chemistry *286*, 17467-17477.
Tchantchou, F., and Zhang, Y. (2013). Selective inhibition of alpha/beta-hydrolase domain 6 attenuates neurodegeneration, alleviates blood brain barrier breakdown, and improves functional recovery in a mouse model of traumatic brain injury. Journal of neurotrauma *30*, 565-579.
Tchkonia, T., Thomou, T., Zhu, Y., Karagiannides, I., Pothoulakis, C., Jensen, M.D., and Kirkland, J.L. (2013). Mechanisms and metabolic implications of regional differences among fat depots. Cell metabolism *17*, 644-656.

Teruel, T., Hernandez, R., and Lorenzo, M. (2001). Ceramide mediates insulin resistance by tumor necrosis factor-alpha in brown adipocytes by maintaining Akt in an inactive dephosphorylated state. Diabetes *50*, 2563-2571.
Thomas, G., Betters, J.L., Lord, C.C., Brown, A.L., Marshall, S., Ferguson, D., Sawyer, J., Davis, M.A., Melchior, J.T., Blume, L.C., et al. (2013). The serine hydrolase ABHD6 Is a critical regulator of the metabolic syndrome. Cell reports *5*, 508-520.
Tiano, J.P., Delghingaro-Augusto, V., Le May, C., Liu, S., Kaw, M.K., Khuder, S.S., Latour, M.G., Bhatt, S.A., Korach, K.S., Najjar, S.M., et al. (2011). Estrogen receptor activation reduces lipid synthesis in pancreatic islets and prevents beta cell failure in rodent models of type 2 diabetes. The Journal of clinical investigation *121*, 3331-3342.
Tran, K.V., Gealekman, O., Frontini, A., Zingaretti, M.C., Morroni, M., Giordano, A., Smorlesi, A., Perugini, J., De Matteis, R., Sbarbati, A., et al. (2012). The vascular endothelium of the adipose tissue gives rise to both white and brown fat cells. Cell metabolism *15*, 222-229.
Tran, T.T., and Kahn, C.R. (2010). Transplantation of adipose tissue and stem cells: role in metabolism and disease. Nature reviews. Endocrinology *6*, 195-213.
Triandafillou, J., and Himms-Hagen, J. (1983). Brown adipose tissue in genetically obese (fa/fa) rats: response to cold and diet. The American journal of physiology *244*, E145-150.
Turpin, S.M., Nicholls, H.T., Willmes, D.M., Mourier, A., Brodesser, S., Wunderlich, C.M., Mauer, J., Xu, E., Hammerschmidt, P., Bronneke, H.S., et al. (2014). Obesity-induced CerS6-dependent C16:0 ceramide production promotes weight gain and glucose intolerance. Cell metabolism *20*, 678-686.
Ueki, K., Kadowaki, T., and Kahn, C.R. (2005). Role of suppressors of cytokine signaling SOCS-1 and SOCS-3 in hepatic steatosis and the metabolic syndrome. Hepatology research : the official journal of the Japan Society of Hepatology *33*, 185-192.
Ueki, K., Kondo, T., and Kahn, C.R. (2004). Suppressor of cytokine signaling 1 (SOCS-1) and SOCS-3 cause insulin resistance through inhibition of tyrosine phosphorylation of insulin receptor substrate proteins by discrete mechanisms. Molecular and cellular biology *24*, 5434-5446.
Ullrich, S., and Wollheim, C.B. (1989). Galanin inhibits insulin secretion by direct interference with exocytosis. FEBS letters *247*, 401-404.
Vaarala, O., Atkinson, M.A., and Neu, J. (2008). The "perfect storm" for type 1 diabetes: the complex interplay between intestinal microbiota, gut permeability, and mucosal immunity. Diabetes *57*, 2555-2562.
van der Lans, A.A., Hoeks, J., Brans, B., Vijgen, G.H., Visser, M.G., Vosselman, M.J., Hansen, J., Jorgensen, J.A., Wu, J., Mottaghy, F.M., et al. (2013). Cold acclimation recruits human brown fat and increases nonshivering thermogenesis. The Journal of clinical investigation *123*, 3395-3403.
van Marken Lichtenbelt, W.D., and Schrauwen, P. (2011). Implications of nonshivering thermogenesis for energy balance regulation in humans. American journal of physiology. Regulatory, integrative and comparative physiology *301*, R285-296.
van Raalte, D.H., and Diamant, M. (2011). Glucolipotoxicity and beta cells in type 2 diabetes mellitus: target for durable therapy? Diabetes research and clinical practice *93 Suppl 1*, S37-46.

Vance, J.E., and Tasseva, G. (2013). Formation and function of phosphatidylserine and phosphatidylethanolamine in mammalian cells. Biochimica et biophysica acta *1831*, 543-554.
Vandevoorde, S., Jonsson, K.O., Labar, G., Persson, E., Lambert, D.M., and Fowler, C.J. (2007). Lack of selectivity of URB602 for 2-oleoylglycerol compared to anandamide hydrolysis in vitro. British journal of pharmacology *150*, 186-191.
Vaughan, M., Berger, J.E., and Steinberg, D. (1964). Hormone-Sensitive Lipase and Monoglyceride Lipase Activities in Adipose Tissue. The Journal of biological chemistry *239*, 401-409.
Vegiopoulos, A., Muller-Decker, K., Strzoda, D., Schmitt, I., Chichelnitskiy, E., Ostertag, A., Berriel Diaz, M., Rozman, J., Hrabe de Angelis, M., Nusing, R.M., et al. (2010). Cyclooxygenase-2 controls energy homeostasis in mice by de novo recruitment of brown adipocytes. Science *328*, 1158-1161.
Vergnes, L., Beigneux, A.P., Davis, R., Watkins, S.M., Young, S.G., and Reue, K. (2006). Agpat6 deficiency causes subdermal lipodystrophy and resistance to obesity. Journal of lipid research *47*, 745-754.
Vilsboll, T., Krarup, T., Madsbad, S., and Holst, J.J. (2003). Both GLP-1 and GIP are insulinotropic at basal and postprandial glucose levels and contribute nearly equally to the incretin effect of a meal in healthy subjects. Regulatory peptides *114*, 115-121.
Virtanen, K.A., Lidell, M.E., Orava, J., Heglind, M., Westergren, R., Niemi, T., Taittonen, M., Laine, J., Savisto, N.J., Enerback, S., et al. (2009). Functional brown adipose tissue in healthy adults. The New England journal of medicine *360*, 1518-1525.
Wallberg-Henriksson, H., and Zierath, J.R. (2015). Metabolism: Exercise remodels subcutaneous fat tissue and improves metabolism. Nature reviews. Endocrinology.
Wang, F., Mullican, S.E., DiSpirito, J.R., Peed, L.C., and Lazar, M.A. (2013a). Lipoatrophy and severe metabolic disturbance in mice with fat-specific deletion of PPARgamma. Proceedings of the National Academy of Sciences of the United States of America *110*, 18656-18661.
Wang, G.X., Zhao, X.Y., Meng, Z.X., Kern, M., Dietrich, A., Chen, Z., Cozacov, Z., Zhou, D., Okunade, A.L., Su, X., et al. (2014). The brown fat-enriched secreted factor Nrg4 preserves metabolic homeostasis through attenuation of hepatic lipogenesis. Nature medicine *20*, 1436-1443.
Wang, L., Teng, R., Di, L., Rogers, H., Wu, H., Kopp, J.B., and Noguchi, C.T. (2013b). PPARalpha and Sirt1 mediate erythropoietin action in increasing metabolic activity and browning of white adipocytes to protect against obesity and metabolic disorders. Diabetes *62*, 4122-4131.
Wang, Q.A., Tao, C., Gupta, R.K., and Scherer, P.E. (2013c). Tracking adipogenesis during white adipose tissue development, expansion and regeneration. Nature medicine *19*, 1338-1344.
Wang, W., Lin, Q., Lin, R., Zhang, J., Ren, F., Zhang, J., Ji, M., and Li, Y. (2013d). PPARalpha agonist fenofibrate attenuates TNF-alpha-induced CD40 expression in 3T3-L1 adipocytes via the SIRT1-dependent signaling pathway. Experimental cell research *319*, 1523-1533.

Wang, Y.X. (2010). PPARs: diverse regulators in energy metabolism and metabolic diseases. Cell research *20*, 124-137.
Watt, M.J., and Spriet, L.L. (2010). Triacylglycerol lipases and metabolic control: implications for health and disease. American journal of physiology. Endocrinology and metabolism *299*, E162-168.
Wendel, A.A., Cooper, D.E., Ilkayeva, O.R., Muoio, D.M., and Coleman, R.A. (2013). Glycerol-3-phosphate acyltransferase (GPAT)-1, but not GPAT4, incorporates newly synthesized fatty acids into triacylglycerol and diminishes fatty acid oxidation. The Journal of biological chemistry *288*, 27299-27306.
Wendel, A.A., Lewin, T.M., and Coleman, R.A. (2009). Glycerol-3-phosphate acyltransferases: rate limiting enzymes of triacylglycerol biosynthesis. Biochimica et biophysica acta *1791*, 501-506.
Westerberg, R., Mansson, J.E., Golozoubova, V., Shabalina, I.G., Backlund, E.C., Tvrdik, P., Retterstol, K., Capecchi, M.R., and Jacobsson, A. (2006). ELOVL3 is an important component for early onset of lipid recruitment in brown adipose tissue. The Journal of biological chemistry *281*, 4958-4968.
Westerberg, R., Tvrdik, P., Unden, A.B., Mansson, J.E., Norlen, L., Jakobsson, A., Holleran, W.H., Elias, P.M., Asadi, A., Flodby, P., et al. (2004). Role for ELOVL3 and fatty acid chain length in development of hair and skin function. The Journal of biological chemistry *279*, 5621-5629.
Whittle, A.J., Carobbio, S., Martins, L., Slawik, M., Hondares, E., Vazquez, M.J., Morgan, D., Csikasz, R.I., Gallego, R., Rodriguez-Cuenca, S., et al. (2012). BMP8B increases brown adipose tissue thermogenesis through both central and peripheral actions. Cell *149*, 871-885.
Wicksteed, B., Brissova, M., Yan, W., Opland, D.M., Plank, J.L., Reinert, R.B., Dickson, L.M., Tamarina, N.A., Philipson, L.H., Shostak, A., et al. (2010). Conditional gene targeting in mouse pancreatic ss-Cells: analysis of ectopic Cre transgene expression in the brain. Diabetes *59*, 3090-3098.
Wiernsperger, N.F. (2005a). Is non-insulin dependent glucose uptake a therapeutic alternative? Part 1: physiology, mechanisms and role of non insulin-dependent glucose uptake in type 2 diabetes. Diabetes & metabolism *31*, 415-426.
Wiernsperger, N.F. (2005b). Is non-insulin dependent glucose uptake a therapeutic alternative? Part 2: Do such mechanisms fulfil the required combination of power and tolerability? Diabetes & metabolism *31*, 521-525.
Wiskerke, J., Irimia, C., Cravatt, B.F., De Vries, T.J., Schoffelmeer, A.N., Pattij, T., and Parsons, L.H. (2012). Characterization of the effects of reuptake and hydrolysis inhibition on interstitial endocannabinoid levels in the brain: an in vivo microdialysis study. ACS chemical neuroscience *3*, 407-417.
Woods, S.C., Seeley, R.J., Porte, D., Jr., and Schwartz, M.W. (1998). Signals that regulate food intake and energy homeostasis. Science *280*, 1378-1383.
Wu, B., Wei, S., Petersen, N., Ali, Y., Wang, X., Bacaj, T., Rorsman, P., Hong, W., Sudhof, T.C., and Han, W. (2015). Synaptotagmin-7 phosphorylation mediates GLP-1-dependent potentiation of insulin secretion from beta-cells. Proceedings of the National Academy of Sciences of the United States of America *112*, 9996-10001.

Wu, J., Bostrom, P., Sparks, L.M., Ye, L., Choi, J.H., Giang, A.H., Khandekar, M., Virtanen, K.A., Nuutila, P., Schaart, G., et al. (2012). Beige adipocytes are a distinct type of thermogenic fat cell in mouse and human. Cell *150*, 366-376.
Wu, J., Cohen, P., and Spiegelman, B.M. (2013). Adaptive thermogenesis in adipocytes: is beige the new brown? Genes & development *27*, 234-250.
Wu, J., and Spiegelman, B.M. (2014). Irisin ERKs the fat. Diabetes *63*, 381-383.
Xie, L., Zhu, D., and Gaisano, H.Y. (2012). Role of mammalian homologue of Caenorhabditis elegans unc-13-1 (Munc13-1) in the recruitment of newcomer insulin granules in both first and second phases of glucose-stimulated insulin secretion in mouse islets. Diabetologia *55*, 2693-2702.
Xu, A., Wang, Y., Keshaw, H., Xu, L.Y., Lam, K.S., and Cooper, G.J. (2003). The fat-derived hormone adiponectin alleviates alcoholic and nonalcoholic fatty liver diseases in mice. The Journal of clinical investigation *112*, 91-100.
Xu, H., Wilcox, D., Nguyen, P., Voorbach, M., Suhar, T., Morgan, S.J., An, W.F., Ge, L., Green, J., Wu, Z., et al. (2006). Hepatic knockdown of mitochondrial GPAT1 in ob/ob mice improves metabolic profile. Biochemical and biophysical research communications *349*, 439-448.
Xue, B., Coulter, A., Rim, J.S., Koza, R.A., and Kozak, L.P. (2005). Transcriptional synergy and the regulation of Ucp1 during brown adipocyte induction in white fat depots. Molecular and cellular biology *25*, 8311-8322.
Yabe, D., and Seino, Y. (2011). Two incretin hormones GLP-1 and GIP: comparison of their actions in insulin secretion and beta cell preservation. Progress in biophysics and molecular biology *107*, 248-256.
Yajima, H., Komatsu, M., Schermerhorn, T., Aizawa, T., Kaneko, T., Nagai, M., Sharp, G.W., and Hashizume, K. (1999). cAMP enhances insulin secretion by an action on the ATP-sensitive K+ channel-independent pathway of glucose signaling in rat pancreatic islets. Diabetes *48*, 1006-1012.
Yamada, M., Miyakawa, T., Duttaroy, A., Yamanaka, A., Moriguchi, T., Makita, R., Ogawa, M., Chou, C.J., Xia, B., Crawley, J.N., et al. (2001). Mice lacking the M3 muscarinic acetylcholine receptor are hypophagic and lean. Nature *410*, 207-212.
Yamauchi, T., and Kadowaki, T. (2013). Adiponectin receptor as a key player in healthy longevity and obesity-related diseases. Cell metabolism *17*, 185-196.
Yamauchi, T., Kamon, J., Minokoshi, Y., Ito, Y., Waki, H., Uchida, S., Yamashita, S., Noda, M., Kita, S., Ueki, K., et al. (2002). Adiponectin stimulates glucose utilization and fatty-acid oxidation by activating AMP-activated protein kinase. Nature medicine *8*, 1288-1295.
Yang, P.Y., Ho, K.H., Chen, H.C., and Chien, M.Y. (2012). Exercise training improves sleep quality in middle-aged and older adults with sleep problems: a systematic review. Journal of physiotherapy *58*, 157-163.
Ye, D.Z., Tai, M.H., Linning, K.D., Szabo, C., and Olson, L.K. (2006). MafA expression and insulin promoter activity are induced by nicotinamide and related compounds in INS-1 pancreatic beta-cells. Diabetes *55*, 742-750.
Ye, L., Wu, J., Cohen, P., Kazak, L., Khandekar, M.J., Jedrychowski, M.P., Zeng, X., Gygi, S.P., and Spiegelman, B.M. (2013). Fat cells directly sense temperature to activate

thermogenesis. Proceedings of the National Academy of Sciences of the United States of America *110*, 12480-12485.
Yen, C.L., Cheong, M.L., Grueter, C., Zhou, P., Moriwaki, J., Wong, J.S., Hubbard, B., Marmor, S., and Farese, R.V., Jr. (2009). Deficiency of the intestinal enzyme acyl CoA:monoacylglycerol acyltransferase-2 protects mice from metabolic disorders induced by high-fat feeding. Nature medicine *15*, 442-446.
Yen, C.L., and Farese, R.V., Jr. (2003). MGAT2, a monoacylglycerol acyltransferase expressed in the small intestine. The Journal of biological chemistry *278*, 18532-18537.
Yen, C.L., Stone, S.J., Cases, S., Zhou, P., and Farese, R.V., Jr. (2002). Identification of a gene encoding MGAT1, a monoacylglycerol acyltransferase. Proceedings of the National Academy of Sciences of the United States of America *99*, 8512-8517.
Yen, C.L., Stone, S.J., Koliwad, S., Harris, C., and Farese, R.V., Jr. (2008). Thematic review series: glycerolipids. DGAT enzymes and triacylglycerol biosynthesis. Journal of lipid research *49*, 2283-2301.
Yin, M.J., Yamamoto, Y., and Gaynor, R.B. (1998). The anti-inflammatory agents aspirin and salicylate inhibit the activity of I(kappa)B kinase-beta. Nature *396*, 77-80.
Yoon, M.J., Lee, G.Y., Chung, J.J., Ahn, Y.H., Hong, S.H., and Kim, J.B. (2006). Adiponectin increases fatty acid oxidation in skeletal muscle cells by sequential activation of AMP-activated protein kinase, p38 mitogen-activated protein kinase, and peroxisome proliferator-activated receptor alpha. Diabetes *55*, 2562-2570.
Yu, C., Chen, Y., Cline, G.W., Zhang, D., Zong, H., Wang, Y., Bergeron, R., Kim, J.K., Cushman, S.W., Cooney, G.J., et al. (2002). Mechanism by which fatty acids inhibit insulin activation of insulin receptor substrate-1 (IRS-1)-associated phosphatidylinositol 3-kinase activity in muscle. The Journal of biological chemistry *277*, 50230-50236.
Yu, S., Levi, L., Siegel, R., and Noy, N. (2012). Retinoic acid induces neurogenesis by activating both retinoic acid receptors (RARs) and peroxisome proliferator-activated receptor beta/delta (PPARbeta/delta). The Journal of biological chemistry *287*, 42195-42205.
Yuan, M., Konstantopoulos, N., Lee, J., Hansen, L., Li, Z.W., Karin, M., and Shoelson, S.E. (2001). Reversal of obesity- and diet-induced insulin resistance with salicylates or targeted disruption of Ikkbeta. Science *293*, 1673-1677.
Zadravec, D., Brolinson, A., Fisher, R.M., Carneheim, C., Csikasz, R.I., Bertrand-Michel, J., Boren, J., Guillou, H., Rudling, M., and Jacobsson, A. (2010). Ablation of the very-long-chain fatty acid elongase ELOVL3 in mice leads to constrained lipid storage and resistance to diet-induced obesity. FASEB journal : official publication of the Federation of American Societies for Experimental Biology *24*, 4366-4377.
Zawalich, W.S., and Rasmussen, H. (1990). Control of insulin secretion: a model involving Ca2+, cAMP and diacylglycerol. Molecular and cellular endocrinology *70*, 119-137.
Zechner, R., Zimmermann, R., Eichmann, T.O., Kohlwein, S.D., Haemmerle, G., Lass, A., and Madeo, F. (2012). FAT SIGNALS--lipases and lipolysis in lipid metabolism and signaling. Cell metabolism *15*, 279-291.
Zhang, J., Gao, Z., Yin, J., Quon, M.J., and Ye, J. (2008). S6K directly phosphorylates IRS-1 on Ser-270 to promote insulin resistance in response to TNF-(alpha) signaling through IKK2. The Journal of biological chemistry *283*, 35375-35382.

Zhang, J., Xu, D., Nie, J., Cao, J., Zhai, Y., Tong, D., and Shi, Y. (2014a). Monoacylglycerol acyltransferase-2 is a tetrameric enzyme that selectively heterodimerizes with diacylglycerol acyltransferase-1. The Journal of biological chemistry *289*, 10909-10918.
Zhang, Q., Miao, Q., Ye, H., Zhang, Z., Zuo, C., Hua, F., Guan, Y., and Li, Y. (2014b). The effects of thyroid hormones on brown adipose tissue in humans: a PET-CT study. Diabetes/metabolism research and reviews *30*, 513-520.
Zhang, Y., Li, R., Meng, Y., Li, S., Donelan, W., Zhao, Y., Qi, L., Zhang, M., Wang, X., Cui, T., et al. (2014c). Irisin stimulates browning of white adipocytes through mitogen-activated protein kinase p38 MAP kinase and ERK MAP kinase signaling. Diabetes *63*, 514-525.
Zhao, S., Mugabo, Y., Iglesias, J., Xie, L., Delghingaro-Augusto, V., Lussier, R., Peyot, M.L., Joly, E., Taib, B., Davis, M.A., et al. (2014). alpha/beta-Hydrolase domain-6-accessible monoacylglycerol controls glucose-stimulated insulin secretion. Cell metabolism *19*, 993-1007.
Zhao, S., Xu, W., Jiang, W., Yu, W., Lin, Y., Zhang, T., Yao, J., Zhou, L., Zeng, Y., Li, H., et al. (2010). Regulation of cellular metabolism by protein lysine acetylation. Science *327*, 1000-1004.
Zhou, G., Sinnett-Smith, J., Liu, S.H., Yu, J., Wu, J., Sanchez, R., Pandol, S.J., Abrol, R., Nemunaitis, J., Rozengurt, E., et al. (2014). Down-regulation of pancreatic and duodenal homeobox-1 by somatostatin receptor subtype 5: a novel mechanism for inhibition of cellular proliferation and insulin secretion by somatostatin. Frontiers in physiology *5*, 226.
Zhu, L., Martinez, M.N., Emfinger, C.H., Palmisano, B.T., and Stafford, J.M. (2014). Estrogen signaling prevents diet-induced hepatic insulin resistance in male mice with obesity. American journal of physiology. Endocrinology and metabolism *306*, E1188-1197.
Zhu, Y., You, W., Wang, H., Li, Y., Qiao, N., Shi, Y., Zhang, C., Bleich, D., and Han, X. (2013). MicroRNA-24/MODY gene regulatory pathway mediates pancreatic beta-cell dysfunction. Diabetes *62*, 3194-3206.
Zygmunt, P.M., Ermund, A., Movahed, P., Andersson, D.A., Simonsen, C., Jonsson, B.A., Blomgren, A., Birnir, B., Bevan, S., Eschalier, A., et al. (2013). Monoacylglycerols Activate TRPV1 - A Link between Phospholipase C and TRPV1. PloS one *8*, e81618.